

---

---

---

---

JSCSEN 77(6)717–857(2012)

---

---

---

ISSN 1820-7421 (Online)

---

---

---

---

---

---

# Journal of the Serbian Chemical Society

---

---

---



---

---

---

VOLUME 77

---

---

No 6

---

---

BELGRADE 2012

---

---

Available on line at



[www.shd.org.rs/JSCS/](http://www.shd.org.rs/JSCS/)

---

---

The full search of JSCS

is available through

DOAJ DIRECTORY OF

OPEN ACCESS

JOURNALS

[www.doaj.org](http://www.doaj.org)



CONTENTS

**Organic Chemistry**

- A. F. M. Motiur Rahman, M. S. Alam and A. A. Kadi: Synthesis and antimicrobial activity of novel tetrabromo-bis(substituted benzyl)cycloalkanones ..... 717  
K. L. Ameta, N. S. Rathore and B. Kumar: Synthesis and *in vitro* anti-breast cancer activity of some novel 1,5-benzothiazepine derivatives ..... 725  
J. Safaei-Ghomi and M. A. Ghasemzadeh: Synthesis of some 3,5-diaryl-2-isoxazoline derivatives in ionic liquids media (Short communication) ..... 733

**Biochemistry and Biotechnology**

- V. D. Vitnik, M. T. Milenković, S. P. Dilber, Ž. J. Vitnik and I. O. Juranić: Improved synthesis and *in vitro* study of antimicrobial activity of  $\alpha,\beta$ -unsaturated and  $\alpha$ -bromo carboxylic acids ..... 741

**Theoretical Chemistry**

- M. Marković, J. Đurđević and I. Gutman: Cyclic conjugation in benzo- and benzocyclobutadieno-annelated terrylenes and higher rylene ..... 751

**Physical Chemistry**

- M. Z. Momčilović, A. E. Onjia, M. M. Purenović, A. R. Zarubica and M. S. Randelović: Removal of a cationic dye from water by activated pinecones ..... 761

**Analytical Chemistry**

- N. Ben Issa, A. D. Marinković and Lj. V. Rajaković: Separation and determination of dimethylarsenate in natural waters ..... 775

**Materials**

- N. D. Abazović, D. J. Jovanović, M. M. Stoiljković, M. N. Mitić, S. P. Ahrenkiel, J. M. Nedeljković and M. I. Čomor: Colloidal chemistry-based synthesis of quantized CuInS<sub>2</sub>/Se<sub>2</sub> nanoparticles ..... 789

**Chemical Engineering**

- S. S. Petrović, J. Ivanović, S. Milovanović and I. Žižović: Comparative analyses of the diffusion coefficients from thyme for different extraction processes ..... 799  
Z. Predojević, B. Škrbić and N. Đurišić-Mladenović: Transesterification of linoleic and oleic sunflower oils to biodiesel using CaO as a solid base catalyst ..... 815

**Environmental**

- I. G. Đalović, D. S. Jocković, G. J. Dugalić, G. F. Bekavac, B. Purar, S. I. Šeremešić and M. D. Jocković: Soil acidity and mobile aluminum status in pseudogley soils in the Čačak-Kraljevo Basin ..... 833  
Lj. Radivojević, S. Gašić, Lj. Šantrić, J. Gajić Umiljendić and D. Marisavljević: Short-time effects of the herbicide nicosulfuron on the biochemical activity of Chernozem soil ..... 845  
*Errata* ..... 857

Published by the Serbian Chemical Society  
Karnegijeva 4/III, 11000 Belgrade, Serbia

Printed by the Faculty of Technology and Metallurgy  
Karnegijeva 4, P.O. Box 35-03, 11120 Belgrade, Serbia



## Synthesis and antimicrobial activity of novel tetrabromo-bis(substituted benzyl)cycloalkanones

A. F. M. MOTIUR RAHMAN<sup>1\*</sup>, MOHAMMAD SAYED ALAM<sup>2,3\*\*</sup>  
and ADNAN A. KADI<sup>1</sup>

<sup>1</sup>Department of Pharmaceutical Chemistry, College of Pharmacy, King Saud University,  
Riyadh 11451, Saudi Arabia, <sup>2</sup>Division of Bioscience, Dongguk University,  
Geyonju 780–714, Republic of Korea and <sup>3</sup>Department of Chemistry,  
Jagannath University, Dhaka 1100, Bangladesh

(Received 8 April 2011, revised 6 January 2012)

**Abstract:** A series of novel tetrabromo-bis(substituted benzyl)cycloalkanones have been synthesized through a rapid, simple, and efficient methodology in an excellent isolated yield and characterized via IR, NMR (<sup>1</sup>H-, <sup>13</sup>C-NMR, DEPT 135, DEPT 90) and mass spectrometry. All compounds were assayed for their *in vitro* antimicrobial activities against eight bacteria and five fungi. They showed stronger antibacterial than antifungal activities. Compounds **4c**, **4d** and **4i**, containing a methoxy or chloro substituent on the *para* or *meta* position of the phenyl ring, showed comparable minimum inhibitory concentration (MIC) values to those of the standard antibiotics streptomycin and tetracycline. Among all the tested compounds, **4i** exhibited good to moderate antifungal activity against all the tested fungal strains used.

**Keywords:** antibacterial; antifungal; tetrabromo-bis-(substituted benzyl)cycloalkanones.

### INTRODUCTION

In the past few decades, the incidence of serious antimicrobial infection has increased dramatically<sup>1</sup> due to the problem of multi-drug resistant microorganisms that has reached alarming levels around the world. For the treatment of microbial infections, the synthesis of new anti-infectious compounds has become a critical need. The organohalogen compounds have received much attention due to their important use in the field of medicinal and agro-chemistry.<sup>2–4</sup> A survey of the literature also revealed that different kinds of bis(substituted benzylidene)cycloalkanones, including organohalogen compounds, have been used for the treatment of the central nervous system, cardiovascular and obesity diseases,

\*,\*\* Corresponding authors. E-mail: \*afmrahman@ksu.edu.sa; \*\*alam\_sms@yahoo.com  
doi: 10.2298/JSC110408005M

and also showed antibacterial,<sup>5</sup> antifungal,<sup>5</sup> anti-angiogenic,<sup>6,7</sup> quinine reductase inducer,<sup>8</sup> cytotoxic,<sup>9,10</sup> and cholesterol-lowering activity.<sup>11</sup>

In 1980, Hoeve and Wynberg<sup>12</sup> prepared tetrabromo-di-*m*-anisalcycloopen-tanone from 2,5-dibenzylidene cycloalkanones using bromine in chloroform in a 47 % yield. Later, in 1988, Desiraju and Kishan<sup>13</sup> used the same starting material and obtained dibromo derivatives in which the bromine addition occurred on the methylene carbon of 2,5-dibenzylidene cycloalkanones. In the present study, we have synthesized and performed antimicrobial evaluation of a series of tetrabromo-bis(substituted benzyl)cycloalkanone analogues (**4a–j**). The structures of the new compounds were established by IR, NMR (<sup>1</sup>H-, <sup>13</sup>C-, DEPT 135 and DEPT 90) and mass spectrometry.

## EXPERIMENTAL

### *Chemistry*

*General.* Melting points were recorded on a Fisher-Jones melting point apparatus and are uncorrected. IR spectra were obtained on an FTIR-300E (Jasco Corporation, Tokyo, Japan) in KBr disc. <sup>1</sup>H-NMR (250 MHz) and <sup>13</sup>C-NMR (62.5 MHz) spectra were recorded on a Bruker 250 spectrometer (Bruker, USA) in CDCl<sub>3</sub> with TMS as an internal standard. ESI-MS were measured on an LCQ advantage-trap mass spectrometer (Thermo Finnigan, San Jose, CA, USA).

### *Synthesis of bis(substituted benzyl)cycloalkanones 3a–j*

The bis(substituted-benzyl)cycloalkanones were obtained by the cross-aldol condensation of substituted aldehydes with cycloalkanones in the presence of sodium acetate-acetic acid, Scheme 1.<sup>14</sup>

### *Synthesis of tetrabromo-bis(substituted benzyl)cycloalkanones 4a–j*

The tetrabromo-bis(substituted benzyl)cycloalkanones (**4a–j**) were prepared by adding a Br<sub>2</sub> solution (2 mmol) in dioxane (10 mL) dropwise over 10 min to a stirred solution of the respective bis(substituted benzyl)cycloalkanone (**3a–j**, 1 mmol) in dioxane (20 mL). The stirring was continued for 3–4 h. The completion of the reaction was monitored by thin layer chromatography (TLC). The solvent was evaporated and the dry residue subjected to column chromatography (*n*-hexane/dichloromethane, 1:1), which afforded the respective compound **4a–j** as a white solid.

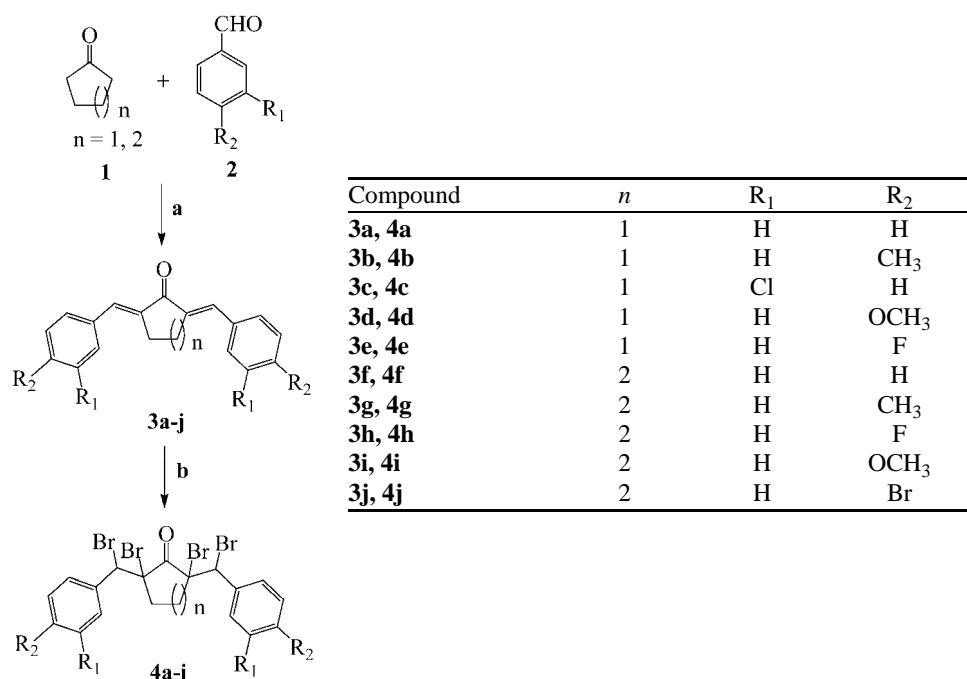
Data of synthesized compounds are given in Supplementary material.

### *Biology*

*Antibacterial screening.* The *in vitro* antibacterial activity of the synthesized compounds **4a–j** were evaluated against eight bacterial strains, *i.e.*, *Staphylococcus aureus* (KCTC 1916), *Bacillus subtilis* (ATCC 6633), *Listeria monocytogenes* (ATCC 19166), *Salmonella enteritidis* (KCCM 12021), *Pseudomonas aeruginosa* (KCTC 2004), *Enterobacter aerogenes* (KCTC 2190), *Salmonella typhimurium* (KCTC 2515) and *Escherichia coli* (ATCC 8739). All the bacterial strains were obtained from the Korea Food and Drug Administration (KFDA), Daegu, South Korea. Cultures of each bacterial strain were maintained on Luria broth (LB) agar medium at 4 °C.

The minimum inhibitory concentrations (MICs) of compounds **4a–j** were tested by the two-fold serial dilution method.<sup>15</sup> The test compounds **4a–j** were incorporated into Luria-

-Broth medium to obtain a concentration of 1,000 µg ml<sup>-1</sup> and serially diluted to a concentration in the range from 500 to 7.8 µg ml<sup>-1</sup>. A standardized suspension (10 µl) of each of the tested organism (10<sup>8</sup> CFU ml<sup>-1</sup>) was transferred to each tube and incubated at 37 °C for 24 h. Control tubes containing only bacterial suspensions were also incubated at 37 °C for 24 h. The lowest concentrations of the test samples that did not show any growth of the tested organism after macroscopic evaluation were determined as the *MICs*.



Scheme 1. Reagents and conditions: a) AcONa, AcOH, 3–8 h, 120 °C;  
b) Br<sub>2</sub>–dioxane, 3–4 h, room temperature.

**Antifungal screening.** The *in vitro* antifungal activities of the synthesized compounds **4a–j** were evaluated against various fungal species, *i.e.*, *Botrytis cinerea* (KACC 40573), *Rhizoctonia solani* (KACC 40111), *Fusarium oxysporum* (KACC 41083), *Sclerotinia sclerotiorum* (KACC 41065) and *Phytophthora capsici* (KACC 40157). The fungal cultures were obtained from the Korean Agricultural Culture Collection (KACC). Cultures of each fungal species were maintained on potato dextrose agar (PDA) slants and stored at 4 °C.

Potato dextrose agar (PDA) medium was used as the basal medium for the antifungal activity assay, which was performed by disc diffusion method.<sup>16</sup> Sterile Whatman No. 1 paper discs (6 mm diameter) were pierced in agar plates, equidistant and near the border, where 10 µl of compounds **4a–j** (200 µg disc<sup>-1</sup>) were applied. A disc of fungal inoculum 6 mm in diameter was removed from the pre-grown cultures of all the tested fungal strains and placed upside down in the center of the Petri dishes. The plates were incubated at 28 °C for 5–7 days, the time in which the growth of the control would have reached the edges of the plates. Discs with CHCl<sub>3</sub> and nystatin were used as negative and positive controls, respectively. The inhibitory activity was measured (in mm) as the diameter of the observed inhibition zones.

The minimum inhibitory concentration (*MIC*) was determined by the two-fold dilution method,<sup>15</sup> against *B. cinerea*, *R. solani*, *F. oxysporum*, *S. sclerotiorum* and *P. capsici*. Samples were dissolved in CHCl<sub>3</sub> accordingly with their respective known weight. These solutions were serially diluted with CHCl<sub>3</sub> and were added to PDA to final concentrations of 500, 250 125 and 62.5, 31.2, 15.6 and 7.8 µg ml<sup>-1</sup>, respectively. A 10 µl spore suspension of each test strain was inoculated in test tubes in PDA medium and incubated for 2–7 days at 28 °C. The control tubes containing PDA medium were inoculated only with fungal suspension. The minimum concentration at which no visible growth was observed was defined as the *MIC*, which was expressed in µg ml<sup>-1</sup>.

## RESULTS AND DISCUSSION

### Chemistry

The synthetic route to the tetrabromo-bis(substituted benzyl)cycloalkanones (**4a–j**) are outlined in Scheme 1. The compounds **4a–j** were obtained from the intermediate compounds **3a–j**, respectively, in excellent yields (70–93 %). The structures of the newly synthesized compounds were established based on their IR, <sup>1</sup>H-NMR, <sup>13</sup>C-NMR, DEPT 135, DEPT 90 and mass spectral data. IR spectra of compounds **4a–j** showed an absorption peak in the 1660–1681 cm<sup>-1</sup> region, indicating the presence of a carbonyl (>C=O) group. In the <sup>1</sup>H-NMR spectra, the characteristic benzylic protons of compounds **4a–j** appeared as a singlet at 5.50–6.03 ppm. The aliphatic protons of the cyclopentanone ring of compounds **4a–e** appeared as two AB-quartets at around 3.28–3.32 and 2.37–2.42 ppm equivalent to two protons, respectively. On the other hand, the six protons of the cyclohexanone ring of compounds **4f–j** were observed as triplets of a doublet at 2.99–3.07 ppm and two multiplets at around 2.14–2.46 and 1.90–2.03 ppm equivalent to two, three and one proton(s), respectively. The aromatic protons of the phenyl groups of compounds **4a–j** appeared in usual way. The methyl protons of compounds **4b** and **4g** were observed as a singlet at 2.35–2.36 ppm, whereas the methoxy protons of compounds **4d** and **4i** appeared as a singlet at 3.81–3.82 ppm. In the <sup>13</sup>C-NMR spectra of compounds **4a–j**, the characteristics carbonyl carbons and benzylic carbons appeared at 197.77–198.57 ppm and 51.40–55.30 ppm, respectively. In addition, the  $\alpha$ -carbons were observed in the range of 63.95–67.98 ppm. In summary, all the newly synthesized compounds exhibited satisfactory spectral data consistent with the proposed structures. In addition, electron spray ionization mass spectra (ESI-MS) of **4a–j** showed a metastable ion peak as [M(<sup>79</sup>Br)+H]<sup>+</sup> (100 %) in the positive mode along with other isotopic peaks.

### Antibacterial activity

The *in vitro* antibacterial activities of the novel compounds **4a–j** were assayed against three Gram-positive bacteria *viz.* *S. aureus*, *B. subtilis* and *L. monocytogenes* and five Gram-negative bacteria, *viz.* *S. enteritidis*, *P. aeruginosa*, *E. aerogenes*, *S. typhimurium* and *E. coli*. The minimum inhibitory concentration

(*MIC* /  $\mu\text{g ml}^{-1}$ ) was determined by the serial dilution method<sup>15</sup> for all the compounds and compared with the controls (streptomycin and tetracycline). The *MIC* values of the tested compounds are presented in Table I, from which it can be seen that all the tetrabromo-bis-benzylcycloalkanone analogues (**4a–j**) showed antibacterial activity against both the Gram-positive and Gram-negative bacteria. Among the tested compounds, compound **4i** exhibited the highest activity against both Gram-positive and Gram-negative strains, followed by compounds **4c** and **4d**. The *MIC* values of compounds **4i**, **4c** and **4d** are almost comparable to those of the standard drugs used in the present study against all bacterial strains.

TABLE I. Antibacterial activity (*MIC* /  $\mu\text{g ml}^{-1}$ ) of compounds **4a–j**

Compound	<i>S. au-reus</i>	<i>B. sub-tillis</i>	<i>L. mono-cytogenes</i>	<i>S. enteri-tidis</i>	<i>P. aeru-ginosa</i>	<i>E. aero-genes</i>	<i>S. typhi-murium</i>	<i>E. coli</i>
<b>4a</b>	125	125	125	125	125	125	62.5	62.5
<b>4b</b>	62.5	62.5	31.2	62.5	125	62.5	62.5	125
<b>4c</b>	31.2	15.6	31.2	15.6	31.2	15.6	31.2	15.6
<b>4d</b>	31.2	15.6	32.2	15.6	31.2	15.6	31.2	31.2
<b>4e</b>	31.2	31.2	31.2	62.5	62.5	31.2	31.2	31.2
<b>4f</b>	62.5	125	62.5	125	62.5	62.5	125	125
<b>4g</b>	62.5	62.5	62.5	62.5	62.5	125	62.5	32.2
<b>4h</b>	31.2	62.5	62.5	62.5	62.5	62.5	31.2	31.2
<b>4i</b>	31.2	15.6	31.2	15.6	31.2	15.6	15.6	15.6
<b>4j</b>	62.5	62.5	31.2	31.2	62.5	31.2	31.2	31.2
Streptomycin	31.2	15.6	31.2	31.2	31.2	15.6	31.2	15.6
Tetracycline	15.6	15.6	31.2	15.6	31.2	15.6	15.6	15.6

Structure–activity relationships (SAR) may be explained briefly as follows: the ring size of cycloalkanones has no strong effect on the antibacterial activity, whereas the unsubstituted compounds (**4a** and **4f**) showed lower activity than the substituted compounds (**4b–d** and **4g–j**). Introduction of hydrophilic substituents (halogen, OMe) at the R<sub>2</sub> or R<sub>1</sub> position resulted in better activity than the hydrophobic substituent (CH<sub>3</sub>). Among the compounds containing halogen substitution at the phenyl ring, the chlorine analogue (**4c**) showed better antibacterial activity than the fluorine or bromine analogues (**4e**, **4h** and **4j**).

#### Antifungal activity

The newly synthesized novel **4a–j** were evaluated for their *in vitro* antifungal activities against five fungal strains, *i.e.*, *B. cinerea*, *R. solani*, *F. oxysporum*, *S. sclerotiorum* and *P. capsici* by disc diffusion methods. The inhibition zones of the synthesized compounds were measured at a dose of 200  $\mu\text{g disc}^{-1}$  and nystatin, a positive control, were evaluated at a dose of 30  $\mu\text{g disc}^{-1}$ . As presented in Table II, among the all tetrabromo-bis-benzylcycloalkanone derivatives (**4a–j**) tested, 5 compounds inhibited the growth of some fungal strains. In detail, compound **4i**

showed good to moderate activity against all the tested fungal strains, while compounds **4d** and **4j** exhibited moderate activity against *R. solani* and *F. oxysporum*. Compounds **4f** and **4h** demonstrated moderate activity against one bacterial strain only. Compounds **4a–c**, **4e** and **4g** showed no activity against all the tested fungal strains. Therefore, the minimum inhibitory concentrations (*MICs*) of compound only **4i** against *B. cinerea*, *R. solani*, *F. oxysporum*, *S. sclerotiorum*, and *P. capsici* were determined and found *MIC* values of 125, 31.2, 31.2, 125 and 250 µg ml<sup>-1</sup>, respectively, were found (Table III).

TABLE II. Antifungal profile of compounds **4a–j** in terms of the inhibition zone in mm (data are means ± SD for at least three experiments. Concentrations of compounds **4a–j** and netilmycin were 200 and 30 µg disc<sup>-1</sup>, respectively)

Compound	<i>B. cinerea</i>	<i>R. solani</i>	<i>F. oxysporum</i>	<i>S. sclerotiorum</i>	<i>P. capsici</i>
<b>4d</b>	—	08±1.1	10±1.1	—	—
<b>4f</b>	—	09±1.1	—	—	—
<b>4h</b>	—	—	07±1.1	—	—
<b>4i</b>	07±1.2	19±1.0	19±1.1	08±1.1	07±1.0
<b>4j</b>	—	11±1.1	11±1.2	—	—
Nystatin	23±1.1	25±1.2	25±1.1	27±1.1	33±1.0

TABLE III. Antifungal activity (*MIC* / µg ml<sup>-1</sup>) of compound **4i**

Compound	<i>B. cinerea</i>	<i>R. solani</i>	<i>F. oxysporum</i>	<i>S. sclerotiorum</i>	<i>P. capsici</i>
<b>4i</b>	125	31.2	31.2	125	250
Nystatin	15.6	15.6	15.6	31.2	30.2

### CONCLUSIONS

In this paper, an efficient synthesis of novel tetrabromo-bis(substituted benzyl)cycloalkanone derivatives and their antimicrobial activities against eight bacterial and five fungal strains were presented. All the tetrabromo-bis(substituted benzyl)cycloalkanone analogues showed potent antibacterial activity compared to their antifungal activity. Compounds **4i**, **4c** and **4d**, having a methoxy- or chloro-substituent on the *para* or *meta* position of the phenyl ring exhibited strong activity against all the tested bacterial strains. Hydrophilic substitution on the phenyl ring resulted in a better antibacterial activity than that of hydrophobic substitution. Among all the tested compounds, **4i** exhibited good antifungal activity against *R. solani* and *F. oxysporum*. The potential antimicrobial activity of compounds **4i**, **4c** and **4d** would be helpful in synthesis of a huge number of tetrabromo-bis(substituted benzyl)cycloalkanone analogues for extensive antimicrobial studies, which could be used to develop more suitable drug candidates.

### SUPPLEMENTARY MATERIAL

Analytical and spectral data of synthesized compounds are available electronically from <http://www.shd.org.rs/JSCS/>, or from the corresponding author on request.



## ИЗВОД

СИНТЕЗА И АНТИМИКРОБНА АКТИВНОСТ НОВИХ  
ТЕТРАБРОМ-БИС(СУПСТИТУИСАНИХ БЕНЗИЛ)ЦИКЛОАЛКАНОНАA. F. M. MOTIUR RAHMAN<sup>1</sup>, MOHAMMAD SAYED ALAM,<sup>2,3</sup> и ADNAN A. KADI<sup>1</sup><sup>1</sup>*Department of Pharmaceutical Chemistry, College of Pharmacy, King Saud University, Riyadh 11451, Saudi Arabia, <sup>2</sup>Division of Bioscience, Dongguk University, Geyonju 780-714, Republic of Korea и*<sup>3</sup>*Department of Chemistry, Jagannath Univeristy, Dhaka 1100, Bangladesh*

Синтетисана је серија нових тетрабром-бис(супституисаних бензил)циклоалканона, брзим и ефикасним поступком. Производи су добијени у високом приносу и охарактерисани су спектроскопским методама (ИЦ, NMR (<sup>1</sup>H-, <sup>13</sup>C-NMR, DEPT 135, DEPT 90)) и масеном спектрометријом. Испитана је *in vitro* антимикробна активност синтетисаних једињења према осам врста бактерија и 5 врста гљива. Тестирана једињења показују добру антибактеријску и антифунгальну активност. Једињења **4c**, **4d** and **4i** која садрже метокси- и хлор-супституенте у *пара* и *мета* положају на фенил групи имају вредности MIC које су близке вредностима које дају стандардни антибиотици стрептомицин и тетрациклин. Од свих испитиваних једињења, дериват **4i** показује добру до умерену активност према све четири врсте гљива.

(Примљено 8. априла 2011, ревидирано 6. јануара 2012)

## REFERENCES

1. C. Lee, *Int. J. Antimicrob. Agents* **32** (2008) S197
2. D. O'Hagen, H. S. Rzepa, *Chem. Commun.* (1997) 645
3. J. T. Welch, *Tetrahedron* **43** (1987) 3123
4. J. Mann, *Chem. Soc. Rev.* **16** (1987) 381
5. K. L. Kirk, *J. Fluorine Chem.* **127** (2006) 1013
6. T. P. Robinson, T. J. Ehlers, R. B. Hubbard, X. Bai, J. L. Arbiser, D. J. Goldsmith, J. P. Bowena, *Bioorg. Med. Chem. Lett.* **13** (2003) 115
7. T. P. Robinson, R. B. Hubbard, T. J. Ehlers, J. L. Arbiser, D. J. Goldsmith, J. P. Bowena, *Bioorg. Med. Chem.* **13** (2005) 4007
8. A. T. Dinkova-Kostova, C. Abeygunawardana, P. Talalay, *J. Med. Chem.* **41** (1998) 5287
9. J. R. Dimmock, M. P. Padmanilayam, G. A. Zello, K. H. Nienaber, T. M. Allen, C. L. Santos, E. De Clercq, J. Balzarini, E. K. Manavathu, J. P. Stables, *Eur. J. Med. Chem.* **38** (2003) 169
10. A. Modzelewska, C. Pettit, G. Achanta, N. E. Davidson, P. Huang, S. R. Khan, *Bioorg. Med. Chem.* **14** (2006) 3491
11. C. Piantadosi, I. H. Hall, J. L. Irvine, G. L. Carlson, *J. Med. Chem.* **16** (1973) 770
12. W. T. Hoeve, H. Wynberg, *J. Org. Chem.* **45** (1980) 2930
13. G. R. Desiraju, K. V. R. Kishan, *Indian J. Chem., B* **27** (1988), 953
14. A. F. M. M. Rahman, B. S. Jeong, D. H. Kim, J. K. Park, E. S. Lee, Y. Jahng, *Tetrahedron* **63** (2007) 2426
15. M. Chandrasekaran, V. Venkatesalu, *J. Ethnopharmacol.* **91** (2004) 105
16. M. E. Duru, A. Cakir, S. Kordali, H. Zengin, M. Harmandar, S. Izumi, T. Hirata, *Fitoterapia* **74** (2003) 170.





SUPPLEMENTARY MATERIAL TO  
**Synthesis and antimicrobial activity of novel  
tetrabromo-bis(substituted benzyl)cycloalkanones**

A. F. M. MOTIUR RAHMAN<sup>1\*</sup>, MOHAMMAD SAYED ALAM<sup>2,3\*\*</sup>  
and ADNAN A. KADI<sup>1</sup>

<sup>1</sup>Department of Pharmaceutical Chemistry, College of Pharmacy, King Saud University,  
Riyadh 11451, Saudi Arabia, <sup>2</sup>Division of Bioscience, Dongguk University,  
Geyonju 780–714, Republic of Korea and <sup>3</sup>Department of Chemistry,  
Jagannath University, Dhaka 1100, Bangladesh

J. Serb. Chem. Soc. 77 (6) (2012) 717–723

ANALYTICAL AND SPECTRAL DATA OF THE SYNTHESIZED COMPOUNDS

**2,5-Dibromo-2,5-bis(α-bromobenzyl)cyclopentanone (4a).** Yield: 418 mg, 70%; m.p.: 178–180 °C (lit. 175 °C<sup>1</sup>); IR (KBr, cm<sup>-1</sup>): 3245, 1664, 1213, 1025, 846; <sup>1</sup>H-NMR (250 MHz, CDCl<sub>3</sub>, δ / ppm): 7.53–7.50 (4H, m, Ar-H), 7.43–7.36 (6H, m, Ar-H), 5.57 (2H, s), 3.32 (2H, ABq, J<sub>AB</sub> = 13.3 Hz), 2.42 (2H, ABq, J<sub>AB</sub> = 13.2 Hz); <sup>13</sup>C-NMR (62.5 MHz, CDCl<sub>3</sub>, δ / ppm): 198.35, 137.35, 129.61, 129.03, 128.35, 67.42, 52.26, 31.67; ESI-MS (m/z): 579.8 [M(79Br)+H]<sup>+</sup>.

**2,5-Dibromo-2,5-bis(α-bromo-p-methylbenzyl)cyclopentanone (4b).** Yield: 462 mg, 76 %; m.p.: 184–185 °C; IR (KBr, cm<sup>-1</sup>): 3252, 1671, 1312, 1007, 820; <sup>1</sup>H-NMR (250 MHz, CDCl<sub>3</sub>, δ / ppm): 7.39 (4H, d, J = 8.1 Hz, Ar-H), 7.18 (4H, d, J = 7.9 Hz, Ar-H), 5.54 (2H, s), 3.31 (2H, ABq, J<sub>AB</sub> = 13.3 Hz), 2.42 (2H, ABq, J<sub>AB</sub> = 13.2 Hz), 2.37 (6H, s, 2×CH<sub>3</sub>); <sup>13</sup>C-NMR (62.5 MHz, CDCl<sub>3</sub>, δ / ppm): 198.50, 139.06, 134.48, 129.47, 129.08, 67.64, 52.36, 32.76, 21.26; ESI-MS (m/z): 607.5 [M(79Br)+H]<sup>+</sup>.

**2,5-Dibromo-2,5-bis(α-bromo-m-chlorobenzyl)cyclopentanone (4c).** Yield: 571 mg, 88 %); m.p.: 190–192 °C; IR (KBr, cm<sup>-1</sup>): 3271, 1665, 1200, 1142, 830; <sup>1</sup>H-NMR (250 MHz, CDCl<sub>3</sub>, δ / ppm): 7.50 (2H, m, Ar-H), 7.41–7.28 (6H, m, Ar-H), 5.49 (2H, s), 3.28 (2H, ABq, J<sub>AB</sub> = 13.3 Hz), 2.40 (2H, ABq, J<sub>AB</sub> = 13.0 Hz); <sup>13</sup>C-NMR (62.5 MHz, CDCl<sub>3</sub>, δ / ppm): 197.82, 139.18, 134.24, 129.63, 129.62, 129.30, 127.90, 66.78, 51.07, 31.58; ESI-MS (m/z): 648.0 [M(79Br)+H]<sup>+</sup>.

**2,5-Dibromo-2,5-bis(α-bromo-p-methoxybenzyl)cyclopentanone (4d).** Yield: 595 mg, 93 %; m.p. 170–172 °C; IR (KBr, cm<sup>-1</sup>): 3301, 1681, 1425, 986, 725; <sup>1</sup>H-NMR (250 MHz, CDCl<sub>3</sub>, δ / ppm): 7.43 (4H, d, J = 8.6 Hz, Ar-H), 6.89 (4H,

\*,\*\* Corresponding authors. E-mail: \*afmrahman@ksu.edu.sa; \*\*alam\_sms@yahoo.com

*d, J = 8.6 Hz, Ar–H), 5.55 (2H, s), 3.82 (6H, s, 2×OCH<sub>3</sub>), 3.30 (2H, ABq, J<sub>AB</sub> = 13.0 Hz), 2.41 (2H, ABq, J<sub>AB</sub> = 13.0 Hz); <sup>13</sup>C-NMR (62.5 MHz, CDCl<sub>3</sub>, δ / ppm): 198.57, 159.87, 130.83, 129.46, 113.68, 67.98, 55.31, 52.38, 31.73; ESI-MS (m/z): 640.0 [M(79Br)+H]<sup>+</sup>.*

**2,5-Dibromo-2,5-bis(α-bromo-p-fluorobenzyl)cyclopentanone (4e).** Yield: 542 mg, 85 %; m.p.: 205–207 °C; IR (KBr, cm<sup>-1</sup>): 3205, 1672, 1201, 1017, 825; <sup>1</sup>H-NMR (250 MHz, CDCl<sub>3</sub>, δ / ppm): 7.49 (4H, dd, J = 8.6, 5.2 Hz, Ar–H), 7.07 (4H, t, J = 8.6 Hz, Ar–H), 5.53 (2H, s), 3.28 (2H, ABq, J<sub>AB</sub> = 13.1 Hz), 2.37 (2H, ABq, J<sub>AB</sub> = 13.2 Hz); <sup>13</sup>C-NMR (62.5 MHz, CDCl<sub>3</sub>, δ / ppm): 198.10, 162.70 (J<sub>C-F</sub> = 247.8 Hz), 133.23 (J<sub>C-F</sub> = 3.6 Hz), 131.43 (J<sub>C-F</sub> = 8.4 Hz), 115.45 (J<sub>C-F</sub> = 21.8 Hz), 67.44, 51.40, 31.61; ESI-MS (m/z): 615.9 [M(79Br)+H]<sup>+</sup>.

**2,5-Dibromo-2,5-bis(α-bromobenzyl)cyclohexanone (4f).** Yield: 523 mg, 76 %; m.p.: 195–196 °C (lit. 193 °C<sup>15</sup>); IR (KBr, cm<sup>-1</sup>): 3201, 1672, 1313, 1102, 742; <sup>1</sup>H-NMR (250 MHz, CDCl<sub>3</sub>, δ / ppm): 7.54–7.50 (4H, m, Ar–H), 7.37–7.32 (6H, m, Ar–H), 6.03 (2H, s), 3.07 (2H, td, J = 14.8, 2.9 Hz), 2.46–2.32 (3H, m), 2.03–1.95 (1H, m); <sup>13</sup>C-NMR (62.5 MHz, CDCl<sub>3</sub>, δ / ppm): 198.13, 136.11, 131.14, 128.85, 127.75, 64.45, 55.30, 33.75, 16.83; ESI-MS (m/z): 593.9 [M(79Br)+H]<sup>+</sup>.

**2,5-Dibromo-2,5-bis(α-bromo-p-methylbenzyl)cyclohexanone (4g).** Yield: 412 mg, 79 %; m.p.: 187–189 °C; IR (KBr, cm<sup>-1</sup>): 3212, 1666, 1210, 1009, 841; <sup>1</sup>H-NMR (250 MHz, CDCl<sub>3</sub>, δ / ppm): 7.39 (4H, d, J = 8.0 Hz, Ar–H), 7.13 (4H, d, J = 7.9 Hz, Ar–H), 5.99 (2H, s), 3.04 (2H, td, J = 14.6, 2.8 Hz), 2.38–2.31 (3H, m), 2.34 (6H, s), 2.00–1.95 (1H, m); <sup>13</sup>C-NMR (62.5 MHz, CDCl<sub>3</sub>, δ / ppm): 198.20, 138.85, 133.24, 130.97, 128.48, 64.77, 55.30, 33.78, 21.19, 16.86; ESI-MS (m/z): 622.0 [M(79Br)+H]<sup>+</sup>.

**2,5-Dibromo-2,5-bis(α-bromo-p-fluorobenzyl)cyclohexanone (4h).** Yield: 555 mg, 88 %; m.p.: 155–158 °C; IR (KBr, cm<sup>-1</sup>): 3195, 1675, 1301, 955, 759; <sup>1</sup>H-NMR (250 MHz, CDCl<sub>3</sub>, δ / ppm): 7.52–7.35 (4H, dd, J = 8.4, 5.3 Hz, Ar–H), 7.03 (4H, t, J = 8.4 Hz, Ar–H), 5.99 (2H, s), 3.00 (2H, td, J = 12.3, 2.8 Hz), 2.40–2.26 (3H, m), 2.00–1.96, (1H, m); <sup>13</sup>C-NMR (62.5 MHz, CDCl<sub>3</sub>, δ / ppm): 197.92, 162.70 (J<sub>C-F</sub> = 247.6 Hz), 132.80 (J<sub>C-F</sub> = 82.5 Hz), 131.93 (J<sub>C-F</sub> = 3.4 Hz), 114.80 (J<sub>C-F</sub> = 21.6 Hz), 64.37, 54.33, 33.61, 16.74; ESI-MS (m/z): 629.9 [M(79Br)+H]<sup>+</sup>.

**2,5-Dibromo-2,5-bis(α-bromo-p-methoxybenzyl)cyclohexanone (4i).** Yield: 523 mg, 80 %; m.p. 170–172 °C; IR (KBr, cm<sup>-1</sup>): 3240, 1662, 1201, 980, 744; <sup>1</sup>H-NMR (250 MHz, CDCl<sub>3</sub>, δ / ppm): 7.45 (4H, d, J = 8.7 Hz, Ar–H), 6.86 (4H, dd, J = 8.8, 2.2 Hz, Ar–H), 5.99 (1H, s), 5.93 (1H, s) 3.81 (6H, s, 2×OCH<sub>3</sub>), 3.34–3.25 (1H, m), 3.02 (1H, t, J = 12.88 Hz), 2.39–2.31 (3H, m), 2.02–1.90 (1H, m); <sup>13</sup>C-NMR (62.5 MHz, CDCl<sub>3</sub>, δ / ppm): 198.19, 159.79, 159.76, 132.26, 128.25, 128.08, 113.13, 113.09, 66.72, 65.16, 55.30, 55.21, 53.90, 33.80, 16.89; ESI-MS (m/z): 654.0 [M(79Br)+H]<sup>+</sup>.

*2,5-Dibromo-2,5-bis( $\alpha$ -bromo-p-bromobenzyl)cyclohexanone (4j).* Yield: 638 mg, 85 %; m.p.: 210–212 °C; IR (KBr, cm<sup>−1</sup>): 3285, 1660, 1201, 955, 885; <sup>1</sup>H-NMR (250 MHz, CDCl<sub>3</sub>,  $\delta$  / ppm): 7.50 (4H, *d*, *J* = 8.5 Hz, Ar-H), 7.38 (4H, *d*, *J* = 8.6 Hz, Ar-H), 5.95 (2H, *s*), 2.99 (2H, *t*, *J* = 14.6 Hz), 2.40–2.14 (3H, *m*), 2.02–1.96 (1H, *dd*, *J* = 14.0, 3.0 Hz); <sup>13</sup>C-NMR (62.5 MHz, CDCl<sub>3</sub>,  $\delta$  / ppm): 197.72, 135.11, 132.67, 130.99, 123.11, 63.95, 54.32, 33.65, 16.73; ESI-MS (*m/z*): 751.8 [M(79Br)+H]<sup>+</sup>.

## REFERENCES

1. P.-Y. Yeh, *Bull. Chem. Soc. Jpn.* **27** (1954) 60.



## Synthesis and *in vitro* anti-breast cancer activity of some novel 1,5-benzothiazepine derivatives

K. L. AMETA\*, NITU S. RATHORE and BIRESH KUMAR

Department of Chemistry, FASC, Mody Institute of Technology and Science,  
Deemed University, Lakshmangarh, Rajasthan-332311, India

(Received 15 July, revised 19 December 2011)

**Abstract:** The title compounds **3a–j**, substituted 1,5-benzothiazepines, were synthesized by the condensation of variously substituted chalcones **1** and 2-aminothiophenol **2** via conventional as well as non-conventional inorganic solid support microwave irradiation methods. The non-conventional protocol offers several advantages, such as simple procedure, fast reaction rate, mild reaction conditions and improved yields, compared to conventional methods. The structures of the products **3a–j** were established by elemental analysis, FTIR, <sup>1</sup>H-NMR, <sup>13</sup>C-NMR and mass spectroscopic studies. The synthesized compounds were also evaluated for their cytotoxicity against the human breast cancer cell line MDA-MB-435, with some exhibiting *in vitro* anti-breast cancer activity.

**Keywords:** 1,5-benzothiazepines; 2-aminothiophenol; chalcones; anti-breast cancer activity.

### INTRODUCTION

Disease poses a major threat to human beings and scientists are fighting to find solutions in the form of various medications. When the era of synthetic drugs began, it opened thousand doors for the development of various synthetic molecules with potential action. Chalcones are the well known intermediates for the synthesis of various differently sized bioactive heterocycles, such as isoxazoles, pyrimidines, pyrazoles, etc., which have been reported to possess various biological activities, such as antimicrobial,<sup>1,2</sup> anti-inflammatory,<sup>3</sup> antimalarial,<sup>4</sup> antioxidant<sup>5</sup> and antitubercular.<sup>6</sup>

Among these chalcone-derived heterocycles, benzothiazepines are well known important nitrogen and sulphur containing compounds that possess a broad spectrum of biological activities, such as antimicrobial,<sup>7,8</sup> anti-convulsant,<sup>9</sup> anti-HIV,<sup>10</sup> anti-cytotoxic,<sup>11</sup> anticancer,<sup>12,13</sup> DPPH free radical scavenger<sup>14</sup> and inhibition of cholinesterases, ureases and  $\alpha$ -glycosidases. Due to biological acti-

\*Corresponding author. E-mail: klameta77@yahoo.co.in  
doi: 10.2298/JSC110715219A

vities, various conventional<sup>15–21</sup> and non-conventional<sup>22–24</sup> approaches have been developed for the synthesis of 1,5-benzothiazepines derivatives.

Cancer is one of the most dangerous, fast propagating diseases of the present century with quite high mortality rates even in developed countries. The situation is even worse in undeveloped countries due to a lack of knowledge, poverty and the non-availability of quality drugs.<sup>25</sup>

As part of our continuing research in the development of new bioactive heterocycles containing nitrogen and sulphur atoms, simple and convenient methods for the transformation of chalcones into 1,5-benzothiazepines by conventional and non-conventional methods are described herein. The non-conventional approaches were based on the observation that organic solvents in classical procedures are used in much larger quantities than the solutes they carry. Furthermore, the employment of solid supports in conjugation with microwaves<sup>26–30</sup> leads to high yields, remarkable reaction rate enhancements, and high catalytic activities with the optimum utilisation of energy.

The anti-breast cancer activity of the synthesised compounds was also investigated.

## EXPERIMENTAL

### *Materials, method and instrumentation*

All the chemicals were of AR grade and were obtained from Sigma–Aldrich and Merck. Melting points (m.p.) were determined in open capillaries on a Veego (VMP-PM) melting point apparatus and are uncorrected. The microwave-assisted reactions were realised using a microwave synthesizer model CATA-R (Catalyst Systems, Pune, India), operating at 700 W, generating 2450 MHz frequency. The purity of the compounds was routinely checked by thin layer chromatography (TLC) with silica gel-G (Merck). The instruments used for obtaining the spectroscopic data were: IR – FTIR spectrophotometer Bruker Alpha-Zn-Se; <sup>1</sup>H-NMR ( $\text{CDCl}_3$ , 500 MHz) and <sup>13</sup>C-NMR ( $\text{CDCl}_3$ , 125 MHz), FT-NMR spectrometer Bruker AV III. The elemental analysis was realised on a Carlo Erba 1108 analyzer and the obtained values were within the  $\pm 0.5\%$  of the theoretical values. Column chromatography was performed on silica gel (Merck, 60–120 mesh).

### *General procedure for the preparing of 1,5-benzothiazepines 3a–j*

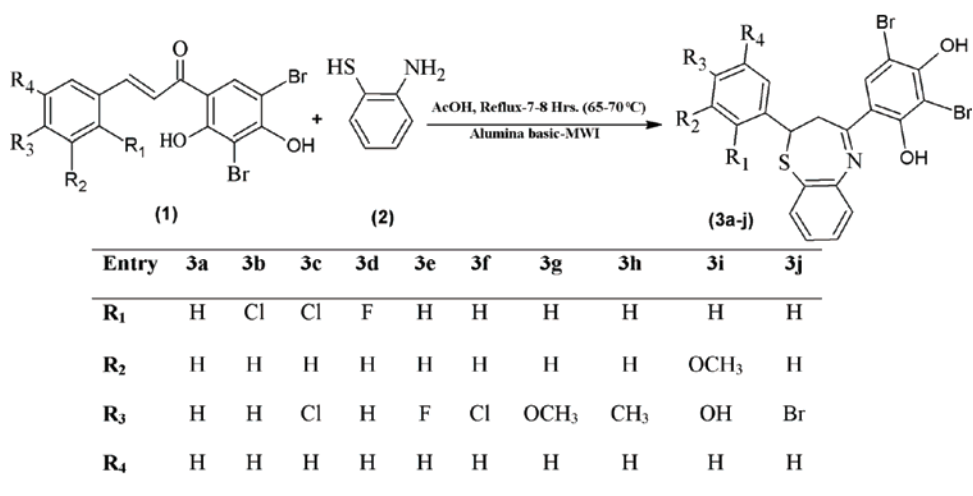
Condensation of the required chalcone (**1**) and 2-aminothiophenol (**2**) afforded the desired products **3a–j** in good yield, as shown in Scheme 1.

*Conventional solution phase method.* Compound **1** (0.010 mol) was dissolved in the minimum quantity of ethanol. To this, 2-aminothiophenol **2** (0.010 mol) was added and the resulting reaction mixture was refluxed for 3 h at 60–70 °C. Then, the mixture was acidified with 5–6 drops of glacial acetic acid and heating was continued for a further 4–5 h. After cooling, the content was poured onto crushed ice. The mixture was filtered and the solid was purified by recrystallization from methanol to afford compound **3a–j**.

*Non-conventional solid phase method.* Compound **1** (0.010 mol) was dissolved in the minimum quantity of DMF. To this, 2-aminothiophenol **2** (0.010 mol) and different inorganic solid supports (4.0 g) was added. The resulting mixture was uniformly mixed with a glass rod and air dried to remove the solvent. The absorbed material was irradiated inside the micro-

wave synthesizer for a specific time at medium power level (700 W). After completion of reaction (monitored by TLC), the reaction mixture was cooled to room temperature and the product was extracted with methanol ( $2 \times 20$  mL). Removal of the solvent and subsequent recrystallization with methanol resulted in analytical samples of **3a–j**. For the biological evaluation, the experimental drugs were solubilised in DMF solvent at 400-fold the desired final maximum test concentration and stored frozen prior to use.

Data of synthesized compounds are given in Supplementary material.



Scheme 1. Preparation route of novel substituted 1,5-benzothiazepines (**3a–j**) from variously substituted chalcones (**1**) and 2-aminothiophenol (**2**) *via* conventional and non-conventional methods. The conventional method involved the 7–8 h reflux whereas the non-conventional method involved 5–7 min under microwave irradiation.

#### Biological evaluation

*Protocol for in vitro anti-cancer screening.* Human tumour breast cancer cell line (MDA-MB-435) was used in this study. The cytotoxic activity was measured *in vitro* for the newly synthesized compounds using the sulforhodamine B stain (SRB) assay method.<sup>31,32</sup> The cell lines were grown in RPMI 1640 medium containing 10 % foetal bovine serum and 2 mM L-glutamine. For the present screening experiment, cells were inoculated into 96-well microtiter plates. For the present screening experiment, cells were inoculated into 96 well microtiter plates in 90  $\mu$ L at plating densities according to the SRB assay method. After cell inoculation, the microtiter plates were incubated at 37 °C, 5 % CO<sub>2</sub>, 95 % air and 100 % relative humidity for 24 h prior to the addition of the experimental drugs. After 24 h, one plate of the cell line was fixed *in situ* with trichloroacetic acid TCA, to represent a measurement of the cell population for the cell line at the time of drug addition ( $T_z$ ). At the time of drug addition, an aliquot of frozen concentrate was thawed and diluted to 10 times the desired final maximum test concentration with complete medium containing test compound at a concentration of 10<sup>-3</sup> M. Additional three 10-fold serial dilutions were made to provide a total of four drug concentrations plus control. Aliquots of 10  $\mu$ L of these different drug dilutions were added to the appropriate microtiter wells already containing 90  $\mu$ L of medium, resulting in the required final drug concentrations. Different concentrations of the compound under test (10<sup>-7</sup>, 10<sup>-6</sup>, 10<sup>-5</sup> and

$10^{-4}$  M) were added to the cell monolayer. Triplicate wells were prepared for each individual concentration.

After compound addition, end point measurement was performed using the "Elisa" test under standard conditions for taking the absorbance at particular wavelength (690 nm reference wavelength). The percent growth was calculated on a plate-by-plate basis for the test wells relative to the control wells. The percent growth was expressed as the ratio of the average absorbance of the test well to the average absorbance of the control wells times 100. Using the six absorbance measurements (time zero ( $T_0$ ), control growth ( $C$ ), and test growth in the presence of drug at the four concentration levels ( $T_i$ )), the percentage growth was calculated at each of the drug concentration levels. Percentage growth inhibition was calculated as:  $100((T_i-T_0)/(C-T_0))$  for concentrations for which  $T_i \geq T_0$ , i.e.,  $(T_i-T_0)$  is positive or zero, or  $100 [(T_i-T_0)/T_0]$  for concentrations for which  $T_i < T_0$ , i.e.,  $(T_i-T_0)$  is negative.

The dose response parameters were calculated for each test compound. The growth inhibition of 50 % ( $GI_{50}$ ) was calculated from  $100((T_i-T_0)/(C-T_0)) = 50$ , which is the drug concentration resulting in a 50 % reduction in the net protein increase (as measured by SRB staining) compared to the control cells during the drug incubation.

## RESULTS AND DISCUSSION

The aim of the present work was to design and synthesize some new 1,5-benzothiazepine derivatives carrying biologically active thiazepine moieties that were expected to have anti-breast cancer activity. Substituted chalcones **1** were reacted with 2-aminothiophenol **2** to give 1,5-benzothiazepine derivatives **3a–j**. The characterization data of the synthesized compounds are tabulated in Table I. The structures of the compounds **3a–j** were determined on the basis of analytical and spectroscopic data (given in the Supplementary material to this paper). Thus, the IR spectra showed bands at around 1606 (C=N), 665 (C–S) and 862 (C–Br). The  $^1\text{H-NMR}$  spectra revealed the presence of a doublet at around  $\delta$  3.32 ppm, corresponding to the  $\text{CH}_2$  group, and a triplet at around  $\delta$  4.98 ppm, corresponding to the CH group.

In view of the immense utility of eco-friendly synthetic approaches, improved syntheses of the 1,5-benzothiazepines were performed under microwave

TABLE I. Characterization data of the synthesized compounds

Entry	Molecular formula	M.p., °C	Reaction time		Yield, %	
			MW, min	Conventional, h	MW	Conventional
<b>3a</b>	$\text{C}_{21}\text{H}_{15}\text{Br}_2\text{NO}_2\text{S}$	80–81	5.0	6.0	78.0	64.0
<b>3b</b>	$\text{C}_{21}\text{H}_{14}\text{Br}_2\text{ClNO}_2\text{S}$	82–83	6.0	6.5	82.0	69.0
<b>3c</b>	$\text{C}_{21}\text{H}_{13}\text{Br}_2\text{Cl}_2\text{NO}_2\text{S}$	89–90	5.5	7.0	84.0	69.0
<b>3d</b>	$\text{C}_{21}\text{H}_{14}\text{Br}_2\text{FNO}_2\text{S}$	81–82	5.0	7.0	83.0	71.0
<b>3e</b>	$\text{C}_{21}\text{H}_{14}\text{Br}_2\text{FNO}_2\text{S}$	87–88	6.0	5.0	86.0	71.0
<b>3f</b>	$\text{C}_{21}\text{H}_{14}\text{Br}_2\text{ClNO}_2\text{S}$	90–91	6.0	6.0	80.0	69.0
<b>3g</b>	$\text{C}_{22}\text{H}_{17}\text{Br}_2\text{NO}_3\text{S}$	82–83	5.0	6.5	89.0	68.0
<b>3h</b>	$\text{C}_{22}\text{H}_{17}\text{Br}_2\text{NO}_2\text{S}$	85–86	7.0	7.5	81.0	68.0
<b>3i</b>	$\text{C}_{22}\text{H}_{17}\text{Br}_2\text{NO}_4\text{S}$	78–79	7.0	6.0	79.0	68.0
<b>3j</b>	$\text{C}_{21}\text{H}_{14}\text{Br}_3\text{NO}_2\text{S}$	93–94	6.0	7.5	90.0	72.0



irradiation. In this context, the suitability of different solid supports, *i.e.*, acidic alumina, basic alumina, neutral alumina, montmorillonite K 10 and  $K_2CO_3$ , were examined. From the results given in Table II, it is clear that basic alumina was the most adaptable and simplest catalyst and gave good yields in the synthesis of the 1,5-benzothiazepines **3a–j**. Finally in order to evaluate the use of microwave irradiation, the 1,5-benzothiazepines were also synthesised under conventional conditions. The yields and reaction times of the two preparation methods are compared in Table I.

TABLE II. Comparative study for the synthesis of **3a–j** by non-conventional MW using different solid supports

Exp. No.	Medium	MW Power, W	Time, min	Temp., °C	Yield, %
1	Alumina acidic	700	9–10	83	57
2	Alumina basic	700	5–7	92	80
3	Alumina neutral	700	11–12	81	64
4	Montmorillonite K 10	700	9–11	80	73
5	Potassium carbonate	700	12–13	72	69

The newly synthesized compounds were evaluated for their *in vitro* cytotoxicity against a human breast cancer cell line (MDA-MB-435) with adriamycin (ADR) as the reference drug. The relationship between control in % growth and molar drug concentration was plotted to obtain the control growth of the breast cancer cell line (MDA-MB-435). The response parameter calculated was the  $GI_{50}$  value, which corresponds to the concentration required for a 50 % inhibition of cell viability (Table III).

TABLE III. *In vitro* anticancer screening of the synthesised compounds against human breast cell line (MDA-MB-435); growth relative to the control (%), each value is the mean  $\pm SD$  of three experiments

Compound	Molar drug concentration, mol dm <sup>-3</sup>				$GI_{50}$ / $\mu M$
	10 <sup>-7</sup>	10 <sup>-6</sup>	10 <sup>-5</sup>	10 <sup>-4</sup>	
<b>3a</b>	100.00 $\pm$ 0.00	100.00 $\pm$ 0.00	37.54 $\pm$ 4.95	–41.23 $\pm$ 16.63	28.0
<b>3b</b>	99.66 $\pm$ 0.39	97.44 $\pm$ 2.60	68.84 $\pm$ 6.13	–46.19 $\pm$ 4.42	32.2
<b>3c</b>	100.00 $\pm$ 0.00	96.72 $\pm$ 3.18	33.62 $\pm$ 3.67	–26.90 $\pm$ 5.27	29.5
<b>3d</b>	90.95 $\pm$ 8.00	99.99 $\pm$ 0.01	88.24 $\pm$ 8.34	80.39 $\pm$ 7.35	>100
<b>3e</b>	97.64 $\pm$ 2.68	95.62 $\pm$ 4.60	77.61 $\pm$ 7.35	–42.53 $\pm$ 4.99	33.9
<b>3f</b>	99.88 $\pm$ 0.20	98.75 $\pm$ 2.01	79.60 $\pm$ 4.71	–38.30 $\pm$ 6.27	36.1
<b>3g</b>	99.43 $\pm$ 1.00	98.97 $\pm$ 1.96	66.40 $\pm$ 3.14	–33.50 $\pm$ 6.83	34.8
<b>3h</b>	98.58 $\pm$ 2.45	96.74 $\pm$ 3.26	84.74 $\pm$ 7.44	–41.03 $\pm$ 10.39	35.7
<b>3i</b>	95.26 $\pm$ 4.56	91.80 $\pm$ 7.10	78.39 $\pm$ 3.18	–47.86 $\pm$ 5.12	31.9
<b>3j</b>	100.00 $\pm$ 0.00	100.00 $\pm$ 0.00	95.98 $\pm$ 3.56	–15.75 $\pm$ 18.88	45.7
ADR	–22.63 $\pm$ 8.93	–39.32 $\pm$ 16.81	–48.07 $\pm$ 19.26	–57.02 $\pm$ 13.25	<0.1



## CONCLUSIONS

By comparing different inorganic solid supports, it was concluded that basic alumina was the most suitable support for the synthesis of 1,5-benzothiazepines via a non-conventional method, giving the products in good yields. It was observed from the obtained results that most of the tested compounds showed some anti-breast cancer activity, as compared to the reference drug. These preliminary results of biologically screening of the tested compounds give an indication of the possible importance of the thiazepine moiety in anti-breast cancer compounds and give an encouraging framework in this field that may lead to the discovery of potent anticancer agents.

## SUPPLEMENTARY MATERIAL

Analytical and spectral data of synthesized compounds are available electronically from <http://www.shd.org.rs/JSCS/>, or from the corresponding author on request.

*Acknowledgements.* The authors are thankful to Prof. B. L. Verma, retd. professor of chemistry, M. L. S. University Udaipur and the Dean, FASC, MITS University, India, for their constant encouragement during this work. Authors are also thankful to the Head, Sophisticated Analytical Instrument Facility, Indian Institute of Technology, Madras, India, for spectral analysis, and the Director, Tata Memorial-ACTRC (The Advanced Centre for Treatment, Research and Education in Cancer) Mumbai, India, for anti-breast cancer activity determinations.

И З В О Д

**СИНТЕЗА НОВИХ ДЕРИВАТА 1,5-БЕНЗОТИАЗЕПИНА И ЊИХОВА  
*IN VITRO* АКТИВНОСТ ПРЕМА КАНЦЕРУ ДОЈКЕ**

K. L. AMETA, NITU S. RATHORE и BIRESH KUMAR

*Department of Chemistry, FASC, Mody Institute of Technology and Science, Deemed University,  
Lakshmangarh, Rajasthan-332311, India*

Супституисани деривати 1,5-бензотиазепина (**3a–j**) синтетисани су реакцијом кондензације супституисаних халкона (**1**) и 2-аминофенола (**2**) класичним и новим поступцима под условима микроталасног озрачивања. Нова метода има неколико предности у поређењу са класичном, као што су једноставнији поступак, краће реакционо време, блажи реакциони услови, побољшан принос. Структуре производа **3a–j** утврђене су на основу елементалне анализе FT-ИЦ,  $^1\text{H}$ -NMR и  $^{13}\text{C}$ -NMR спектроскопије и масене спектрометрије. Испитана је цитотоксична активност синтетисаних једињења према ћелијској линији канцера дојке MDA-MB-435.

(Примљено 15. јула, ревидирано 19. децембра 2011)

## REFERENCES

1. P. M. Sivakumar, S. Ganesan, P. Veluchamy, M. Doble, *Chem. Biol. Drug Des.* **76** (2010) 407
2. A. R. Trivedi, D. K. Dodiya, N. R. Ravat, V. H. Shah, *Arkivoc* **XI** (2008) 131
3. F. Herencia, M. L. Ferrandiz, A. Ubeda, J. N. Dominguez, J. E. Charris, G. M. Lobo, M. J. Alcaraz, *Bioorg. Med. Chem. Lett.* **8** (1998) 1169
4. X. Wu, P. Wilairat, M. N. Go, *Bioorg. Med. Chem. Lett.* **12** (2002) 2299

5. J. H. Cheng, C. F. Hung, S. C. Yang, J. P. Wang, S. J. Won, C. H. Lin, *Bioorg. Med. Chem.* **16** (2008) 7270
6. Y. M. Lin, Y. Zhou, M. T. Flavin, L. M. Zhou, W. Nie, F. C. Chen, *Bioorg. Med. Chem.* **10** (2008) 2795
7. S. Pant, P. Sharma, A. Sharma, R. Mishra, U. C. Pant, *J. Indian Chem. Soc.* **85** (2008) 406
8. P. Zhang, L. Z. Wang, H. S. Wu, J. M. Lan, Y. Li, Y. X. Wang, *Chin. Chem. Lett.* **20** (2009) 660
9. J. G. De. Sarro, A. Chimirri, A. De. Sarro, *Eur. J. Med. Chem.* **30** (1995) 925
10. G. Grandolini, L. Perioli, V. Ambrogi, *Eur. J. Med. Chem.* **34** (1999) 701
11. A. Garofalo, G. Balconi, M. Botta, F. Corelli, M. D. Incalci, G. Frabizi, I. Fiorini, D. Lamba, V. Nacci, *Eur. J. Med. Chem.* **28** (1993) 213
12. A. K. Sharma, G. Singh, A. K. Yadav, L. Prakash, *Molecules* **2** (1997) 129
13. P. Lawerence, J. Tordibano, M. J. Miller, *Org. Lett.* **11** (2009) 1575
14. F. Ansari, S. Umbreen, L. Hussain, T. Makhboor, S. Nawas, M. A. Lodhi, S. N. Khan, F. Shaheen, M. I. Choudhary, A. U. Rahman, *Chem. Biodiversity* **2** (2005) 487
15. D. S. Ghotekar, R. S. Joshi, P. G. Mandhane, S. S. Bhagat, C. H. Gill, *Indian J. Chem., B* **49** (2010) 1267
16. A. Levai, *J. Heterocycl. Chem.* **37** (2000) 199
17. A. Levai, A. Kiss-Szikszai, *Arkivoc* **I** (2008) 65
18. G. L. Khatik, R. Kumar, A. K. Chakraborti, *Synthesis* **4** (2007) 541
19. G. L. Khatik, G. Sharma, R. Kumar, A. K. Chakraborti, *Tetrahedron* **63** (2007) 1200
20. G. Sharma, R. Kumar, A. K. Chakraborti, *Tetrahedron Lett.* **49** (2008) 4269
21. G. Sharma, R. Kumar, A. K. Chakraborti, *Tetrahedron Lett.* **49** (2008) 4272
22. V. M. Patel, K. R. Desai, *Indian J. Chem., B* **43** (2004) 199
23. C. B. W. Phippen, C. S. P. McErlean, *Tetrahedron Lett.* **52** (2011) 1490
24. K. G. Desai, K. R. Desai, *Indian J. Chem., B* **46** (2007) 1179
25. M. E. Wolff, Burger Medicinal Chemistry and Drug Discovery, 5<sup>th</sup> ed., Wiley, New York 1991, p. 611
26. U. S. Gahlot, S. S. Rao, S. S. Dulawat, K. L. Ameta, B. L. Verma, *Afinidad* **60** (2003) 558
27. R. S. Varma, *Green Chem.* **1** (1990) 43
28. K. L. Ameta, B. Kumar, N. S. Rathore, *E-J. Chem.* **8** (2011) 665
29. K. L. Ameta, N. S. Rathore, B. Kumar, *An. Univ. Bucuresti Chimie* **20** (2011) 15
30. K. L. Ameta, B. L. Verma, *J. Indian Chem. Soc.* **79** (2002) 840
31. Michael R. Boyd, The NCI *in vitro* anticancer drug discovery screen. Concept, implementation and operation, 1985–1995, [http://home.ncicrf.gov/mtdp/catalog/full\\_text/paper309/Paper309.pdf](http://home.ncicrf.gov/mtdp/catalog/full_text/paper309/Paper309.pdf) (accessed june 2012)
32. V. Vichai, K. Kirtikar, *Nat. Protoc.* **1** (2006) 1112.







SUPPLEMENTARY MATERIAL TO  
**Synthesis and *in vitro* anti-breast cancer activity of  
some novel 1,5-benzothiazepine derivatives**

K. L. AMETA\*, NITU S. RATHORE and BIRESH KUMAR

Department of Chemistry, FASC, Mody Institute of Technology and Science  
(Deemed University) Lakshmangarh, Rajasthan-332311, India

J. Serb. Chem. Soc. 77 (6) (2012) 725–731

ANALYTICAL AND SPECTRAL DATA OF THE NEWLY SYNTHESIZED COMPOUNDS

**2,4-Dibromo-6-(2-phenyl-2,3-dihydro-1,5-benzothiazepin-4-yl)benzene-1,3-diol (3a).** Yield: 78 %; m.p.: 80–81 °C; Anal. Calcd. for C<sub>21</sub>H<sub>15</sub>Br<sub>2</sub>NO<sub>2</sub>S (FW 504.80): C, 49.92; H, 2.97; O, 6.34; N, 2.77 %. Found: C, 49.86; H, 2.92; O, 6.40; N, 2.82 %; IR (KBr, cm<sup>-1</sup>): 3372 (O–H stretching), 3289 (aliphatic C–H stretching), 3059–3008 (aromatic C–H stretching), 1606 (C=N), 1575 (C=C), 862 (C–Br), 666 (C–S); <sup>1</sup>H-NMR (500 MHz, CDCl<sub>3</sub>, δ / ppm): 9.2–8.7 (2H, *brs*, aromatic-OH), 7.86 (1H, *s*, aromatic), 7.56–7.10 (9H, *m*, aromatic), 4.9 (1H, *t*, *J* = 11.2 Hz, CH), 3.35 (2H, *d*, *J* = 12.2 Hz, CH<sub>2</sub>); <sup>13</sup>C-NMR (125 MHz, CDCl<sub>3</sub>, δ / ppm): 162.52 (C=N), 158.59 (C–OH), 155.42 (C’–OH), 140.62, 131.49, 129.62, 128.57, 126.50, 116.99 (aromatic-C), 140.54 (C–S), 108.81 (C’–Br), 94.60 (C–Br), 55.37 (CH<sub>2</sub>), 52.63 (CH); MS (*m/z*): 506.80 [M+2+H]<sup>+</sup>.

**2,4-Dibromo-6-[2-(2-chlorophenyl)-2,3-dihydro-1,5-benzothiazepin-4-yl]benzene-1,3-diol (3b).** Yield: 82 %; m.p.: 82–83 °C. Anal. Calcd. for C<sub>21</sub>H<sub>14</sub>Br<sub>2</sub>ClNO<sub>2</sub>S (FW 539.30): C, 46.73; H, 2.60; O, 5.94; N, 2.60 %. Found: C, 46.80; H, 2.67; O, 5.90; N, 2.53 %; IR (KBr, cm<sup>-1</sup>): 3378 (O–H stretching), 3298 (aliphatic C–H stretching), 3061–3018 (aromatic C–H stretching), 1629 (C=N), 1571 (C=C), 862 (C–Br), 753 (C–Cl stretching of chlorine), 666 (C–S); <sup>1</sup>H-NMR (500 MHz, CDCl<sub>3</sub>, δ / ppm): 9.5–8.4 (2H, *brs*, aromatic-OH), 7.86 (1H, *s*, aromatic), 7.45–7.15 (8H, *m*, aromatic), 4.98 (1H, *t*, *J* = 11.1 Hz, CH), 3.54 (2H, *d*, *J* = 12.2 Hz, CH<sub>2</sub>); <sup>13</sup>C-NMR (125 MHz, CDCl<sub>3</sub>, δ / ppm): 165.50 (C=N), 158.53 (C–OH), 154.52 (C’–OH), 140.44 (C–S), 139.51, 131.49, 129.93, 128.07, 127.85, 126.50, 116.99 (aromatic-C), 131.48 (C–Cl), 107.80 (C’–Br), 94.51 (C–Br), 53.63 (CH<sub>2</sub>), 49.39 (CH); MS (*m/z*): 541.30 [M+2+H]<sup>+</sup>.

\*Corresponding author. E-mail: klameta77@yahoo.co.in

**2,4-Dibromo-6-[2-(2,4-dichlorophenyl)-2,3-dihydro-1,5-benzothiazepin-4-yl]benzene-1,3-diol (3c).** Yield: 84 %; m.p.: 89–90 °C. Anal. Calcd. for C<sub>21</sub>H<sub>13</sub>Br<sub>2</sub>Cl<sub>2</sub>NO<sub>2</sub>S (FW 573.80): C, 43.92; H, 2.26; O, 5.58; N, 2.44 %. Found: C, 43.86; H, 2.21; O, 5.54; N, 2.50 %. IR (KBr, cm<sup>-1</sup>): 3370 (O–H stretching), 3288 (aliphatic C–H stretching), 3060 (aromatic C–H stretching), 2830 (OCH<sub>3</sub>), 848–825 (C–Cl stretching of chlorine), 1606 (C=N), 1564 (C=C), 862 (C–Br), 665 (C–S); <sup>1</sup>H-NMR (500 MHz, CDCl<sub>3</sub>, δ / ppm): 9.6–8.53 (2H, *brs*, aromatic–OH), 7.86 (1H, *s*, aromatic), 7.50–7.16 (7H, *m*, aromatic), 4.97 (1H, *t*, *J* = 11.2 Hz, CH), 3.46 (2H, *d*, *J* = 12.3 Hz, CH<sub>2</sub>); <sup>13</sup>C-NMR (125 MHz, CDCl<sub>3</sub>, δ / ppm): 166.43 (C=N), 159.76 (C–OH), 156.26 (C’–OH), 139.63 (C–S), 133.66, 131.69, 129.11, 128.07, 127.75, 126.50 (aromatic-C), 132.71 (C–Cl), 109.38 (C’–Br), 95.31 (C–Br), 54.46 (CH<sub>2</sub>), 50.35 (CH); MS (*m/z*): 575.80 [M+2+H]<sup>+</sup>.

**2,4-Dibromo-6-[2-(2-fluorophenyl)-2,3-dihydro-1,5-benzothiazepin-4-yl]benzene-1,3-diol (3d).** Yield: 83 %; m.p.: 81–82 °C. Anal. Calcd. for C<sub>21</sub>H<sub>14</sub>Br<sub>2</sub>FNO<sub>2</sub>S (FW 522.80): C, 48.20; H, 2.68; O, 6.12; N, 2.68 %. Found: C, 48.27; H, 2.61; O, 6.06; N, 2.72 %. IR (KBr, cm<sup>-1</sup>): 3368 (O–H stretching), 3284 (aliphatic C–H stretching), 3056–3005 (aromatic C–H stretching), 1605 (C=N), 1581 (C=C), 1244 (C–F stretching), 862 (C–Br), 660 (C–S); <sup>1</sup>H-NMR (500 MHz, CDCl<sub>3</sub>, δ / ppm): 9.8–8.54 (2H, *brs*, aromatic–OH), 7.82 (1H, *s*, aromatic), 7.30–6.85 (8H, *m*, aromatic), 5.01 (1H, *t*, *J* = 11.1 Hz, CH), 3.45 (2H, *d*, *J* = 12.2 Hz, CH<sub>2</sub>); <sup>13</sup>C-NMR (125 MHz, CDCl<sub>3</sub>, δ / ppm): 166.78 (C=N), 150.56 (C–OH), 148.66 (C’–OH), 138.93 (C–S), 136.66, 132.02, 130.98, 128.77, 125.92, 116.74, 115.63 (aromatic-C), 108.08 (C’–Br), 95.35 (C–Br), 55.51 (CH<sub>2</sub>), 53.71 (CH); MS (*m/z*): 524.80 [M+2+H]<sup>+</sup>.

**2,4-Dibromo-6-[2-(4-fluorophenyl)-2,3-dihydro-1,5-benzothiazepin-4-yl]benzene-1,3-diol (3e).** Yield: 86 %; m.p.: 87–88 °C. Anal. Calcd. for C<sub>21</sub>H<sub>14</sub>Br<sub>2</sub>FNO<sub>2</sub>S (FW 522.80): C, 48.21; H, 2.68; O, 6.12; N, 2.68 %. Found: C, 48.16; H, 2.75; O, 6.18; N, 2.61 %. IR (KBr, cm<sup>-1</sup>): 3368 (O–H stretching), 3284 (aliphatic C–H stretching), 3058–3005 (aromatic C–H stretching), 1605 (C=N), 1581 (C=C), 1244 (C–F stretching), 862 (C–Br), 660 (C–S); <sup>1</sup>H-NMR (500 MHz, CDCl<sub>3</sub>, δ / ppm): 9.6–8.42 (2H, *brs*, aromatic–OH), 7.86 (1H, *s*, aromatic), 7.39–6.85 (8H, *m*, aromatic), 4.98 (1H, *t*, *J* = 11.3 Hz, CH), 3.25 (2H, *d*, *J* = 12.1 Hz, CH<sub>2</sub>); <sup>13</sup>C-NMR (125 MHz, CDCl<sub>3</sub>, δ / ppm): 165.93 (C=N), 162.42 (C–F), 158.56 (C–OH), 157.79 (C’–OH), 139.57 (C–S), 136.56, 132.42, 129.53, 128.77, 125.98, 117.98, 116.99 (aromatic-C), 108.98 (C’–Br), 96.32 (C–Br), 54.52 (CH<sub>2</sub>), 51.29 (CH); MS (*m/z*): 524.80 [M+2+H]<sup>+</sup>.

**2,4-Dibromo-6-[2-(4-chlorophenyl)-2,3-dihydro-1,5-benzothiazepin-4-yl]benzene-1,3-diol (3f).** Yield: 80 %; m.p.: 90–91 °C. Anal. Calcd. for C<sub>21</sub>H<sub>14</sub>Br<sub>2</sub>ClNO<sub>2</sub>S (FW 539.30): C, 46.73; H, 2.60; O, 5.93; N, 2.59 %. Found: C, 46.78; H, 2.64; O, 5.87; N, 2.64 %. IR (KBr, cm<sup>-1</sup>): 3372 (O–H stretching), 3291 (aliphatic C–H stretching), 3060–3009 (aromatic C–H stretching), 1606



(C=N), 1581 (C=C), 862 (C–Br), 848 (C–Cl stretching of chlorine), 666 (C–S); <sup>1</sup>H-NMR (500 MHz, CDCl<sub>3</sub>, δ / ppm): 9.40–8.57 (2H, *trs*, aromatic–OH), 7.72 (1H, *s*, aromatic), 7.20–7.15 (8H, *m*, aromatic), 5.14 (1H, *t*, J = 11.4 Hz, CH), 3.44 (2H, *d*, J = 12.3 Hz, CH<sub>2</sub>); <sup>13</sup>C-NMR (125 MHz, CDCl<sub>3</sub>, δ / ppm): 164.77 (C=N), 159.06 (C–OH), 156.29 (C’–OH), 141.97 (C–S), 138.36, 131.97, 129.63, 130.23, 128.37, 127.78, 116.72, 115.63 (aromatic-C), 131.72 (C–Cl), 109.63 (C’–Br), 95.32 (C–Br), 55.02 (CH<sub>2</sub>), 49.73 (CH); MS (*m/z*): 541.30 [M+2+H]<sup>+</sup>.

**2,4-Dibromo-6-[2-(4-methoxyphenyl)-2,3-dihydro-1,5-benzothiazepin-4-yl]-benzene-1,3-diol (3g).** Yield: 89 %; m.p.: 82–83 °C. Anal. Calcd. for C<sub>22</sub>H<sub>17</sub>Br<sub>2</sub>NO<sub>3</sub>S (FW 534.80): C, 49.36; H, 3.18; O, 8.97; N, 2.62 %. Found: C, 49.31; H, 3.25; O, 8.91; N, 2.65 %. IR (KBr, cm<sup>-1</sup>): 3377 (O–H stretching), 3298 (aliphatic C–H stretching), 3061–3018 (aromatic C–H stretching), 2830 (OCH<sub>3</sub>), 1611 (C=N), 1581 (C=C), 862 (C–Br), 671 (C–S); <sup>1</sup>H-NMR (500 MHz, CDCl<sub>3</sub>, δ / ppm): 9.6–8.34 (2H, *trs*, aromatic–OH), 7.76 (1H, *s*, aromatic), 7.41–7.19 (8H, *m*, aromatic), 5.16 (1H, *t*, J = 11.2 Hz, CH), 3.87 (3H, *s*, OCH<sub>3</sub>), 3.32 (2H, *d*, J = 12.2 Hz, CH<sub>2</sub>); <sup>13</sup>C-NMR (125 MHz, CDCl<sub>3</sub>, δ / ppm): 34.77 (OCH<sub>3</sub>), 164.07 (C=N), 159.96 (C–OH), 158.02 (C’–OH), 159.14, 131.85, 129.62, 128.64, 127.78, 113.74 (aromatic-C), 139.93 (C–S), 107.97 (C’–Br), 96.23 (C–Br), 55.92 (CH<sub>2</sub>), 54.03 (CH); MS (*m/z*): 536.80 [M+2+H]<sup>+</sup>.

**2,4-Dibromo-6-[2-(4-methylphenyl)-2,3-dihydro-1,5-benzothiazepin-4-yl]-benzene-1,3-diol (3h).** Yield: 81 %; m.p.: 85–86 °C. Anal. Calcd. for C<sub>22</sub>H<sub>17</sub>Br<sub>2</sub>NO<sub>2</sub>S (FW 518.80): C, 50.88; H, 3.28; O, 6.17; N, 2.70 %. Found: C, 50.83; H, 3.32; O, 6.20; N, 2.74 %. IR (KBr, cm<sup>-1</sup>): 3371 (O–H stretching), 3289 (aliphatic C–H stretching), 3008–3059 (aromatic C–H stretching), 2913 (CH<sub>3</sub>), 1606 (C=N), 1581 (C=C), 862 (C–Br), 627 (C–S); <sup>1</sup>H-NMR (500 MHz, CDCl<sub>3</sub>, δ / ppm): 9.5–8.52 (2H, *trs*, aromatic–OH), 7.76 (1H, *s*, aromatic), 7.22–6.96 (8H, *m*, aromatic), 5.21 (1H, *t*, J = 11.3 Hz, CH), 3.38 (2H, *d*, J = 12.1 Hz, CH<sub>2</sub>), 2.63 (3H, *s*, –CH<sub>3</sub>); <sup>13</sup>C-NMR (125 MHz, CDCl<sub>3</sub>, δ / ppm): 165.93 (C=N), 159.06 (C–OH), 157.53 (C’–OH), 139.52, 131.65, 129.32, 126.89, 117.06, 105.71 (aromatic-C), 141.03 (C–S), 107.91 (C’–Br), 96.93 (C–Br), 55.27 (CH<sub>2</sub>), 51.93 (CH), 21.18 (CH<sub>3</sub>); MS (*m/z*): 520.80 [M+2+H]<sup>+</sup>.

**2,4-Dibromo-6-[2-(4-hydroxy-3-methoxyphenyl)-2,3-dihydro-1,5-benzothiazepin-4-yl]benzene-1,3-diol (3i).** Yield: 79 %; m.p.: 78–79 °C. Anal. Calcd. for C<sub>22</sub>H<sub>17</sub>Br<sub>2</sub>NO<sub>4</sub>S (FW 550.80): C, 47.93; H, 3.09; O, 11.62; N, 2.54 %. Found: C, 47.89; H, 3.14; O, 11.66; N, 2.46 %. IR (KBr, cm<sup>-1</sup>): 3373 (O–H stretching), 3291 (aliphatic C–H stretching), 3060–3009 (aromatic C–H stretching), 2848 (OCH<sub>3</sub>), 1606 (C=N), 1581 (C=C), 862 (C–Br), 665 (C–S); <sup>1</sup>H-NMR (500 MHz, CDCl<sub>3</sub>, δ / ppm): 9.96 (1H, *s*, aromatic–OH), 9.0–8.32 (2H, *trs*, aromatic–OH), 7.82 (1H, *s*, aromatic), 7.26–7.16 (7H, *m*, aromatic), 5.26 (1H, *t*, J = 11.1 Hz, CH), 3.87 (3H, *s*, –OCH<sub>3</sub>), 3.37 (2H, *d*, J = 12.4 Hz, CH<sub>2</sub>); <sup>13</sup>C-NMR (125 MHz, CDCl<sub>3</sub>, δ / ppm): 35.40 (OCH<sub>3</sub>), 167.53 (C=N), 159.77 (C–OH), 156.67 (C’–OH),



150.13, 145.00, 131.93, 129.62, 128.09, 121.04, 122.35, 116.37, 111.95 (aromatic-C), 141.03 (C–S), 108.51 (C’–Br), 97.07 (C–Br), 55.78 (CH<sub>2</sub>), 54.47 (CH); MS (*m/z*): 552.80 [M+2+H]<sup>+</sup>.

*2,4-Dibromo-6-[2-(4-bromophenyl)-2,3-dihydro-1,5-benzothiazepin-4-yl]-benzene-1,3-diol (3j).* Yield: 90 % m.p.: 93–94 °C. Anal. Calcd. for C<sub>21</sub>H<sub>14</sub>Br<sub>3</sub>NO<sub>2</sub>S (FW 583.70): C, 43.17; H, 2.40; O, 5.48; N, 2.40 %. Found: C, 43.11; H, 2.45; O, 5.41; N, 2.39 %; IR (KBr, cm<sup>-1</sup>): 3377 (O–H stretching), 3298 (aliphatic C–H stretching), 3061–3018 (aromatic C–H stretching), 2830 (OCH<sub>3</sub>), 1611 (C=N), 1581 (C=C), 869 (C–Br), 671 (C–S); <sup>1</sup>H-NMR (500 MHz, CDCl<sub>3</sub>, δ / ppm): 9.7–8.42 (2H, *brs*, aromatic–OH), 7.82 (1H, *s*, aromatic), 7.52–6.99 (8H, *m*, aromatic), 5.18 (1H, *t*, *J* = 11.2 Hz, CH), 3.52 (2H, *d*, *J* = 12.3 Hz, CH<sub>2</sub>); <sup>13</sup>C-NMR (125 MHz, CDCl<sub>3</sub>, δ / ppm): 166.03 (C=N), 159.37 (C–OH), 157.47 (C’–OH), 141.03 (C–S), 137.43, 131.43, 130.96, 129.62, 128.69, 121.45 (aromatic-C), 108.51 (C’–Br), 97.07 (C–Br), 54.98 (CH<sub>2</sub>), 51.47 (CH); MS (*m/z*): 585.70 [M+2+H]<sup>+</sup>.



SHORT COMMUNICATION

**Synthesis of some 3,5-diaryl-2-isoxazoline derivatives  
in ionic liquids media**

JAVAD SAFAEI-GHOMI\* and MOHAMMAD ALI GHASEMZADEH

*Department of Chemistry, Qom Branch, Islamic Azad University, Qom, I. R. Iran*

(Received 31 August, revised 19 December 2011)

**Abstract:** Biologically active isoxazoline derivatives were efficiently synthesized in excellent yields and in smaller reaction times using mild, effective and environmentally friendly butylmethyimidazolium bromide as the solvent and catalyst. By use of this catalyst, isoxazoline derivatives were produced *via* cyclization reaction of a chalcone and hydroxylamine hydrochloride in the ionic liquid media. The separation of the product was facile and the catalyst could be separated and recycled. The method is very rapid, safe and avoids the use of hazardous and expensive reagents and solvents.

**Keywords:** isoxazoline; cyclization reaction; ionic liquids; butylmethyimidazolium bromide; multi-component reactions; biological activities.

INTRODUCTION

Compounds incorporating heterocyclic ring systems continue to attract considerable interest due to the wide range of their biological activities. Amongst them, five-membered heterocyclic compounds occupy a unique place in the realm of natural and synthetic organic chemistry. Isoxazolines as heterocyclic compounds have found wide application as pharmaceutical and agrochemical agents. For instance, isoxazolines possess biological activities,<sup>1–8</sup> such as insecticidal, antibacterial, antibiotic, antitumour, antifungal, antimicrobial activity, and anti-inflammatory and analgesic. In addition, isoxazoline derivatives have played a crucial role in the theoretical development of heterocyclic chemistry and are also used extensively in organic synthesis.<sup>9,10</sup> Consequently, much attention has been paid to the development of new methodologies for their preparation. Several methods have been reported for the synthesis of isoxazoline derivatives. The synthetic routes for the preparation of isoxazoline derivatives mainly are cyclization reaction of chalcones,<sup>11–14</sup> 1,3-dipolar cycloaddition of oximes to alkenes,<sup>15,16</sup>

\*Corresponding author. E-mail: safaei@kashanu.ac.ir  
doi: 10.2298/JSC110831001S

direct transformation of 3-arylpropargyl hydroxylamines hydrochlorides,<sup>17</sup> reaction of alkenes or alkynes with ketones,<sup>18</sup> 1,3-dipolar cycloaddition of nitrile oxides to vinylic compounds<sup>19</sup> and cyclization of *O*-propargylic hydroxylamines.<sup>20</sup>

In accordance with the significance of the application these compounds, a mild and efficient route to the synthesis of isoxazoline derivatives in ionic liquid media is reported herein.

In the past decade, ionic liquids have received substantial attention in organic synthesis because of their environmentally benign nature, high polarity, and good thermal stability. Often shorter reaction times, high yields, cleaner reaction products and high selectivity are obtained from ionic-liquid reaction media.<sup>21,22</sup> Ionic liquids (ILs) have attracted increasing interest recently in the context of green organic synthesis. Although ionic liquids were initially introduced as alternative green reaction media because of their unique chemical and physical properties of non-volatility, non-inflammability, negligible vapor pressure, reusability and high thermal stability, today they have marched far beyond this boundary, showing their significant role in controlling reactions as solvents or catalysts.<sup>23,24</sup>

There are many reports concerning the applications of ionic liquids as solvents and catalysts in organic reactions, such as Friedel–Crafts reaction,<sup>25</sup> Diels–Alder reaction,<sup>26,27</sup> Biginelli reaction,<sup>28</sup> Beckmann rearrangement,<sup>29</sup> Michael reaction,<sup>30</sup> reduction of aldehydes,<sup>31</sup> electrophilic substitution of aromatic rings,<sup>32,33</sup> 1,3-dipolar cycloaddition<sup>34,35</sup> and other reactions.<sup>36–38</sup>

In the continuation of ongoing studies on the application of IL media, it was found that dialkylimidazolium halide derivatives have many advantages over conventional solvents.<sup>39–42</sup> These reagents are safe, easy to handle, environmentally benign and present fewer disposal problems. Therefore, butylmethylimidazolium bromide ([bmim]Br) (Scheme 1) could be an excellent candidate for employment in organic reactions. The advantage of these methods over conventional methods is that they provide greater selectivity, enhanced reaction rates, cleaner products and manipulative simplicity. According to the development of methods that consist of using environmentally friendly reagents and in continuation of our ongoing program to develop environmentally benign methods, the use of an ionic liquid in the synthesis of isoxazoline derivatives in a mild, facile and clean manner is reported herein.



Scheme 1. 1-Butyl-3-methylimidazolium bromide ([bmim]Br).

## EXPERIMENTAL

Butylmethylimidazolium bromide ([bmim]Br) was purchased from Fluka. All melting points are uncorrected and were determined in a capillary tube using a Boetius melting point

microscope. The Fourier transform infrared (FTIR) spectra were recorded on a Nicolet Magna 550 spectrometer (KBr). The  $^1\text{H}$ - and  $^{13}\text{C}$ -NMR spectra were obtained on a Bruker 400 MHz spectrometer in  $\text{CDCl}_3$  as solvent using tetramethylsilane (TMS) as an internal standard. All reactions were monitored and checked by thin layer chromatography (TLC) using hexane/ethyl acetate (8:2) and the spots were examined using a UV lamp. The elemental analyses (C, H, N) were obtained from a Carlo ERBA Model EA 1108 analyzer. The mass spectra were recorded on a Joel D-30 instrument at an ionization potential of 70 eV.

#### *General procedures for the synthesis of chalcones **1a–j***

Chalcone derivatives have been prepared by condensation of various aromatic aldehydes and acetophenones in alkaline ethanol according to the procedure reported by Nielsen *et al.*<sup>43</sup>

To a mixture of NaOH (2.5 g) in 20 ml water and 15 ml EtOH, was added 0.050 mol of the required acetophenone derivative and the solution was stirred at 0–5 °C for 10 min, then 0.050 mol of the required aromatic aldehyde was added and the reaction mixture was refluxed for an appropriate time. After completion of reaction, as indicated by TLC using hexane/ethyl acetate (7:3) the residue was filtered, washed with water and recrystallized from ethanol.

#### *Typical procedures for the synthesis of isoxazolines **3a–j***

*Conventional heating.* Hydroxylamine hydrochloride (0.010 mol) was dissolved in water (5 ml) and added to a solution of chalcone (0.01 mol) in pyridine (10 ml). The reaction mixture was refluxed (magnetic stirring) on oil bath for 3 h. After completion of the reaction, observed by TLC using hexane/ethyl acetate (8:2), the mixture was cooled to room temperature, poured into ice-cold water and then acidified with dilute acetic acid. The obtained solid was filtered, washed with water and recrystallized from ethanol.

*[Bmim]Br method.* A mixture of chalcone (0.010 mol), hydroxylamine hydrochloride (0.010 mol) and [bmim]Br (0.76 g, 0.0035 mol) was stirred at room temperature for the appropriate period. After completion of the reaction, as indicated by TLC using hexane/ethyl acetate (8:2), the reaction mixture was extracted with diethyl ether (3×10 ml). The organic layer was evaporated under reduced pressure and the solid residue was recrystallized from ethanol. The immiscible ionic liquid phase was recovered and heated for 3 h under vacuum for further use. The best results were obtained with a molar ratio of 1:1:0.35 of chalcone, hydroxylamine hydrochloride and [bmim]Br.

Data of synthesized compounds are given in Supplementary material.

## RESULTS AND DISCUSSION

In this research, the ring closure reaction of chalcone **1** and hydroxylamine hydrochloride **2** occurred under I) conventional and II) in the presence of [bmim]Br to afford the isoxazoline derivatives **3** (Scheme 2). The reactions were performed using  $\alpha,\beta$ -unsaturated carbonyl compounds with diverse substituents. The results of the experiments are summarized in Table I.

A possible mechanism for this reaction, proposed based on our experimental results together with some literature data for the cyclization reaction of chalcone, is that it is realized in two steps; first nucleophilic attack of the carbonyl group by the  $\text{NH}_2$  moiety occurs, which is followed by oxime formation and then intramolecular cyclization leads to the five-membered ring products.<sup>12,13</sup>

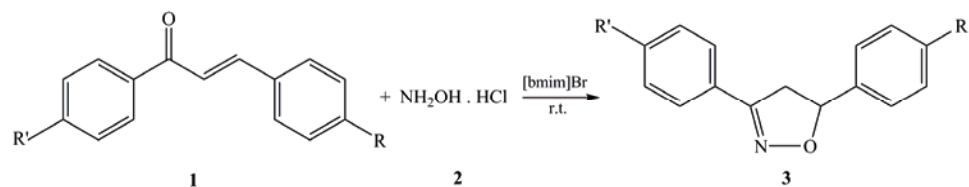
Scheme 2. Preparation of isoxazolines **3** in [bmim]Br.

TABLE I. One-pot synthesis of substituted isoxazolines catalyzed by ([bmim]Br)

Entry	R	R'	Product	M.p., °C	
				Found	Reported
1	H	H	<b>3a</b>	150–152	151–152 <sup>11</sup>
2	CH <sub>3</sub>	H	<b>3b</b>	167–168	168 <sup>11</sup>
3	Cl	H	<b>3c</b>	174–175	175 <sup>11</sup>
4	OCH <sub>3</sub>	H	<b>3d</b>	149–150	148–151 <sup>12</sup>
5	NO <sub>2</sub>	Br	<b>3e</b>	150–151	150–151 <sup>15</sup>
6	OH	H	<b>3f</b>	149–150	— <sup>a</sup>
7	OH	CH <sub>3</sub>	<b>3g</b>	140–142	— <sup>a</sup>
8	NO <sub>2</sub>	CH <sub>3</sub>	<b>3h</b>	121–123	122–123 <sup>15</sup>
9	Br	CH <sub>3</sub>	<b>3i</b>	142–143	142–143 <sup>15</sup>
10	OCH <sub>3</sub>	Br	<b>3j</b>	168–170	— <sup>a</sup>

<sup>a</sup>Compounds **3f**, **3g** and **3j** are new products

The one-pot condensation of  $\alpha,\beta$ -unsaturated carbonyl compounds and hydroxylamine hydrochloride proceeded in the presence of the ionic liquid smoothly to give the corresponding products in high yields and shorter reaction times in comparison to thermal heating method; the results are summarized in Table II. It was found that [bmim]Br is a fairly good catalytic medium for this reaction. Compared with traditional catalysts, such as AcOH, KOH and NaOH, [bmim]Br not only gives higher yields but also takes much less time and can be easily recycled. Compared with traditional solvents, ionic liquids can be easily reused.

TABLE II. Comparison of the two methods for the synthesis of 3,5-diaryl-2-isoxazolines

Product	Conventional conditions		Stirred in [bmim]Br	
	Time, h	Yield, %	Time, min	Yield, %
<b>3a</b>	3.5	35	52	63
<b>3b</b>	3.5	45	50	70
<b>3c</b>	3	50	48	78
<b>3d</b>	3	52	46	80
<b>3e</b>	3	60	45	87
<b>3f</b>	3	60	44	82
<b>3g</b>	3	55	52	75
<b>3h</b>	3	60	42	84
<b>3i</b>	3	52	44	82
<b>3j</b>	3	50	45	80

As mentioned earlier, one of the goals in the use of ionic liquids is to identify and exploit the advantages these compounds can offer over conventional organic solvents besides their greener nature. It has been documented that, compared with classical organic solvents, reactions carried out in ionic liquids often offer enhanced reactivity, better yields and simpler operational process. These advantages were confirmed in the present paper for the synthesis of 3,5-diaryl-2-isoxazoline. The obtained results can be explained by the better catalytic and coordinative properties<sup>44,45</sup> of this kind of ionic liquids in comparison to other methods.

#### CONCLUSIONS

In conclusion, the ionic liquid promoted one-pot annulation reactions of chalcones and hydroxylamine hydrochloride and was proved an efficient medium for the synthesis of isoxazoline derivatives. Compared with conventional organic solvents, the use of [bmim]Br had several advantages, *i.e.*, high yields, mild conditions and simpler procedure in shorter reaction times. In addition, the ionic liquid used can be easily recovered and effectively reused at least 5 times more without any significant loss in efficiency.

#### SUPPLEMENTARY MATERIAL

Spectral data of the compounds are available electronically from <http://www.shd.org.rs/JSCS/>, or from the corresponding author on request.

*Acknowledgement.* The authors gratefully acknowledge the financial support of this work by the Research Affairs Office of the Islamic Azad University, Qom Branch, Qom, I. R. Iran.

#### ИЗВОД

#### СИНТЕЗА НОВИХ ДЕРИВАТА 3,5-ДИАРИЛ-2-ИЗОКСАЗОЛИНА У ЈОНСКИМ ТЕЧНОСТИМА

JAVAD SAFAEI-GHOMI и MOHAMMAD ALI GHASEMZADEH

*Department of Chemistry, Qom Branch, Islamic Azad University, Qom, I. R. Iran*

Биолошки активни деривати изоксазолина синтетисани су у одличном приносу, у присуству бутилметилимидазолијум-бромида као раствараца и катализатора. Производи су добијени реакцијом циклизације халкона и хидроксиламин-хидрохлорида. Производи су лако раздвојени, а катализатор је могуће одвојити и поновно користити. Описаны поступак је кратак и омогућава да се избегне употреба опасних и скупих реагенаса и раствараца.

(Примљено 31. августа, ревидирано 19. децембра 2011)

#### REFERENCES

1. R. Huisgen, *Angew. Chem. Int. Ed. Engl.* **2** (1963) 565
2. P. Caramella, P. Grunanger, *1,3-Dipolar Cycloaddition Chemistry*, Vol. 1, Wiley, New York, USA, 1984
3. V. M. Barot, *Oriental J. Chem.* **16** (2000) 177

4. M. D. Ankhiala, M. V. Hathi, *J. Indian Chem. Soc.* **71** (1994) 587
5. C. J. Shishoo, M. B. Devani, G. V. Ullas, S. Ananhan, V. S. Bhadti, *J. Heterocycl. Chem.* **18** (1981) 43
6. B. L. Varma, *Indian. J. Heterocycl. Chem.* **13** (2003) 111
7. R. P. Tangallapally, S. D. Rakesh, N. Budha, B. Meibohm, *Bioorg. Med. Chem. Lett.* **17** (2007) 6638
8. A. G. Habeeb, P. N. Praveen, R. E. Knaus, *J. Med. Chem.* **44** (2001) 2921
9. Y. V. Tomilovi, G. P. Okonishnikova, E. V. Shulishov, O. M. Nefedov, *Russ. Chem. Bull.* **44** (1995) 2114
10. E. I. Klimova, M. Marcos, T. B. Klimova, A. T. Cecilio, A. T. Ruben, R. R. Lena, *J. Organomet. Chem.* **106** (1999) 585
11. M. Venugopal, P. T. Perumal, *Proc. Indian Acad. Sci. (Chem. Sci.).* **105** (1993) 19
12. M. Kidwai, P. Misra, *Synth. Commun.* **29** (1999) 3237
13. A. Voskienė, V. Mickevičius, *Chem. Heterocycl. Compd.* **45** (2009) 1485
14. T. Shah, V. Desai, *J. Serb. Chem. Soc.* **72** (2007) 443
15. A. Tavares, O. M. S. Ritter, U. B. Vasconcelos, B. C. Arruda, A. Schrader, P. H. Schneider, A. A. Merlo, *Liquid Cryst.* **37** (2010) 159
16. R. Maurya, A. Ahmad, P. Gupta, K. Chand, M. Kumar, P. Rawat, N. Rasheed, G. Palit, *Med. Chem. Res.* **20** (2011) 139
17. L. Pennicott, S. Lindell, *Synlett* **3** (2006) 463
18. K. I. Itoh, H. Sakamaki, N. Nakazato, A. Horiuchi, E. Horn, C. A. Horiuchi, *Synthesis* **20** (2005) 3541
19. I. N. N. Namboothiri, N. Rastogi, *Top. Heterocycl. Chem.* **12** (2008) 1
20. D. W. Knight, A. J. Proctor, J. M. Clough, *Synlett* **4** (2010) 628
21. H. Olivier-Bourbigou, L. Magna, *J. Mol. Catal.* **419** (2002) 182
22. D. Zhao, M. Wu, Y. Kou, E. Min, *Catal. Today* **74** (2002) 157
23. P. Wasserscheid, T. Welton, *Ionic Liquids in Synthesis*, Wiley-VCH Verlag, Stuttgart, Germany, 2002
24. A. P. M. Martins, P. F. Clarissa, N. M. Dayse, N. Zanatta, G. H. Bonacorso, *Chem. Rev.* **108** (2008) 2015
25. A. Stark, B. L. MacLean, R. D. Singer, *J. Chem. Soc., Dalton Trans. I* (1999) 63
26. T. Fischer, A. Sethi, T. Welton, J. Woolf, *Tetrahedron Lett.* **40** (1999) 793
27. P. Ludley, N. Karodia, *Tetrahedron Lett.* **42** (2001) 2011
28. J. J. Peng, Y. Q. Deng, *Tetrahedron Lett.* **42** (2001) 5917
29. R. X. Ren, L. D. Zueva, W. Ou, *Tetrahedron Lett.* **42** (2001) 8441
30. B. C. Ranu, S. S. Dey, *Tetrahedron* **60** (2004) 4183
31. G. W. Kabalka, R. R. Malladi, *Chem. Commun.* **22** (2000) 2191
32. K. K. Laali, V. J. Gettwert, *J. Org. Chem.* **66** (2001) 35
33. F. Zulfiqar, T. Kitazume, *Green Chem.* **2** (2000) 296
34. J. F. Dubreuil, J. P. Bazureau, *Tetrahedron Lett.* **41** (2000) 7351
35. D. Conti, M. Rodriguez, A. Segal, M. Taddei, *Tetrahedron Lett.* **44** (2003) 5327
36. A. R. Hajipour, Z. Nasreesfahani, A. E. Ruoho, *Org. Prep. Proc. Int.* **40** (2008) 385
37. A. Zare, A. Hasaninejad, M. Shekouhy, A. R. M. Zare, *Org. Prep. Proc. Int.* **40** (2008) 457
38. A. R. Williams, A. J. Angel, K. L. French, D. R. Hurst, D. D. Beckman, C. F. Beam, *Synth. Commun.* **29** (1999) 1977
39. J. Safaei-Ghomi, A. R. Hajipour, *J. Chin. Chem. Soc.* **56** (2009) 416

40. J. Safaei-Ghom, M. Taheri, M. A. Ghasemzadeh, *Org. Prep. Proc. Int.* **42** (2010) 485
41. J. Safaei-Ghom, A. R. Hajipour, M. Esmaeili, *Dig. J. Nanomater. Bios.* **5** (2010) 865
42. J. Safaei-Ghom, A. R. Hajipour, *Org. Prep. Proc. Int.* **43** (2011) 372
43. A. T. Nielsen, W. J. Houlihan, *Org. React.* **16** (1968) 1
44. Y. Chen, Y. Zu, Y. Fu, X. Zhang, P. Yu, G. Sun, T. Efferth, *Molecules* **15** (2010) 9486
45. S. Kantevari, M. V. Chary, A. P. Rudra Das, S. V. N. Vuppalapati, N. Lingaiah, *Catal. Commun.* **9** (2008) 1575.





SUPPLEMENTARY MATERIAL TO  
**Synthesis of some 3,5-diarylisoazoline derivatives  
in ionic liquids media**

JAVAD SAFAEI-GHOMI\* and MOHAMMAD ALI GHASEMZADEH

Department of Chemistry, Qom Branch, Islamic Azad University, Qom, I. R. Iran

J. Serb. Chem. Soc. 77 (6) (2012) 733–739

SPECTRAL DATA FOR THE COMPOUNDS

**3,5-Diphenyl-2-isoxazoline (3a).** White crystals; FTIR (KBr,  $\text{cm}^{-1}$ ): 1640 (C=N), 1580, 1472, 1434 (C=C);  $^1\text{H-NMR}$  (400 MHz,  $\text{CDCl}_3$ ,  $\delta$  / ppm): 2.7 (1H, *dd*,  $^2J_{\text{gem}} = 14.5$  Hz,  $^3J_{\text{trans}} = 6.6$  Hz, CHHCH), 3.1 (1H, *dd*,  $^2J_{\text{gem}} = 14.5$  Hz,  $^3J_{\text{cis}} = 8.7$  Hz, CHHCH), 5.2 (1H, *dd*,  $^3J_{\text{cis}} = 8.6$  Hz,  $^3J_{\text{trans}} = 6.5$  Hz, CHHCH), 6.9–7.8 (10H, *m*, Ar–H);  $^{13}\text{C-NMR}$  (100 MHz,  $\text{CDCl}_3$ ,  $\delta$  / ppm): 38.5, 75.2, 121.3, 125.2, 128.1, 130.0, 133.2, 137.2, 140.1, 142.5, 148.3.

**3-Phenyl-5-p-tolyl-2-isoxazoline (3b).** Yellow crystals; FTIR (KBr,  $\text{cm}^{-1}$ ): 1642 (C=N), 1595, 1475, 1430 (C=C);  $^1\text{H-NMR}$  (400 MHz,  $\text{CDCl}_3$ ,  $\delta$  / ppm): 2.1 (3H, *s*,  $\text{CH}_3$ ), 2.8 (1H, *dd*,  $^2J_{\text{gem}} = 14.4$  Hz,  $^3J_{\text{trans}} = 6.6$  Hz, CHHCH), 3.1 (1H, *dd*,  $^2J_{\text{gem}} = 14.4$  Hz,  $^3J_{\text{cis}} = 8.7$  Hz, CHHCH), 5.4 (1H, *dd*,  $^3J_{\text{cis}} = 8.7$  Hz,  $^3J_{\text{trans}} = 6.5$  Hz, CHHCH), 6.88–7.75 (9H, *m*, Ar–H);  $^{13}\text{C-NMR}$  (100 MHz,  $\text{CDCl}_3$ ,  $\delta$  / ppm): 21.5, 38.2, 75.5, 121.1, 125.7, 127.2, 132.2, 134.6, 137.5, 138.2, 142.2, 147.1.

**5-(4-Chlorophenyl)-3-phenyl-2-isoxazoline (3c).** White crystals; FTIR (KBr,  $\text{cm}^{-1}$ ): 1645 (C=N), 1602, 1467, 1441 (C=C);  $^1\text{H-NMR}$  (400 MHz,  $\text{CDCl}_3$ ,  $\delta$  / ppm): 2.8 (1H, *dd*,  $^2J_{\text{gem}} = 14.6$  Hz,  $^3J_{\text{trans}} = 6.6$  Hz, CHHCH), 3.2 (1H, *dd*,  $^2J_{\text{gem}} = 14.6$  Hz,  $^3J_{\text{cis}} = 8.5$  Hz, CHHCH), 5.3 (1H, *dd*,  $^3J_{\text{cis}} = 8.5$  Hz,  $^3J_{\text{trans}} = 6.6$  Hz, CHHCH), 6.92–7.81 (9H, *m*, Ar–H);  $^{13}\text{C-NMR}$  (100 MHz,  $\text{CDCl}_3$ ,  $\delta$  / ppm): 37.7, 76.2, 120.3, 123.6, 127.2, 130.6, 133.4, 137.8, 143.2, 148.5, 155.8.

**5-(4-Methoxyphenyl)-3-phenyl-2-isoxazoline (3d).** White crystals; FTIR (KBr,  $\text{cm}^{-1}$ ): 1640 (C=N), 1590, 1485, 1442 (C=C);  $^1\text{H-NMR}$  (400 MHz,  $\text{CDCl}_3$ ,  $\delta$  / ppm): 2.9 (1H, *dd*,  $^2J_{\text{gem}} = 14.5$  Hz,  $^3J_{\text{trans}} = 6.4$  Hz, CHHCH), 3.3 (1H, *dd*,  $^2J_{\text{gem}} = 14.5$  Hz,  $^3J_{\text{cis}} = 8.8$  Hz, CHHCH), 3.6 (3H, *s*,  $\text{OCH}_3$ ), 5.2 (1H, *dd*,  $^3J_{\text{cis}} = 8.7$  Hz,  $^3J_{\text{trans}} = 6.5$  Hz, CHHCH), 6.78–7.68 (9H, *m*, Ar–H);  $^{13}\text{C-NMR}$  (100 MHz,  $\text{CDCl}_3$ ,  $\delta$  / ppm): 37.7, 76.2, 120.3, 123.6, 127.2, 130.6, 133.4, 137.8, 143.2, 148.5, 155.8.

\*Corresponding author. E-mail: safaei@kashanu.ac.ir

<sup>1</sup>-NMR (100 MHz, CDCl<sub>3</sub>,  $\delta$  / ppm): 38.4, 51.5, 75.7, 122.8, 124.6, 126.9, 130.1, 132.5, 136.8, 137.9, 139.2, 144.1.

**3-(4-Bromophenyl)-5-(4-nitrophenyl)-2-isoxazoline (3e).** Yellow crystals; FTIR (KBr, cm<sup>-1</sup>): 1642 (C=N), 1590, 1477, 1445 (C=C); <sup>1</sup>H-NMR (400 MHz, CDCl<sub>3</sub>,  $\delta$  / ppm): 2.8 (1H, dd,  $^2J_{\text{gem}} = 14.8$  Hz,  $^3J_{\text{trans}} = 6.5$  Hz, CHHCH), 3.3 (1H, dd,  $^2J_{\text{gem}} = 14.8$  Hz,  $^3J_{\text{cis}} = 8.3$  Hz, CHHCH), 5.4 (1H, dd,  $^3J_{\text{cis}} = 8.4$  Hz,  $^3J_{\text{trans}} = 6.5$  Hz, CHHCH), 7.12–7.97 (8H, m, Ar-H); <sup>13</sup>C-NMR (100 MHz, CDCl<sub>3</sub>,  $\delta$  / ppm): 38.3, 76.3, 123.2, 125.1, 127.8, 129.5, 133.8, 139.5, 145.4, 149.2, 154.7.

**5-(4-Hydroxyphenyl)-3-phenyl-2-isoxazoline (3f).** White crystals; Anal. Calcd. for C<sub>15</sub>H<sub>13</sub>NO<sub>2</sub>: C, 75.30; H, 5.48; N, 5.85 %. Found: C, 75.25; H, 5.51; N, 5.89 %; FTIR (KBr, cm<sup>-1</sup>): 1640 (C=N), 1595, 1472, 1440 (C=C); <sup>1</sup>H-NMR (400 MHz, CDCl<sub>3</sub>,  $\delta$  / ppm): 3.0 (1H, dd,  $^2J_{\text{gem}} = 14.7$  Hz,  $^3J_{\text{trans}} = 6.3$  Hz, CHHCH), 3.3 (1H, dd,  $^2J_{\text{gem}} = 14.7$  Hz,  $^3J_{\text{cis}} = 8.5$  Hz, CHHCH), 5.1 (1H, bs, OH), 5.6 (1H, dd,  $^3J_{\text{cis}} = 8.6$  Hz,  $^3J_{\text{trans}} = 6.3$  Hz, CHHCH), 6.75–7.57 (9H, m, Ar-H); <sup>13</sup>C-NMR (100 MHz, CDCl<sub>3</sub>,  $\delta$  / ppm): 38.2, 76.1, 122.5, 124.8, 127.3, 128.8, 131.5, 134.4, 137.8, 139.9, 144.3; MS-EI (*m/z*): 239 (M<sup>+</sup>).

**5-(4-Hydroxyphenyl)-3-p-tolyl-2-isoxazoline (3g).** White crystals; Anal. Calcd. for C<sub>16</sub>H<sub>15</sub>NO<sub>2</sub>: C, 75.87; H, 5.97; N, 5.53 %. Found: C, 75.91; H, 5.99; N, 5.85 %; FTIR (KBr, cm<sup>-1</sup>): 1645 (C=N), 1585, 1483, 1440 (C=C); <sup>1</sup>H-NMR (400 MHz, CDCl<sub>3</sub>,  $\delta$  / ppm): 2.1 (3H, s, CH<sub>3</sub>), 2.9 (1H, dd,  $^2J_{\text{gem}} = 14.6$  Hz,  $^3J_{\text{trans}} = 6.4$  Hz, CHHCH), 3.4 (1H, dd,  $^2J_{\text{gem}} = 14.6$  Hz,  $^3J_{\text{cis}} = 8.2$  Hz, CHHCH), 5.1 (1H, bs, OH) 5.5 (1H, dd,  $^3J_{\text{cis}} = 8.3$  Hz,  $^3J_{\text{trans}} = 6.5$  Hz, CHHCH), 6.88–7.67 (8H, m, Ar-H); <sup>13</sup>C-NMR (100 MHz, CDCl<sub>3</sub>,  $\delta$  / ppm): 21.3, 37.9, 75.8, 122.2, 124.4, 125.8, 127.3, 134.6, 138.3, 141.1, 143.5, 148.5; MS-EI (*m/z*): 253(M<sup>+</sup>).

**5-(4-Nitrophenyl)-3-p-tolyl-2-isoxazoline (3h).** Yellow crystals; FTIR (KBr, cm<sup>-1</sup>): 1645 (C=N), 1595, 1480, 1442 (C=C); <sup>1</sup>H-NMR (400 MHz, CDCl<sub>3</sub>,  $\delta$  / ppm): 2.2 (3H, s, CH<sub>3</sub>), 2.8 (1H, dd,  $^2J_{\text{gem}} = 14.8$  Hz,  $^3J_{\text{trans}} = 6.6$  Hz, CHHCH), 3.2 (1H, dd,  $^2J_{\text{gem}} = 14.8$  Hz,  $^3J_{\text{cis}} = 8.1$  Hz, CHHCH), 5.3 (1H, dd,  $^3J_{\text{cis}} = 8.1$  Hz,  $^3J_{\text{trans}} = 6.5$  Hz, CHHCH), 6.95–7.81 (8H, m, Ar-H); <sup>13</sup>C-NMR (100 MHz, CDCl<sub>3</sub>,  $\delta$  / ppm): 21.2, 38.2, 76.5, 123.7, 124.1, 126.9, 129.2, 134.5, 140.3, 145.7, 150.2, 154.6.

**5-(4-Bromophenyl)-3-p-tolyl-2-isoxazoline (3i).** White crystals; FTIR (KBr, cm<sup>-1</sup>): 1644 (C=N), 1588, 1472, 1448 (C=C); <sup>1</sup>H-NMR (400 MHz, CDCl<sub>3</sub>,  $\delta$  / ppm): 2.1 (3H, s, CH<sub>3</sub>), 3.0 (1H, dd,  $^2J_{\text{gem}} = 14.5$  Hz,  $^3J_{\text{trans}} = 6.7$  Hz, CHHCH), 3.4 (1H, dd,  $^2J_{\text{gem}} = 14.5$  Hz,  $^3J_{\text{cis}} = 8.1$  Hz, CHHCH), 5.3 (1H, dd,  $^3J_{\text{cis}} = 8.1$  Hz,  $^3J_{\text{trans}} = 6.6$  Hz, CHHCH), 6.92–7.75 (8H, m, Ar-H); <sup>13</sup>C-NMR (100 MHz, CDCl<sub>3</sub>,  $\delta$  / ppm): 21.2, 38.1, 75.6, 120.1, 123.2, 126.7, 129.3, 133.8, 136.3, 139.5, 142.4, 148.1.



*3-(4-Bromophenyl)-5-(4-methoxyphenyl)-2-isoxazoline (3j).* White crystals; Anal. Calcd. for C<sub>16</sub>H<sub>14</sub>BrNO<sub>2</sub>: C, 57.85; H, 4.25; N, 4.22 %. Found: C, 57.94; H, 4.21; N, 4.16 %; FTIR (KBr, cm<sup>-1</sup>): 1642 (C=N), 1592, 1475, 1440 (C=C); <sup>1</sup>H-NMR (400 MHz, CDCl<sub>3</sub>, δ/ ppm): 2.8 (1H, *dd*, <sup>2</sup>J<sub>gem</sub> = 14.7 Hz, <sup>3</sup>J<sub>trans</sub> = 6.6 Hz, CHHCH), 3.3 (1H, *dd*, <sup>2</sup>J<sub>gem</sub> = 14.7 Hz, <sup>3</sup>J<sub>cis</sub> = 8.5 Hz, CHHCH), 3.6 (3H, *s*, OCH<sub>3</sub>), 5.4 (1H, *dd*, <sup>3</sup>J<sub>cis</sub> = 8.6 Hz, <sup>3</sup>J<sub>trans</sub> = 6.6 Hz, CHHCH), 6.85–7.71 (8H, *m*, Ar-H); <sup>13</sup>C-NMR (100 MHz, CDCl<sub>3</sub>, δ/ ppm): 38.2, 52.4, 75.9, 121.5, 123.4, 125.9, 132.3, 134.5, 137.6, 140.2, 144.1, 149.3; MS-EI (*m/z*): 333 (M+2)<sup>+</sup>.



## Improved synthesis and *in vitro* study of antimicrobial activity of $\alpha,\beta$ -unsaturated and $\alpha$ -bromo carboxylic acids

VESNA D. VITNIK<sup>1\*\*#</sup>, MARINA T. MILENKOVIĆ<sup>2</sup>, SANDA P. DILBER<sup>3</sup>,  
ŽELJKO J. VITNIK<sup>4#</sup> and IVAN O. JURANIĆ<sup>1#</sup>

<sup>1</sup>Department of Chemistry ICTM, University of Belgrade, Studentski trg 12–16, 11000

Belgrade, Serbia, <sup>2</sup>Department of Microbiology and Immunology, Faculty of Pharmacy,

University of Belgrade, Vojvode Stepe 450, 11221 Belgrade, Serbia, <sup>3</sup>Department of  
Organic Chemistry, Faculty of Pharmacy, University of Belgrade, Vojvode Stepe 450,

11221 Belgrade, Serbia and <sup>4</sup>Faculty of Chemistry, University of Belgrade,  
Studentski trg 12–16, 11000 Belgrade, Serbia

(Received 4 November 2011, revised 16 January 2012)

**Abstract:** A series of  $\alpha,\beta$ -unsaturated and  $\alpha$ -bromo carboxylic acids were identified as potent antimicrobial agents. The antimicrobial activity was evaluated using the broth microdilution method. All acids **1–12** exhibited a significant activity against nine laboratory control strains of bacteria and two strains of yeast *Candida albicans*. The tested acids were efficiently prepared by optimized phase-transfer-catalyzed (PTC) reactions of ketones with bromoform and aqueous lithium hydroxide in alcoholic solvent with triethylbenzyl ammonium chloride (TEBA) as catalyst.

**Keywords:** antimicrobial activity; one-pot synthesis; ketones; bromoform.

### INTRODUCTION

Fungal and bacterial infections are important problems in phytopathology, agriculture, the food industry and especially in medicine. Bacterial resistance to antimicrobial agents has become a serious problem worldwide, with resistance mechanisms having been identified and described for all known antibiotics currently available for clinical use.<sup>1</sup>

The development of new antimicrobial agents represents an important field in medicinal chemistry, due to the increasing problem of the formation of resistant strains of bacterial pathogens. Natural products often represent important lead structures for the development of new antibiotics.

\* Corresponding author. E-mail: vesnak@chem.bg.ac.rs

# Serbian Chemical Society member.

doi: 10.2298/JSC111104016V

The potential antimicrobial activity of  $\alpha,\beta$ -unsaturated carbonyl compounds continues to receive attention, and several substances exhibiting this function, are used in therapy, for example (Fig. 1), ciprofloxacin<sup>2</sup> and minocycline<sup>3</sup> are members of the antibiotics group, and are commonly used to treat a variety of infections. Helenalin,<sup>4</sup> a sesquiterpene lactone with potent anti-inflammatory and antitumor effects, can also reduce the severity of *Staphylococcus aureus* infection in animals. Some  $\alpha,\beta$ -unsaturated carbonyl compounds with different biological activity are shown in Fig. 1. Etacrynic acid<sup>5</sup> is a loop diuretic used to treat high blood pressure. Digoxin<sup>6</sup> is a cardiac glycoside used in the treatment of congestive heart failure and cardiac arrhythmia. Risperidone,<sup>7</sup> a second generation anti-psychotic, is used to treat schizophrenia. Rofecoxib<sup>8</sup> is a non-steroidal anti-inflammatory drug, which has now been withdrawn due to safety concerns. Dimethyl fumarate<sup>9</sup> is used to treat psoriasis.

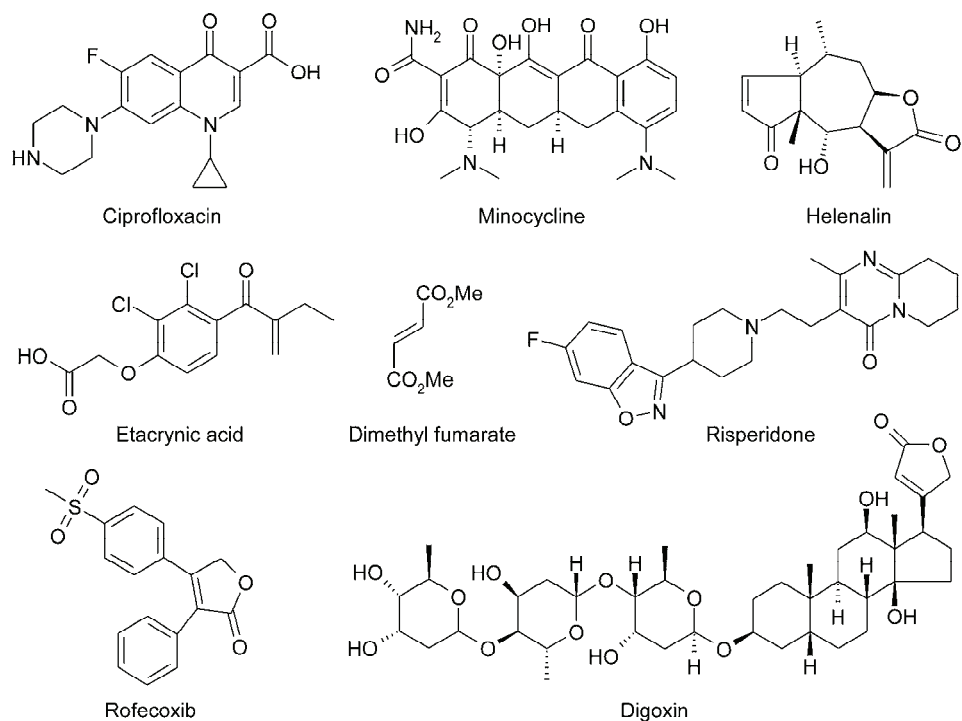


Fig. 1. Structures of several significant  $\alpha,\beta$ -unsaturated carbonyl compounds currently used in medical therapy.

It is generally assumed and confirmed by experimental evidence that the activity of this class of compounds is due to the alkylation of nucleophilic groups, such as amino groups or sulfhydryls, of biomolecules.<sup>10</sup> The reaction involves a

Michael-type addition of the nucleophile to the activated double bond of  $\alpha,\beta$ -unsaturated carbonyl compounds.

The synthesis of  $\alpha,\beta$ -unsaturated carboxylic acids has gained considerable attention<sup>11</sup> because of the biologically important properties of these acids and their use as precursors for the preparation of biologically active compounds.<sup>12</sup> These acids are known for their broad spectrum of activity, for example: anti-fungal activity of derivatives of tiglic acid and cyclohex-1-enecarboxylic acid.<sup>13</sup> Derivatives of cyclohex-1-enecarboxylic acid are effective in controlling weeds in rice paddies and in vegetable fields.<sup>14</sup> The structural analogue of the anti-epileptic drug sodium valproate (VPA, 2-propylpentanoic acid) possessing an  $\alpha,\beta$ -unsaturated carboxyl group, is 1-cyclohept-1-enecarboxylic acid, which has very low activity.<sup>15</sup> Atropic acid and  $\beta,\beta$ -dimethylatropic acid are plant growth regulators.<sup>16</sup> Pyrethrins are natural organic compounds with potent insecticidal activity. Pyrethrin I and pyrethrin II are structurally related esters with a cyclopropane core, (+)-*trans*-chrysanthemic acid in the case of pyrethrin I. Natural chemical pyrethrins produced by the flowers of pyrethrums (*Chrysanthemum cinerariaefolium* and *C. coccineum*) have the synthetic analog pyrethroid, which now constitutes a major proportion of the synthetic insecticides.<sup>17</sup> A large number of known drugs arise from the reduction of appropriate precursors ( $\alpha,\beta$ -unsaturated carboxylic acids), for example, Ariflo,<sup>18</sup> an orally active second-generation phosphodiesterase type 4 inhibitor (PDE4) inhibitor for the treatment of asthma, as well as non-steroidal anti-inflammatory drugs, such as ibuprofen<sup>19</sup> and naproxen.<sup>20</sup>

## EXPERIMENTAL

### Reagents and chemicals

All used chemicals were of analytical reagent grade, purchased from Aldrich, Fluka or Merck, and were used without further purification.

### Measurements

The NMR spectra for samples were recorded on a Varian Gemini 2000, <sup>1</sup>H-NMR at 200 MHz, <sup>13</sup>C-NMR at 50 MHz, in deuterated chloroform. Chemical shifts are expressed in ppm using tetramethylsilane as the internal standard. The IR spectra were recorded on Nicolet 6700 FT instrument, and are expressed in cm<sup>-1</sup>. Melting points were determined on a Boetius PMHK apparatus and are not corrected.

### Typical procedure for the synthesis of cyclopent-1-enecarboxylic acid (8)

A flask was charged with LiOH solution (1.18 mol, 49.93 g, in 50 ml H<sub>2</sub>O), *t*-BuOH (250 ml), cyclopentanone (0.059 mol, 5.0 g) and TEBA (0.029 mol, 6.8 g). The mixture was stirred vigorously (large egg-shaped stirring bar) at 45–50 °C (water bath), while bromoform (0.24 mol, 60 g) was added dropwise from a dropping funnel ( $\approx$ 60 min.). The stirring was continued for 24 h at room temperature. Then (0.12 mol, 30 g) of bromoform was added, and the stirring continued for 12 h at room temperature; H<sub>2</sub>O (300 ml) was added and the organic layer (lower one) discarded. The aqueous layer was extracted with toluene (2×70 ml), then acidified with HCl (20 %) to pH around 1. The separated oil was extracted with toluene (3×70

ml), dried (anh. MgSO<sub>4</sub>), concentrated and crystallized from toluene. Cyclopent-1-enecarboxylic acid was obtained as white crystals.

#### In vitro antibacterial activity

The antimicrobial activity was evaluated using nine laboratory control strains of bacteria, *i.e.*, the Gram-positive *Staphylococcus aureus* (ATCC 25923), *Staphylococcus epidermidis* (ATCC 12228), *Micrococcus luteus* (ATCC 9341), *Micrococcus flavus* (ATCC 10240), *Enterococcus faecalis* (ATCC 29212), *Bacillus subtilis* (ATCC 6633) and the Gram-negative *Escherichia coli* (ATCC 25922), *Klebsiella pneumoniae* (NCIMB 9111), *Pseudomonas aeruginosa* (ATCC 27853), and two strains of yeast *Candida albicans* (ATCC 10231 and ATCC 10259). A broth microdilution method was used to determine the minimal inhibitory concentrations (*MICs*) of tested compounds according to the Clinical and Laboratory Standards Institute (CLSI 2005).<sup>21</sup>

All tests were performed in Müller–Hinton broth for the bacterial strains and in Sabouraud dextrose broth for the *Candida albicans*. Overnight broth cultures of each strain were prepared, and the final concentration in each well was adjusted to 2×10<sup>6</sup> CFU ml<sup>-1</sup> for the bacteria and 2×10<sup>7</sup> CFU ml<sup>-1</sup> for the yeasts. The investigated acids were dissolved to 1 % in dimethyl sulfoxide (DMSO) and then diluted to the highest test concentration. Serial doubling dilutions of the compounds were prepared in 96-well micotiter plates over the concentration range 31.25–1000 µg ml<sup>-1</sup>. In the tests, triphenyltetrazolium chloride (TTC) (Aldrich, USA) was also added to the culture medium as a growth indicator. The final concentration of TTC after inoculation was 0.05 %. The microbial growth was determined after 24 h incubation at 37 °C for the bacteria and at 25 °C after 48 h for the fungi. The *MIC* is defined as the lowest concentration of a compound at which the microorganism does not demonstrate visible growth. All determinations were performed in duplicate and two positive growth controls were included.

#### RESULTS AND DISCUSSION

Herein, an optimized, convenient synthesis of  $\alpha,\beta$ -unsaturated and  $\alpha$ -bromo carboxylic acids, by phase-transfer-catalyzed reactions of ketones with bromoform and aqueous lithium hydroxide in an alcoholic solvent is reported.

#### Chemistry

As a part of efforts to synthesize various novel  $\alpha,\beta$ -unsaturated carboxylic acids, a substantially improved and modified synthesis of them has been developed.<sup>22</sup> It also provides access to numerous other conjugated acids.

All the investigated acids (Fig. 2) were synthesized in one-pot phase-transfer reactions of ketones with bromoform (Scheme 1). The acids **1–7**, **11** and **12** were synthesized in satisfactory yields, as is reported in a previous paper.<sup>22</sup> The acids **8–10** were obtained in the improved synthesis in the present work (Scheme 2).

In a previous study, conjugated acids **1–10** were obtained from the corresponding cyclic or aromatic ketones. Bromo acids, 4-bromo-piperidine-1,4-dicarboxylic acid mono-*tert*-butyl ester **11** and 4-bromo-piperidine-1,4-dicarboxylic acid monoethyl ester **12** were obtained from 4-oxo-piperidine-1-carboxylic acid *tert*-butyl ester and 4-oxo-piperidine-1-carboxylic acid ethyl ester. The published syntheses of the cyclic carboxylic acids **8–10** suffered from low yields (35–75

$\%$ ).<sup>22</sup> In general, ketones with larger ring size (cycloheptanone and cyclododecanone) were found to be much less reactive than the model ketone (cyclohexanone). Due to steric hindrance, the reaction is slow.<sup>22</sup> Various solvents and reagents were tested, usually resulting in lower yields or giving various side products. Their synthesis presented herein was accomplished in one-step, starting from cyclic ketones, Scheme 2. In this research, the reaction conditions were optimized regarding the reaction temperature, molar ratio of the reactants and the catalyst. Optimal molar proportion of the reagents was found to be 6 eq. of  $\text{CHBr}_3$  and 20 eq. of LiOH per 1 eq. of ketone, with solvents (*t*-BuOH/ $\text{H}_2\text{O}$ ) and the phase-transfer catalyst TEBA. Lower ratios diminished the yields while higher proportions did not lead to further improvements.

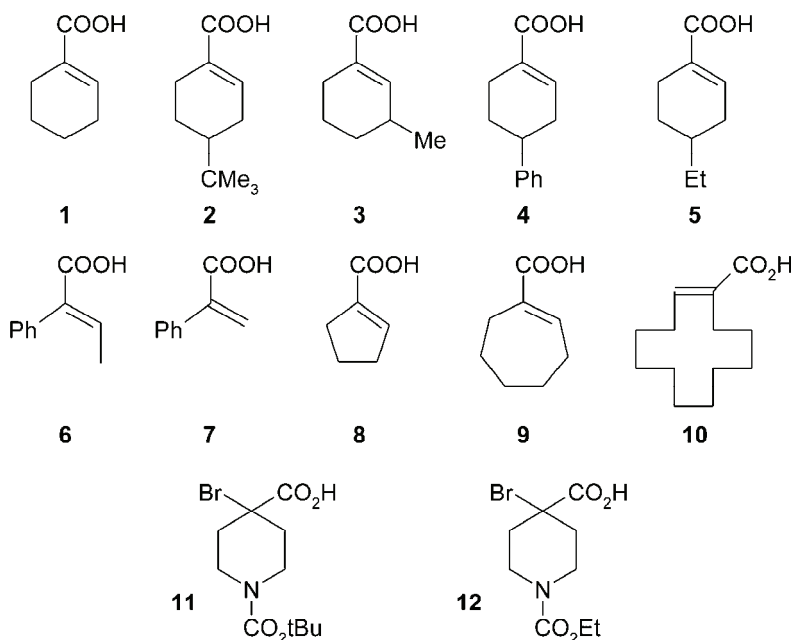
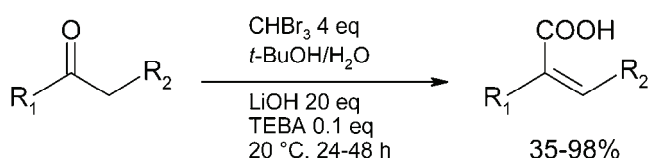


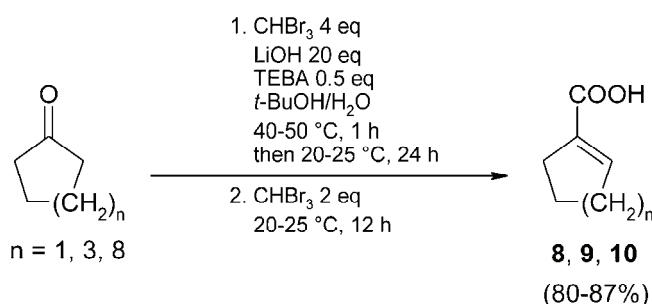
Fig. 2. Investigated acids **1–12**, synthesized in a one-pot phase-transfer reaction of ketones with bromoform.



$\text{R}_1, \text{R}_2 = \text{cycloalkyl, alkyl, aryl}$

Scheme 1. One-pot reaction of ketones with bromoform.<sup>22</sup>

Although these kinds of reaction of cyclohexanone and analogs are usually performed at 20 °C,<sup>22</sup> it was found that subsequent heating at 40–50 °C for the first hour of reaction was necessary to achieve nearly quantitative yields, as given in Scheme 2. Finally, acceptable yields and purity of acids **8–10** were obtained using lithium hydroxide (20 eq.), heated *t*-BuOH/H<sub>2</sub>O (40–50 °C) with the gradual addition of bromoform (4 eq., 1 h). After 24 h, the addition of two further equivalents of CHBr<sub>3</sub> dramatically improved the yields and the reaction rate. A number of solvent systems were examined (PhMe/H<sub>2</sub>O, DMSO, CH<sub>2</sub>Cl<sub>2</sub>/H<sub>2</sub>O, THF/H<sub>2</sub>O, *i*-PrOH/H<sub>2</sub>O, *t*-BuOH/H<sub>2</sub>O and *t*-PentOH/H<sub>2</sub>O). The optimal yields, purity and reaction rate were achieved in a *t*-BuOH/H<sub>2</sub>O mixture (5:1), in the presence of ≈0.5 eq. of TEBA. The products were isolated and recrystallized from toluene. All the synthesized compounds were fully characterized by instrumental methods, and the purity confirmed by GC, TLC, and MS.



Scheme 2. Optimized one-pot reaction of cyclic ketones with bromoform.

It should be stressed that the reaction protocol presented herein is applicable to a variety of ketones.

#### Characterization data of the compounds

**Cyclopent-1-enecarboxylic acid (8).** Yield: 5.7 g, 87 %; m.p: 120–121 °C (lit. 121 °C<sup>23</sup>); IR (KBr, cm<sup>−1</sup>): 3100–3150 (O–H stretching of COOH group), 2967 (=C–H stretching of vinyl group), 2863 (−C–H stretching of CH<sub>2</sub> group), 1724 (C=O stretching of COOH group), 1429 (C=C stretching of vinyl group), 1294 (C–O stretching of COOH group), 952 (C=CH bending of vinyl group); <sup>1</sup>H-NMR (200 MHz, CDCl<sub>3</sub>, δ / ppm): 11.08 (1H, *s*), 6.94 (1H, *t*, *J* = 2 Hz), 2.49 (4H, *m*), 2.06 (2H, *m*); <sup>13</sup>C-NMR (50 MHz CDCl<sub>3</sub>, δ / ppm): 171.02 (CO), 147.07 (CH), 136.07 (C), 33.54 (CH<sub>2</sub>), 30.88 (CH<sub>2</sub>), 23.07 (CH<sub>2</sub>).

**Cyclohept-1-enecarboxylic acid (9).** Yield: 5.0 g, 85 %; m.p: 53 °C (lit. 51 °C<sup>23</sup>); IR (KBr, cm<sup>−1</sup>): 3150–3200 (O–H stretching of COOH group), 2932 (=C–H stretching of vinyl group), 2860 (−C–H stretching of CH<sub>2</sub> group), 1703 (C=O stretching of COOH group), 1450 (C=C stretching of vinyl group), 1288 (C–O stretching of COOH group), 951 (C=CH bending of vinyl group); <sup>1</sup>H-NMR

(200 MHz, CDCl<sub>3</sub>,  $\delta$  / ppm): 12 (1H, s), 7.2 (1H, t,  $J$  = 7 Hz), 2.6 (2H, m), 2.25 (2H, m), 1.8 (2H, m), 1.6 (4H, m); <sup>13</sup>C-NMR (50 MHz, CDCl<sub>3</sub>,  $\delta$  / ppm): 174.04 (CO), 147.46 (CH), 135.89 (C), 31.93 (CH<sub>2</sub>), 28.93 (CH<sub>2</sub>), 26.82 (CH<sub>2</sub>), 26.06 (CH<sub>2</sub>), 25.55 (CH<sub>2</sub>).

*Cyclododec-1-enecarboxylic acid (**10**)*. Yield: 4.61 g, 80 %; m.p: 121–122 °C (lit. 120–123 °C<sup>24</sup>); IR (KBr, cm<sup>−1</sup>): 2958, 2865 (−C—H stretching of CH<sub>2</sub> group), 1682 (C=O stretching of COOH group), 1424 (C=C stretching of vinyl group), 1280 (C—O stretching of COOH group), 932 (C=CH bending of vinyl group); <sup>1</sup>H-NMR (200 MHz, CDCl<sub>3</sub>,  $\delta$  / ppm): 10.47 (1H, s), 7.14 (1H, t,  $J$  = 8 Hz), 2.45 (2H, m), 1.9 (2H, m), 0.95 (16H, m); <sup>13</sup>C-NMR (50 MHz, CDCl<sub>3</sub>,  $\delta$  / ppm): 173.13 (CO), 143.22 (CH), 129.56 (C), 43.09 (CH<sub>2</sub>), 34.92 (CH<sub>2</sub>), 32.42 (CH<sub>2</sub>), 32.06 (CH<sub>2</sub>), 27.69 (CH<sub>2</sub>), 27.40 (CH<sub>2</sub>), 27.06 (CH<sub>2</sub>), 25.1 (CH<sub>2</sub>), 23.4 (CH<sub>2</sub>), 21.76 (CH<sub>2</sub>).

Characterization data of compounds (**1–7**, **11** and **12**) are given in a previous paper.<sup>22</sup>

#### Biological results and discussion

The antimicrobial activity of  $\alpha,\beta$ -unsaturated and  $\alpha$ -bromo-carboxylic acids was tested against ATCC strains of bacteria and two strains of yeast *Candida albicans*. As a standard for the comparison with the synthesized compounds, a well-known drug ampicillin was used. The inhibitory properties of the acids were observed within the concentration range 0.10 to 1.0 mg ml<sup>−1</sup>. Minimal inhibitory concentrations (*MICs*) of tested acids are presented in Table I. The maximum activity was exhibited by the acids **8–10**. The Gram-positive bacteria were more sensitive to the tested acids than the Gram-negative bacteria. The most resistant bacterial strain was the Gram-negative *P. aeruginosa*, which is known to have a high level of intrinsic resistance to virtually all known antimicrobials and antibiotics, due to its very restrictive outer membrane barrier, which is highly resistant even to synthetic drugs.<sup>25</sup>

From the biological data (Table I), it was observed that cyclohex-1-enecarboxylic acid **1** was almost inactive against all the tested strains. As can be seen in Table I, most of the conjugated acids **2–10** generally showed antifungal and antibacterial activity against all the tested fungal and bacterial strains. The activities of compounds **3** and **5** were higher in comparison to those of compounds **2** and **4** because of the steric hindrance (*tert*-butyl and phenyl group) in the series of the substituted cyclohex-1-enecarboxylic acids. The cyclic acids **8–10** showed good inhibitory effects against all the Gram-positive bacteria and the two strains of yeast *C. albicans*. Furthermore, the aromatic acids **6** and **7** showed good antibacterial and antifungal activities. The acids **11** and **12**, the activities of which are unknown in the literature, showed good antifungal activity with an *MIC* value of

0.1 mg ml<sup>-1</sup>. It is evident that the studied compounds exhibit much lower anti-bacterial activities than ampicillin.

In a previous study,<sup>22</sup> undesirable cytotoxic effects of the investigated compounds were determined on immune competent cells, the normal peripheral blood mononuclear cells. All the compounds examined in this work did not affect proliferation of healthy human blood peripheral mononuclear cells (PBMC and PBMC + PHA),  $IC_{50} > 200 \mu\text{M}$ ; hence, they could be safely used as potential antibiotics.

TABLE I. Antimicrobial activity of the tested  $\alpha,\beta$ -unsaturated and  $\alpha$ -bromo-carboxylic acids (n.t. – not tested)

Microorganism	MIC / mg ml <sup>-1</sup>												Ampicillin
	1	2	3	4	5	6	7	8	9	10	11	12	
<i>S. aureus</i> ATCC 25923	>1.0	0.5	0.5	0.2	1.0	1.0	1.0	0.5	0.5	0.5	1.0	>1.0	0.0005
<i>S. epidermidis</i> ATCC 12228	0.2	0.5	0.2	1.0	0.2	0.5	0.5	0.1	0.2	0.2	1.0	0.5	0.0002
<i>M. luteus</i> ATCC 9341	>1.0	1.0	0.2	0.5	1.0	n.t.	n.t.	0.2	0.2	0.2	n.t.	n.t.	0.002
<i>M. flavus</i> ATCC 10240	1.0	>1.0	0.5	0.1	1.0	n.t.	n.t.	0.2	0.2	0.2	n.t.	n.t.	0.003
<i>E. faecalis</i> ATCC 29212	>1.0	>1.0	1.0	>1.0	1.0	0.2	1.0	0.1	0.2	0.2	>1.0	>1.0	0.0005
<i>B. subtilis</i> ATCC 6633	1.0	1.0	0.2	0.2	0.5	0.2	>1.0	0.2	0.2	0.2	>1.0	1.0	n.t.
<i>E. coli</i> ATCC 25922	>1.0	1.0	1.0	>1.0	>1.0	>1.0	>1.0	0.2	0.5	0.5	>1.0	>1.0	0.002
<i>K. pneumoniae</i> ATCC 13883	>1.0	>1.0	>1.0	>1.0	>1.0	>1.0	>1.0	0.2	0.2	0.5	>1.0	1.0	0.004
<i>P. aeruginosa</i> ATCC 27853	>1.0	1.0	>1.0	>1.0	>1.0	>1.0	>1.0	1.0	0.5	1.0	>1.0	1.0	0.003
<i>C. albicans</i> ATCC 10259	>1.0	1.0	0.5	>1.0	>1.0	0.1	0.2	0.5	0.2	0.5	0.1	0.1	n.t.

#### CONCLUSIONS

The tested compounds exhibited significant antimicrobial and antifungal activities and could be considered as the potential antimicrobial agents. Previous cytotoxicity studies revealed low toxicity of these compounds,<sup>22</sup> which renders them as harmless drugs against various microbial and micro-fungal strains. Further studies are planned to elucidate the possible mechanism/mechanisms of action of these compounds.

*Acknowledgements.* This work was financially supported by the Ministry of Education and Science of the Republic of Serbia, under Grant Nos. 172035, 172041 and 173021.



И З В О Д

ОПТИМИЗАЦИЈА СИНТЕЗЕ И *IN VITRO* ПРОУЧАВАЊЕ АНТИМИКРОБНОГ ДЕЈСТВА  
 $\alpha,\beta$ -НЕЗАСИЋЕНИХ И  $\alpha$ -БРОМКАРБОКСИЛНИХ КИСЕЛИНА

ВЕСНА Д. ВИТНИК<sup>1</sup>, МАРИНА Т. МИЛЕНКОВИЋ<sup>2</sup>, САНДА П. ДИЛБЕР<sup>3</sup>,  
 ЖЕЉКО Ј. ВИТНИК<sup>4</sup> и ИВАН О. ЈУРАНИЋ<sup>1</sup>

<sup>1</sup>ИХТМ – Центар за хемију, Универзитет у Београду, Студенчески парк 12–16, 11000 Београд, <sup>2</sup>Институт за микробиологију и имунологију, Фармацевтички факултет, Универзитет у Београду, Војводе Степе 450, 11221 Београд, <sup>3</sup>Институт за органску хемију, Фармацевтички факултет, Универзитет у Београду, Војводе Степе 450, 11221 Београд и <sup>4</sup>Хемијски факултет, Универзитет у Београду, Студенчески парк 12–16, 11000 Београд

У овом раду је приказано *in vitro* испитивање антимикробног дејства серије  $\alpha,\beta$ -незасићених и  $\alpha$ -бромкарбоксилних киселина и показано је да су оне потенцијално добри антимикробни агенци. Све киселине **1–12** показале су значајну активност према девет сојева бактерија и два соја гљивица *Candida albicans*. Испитивање киселине синтетисане су у оптимизованој реакцији кетона са бромоформом и литијум-хидроксидом у смеси растворача (*пирец*-бутанол/вода). Као катализатор за пренос између фаза употребљен је триетилбензиламонијум-хлорид (ТЕБА).

(Примљено 4. новембра 2011, ревидирано 16. јануара 2012)

## REFERENCES

1. A. C. Fluit, M. E. Jones, F.-J. Schmitz, J. Acar, R. Gupta, J. Verhoef, *Clin. Infect. Dis.* **30** (2000) 454
2. J. A. Hoogkamp-Korstanje, S. J. Klein, *J. Antimicrob. Chemother.* **18** (1986) 407
3. T. M. Tikka, J. E. Koistinaho, *J. Immunol.* **166** (2001) 7527
4. D. Boulanger, E. Brouilette, F. Jaspar, F. Malouin, J Mainil, F. Bureau, P. Lekeux, *Vet. Microbiol.* **119** (2007) 330
5. J. C. Somberg, J. Molnar, *Am. J. Ther.* **16** (2009) 102
6. C. Sticherling, H. Oral, J. Horrocks, S. P. Chough, R. L. Baker, M. H. Kim, K. Wasmer, F. Pelosi, B. P. Knight, G. F. Michaud, S. A. Strickberger, F. Morady, *Circulation* **102** (2000) 2503
7. C. J. Lane, E. T. C. Ngan, L. N. Yatham, T. J. Ruth, P. F. Liddle, *J. Psychiatry Neurosci.* **29** (2004) 30
8. N. M. Davies, X. W. Teng, N. M. Skjodt, *Clin. Pharmacokinet.* **42** (2003) 545
9. T. J. Schmidt, M. Aku, U. Mrowietz, *Bioorg. Med. Chem.* **15** (2007) 333
10. P. Tronche, P. Bastide, R. Cluzel, J. Couquelet, *Sci. Med.* **2** (1971) 35
11. A. Silveira Jr., Y. R. Mehra, W. A. Atwell, *J. Org. Chem.* **42** (1977) 3892
12. a) J. Palaty, F. Abbott, *J. Med. Chem.* **38** (1995) 3398; b) N. F. Badham, J-H. Chen, P. G. Cummings, P. C. Dell'Orco, A. M. Diederich, A. M. Eldridge, W. L. Mendelson, R. J. Mills, V. J. Novack, M. A. Olsen, A. M. Rustum, K. S. Webb, S. Yang, *Org. Process Res. Dev.* **7** (2003) 101
13. P. Chakravarthy, Y. Hiratsuka, L. S. Trifonov, W. A. Ayer, Z. *Pflanzenkr. Pflanzenschutz* **104** (1997) 254
14. K. Matsui, K. Matsuya, H. Ohta, S. Motojima, M. Nakazawa, Japan Patent JP 49000431 A (1974)
15. C. Redecker, U. Altrup, D. Hoppe, R. Dusing, E.-J. Speckmann, *Neuropharmacology* **39** (2000) 254
16. K. Kazuyoshi, F. Toshio, M. Tetsou, *Agric. Biol. Chem.* **30** (1966) 261



17. J. H. Babler, K. P. Spina, *Tetrahedron Lett.* **26** (1985) 1923
18. H. Ochiai, T. Ohtani, A. Ishida, K. Kishikawa, T. Obata, H. Nakaia, M. Toda, *Bioorg. Med. Chem. Lett.* **14** (2004) 1323
19. H. Kamekawa, H. Senboku, M. Tokuda, *Electrochim. Acta* **42** (1997) 2117
20. T. Ohta, H. Takaya, M. Kitamura, K. Nagai, R. Noyori, *J. Org. Chem.* **52** (1987) 3174
21. Clinical and Laboratory Standards Institute (CLSI), *Performance Standards for Antimicrobial Susceptibility Testing: 15<sup>th</sup> Informational Supplement. CLSI Document M100-S15*. Wayne, PA, USA, 2005
22. V. D. Vitnik, M. D. Ivanović, Ž. J. Vitnik, J. B. Đorđević, Ž. S. Žižak, Z. D. Juranić, I. O. Juranić, *Synth. Commun.* **39** (2009) 1457
23. O. H. Wheeler, I. Lerner, *J. Am. Chem. Soc.* **78** (1956) 63
24. A. Silveira Jr., Y. R. Mehra, W. A. Atwell, *J. Org. Chem.* **42** (1977) 3892
25. C. M. Mann, S. D. Cox, J. L. Markham, *Lett. Appl. Microbiol.* **30** (2000) 294.



## Cyclic conjugation in benzo- and benzocyclobutadieno-annelated terrylenes and higher rylene

MARIJA MARKOVIĆ, JELENA ĐURĐEVIĆ and IVAN GUTMAN\*#

Faculty of Science, University of Kragujevac, P. O. Box 60, 34000 Kragujevac, Serbia

(Received 31 January 2012)

**Abstract:** The effect of benzo- and benzocyclobutadieno-annelation on cyclic conjugation in terrylene and the higher members of the rylene homologous series are examined. Some peculiar regularities are established, which could not be observed in the case of perylene (the first member of the rylene series).

**Keywords:** cyclic conjugation; energy effect (of cyclic conjugation); terrylene; quaterrylene; rylene.

### INTRODUCTION

In this work, we are concerned with the cyclic conjugation in the benzo- and benzocyclobutadieno-annelated derivatives of the rylene homologous series of benzenoid hydrocarbons, Fig. 1. What is meant under “linear” and “angular” benzo- and benzocyclobutadieno-annelation is clarified in Fig. 2.

A method for calculating the energy effect *ef* of cyclic conjugation in individual rings of polycyclic conjugated compounds was conceived in the 1970s by one of the present authors.<sup>1</sup> Its details and an exhaustive bibliography can be found in the reviews,<sup>2,3</sup> whereas the mathematical details by which the quantity *ef* is computed are outlined in recent articles.<sup>4,5</sup>

When the *ef*-method was applied to benzo-annelated perylenes,<sup>6,7</sup> a remarkable phenomenon was discovered: Contrary to what standard methods<sup>8–10</sup> predict, benzo-annelation significantly influences the intensity of cyclic conjugation in the “empty” central ring of perylene; in some cases it even exceeds the intensity of cyclic conjugation in the “full” rings. Characteristic results of this kind are shown in Fig. 3.

Eventually, systematic studies<sup>11–15</sup> revealed that the first observations made in the case of perylene are general regularities that can be stated as follows:

*Rule 1.* Angular benzo-annelation increases the intensity of cyclic conjugation.

\* Corresponding author. E-mail: gutman@kg.ac.rs; jddjurdjevic@gmail.com

# Serbian Chemical Society member.

doi: 10.2298/JSC120131012M

*Rule 2.* Linear benzo-annelation decreases the intensity of cyclic conjugation.

*Rule 3.* The effect of angular benzo-annelation is stronger than the effect of linear benzo-annelation.

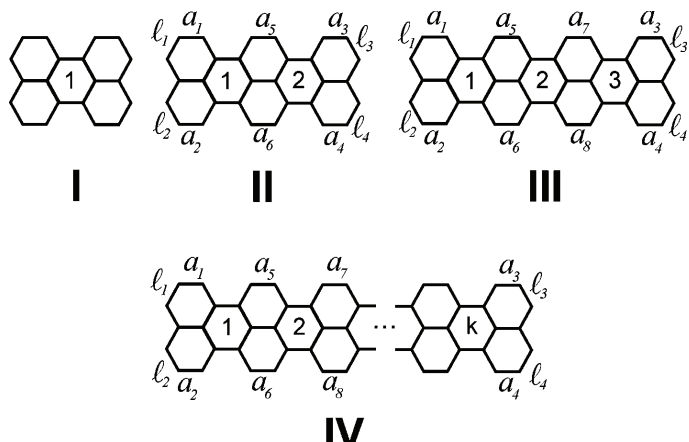


Fig. 1. The first three members of the rylene homologous series: perylene (I), terrylene (II), and quaterrylene (III), their general formula (IV), and the labeling of their annelation sites; sites marked by  $a$  pertain to angular, and those marked by  $\ell$  to linear annelation, cf. Fig. 2. The “empty” rings are labeled by  $1, 2, \dots, k$ . According to classical Kekulé-structure-based theories, the “empty” rings are devoid of any cyclic conjugation, implying that rylenes should be viewed as consisting of several independent naphthalene fragments. The present approach shows that this is an oversimplification and that cyclic conjugation in the “empty” rings is far from negligible, and is much influenced by benzo- and benzocyclobutadieno-annelation.

Rules 1–3 summarize the results of a large number of calculations. In addition, their general validity was recently confirmed by means of theoretical arguments.<sup>16</sup> Recalling that in some polycyclic conjugated systems (*e.g.*, in perylene<sup>6,7</sup>), as a consequence of Rules 1–3, the conjugation pattern significantly differs from what previous theories<sup>8–10</sup> based on the analysis of Kekulé structures would predict. One could even speak of the “breakdown of the Kekulé-structure model”.<sup>17</sup>

Another way to attach a six-membered ring to a conjugated system is the benzocyclobutadieno-annelation, Fig. 2. The effect of such an annelation was also studied in due detail.<sup>18–23</sup> In many cases, but not all,<sup>22,23</sup> the following regularities could be envisaged:

*Rule 4.* Angular benzocyclobutadieno-annelation decreases the intensity of cyclic conjugation.

*Rule 5.* Linear benzocyclobutadieno-annelation increases the intensity of cyclic conjugation.

*Rule 6.* The effect of linear benzocyclobutadieno-annelation is stronger than the effect of angular benzocyclobutadieno-annelation.

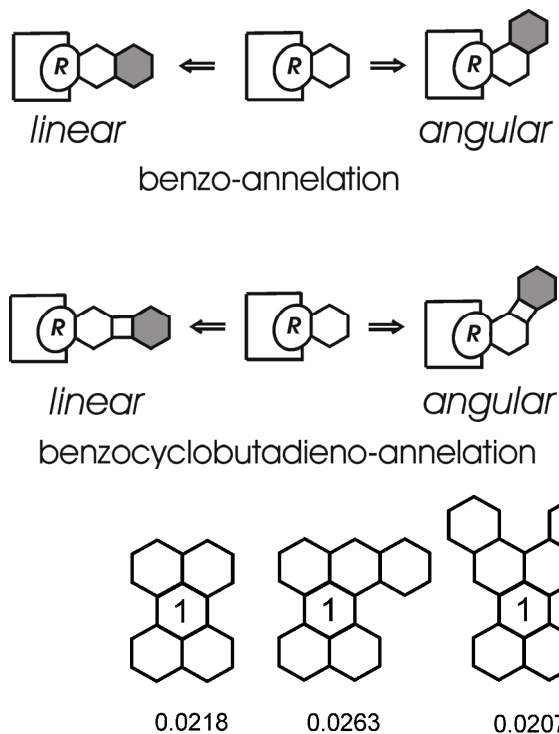


Fig. 2. Modes of benzo- and benzocyclobutadieno-annelation with regard to the ring  $R$ .

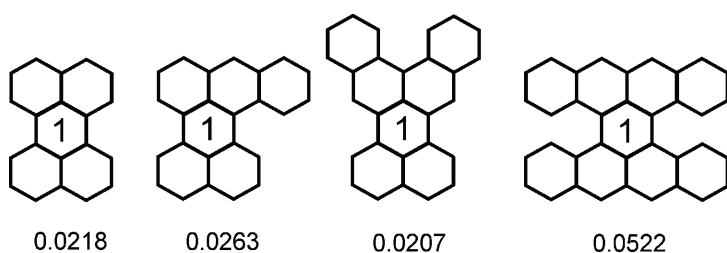


Fig. 3. Energy effects of the central “empty” ring (1) of perylene and its angularly annelated benzo-derivatives. The greater is the number of angular benzo-annelations, the greater is  $ef$ . In tetra-angularly annelated perylene, each of the four six-membered rings adjacent to ring 1 has  $ef = 0.0437$ , which is smaller than  $ef(1) = 0.0522$ . This contradicts the predictions of classical theories,<sup>8–10</sup> according to which there is no cyclic conjugation in the “empty” ring.

A remarkable violation of Rule 4 was found in the case of benzocyclobutadieno-annelated perylenes.<sup>23</sup> Surprisingly, in these polycyclic systems, angularly annelated benzocyclobutadieno-fragments have practically no effect on the  $ef$ -value of the “empty” central ring. Characteristic results of this kind are shown in Fig. 4.

The evident question that could be asked at this point is whether analogous regularities also exist in the higher members of the rylene series, in particular in terrylene and quaterrylene, *cf.* Fig. 1. The importance of knowing the answer to this question lies in the fact that oligorylenes (the first few, experimentally available, members of the rylene series) possess interesting and non-standard optical and optoelectronic properties.<sup>24–26</sup> These are primarily caused by the  $\pi$ -electrons, the degree of delocalization of which is significantly influenced by conjugation in the “empty” rings. Thus, by means of appropriately combined benzo- and benzocyclobutadieno-annelation, a fine-tuning of the optical and optoelectronic pro-

perties of these compounds could be achieved, which would be of evident value for their practical (technical) applications.

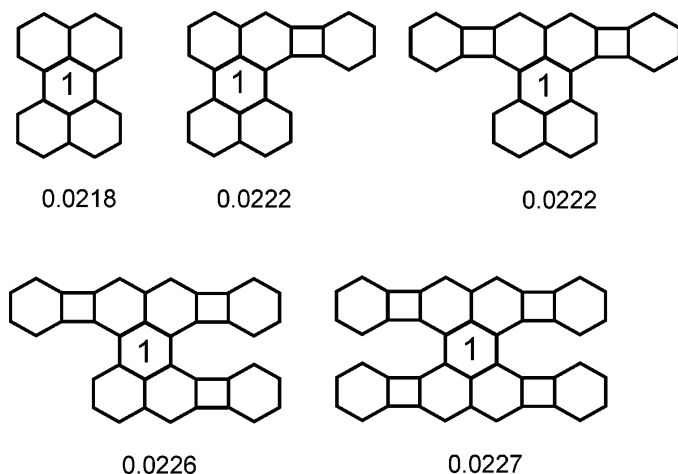


Fig. 4. Energy effects  $ef$  of the central ring (1) of various angularly benzocyclobutadieno-annelated perylenes. Practically, angular benzocyclobutadieno-annelation has an influence on the value of  $ef$ . These results should be compared with those in Fig. 6.

In what follows, some partial answers to the above question are offered.

#### NUMERICAL WORK

The energy effects,  $ef$ , of the six-membered rings were calculated by means of a several times previously described<sup>1–7</sup> graph-theoretical method, using in-house software. As usual, the  $ef$  values are given in the units of the HMO carbon–carbon resonance integral  $\beta$ . Thus, positive  $ef$  values indicate thermodynamic stabilization caused by cyclic conjugation. The greater is  $ef$ , the greater is the intensity of cyclic conjugation in the underlying ring.

There are 3 monobenzo-, 14 dibenzo-, 24 tribenzo-, 32 tetrabenzo-, 18 pentabenzo- and 7 hexabenzo-annelated terrylenes, *i.e.*, a total of 98 benzo-annelated congeners. Exactly the same counts apply to benzocyclobutadieno-annelated terrylenes. All calculated  $ef$ -values of the six-membered rings of these derivatives of terrylene are available from the authors (M.M.) upon request.

The number of terrylene derivatives possessing both benzo- and benzocyclobutadieno-annelations is several hundred. Their  $ef$  values were not calculated.

#### CONJUGATION IN BENZO-ANNELATED TERRYLENE AND HIGHER RYLENES

The  $ef$ -values of benzo-annelated terrylenes and higher ryles are found to obey fully the Rules 1–3. A few characteristic examples are depicted in Fig. 5.

A structural feature that does not exist in perylene is the sites  $a_5$ ,  $a_6$ ,... (see Fig. 1).

Benzo-annelation on these sites also obeys Rules 1 and 3, but the effect is somewhat weaker than at the terminal sites  $a_1$ – $a_4$ . Examples: For  $a_1$ - and  $(a_1,a_2)$ -annelation  $ef = 0.0293$  and  $ef = 0.0367$ , whereas for  $a_5$ - and  $(a_5,a_6)$ -annelation  $ef$

= 0.0287 and  $ef = 0.0352$ . Consistently, the  $ef$  values for ( $a_1, a_5$ )- and ( $a_1, a_6$ )-annelation are 0.0355 and 0.0358, which lie between 0.0287 and 0.0367.

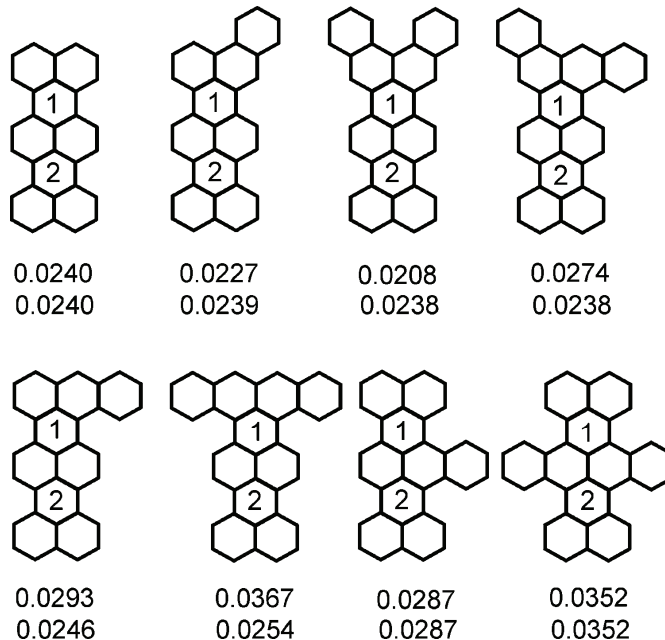


Fig. 5. Energy effects,  $ef$ , of the two “empty” rings in benzo-annelated terrylenes; the numbers below the structures are  $ef(1)$  and  $ef(2)$ , in that order. Rules 1–3 are satisfied in all cases.

In the higher rylenes, there are several “empty” rings and annelation influences all their energy effects. This can be seen from the examples depicted in Fig. 5. In order to show how fast this “transmission” of annelation effect decreases, the sixth member of the rylene series ( $k=6$ , see Fig. 1) is considered. For the non-annelated species,  $ef(1) = ef(6) = 0.0252$ ,  $ef(2) = ef(5) = 0.0282$  and  $ef(3) = ef(4) = 0.0290$ . For the ( $a_1, a_2$ )-dibenzo derivative,  $ef(1) = 0.0396$ ,  $ef(2) = 0.0305$ ,  $ef(3) = 0.0301$ ,  $ef(4) = 0.0296$ ,  $ef(5) = 0.0285$  and  $ef(6) = 0.0253$ .

For the ( $\ell_1, \ell_2$ )-dibenzo derivative, the attenuation of the annelation effect is even faster:  $ef(1) = 0.0216$ ,  $ef(2) = 0.0279$ ,  $ef(3) = 0.0289$ ,  $ef(4) = 0.0289$ ,  $ef(5) = 0.0281$  and  $ef(6) = 0.0252$ .

#### CONJUGATION IN BENZOCYCLOBUTADIENO-ANNELATED TERRYLENE AND HIGHER RYLENES

In the case of benzocyclobutadieno-annelation, the first point to be examined is whether violation of Rule 4 also occurs at the higher members of the rylene series. The findings are surprising: the same as in the case of perylene, angular benzocyclobutadieno-annelation in the terminal positions  $a_1-a_4$  has a negligible influence on cyclic conjugation in the “empty” rings of terrylene; examples are

given in Fig. 6. On the other hand, angular benzocyclobutadieno-annelation in the lateral positions  $a_5$ ,  $a_6$ ,... diminishes the  $ef$  values, thus obeying Rule 4; examples are given in Fig. 7. From the examples given in Fig. 7, it is seen that the same regularity also applies to benzocyclobutadieno-annelated quaterrylenes.

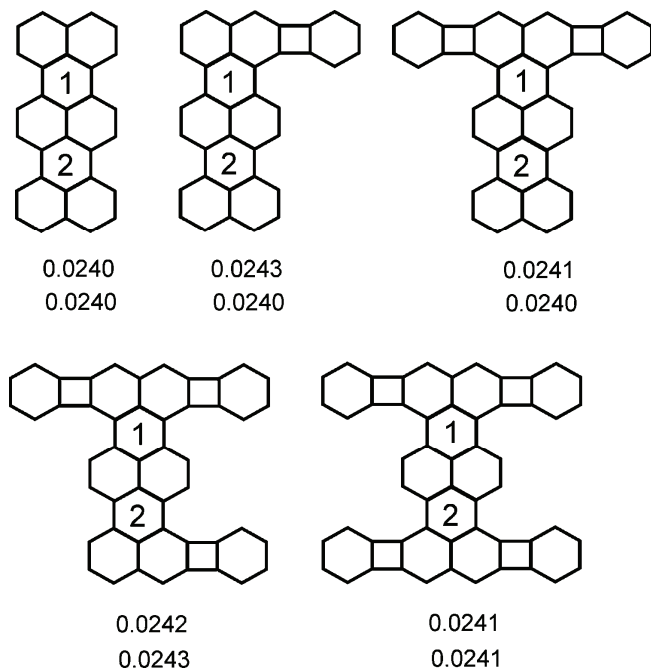


Fig. 6. Energy effects,  $ef$ , of the “empty” rings of benzocyclobutadieno-derivatives of terrylene, annelated in terminal positions  $a_1$ ,  $a_2$ ,  $a_3$  and  $a_4$ . The numbers below the structures are  $ef(1)$  and  $ef(2)$ , in that order. Practically, such angular benzocyclobutadieno-annelation has an influence on the value of  $ef$ . These results should be compared with those in Fig. 4.

The present calculations confirmed that Rules 5 and 6 apply without a single exception. A few illustrative examples are provided in Fig. 8.

The results of the present work indicate that there exists an annelation mode (or, more precisely, an angular benzocyclobutadieno-annelation mode) that leaves the pattern of cyclic conjugation in the members of the rylene homologous series essentially unchanged. The theoretical explanation of why this is so remains a task for the future. Other annelation modes obey the relatively “reasonable” regularities stated here as Rules 1–6. By employment of these rules, it would be possible to design oligorylenes with the desired conjugation patterns, thus possessing optical and optoelectronic properties required for technical applications.

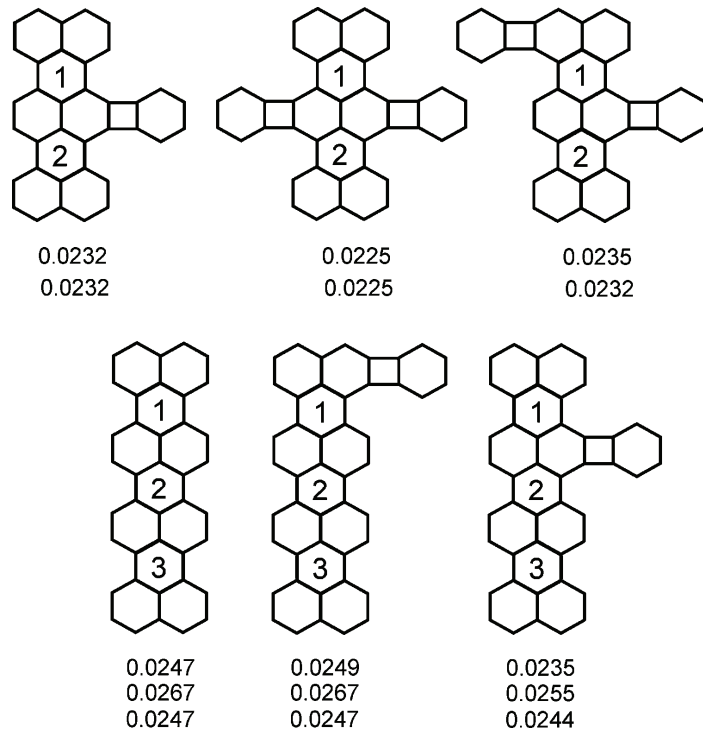


Fig. 7. The above three examples illustrate that contrary to angular benzocyclobutadieno-annealing in terminal positions, annealing in lateral positions  $a_5, a_6, \dots$  obeys Rule 4 and diminishes the intensity of cyclic conjugation in the “empty” rings of terrylene. The three examples below show that the same regularities also hold in the case of higher members of the rylene homologous series. The numbers below the structures are  $ef(1)$ ,  $ef(2)$ , and, where applicable,  $ef(3)$ , in that order.

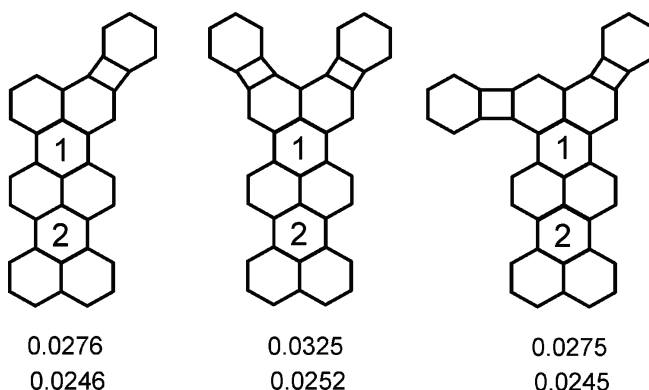


Fig. 8. Examples confirming that Rules 5 and 6 hold in the case of benzocyclobutadieno-annealed terrylenes. The numbers below the structures are  $ef(1)$  and  $ef(2)$ , in that order.  
Note that the  $ef$ -values in the  $\ell_1$ - and  $(\ell_1, a_2)$ -derivatives are practically identical; this is the consequence of the non-validity of Rule 4, cf. Fig. 6.

*Acknowledgement.* The authors thank the Ministry of Education and Science of the Republic of Serbia for support (Grant No. 174033).

## ИЗВОД

## ЦИКЛИЧНА КОНЈУГАЦИЈА У БЕНЗО- И БЕНЗОЦИКЛОБУТАДИЕНО-АНЕЛИРАНИМ ТЕРИЛЕНИМА И ВИШИМ РИЛЕНИМА

МАРИЈА МАРКОВИЋ, ЈЕЛЕНА ЂУРЂЕВИЋ И ИВАН ГУТМАН

*Природно-математички факултет Универзитета у Крагујевцу*

Испитиван је утицај бензо- и бензоциклогидиенске анелације на цикличну конјугацију у терилену и вишим члановима риленског хомологног низа. Установљене су извесне неочекиване правила, које нису могле бити уочене у случају перилена (првог члана риленског низа).

(Примљено 31. јануара 2012)

## REFERENCES

1. I. Gutman, S. Bosanac, *Tetrahedron* **33** (1977) 1809
2. I. Gutman, *Monatsh. Chem.* **136** (2005) 1055
3. I. Gutman, in: A. Graovac, I. Gutman, D. Vukičević (Eds.), *Mathematical Methods and Modelling for Students of Chemistry and Biology*, Hum, Zagreb, 2009, pp. 13–27
4. I. Gutman, *Int. J. Chem. Model.* **2** (2010) 335
5. I. Gutman, G. V. Milovanović, *Bull. Acad. Serb. Sci. Arts (Cl. Sci. Math. Natur.)* **143** (2011) 1
6. I. Gutman, N. Turković, J. Jovičić, *Monatsh. Chem.* **135** (2004) 1389
7. I. Gutman, B. Furtula, J. Đurđević, R. Kovačević, S. Stanković, *J. Serb. Chem. Soc.* **70** (2005) 1023
8. I. Gutman, S. J. Cyvin, *Introduction to the Theory of Benzenoid Hydrocarbons*, Springer-Verlag, Berlin, 1989
9. M. Randić, *Chem. Rev.* **103** (2003) 3449
10. A. T. Balaban, *Polycycl. Arom. Comp.* **24** (2004) 83
11. I. Gutman, J. Đurđević, A. T. Balaban, *Polycycl. Arom. Comp.* **29** (2009) 3
12. J. Đurđević, I. Gutman, J. Terzić, A. T. Balaban, *Polycycl. Arom. Comp.* **29** (2009) 90
13. I. Gutman, J. Đurđević, *J. Serb. Chem. Soc.* **74** (2009) 765
14. S. Jeremić, S. Radenković, I. Gutman, *J. Serb. Chem. Soc.* **75** (2010) 943
15. A. T. Balaban, I. Gutman, S. Jeremić, J. Đurđević, *Monatsh. Chem.* **142** (2011) 53
16. I. Gutman, A. T. Balaban, *J. Serb. Chem. Soc.* **76** (2011) 1505
17. I. Gutman, S. Marković, S. Jeremić, *Polycycl. Arom. Comp.* **30** (2010) 240
18. A. T. Balaban, J. Đurđević, I. Gutman, S. Jeremić, S. Radenković, *J. Phys. Chem., A* **114** (2010) 5870
19. A. T. Balaban, I. Gutman, S. Marković, D. Simijonović, J. Đurđević, *Polycycl. Arom. Comp.* **31** (2011) 339
20. A. T. Balaban, I. Gutman, S. Marković, D. Simijonović, *Monatsh. Chem.* **142** (2011) 797
21. I. Gutman, B. Furtula, A. T. Balaban, *J. Serb. Chem. Soc.* **76** (2011) 733
22. I. Gutman, *Indian J. Chem., A* **50** (2011) 670
23. I. Gutman, B. Stojanovska, *Maced. J. Chem. Chem. Eng.* **30** (2011) 235



24. *Electronic Materials: The Oligomer Approach*, K. Müllen, G. Wegner, Eds., Wiley-VCH, Weinheim, 1998
25. J. Wu, A. Pisula, K. Müllen, *Chem. Rev.* **107** (2007) 718
26. T. M. Figueira-Dharte, K. Müllen, *Chem. Rev.* **111** (2011) 7260.







## Removal of a cationic dye from water by activated pinecones

MILAN Z. MOMČILOVIĆ<sup>1\*</sup>, ANTONIJE E. ONJIA<sup>1</sup>, MILOVAN M. PURENOVIĆ<sup>2</sup>,  
ALEKSANDRA R. ZARUBICA<sup>2</sup> and MARJAN S. RANDELOVIĆ<sup>2</sup>

<sup>1</sup>The Vinča Institute of Nuclear Sciences, P. O. Box 522, University of Belgrade,  
11001 Belgrade, Serbia and <sup>2</sup>Department of Chemistry, Faculty of Sciences and  
Mathematics, University of Niš, Višegradska 33, 18 000 Niš, Serbia

(Received 17 May, revised 8 November 2011)

**Abstract:** Adsorption of a cationic phenoxyazine dye, Methylene Blue onto activated carbon prepared from pinecones was investigated. The parameters contact time, dye concentration and pH were varied. The kinetic data were found to follow closely the pseudo-second-order kinetic model. The equilibrium data were best represented by the Langmuir isotherm with a maximum adsorption capacity of 233.1 mg g<sup>-1</sup>. The adsorption was favored by using a higher solution pH. Textural analysis by nitrogen adsorption was used to determine the specific surface area and pore structure of the obtained carbon. Boehm titrations revealed that carboxylic groups were present in a high degree on the carbon surface. The results indicate that the presented method for activation of pinecones could yield activated carbon with significant porosity, a developed surface reactivity and a considerable adsorption affinity toward the cationic dye Methylene Blue.

**Keywords:** activated carbon; adsorption; kinetics; Methylene Blue.

### INTRODUCTION

Activated carbons are considered one of the most effective adsorbents with a wide range of applications due to their high surface areas, surface reactivity and large adsorption capacities. The structure of activated carbons was shown to be composed of microcrystallites consisting of fused hexagonal rings, the reactive edges of which contain a variety of functional groups.<sup>1</sup> The size of microcrystallites is influenced by the temperature of carbonization and the structure of the precursor.<sup>2</sup> For industrial production of activated carbons, carbonaceous precursors such as coconut shell, coal, wood and peat are used. However, since commercial activated carbons are rather expensive, some alternative precursors are required for the production of cheaper adsorbent with the same, or even better,

\*Corresponding author. E-mail: milanmomcilovic@yahoo.com  
doi: 10.2298/JSC110517162M

quality. The thermochemical conversion of waste biomass into activated carbon is a method of growing prominence in innovating economical solutions for activated carbon production. For this purpose, there are numerous studies on application of lignocellulosic waste biomass, such as: nutshells,<sup>3</sup> fruit stones of different origin,<sup>4,5</sup> sawdust,<sup>6</sup> cotton stalks,<sup>7</sup> corn stover,<sup>8</sup> corncob,<sup>9</sup> organic peel,<sup>10</sup> etc.

The European Black Pine (*Pinus nigra*) is a species of pine occurring across large areas of Europe and northwest Africa. It is a large evergreen tree that is frequently used as an ornament in parks. Its pinecones are 5–10 cm long, have rounded spirally arranged scales that contain a lot of lignin and resins. They usually fall from the tree in October and November. On park footpaths, they can be considered as municipal waste that has to be collected, transported and disposed of.

In this study, the cones of the European Black Pine were used for the preparation of powdered activated carbon, which was further characterized by its pore structure and surface chemistry. In addition, the batch adsorption of Methylene Blue (MB) onto the obtained carbon was investigated. MB (Fig. 1) is a basic cationic phenoxyazine dye that is commonly used as an adsorbate for the investigation of the adsorptive properties of novel activated carbons.

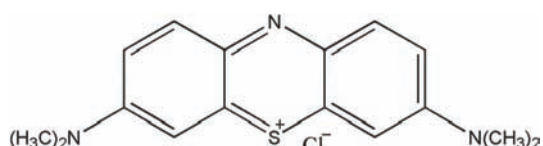


Fig. 1. Structural formula of Methylene Blue.

The goal of this study was to investigate isotherms and kinetics of adsorption of the cationic dye MB onto the powdered activated carbon obtained from pinecones. Pinecones were chosen since they are a low-cost and locally abundant raw material that can frequently emerge as a municipal waste. To the best of our knowledge, this material has not hitherto been used for the synthesis of activated carbon.

## EXPERIMENTAL

### *Preparation of pinecone activated carbon (PCAC)*

The pinecones were collected in Čair Park in Niš, Serbia. First, they were milled and sieved through a sieve of mesh size 0.841 mm. The cone dust was impregnated with 85 mass % H<sub>3</sub>PO<sub>4</sub> (Merck) in weight ratio of 1:1. The resulting slurry was transferred to several ceramic crucibles and placed in a programmable muffle furnace to undergo a two-stage activation process. The first stage was semi-carbonization with a heating rate of 6 °C min<sup>-1</sup> up to 170 °C and 60 min holding at this temperature. Subsequently, the heating was continued at a rate of 8 °C min<sup>-1</sup> up to 500 °C with a 60 min soaking time. Both stages were performed under a nitrogen flow of 100 cm<sup>3</sup> min<sup>-1</sup>. The product was cooled to room temperature, washed with 100 cm<sup>3</sup> of warm 0.1 M HCl and then with hot distilled water until the pH of the washings reached 5.3. After drying at 110 °C overnight, the material was crushed in a mortar and sieved through a

0.149 mm mesh sieve. The obtained black powder was denoted as PCAC and stored in an airtight bottle for further analysis.

#### *Physical characterization*

The surface morphology of the PCAC samples was analyzed before and after MB adsorption by scanning electron microscopy using a JEOL JSM 5300 microscope (Japan). The gold sputtered samples were placed in the SEM specimen chamber and observed at an accelerating voltage of 30 kV.

Nitrogen adsorption isotherms were determined at -196 °C using a Sorptomatic 1990 instrument (Thermo Fisher Scientific, USA). Before the measurements, the carbon samples were out-gassed for 4 h at room temperature, then for 8 h at 110 °C and finally 12 h at 200 °C. The specific surface area of the PCAC was calculated using the BET method.<sup>11</sup> The cumulative pore volume (cm<sup>3</sup> g<sup>-1</sup>), the median pore diameter (nm) and the area of the mesopores (m<sup>2</sup> g<sup>-1</sup>) were calculated using Barrett–Joyner–Halenda method.<sup>12</sup> The Dubinin–Radushkevich Equation was applied to obtain the micropore volume.<sup>13</sup>

The ash and moisture content analysis of the PCAC followed ASTM D 2866-94<sup>14</sup> and ASTM D 2867-04, respectively.<sup>15</sup>

#### *Surface chemistry characterization*

Oxygen-containing surface functional groups were determined according to the Boehm method.<sup>16</sup> PCAC samples (0.5 g) were placed in PVC bottles of 100 cm<sup>3</sup> capacity with 40 cm<sup>3</sup> of the following 0.1 M solutions: NaOH, Na<sub>2</sub>CO<sub>3</sub>, NaHCO<sub>3</sub> and HCl. The bottles were sealed and shaken for 24 h and then filtrated using Whatman 44 filter paper. Excess of residual base in 20 cm<sup>3</sup> of filtrates from the NaOH, Na<sub>2</sub>CO<sub>3</sub> and NaHCO<sub>3</sub> probes was pH-metrically titrated in open system using 0.1 M HCl standard solution. The excess residual acid in 20 cm<sup>3</sup> filtrate from the HCl probe was titrated using a 0.1 M standard NaOH solution. The reaction between the reagents and the acidic oxygen containing functional groups on the carbon surface is based on the difference in acid/base strength (carboxylic>lactonic>phenolic). It was assumed that NaOH neutralizes carboxylic, lactonic and phenolic groups; Na<sub>2</sub>CO<sub>3</sub>, carboxylic and lactonic groups; NaHCO<sub>3</sub>, carboxylic groups only. The phenolic groups were determined from the differences in the neutralization by NaOH and Na<sub>2</sub>CO<sub>3</sub>. The quantity of surface basic groups was calculated from the titration with 0.1 M HCl. A blank was not used in the analysis.

Carbon particles in an aqueous medium adsorb H<sup>+</sup> or OH<sup>-</sup> rendering their surface positively or negatively charged. The pH value when the carbon surface has zero net charge is known as pH<sub>PZC</sub>. The pH<sub>p.z.c.</sub> of the PCAC was determined by the modified pH drift method which can be described as follows: 30 cm<sup>3</sup> of 0.1 M KNO<sub>3</sub> solution was added to a series of PVC bottles and their pH values were adjusted in the range from 2 to 12 using small amounts of 0.01 M HCl and/or NaOH. When the pH values became constant, they were measured using a pH meter SensION3 (Hach, USA) and the values denoted as pH<sub>initial</sub>. Then, 0.1 g of carbon samples were added to the bottles that were then well-sealed and shaken for 24 h to reach equilibrium. After 24 h, the pH values of the suspensions were measured and denoted as pH<sub>final</sub>. pH<sub>p.z.c.</sub> is regarded as the pH value when pH<sub>initial</sub> is equal to pH<sub>final</sub>.<sup>17</sup>

#### *Batch adsorption experiments*

MB (C<sub>16</sub>H<sub>18</sub>CIN<sub>3</sub>S, CI = 52015, M<sub>r</sub> = 319.86 g mol<sup>-1</sup>, λ<sub>max</sub> = 662 nm) supplied by Riedel-de-Haen (Germany) was dried for 2 h at 90 °C prior to use. A stock solution of 1000 mg dm<sup>-3</sup> was prepared using distilled water and afterwards diluted to the required concentrations.

The adsorption equilibrium studies were performed by contacting 0.1 g of PCAC with 50 cm<sup>3</sup> of MB solutions, the initial concentrations of which were 300, 350, 400, 450 and 500 mg dm<sup>-3</sup>. The suspensions were stirred using a mechanical magnetic stirrer at 120 rpm in a set of stoppered Erlenmeyer flasks. After 60 min, the suspensions were filtered using filter paper Whatman 44 and the residual MB concentrations were determined by microprocessor-controlled photometer MultiDirect (Lovibond, Germany) at 660 nm. For kinetic studies, MB solutions of 400 mg dm<sup>-3</sup> were stirred in the same manner for 5 to 80 min. An interval of 60 min was established to be enough to reach equilibrium. The effect of solution pH was examined in the range from 3 to 10 by contacting 0.1 g of PCAC with 50 cm<sup>3</sup> of 400 mg dm<sup>-3</sup> MB solutions for 60 min. In all the cases, the adsorption capacity,  $q$  (mg g<sup>-1</sup>), was calculated as:

$$q = \frac{(c_0 - c) V}{W} \quad (1)$$

where  $c_0$  (mg dm<sup>-3</sup>) is the initial MB concentration,  $V$  (dm<sup>3</sup>) is the volume of the solution,  $W$  (g) is the mass of PCAC and  $c$  (mg dm<sup>-3</sup>) is the residual MB concentration at equilibrium or at any time  $\tau$  (min), which then defines  $q_e$  or  $q_\tau$  (mg g<sup>-1</sup>), respectively. The experimental data were fitted to kinetic and isotherm theoretical models.

All adsorption experiments were performed in triplicate at ambient temperature (25 °C) and the average value was used. The chemicals used in the whole study were reagent grade.

## RESULTS AND DISCUSSION

### *Physical characteristics*

Micrographs of the PCAC samples before and after adsorption of MB are shown in Fig. 2. The micrographs show that the adsorption process did not significantly change the morphology of the surface matrix of the carbon samples. However, slight differences in the number and shape of cracks and attached fine particles over the carbon surface are evident.

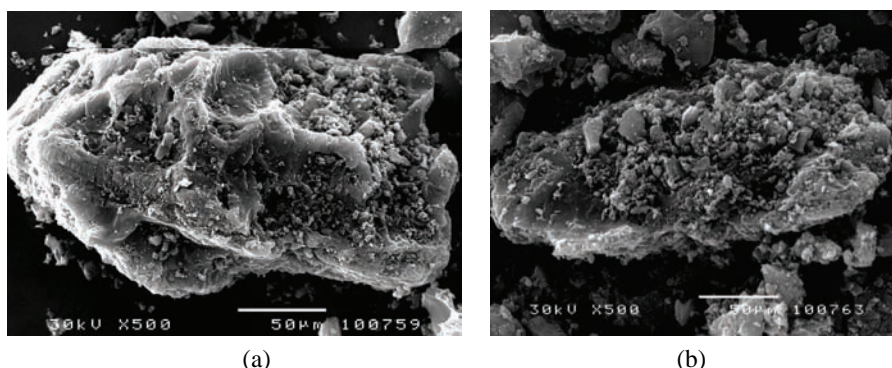


Fig. 2. SEM Micrographs of the carbon particles a) before and b) after MB adsorption.

A textural study revealed that the PCAC had a relatively high specific surface area, measured by nitrogen adsorption. The porosity characteristics and the determined MB adsorption capacities for the PCAC are given in Table I, together

with the corresponding values for other activated carbons obtained from various precursors.

TABLE I. Comparison of maximum MB adsorption capacities of carbons derived from various lignocellulosic precursors

Adsorbent	BET Specific surface area $\text{m}^2 \text{ g}^{-1}$	Mesopore volume $\text{cm}^3 \text{ g}^{-1}$	Micropore volume $\text{cm}^3 \text{ g}^{-1}$	Adsorption conditions	Adsorption capacity for MB $\text{mg g}^{-1}$
Activated sunflower oil cake <sup>25</sup>	240	0.0063	0.111	$c_{i(\text{MB})} = 0\text{--}250 \text{ mg dm}^{-3}$ adsorbent dose $2 \text{ g dm}^{-3}$ , $T = 25^\circ\text{C}$	16
Pinecone activated carbon (this work)	1094	0.70	0.395	$c_{i(\text{MB})} = 300\text{--}500 \text{ mg dm}^{-3}$ adsorbent dose $2 \text{ g dm}^{-3}$ $T = 25^\circ\text{C}$ , pH 6	233
Vetiver roots activated carbon <sup>21</sup>	1272	0.80	0.390	$c_{i(\text{MB})} = 50\text{--}300 \text{ mg dm}^{-3}$ adsorbent dose $400 \text{ mg dm}^{-3}$ , $T = 25^\circ\text{C}$ , pH 4–5	394
Bamboo-based activated carbon <sup>26</sup>	1355	0.14	0.485	$c_{i(\text{MB})} = 0\text{--}250 \text{ mg dm}^{-3}$ adsorbent dose $1 \text{ g dm}^{-3}$ $T = 25^\circ\text{C}$	183
Bituminous coal-based activated carbon <sup>27</sup>	875	/	0.390	$c_{i(\text{MB})} = 100\text{--}1000 \text{ mg dm}^{-3}$ , adsorbent dose $1 \text{ g dm}^{-3}$ , pH 4	298

### Surface chemistry

The characteristics of the pinecone activated carbon and the results of the Boehm titration are given in Table II. Functional groups are important since they determine the acid–base character of activated carbons. Their electrical charge may also influence the adsorption of target molecules. Carboxylic groups were the major oxygen-containing surface functional groups on the PCAC surface. Only a small number of phenolic groups were found. The neutralization with HCl revealed the total amount of basic groups and showed that the number of acidic groups present was more than double the number of basic groups, probably due to the production method that involved phosphoric acid as the activating agent. In comparison to other activated carbons, the PCAC possessed a high number of functional groups (Table III).

The result of the  $\text{pH}_{\text{p.z.c.}}$  determination is presented in Table II. The low  $\text{pH}_{\text{p.z.c.}}$  value is consistent with the results of the Boehm titrations, which showed a dominance of acidic groups at the surface of the PCAC. At native (unadjusted) pH of MB solution, the PCAC surface was most probably negatively charged, which leads to an electrostatic attraction between the carbons surface and the MB cation.

TABLE II. Characteristics of the studied pinecone activated carbon

Parameter	Value
Yield, %	55.7
pH <sub>D.Z.C.</sub>	3.06
Contact pH	3.51
Ash, %	6.35
Moisture, %	2.87
Density, g cm <sup>-3</sup>	1.58
Textural properties	
$S_{BET}$ / m <sup>2</sup> g <sup>-1</sup>	1094.1
Mesopore volume, cm <sup>3</sup> g <sup>-1</sup>	0.701
Mesopore area, m <sup>2</sup> g <sup>-1</sup>	481.65
Micropore volume, cm <sup>3</sup> g <sup>-1</sup>	0.395
Median pore diameter, nm	7.68
Surface functional groups, meq g <sup>-1</sup>	
Acidic groups	2.958
Carboxylic	1.742
Lactonic	0.723
Phenolic	0.493
Basic groups	1.357

TABLE III. Results of the Boehm titrations for activated carbons from various sources

Adsorbent	Synthesis parameters	Phenolic meq g <sup>-1</sup>	Lactonic meq g <sup>-1</sup>	Carboxylic meq g <sup>-1</sup>	Total acidic meq g <sup>-1</sup>	Total basic meq g <sup>-1</sup>
Jute fiber carbon <sup>28</sup>	Precursor: 15 % H <sub>3</sub> PO <sub>4</sub> 1:3, hot air oven, 12 h	0.045	0.01	0.025	0.08	–
Activated jackfruit peel waste <sup>29</sup>	Precursor: 85 % H <sub>3</sub> PO <sub>4</sub> 1:3, 550 °C, 45 min, N <sub>2</sub> , washing with warm distilled water	0.261	0.391	0.737	1.389	1.025
Pinecone activated carbon (this work)	Precursor: 85 % H <sub>3</sub> PO <sub>4</sub> 1:3, 500 °C, 60 min, N <sub>2</sub> , washing with warm HCl and distilled water	0.493	0.723	1.742	2.958	1.357
Activated sunflower oil cake <sup>25</sup>	Precursor: H <sub>2</sub> SO <sub>4</sub> 1:1.9, 600 °C, 120 min, N <sub>2</sub> , washing with hot and cold distilled water	0.362	0.125	0.325	0.812	–
Bamboo-based activated carbon <sup>26</sup>	Precursor: H <sub>3</sub> PO <sub>4</sub> 1:3, 600 °C, 90 min, N <sub>2</sub> , washing with distilled water	0.12	0.16	0.74	1.02	0.025

### Adsorption kinetics

The experiments of adsorption kinetics were performed to establish the effect of time on the adsorption process (Fig. 3). Four theoretical kinetic models were applied.

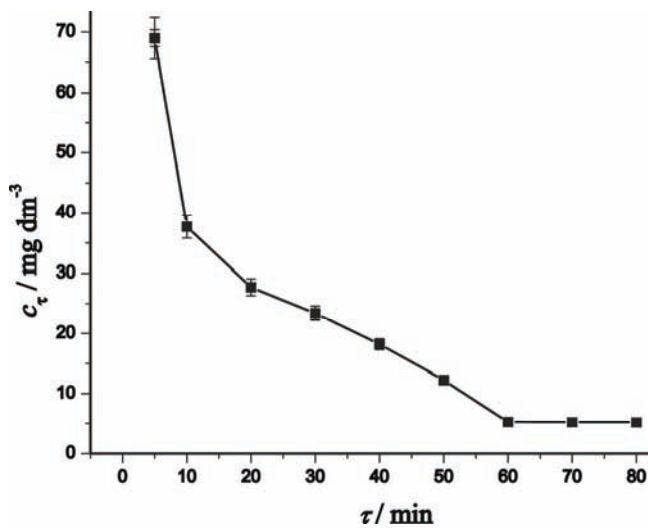


Fig. 3. Effect of contact time on MB adsorption by PCAC.

The pseudo-first-order kinetic model defined by Lagergren is one of the most used adsorption models defining the adsorption of an adsorbate from a solution.<sup>18</sup> It can be written as:

$$\ln(q_e - q_\tau) = \ln q_e - k_1 \tau \quad (2)$$

where  $k_1$  ( $\text{g mg}^{-1} \text{ min}^{-1}$ ) is the rate constant of pseudo-first-order adsorption. The values of  $k_1$  were obtained from the slopes of the linear plots of  $\ln(q_e - q_\tau)$  vs.  $\tau$  (Fig. 4a).

The pseudo-second-order kinetic model may be expressed as:

$$\frac{\tau}{q_\tau} = \frac{1}{k_2 q_e^2} + \frac{1}{q_e} \tau \quad (3)$$

where  $k_2$  ( $\text{g mg}^{-1} \text{ min}^{-1}$ ) is the equilibrium rate constant for a pseudo-second-order adsorption and was calculated from the plot of  $t/q_\tau$  against  $\tau$  (Fig. 4b).<sup>19</sup>

The Elovich model is represented as:

$$q_\tau = \frac{1}{\beta} \ln(\alpha\beta) + \frac{1}{\beta} \ln \tau \quad (4)$$

where  $\alpha$  ( $\text{mg g}^{-1} \text{ min}^{-1}$ ) and  $\beta$  ( $\text{g mg}^{-1}$ ) are constants of the adsorption and were determined from a plot  $q_\tau$  vs.  $\ln \tau$  (Fig. 4c).<sup>20</sup>

A Weber and Morris plot is used to examine the intraparticle diffusion model.<sup>21</sup> This model is defined by the following equation:

$$q_\tau = k_i \tau^{1/2} \quad (5)$$

where  $k_i$  is the constant of adsorption and was determined from a plot  $q_\tau$  vs.  $\tau^{1/2}$  (Fig. 4d).

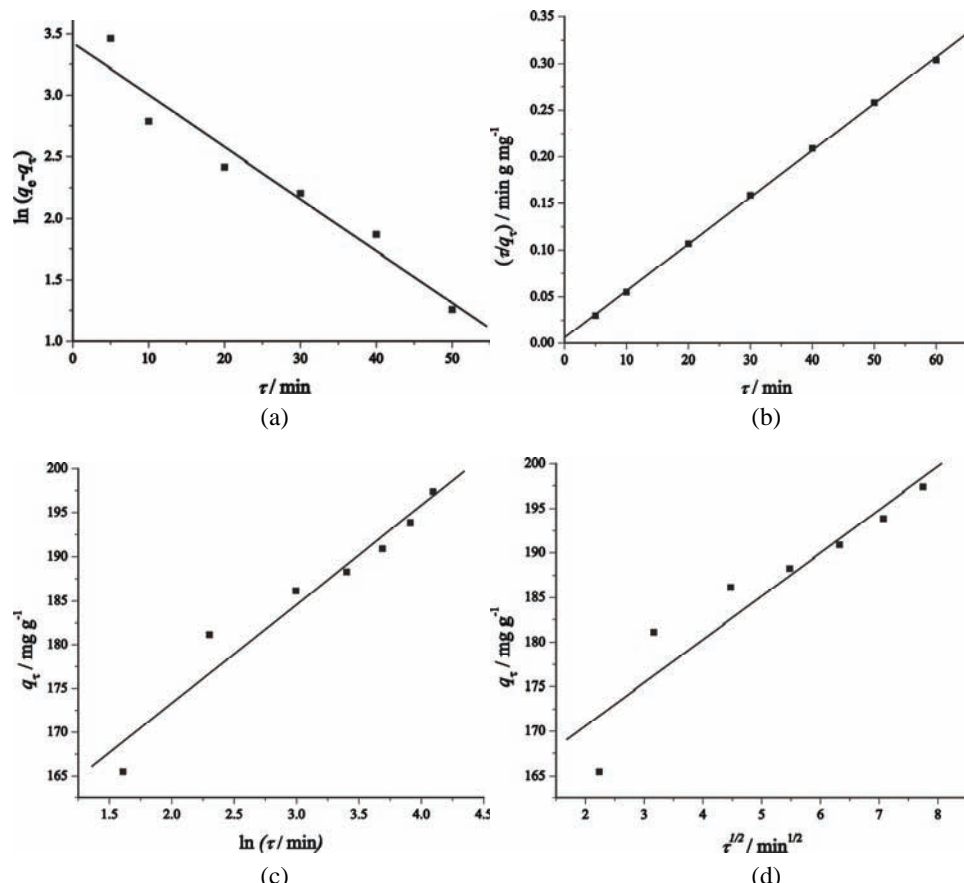


Fig. 4. Kinetic models for the adsorption of MB onto pinecone activated carbon: a) pseudo-first-order, b) pseudo-second-order, c) Elovich model and d) intraparticle diffusion model.

The validity of the exploited models is verified by the correlation coefficient,  $r^2$  (Table IV). The comparison of the  $r^2$  values for the different models implies that the pseudo-second-order kinetic model represents the data in the best way. Hence, it could be concluded that the overall rate of MB adsorption onto the PCAC was controlled by chemisorption processes. The establishment of chemical bonds

and the overlapping of orbitals is, thus, a very probable mechanism of binding of MB to the carbon surface.

TABLE IV. Kinetic parameters for the adsorption of MB onto pinecone activated carbon

Kinetic model	Value
Pseudo-first-order	
$k_1 / \text{g mg}^{-1} \text{ min}^{-1}$	-0.04229
$r^2$	0.97221
Pseudo-second-order	
$k_2 / \text{g mg}^{-1} \text{ min}^{-1}$	0.004
$q_e / \text{mg g}^{-1}$	199.2
$r^2$	0.999
Elovich Equation model	
$\alpha / \text{mg g}^{-1} \text{ min}^{-1}$	7368133
$B / \text{g mg}^{-1}$	0.088
$r^2$	0.971
Intraparticle diffusion model	
$k_i / \text{g mg}^{-1} \text{ min}^{-1}$	4.853
$r^2$	0.937

#### Adsorption isotherms

Adsorption isotherms are used as a function of adsorbate concentration on the adsorbent surface at a constant temperature (Fig. 5). In this study, the equilibrium data were analyzed by considering the linearized Langmuir, Freundlich and Temkin isotherm model equations.

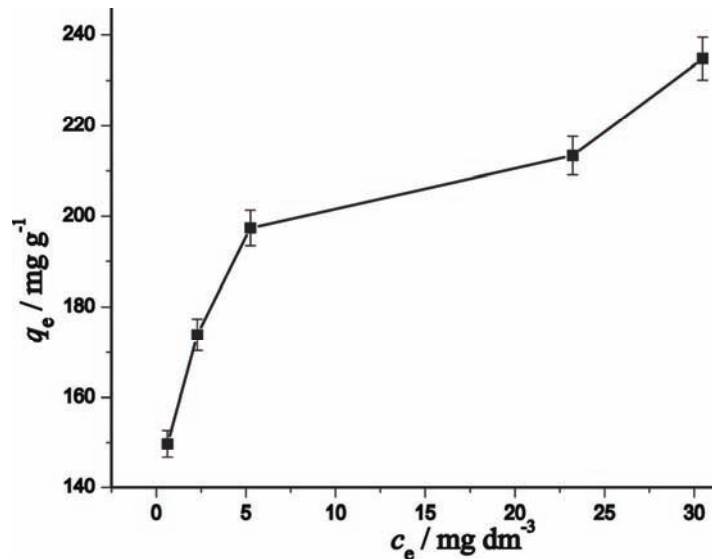


Fig. 5. Adsorption isotherm of MB by PCAC at 25 °C.

The Langmuir isotherm model is given below:

$$\frac{c_e}{q_e} = \frac{1}{q_{\max} K_L} + \frac{1}{q_{\max}} c_e \quad (6)$$

where  $K_L$  is the Langmuir equilibrium constant ( $\text{dm}^3 \text{ mg}^{-1}$ ) and  $q_{\max}$  ( $\text{mg g}^{-1}$ ) is the maximum adsorption capacity (Fig. 6a).<sup>22</sup> The most important feature of Langmuir isotherm is called the Separation Factor,  $R_L$ , which is defined as:

$$R_L = \frac{1}{1 + K_L c_0} \quad (7)$$

The value of the Separation Factor defines the types of isotherms: unfavorable ( $R_L > 1$ ), linear ( $R_L = 1$ ), irreversible ( $R_L = 0$ ), and favorable  $0 < R_L < 1$ .

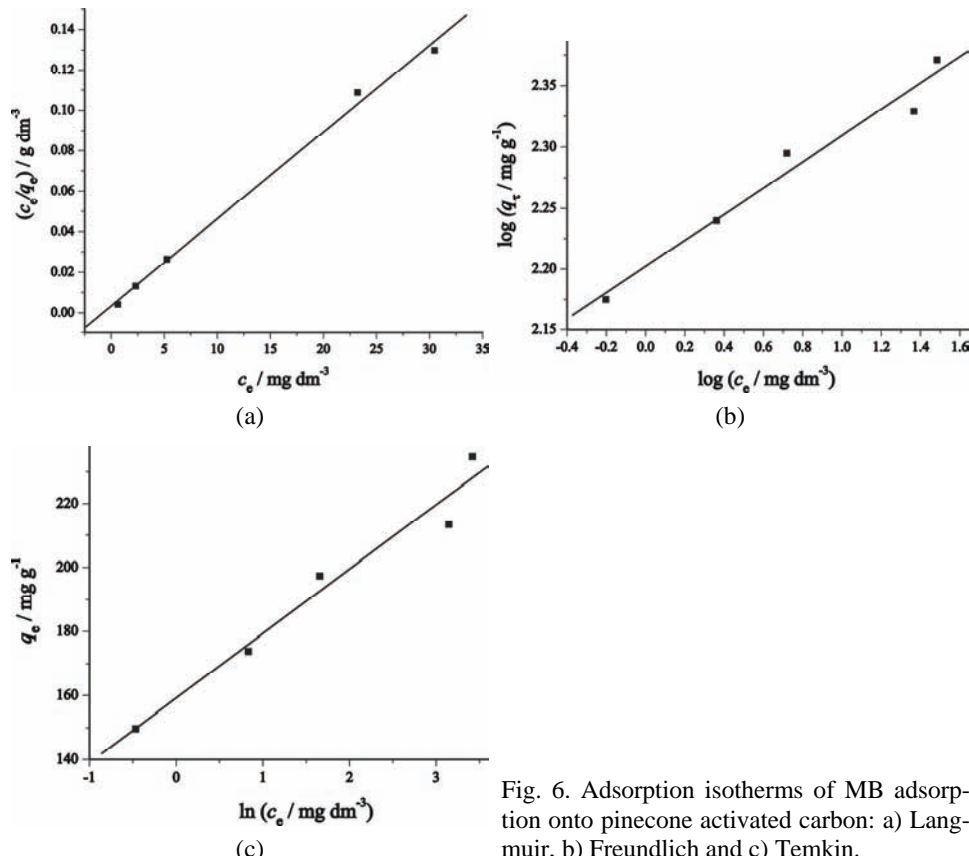


Fig. 6. Adsorption isotherms of MB adsorption onto pinecone activated carbon: a) Langmuir, b) Freundlich and c) Temkin.

The Freundlich adsorption isotherm is based on the adsorption onto heterogeneous surfaces.<sup>27</sup> The equation of the Freundlich adsorption isotherm is:

$$\ln q_e = \ln K_F + \frac{1}{n} \ln c_e \quad (8)$$

where  $K_F$  ((mg g<sup>-1</sup>) (dm<sup>3</sup> mg<sup>-1</sup>)<sup>1/n</sup>) is the Freundlich constant and  $n$  is Freundlich exponent, which were determined from the plot shown in Fig. 6b.

The Temkin isotherm is represented by the following equation:

$$q_e = A + B \ln c_e \quad (9)$$

where  $A$  and  $B$  (dm<sup>3</sup> g<sup>-1</sup>) are constants easily determined from a plot of  $q_e$  vs.  $c_e$  (Fig. 6c).<sup>24</sup>

The Langmuir isotherm fits quite well with the experimental data quite well ( $r^2 = 0.997$ ) whereas the lower correlation coefficients ( $r^2 = 0.984$  and  $r^2 = 0.852$ ) show that the agreement of the Freundlich and Temkin isotherms with the experimental data was worse (Table V). The Langmuir isotherm assumes a monolayer adsorption onto the carbon surface containing a finite number of adsorption sites. The adsorption process is supposed to be uniform with no transmigration of the adsorbate in the plane of the surface.

TABLE V. The equilibrium model parameters for the adsorption of MB onto pinecone activated carbon

Equilibrium model	Value
Langmuir isotherm	
$K_L$ / dm <sup>3</sup> g <sup>-1</sup>	1.262
$q_{\max}$ / mg g <sup>-1</sup>	233.1
$R_L$	0.0016
$r^2$	0.997
Freundlich model	
$K_F$ / (mg g <sup>-1</sup> ) (dm <sup>3</sup> mg <sup>-1</sup> ) <sup>1/n</sup>	159.24
$n$	9.3248
$r^2$	0.984
Temkin isotherm	
$A$	159.21
$B$ / dm <sup>3</sup> g <sup>-1</sup>	20.156
$r^2$	0.852

Table III indicates that the activated carbon studied in this work showed a considerably large adsorption capacity for MB along with a high specific surface area and mesopore volume.

#### Influence of pH on adsorption

The pH of the solution was reported to be a significant factor that influences the adsorption of MB as it controls the electrostatic interactions between the carbon surface and adsorbate.<sup>25</sup> The pH of the suspension in all kinetic and equilibrium experiments was 6.3. In the case of different pH values, it was estab-

blished that the adsorption of MB increased with the increasing pH (Fig. 7). Lower adsorption of MB at acidic pH is due to the presence of excess H<sup>+</sup> that compete with the MB cations for the adsorption sites. As the surface becomes less positive with increasing suspension pH, the electrostatic repulsion of the MB cations is lower, which results in a higher adsorption. At pH values higher than the pH<sub>p.z.c.</sub>, the surface is considered to be negatively charged with predominantly strong electrostatic attraction towards the MB cations.

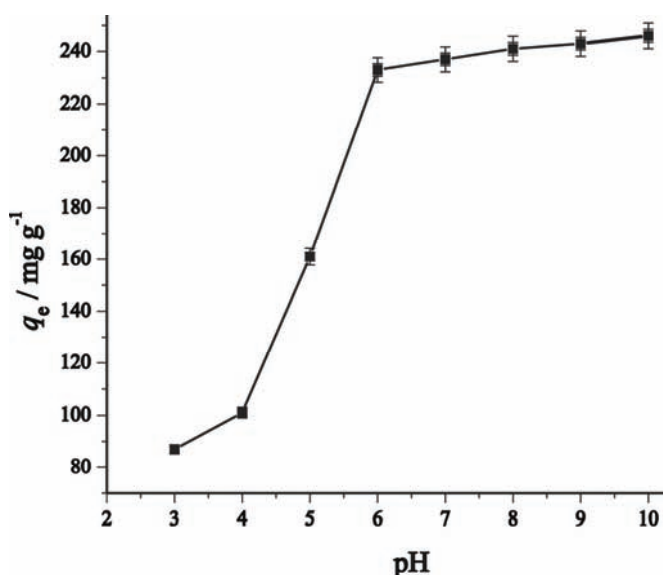


Fig. 7. Effect of pH on the adsorption of MB onto pinecone activated carbon.

#### CONCLUSIONS

In this work, pinecones were efficiently utilized as the raw material for the production of activated carbon with a high specific surface area. The adsorption experiments showed a significant adsorption affinity of the PCAC towards MB with maximum adsorption capacity of 233.1 mg g<sup>-1</sup>. The adsorption of MB onto the carbon particles was found to be a fast process that reaches equilibrium in 60 min. The results of the kinetic study were best fitted by the pseudo-second-order model, which suggests the establishment of chemical bonds between MB and the carbon surface (chemisorption). The equilibrium data agreed well with the Langmuir isotherm model, implying a monolayer adsorption. The obtained  $R_L$  value for the adsorption of MB onto the PCAC was less than 1 and greater than zero, indicating favorable adsorption. Increasing the suspension pH led to a higher uptake of MB because protons compete with the MB cations for the adsorption sites under acidic conditions. The Boehm titration revealed that most of the acidic groups on the carbon surface were carboxyl groups followed by lactonic and

phenolic groups. SEM images showed that the adsorption of MB did not change the carbon surface significantly.

*Acknowledgements.* The authors are grateful to the Ministry of Education and Science of the Republic of Serbia for financial support of this research through Project III 43009.

#### ИЗВОД

#### УКЛАЊАЊЕ КАТЈОНСКЕ БОЈЕ ИЗ ВОДЕ ПОМОЋУ АКТИВИРАНИХ БОРОВИХ ШИШАРКИ

МИЛАН З. МОМЧИЛОВИЋ<sup>1</sup>, АНТОНИЈЕ Е. ОЊИА<sup>1</sup>, МИЛОВАН М. ПУРЕНОВИЋ<sup>2</sup>,  
АЛЕКСАНДРА Р. ЗАРУБИЦА<sup>2</sup> и МАРЈАН С. РАНЂЕЛОВИЋ<sup>2</sup>

<sup>1</sup>Институут за нуклеарне науке „Винча“, Ј. Џр. 522, 11001 Београд и <sup>2</sup>Одсек за хемију, Природно-математички факултет, Универзитет у Нишу, Вишеградска 33, 18000 Ниш

Адсорпција катјонске фенотиазинске боје метилен плаво на активном угљу добијеном из шишарке црног бора је испитана уз промену времена контакта, концентрације боје и pH вредности. Утврђено је да се подаци кинетичких испитивања најбоље слажу са моделом псевдо-другог реда. Подаци равнотежних испитивања се најбоље поклапају са Ленгмировим моделом уз максимални адсорpcionи капацитет од  $233,1 \text{ mg g}^{-1}$ . Адсорпција је фаворизована на вишем pH вредностима. Текстурална анализа извршена проучавањем адсорпције азота је искоришћена да се одреди специфична површина и структура пора добијеног материјала. Боемове титрације су доказале да су карбоксилне групе присутне у највећој мери од свих киселих кисеоничних група на површини активног угља. Резултати ове студије указују да се описаном методом за активацију борових шишарки може добити активни угљ који има значајну порозност, развијену површинску реактивност и висок адсорpcionи капацитет према катјонској боји метилен плаво.

(Примљено 18. маја, ревидирано 8. новембра 2011)

#### REFERENCES

1. S. D. Faust, O. M. Aly, *Chemistry of water treatment*, 2<sup>nd</sup> ed., Taylor and Francis Group, London, UK, 1998, p.134
2. J. W. Hassler, *Activated Carbon*, Chemical Publishing, New York, 1974, p. 85
3. J. H. T. Horikawa, I. Takeda, K. Muroyama, F. N. Ani, *Carbon* **40** (2002) 2381
4. M. G. Lussier, J. C. Shull, D. J. Miller, *Carbon* **32** (1994) 1493
5. M. Soleimani, T. Kagazchi, *Bioresour. Technol.* **99** (2008) 5374
6. C. Srinivasakannan, M. Z. A. Bakar, *Biomass Bioenergy* **27** (2004) 89
7. K. Li, Z. Zheng, Y. Li, *J. Hazard. Mater.* **181** (2010) 440
8. M. Fan, W. Marshall, D. Daugaard, R. C. Brown, *Bioresour. Technol.* **93** (2004) 103
9. A.-N. A. El-Hendawy, S. E. Samrab, B. S. Girgis, *Colloids Surf., A* **180** (2001) 209
10. E. S. Z. El-Ashtoukhy, N. K. Amin, O. Abdelwahab, *Desalination* **223** (2008) 162
11. S. Brunauer, P. H. Emmett, E. Teller, *J. Am. Chem. Soc.* **60** (1938) 309
12. E. P. Barrett, L. G. Joyner, P. P. Halenda *J. Am. Chem. Soc.* **73** (1951) 373
13. F. Rouquerol, J. Rouquerol, K. Sing, *Adsorption by powders and porous solids*, Academic Press, London, UK, 1999, p. 111
14. ASTM D 2866-94, *Standard Test Method for Total Ash content of Activate Carbon*, ASTM International, West Conshohocken, PA, USA, 1996

15. ASTM D 2867-95, *Standard Test Method for Moisture in Activate Carbon*, ASTM International, West Conshohocken, PA, USA, 1996
16. S. L. Goertzen, K. D. Theriault, A. M. Oickle, A. C. Tarasuk, H. A. Andreas, *Carbon* **48** (2010) 1252
17. D. Prahas, Y. Kartika, N. Indraswati, S. Ismadji, *Chem. Eng. J.* **140** (2008) 32
18. M. Dogan, H. Abak, M. Alkan, *J. Hazard. Mater.* **164** (2009) 172
19. A. S. Franca, L. S. Oliveira, M. E. Ferreira, *Desalination* **249** (2009) 267
20. F. Wu, R. Tseng, R. Juang, *Chem. Eng. J.* **150** (2009) 366
21. S. Altenor, B. Carene, E. Emmanuel, J. Lambert, J. Ehrhardt, S. Gaspard, *J. Hazard. Mater.* **165** (2009) 1029
22. Y. Liu, *Colloids Surf., A* **274** (2006) 34
23. C. A. Coles, R. N. Yong, *Eng. Geol.* **85** (2006) 19
24. B. H. Hameed, A. A. Ahmad, *J. Hazard. Mater.* **164** (2009) 870
25. S. Karagoz, T. Tay, S. Ucar, M. Erdem, *Bioresour. Technol.* **99** (2008) 6214
26. Q. Liu, T. Zheng, N. Li, P. Wang, G. Abulikemu, *Appl. Clay Sci.* **56** (2010) 3309
27. E. N. El Qada, S. J. Allen, G. M. Walker, *Chem. Eng. J.* **124** (2006) 103
28. S. Senthilkumaar, P. R. Varadarajan, K. Porkodi, C. V. Subbhuraam, *J. Colloid Interface Sci.* **284** (2005) 78
29. D. Prahas, Y. Kartika, N. Indraswati, S. Ismadji, *Chem. Eng. J.* **140** (2008) 32.



*J. Serb. Chem. Soc.* 77 (6) 775–788 (2012)  
JSCS-4308

# Journal of the Serbian Chemical Society

JSCS-info@shd.org.rs • www.shd.org.rs/JSCS

UDC 628.161.2:546.19+547:543.62

Original scientific paper

## Separation and determination of dimethylarsenate in natural waters

NUREDDIN BEN ISSA\*, ALEKSANDAR D. MARINKOVIĆ\*#  
and LJUBINKA V. RAJAKOVIĆ#

Faculty of Technology and Metallurgy, University of Belgrade, Kariđelova 4,  
11120 Belgrade, P. O. Box 3503, Serbia

(Received 11 May 2011, revised 1 February 2012)

**Abstract:** A simple and efficient method for the separation and determination of dimethylarsenate DMAAs(V) was developed in this work. Two resins, a strong base anion exchange (SBAE) resin and iron-oxide coated hybrid (HY) resin were tested. By simple adjustment of the pH value of water to 7.00, DMAAs(V) passed through the HY column without any changes, while all other arsenic species (inorganic arsenic and monomethylarsonate, MMAAs(V)) were quantitatively bonded on the HY resin. The resin capacity was calculated according to the breakthrough point in a fixed bed flow system. At pH 7.00, the HY resin bonded more than 4150 µg g<sup>-1</sup> of As(III), 3500 µg g<sup>-1</sup> of As(V) and 1500 µg g<sup>-1</sup> of MMAAs(V). Arsenic adsorption behavior in the presence of impurities showed tolerance with the respect to potential interference of anions commonly found in natural water. DMAAs(V) was determined in the effluent by inductively coupled plasma mass spectrometry (ICP-MS). The detection limit was 0.03 µg L<sup>-1</sup> and the relative standard deviation (*RSD*) was between 1.1–7.5 %. The proposed method was established by application of standard procedures, *i.e.*, using an external standard, certified reference material and by the standard addition method.

**Keywords:** arsenic species; dimethylarsenate; hybrid resin; exchange; adsorption; inductively coupled plasma mass spectrometry (ICP-MS).

### INTRODUCTION

Arsenic is typically found in areas with active volcanism, geothermal waters, soil and bedrock.<sup>1–3</sup> Traces of arsenic are found in groundwater, lakes, rivers and ocean water. It is also released during human activities in areas of wood preservation, agriculture, mining<sup>3</sup> and energy production from fossil fuels.<sup>2,3</sup> Many water sources in the world containing high concentration of arsenic cause health

\* Corresponding author. E-mail: marinko@tmf.bg.ac.rs

# Serbian Chemical Society member.

• On sabbatical leave at the University of Belgrade.

doi: 10.2298/JSC110510010B

problems or diseases such as cancer.<sup>3–7</sup> The provisional guideline value for arsenic in drinking water of the World Health Organization, WHO, is  $10 \mu\text{g L}^{-1}$  (WHO, 1993). Inorganic arsenic, iAs, has two predominant oxidation states in most environmental systems, As(III) and As(V), which are mostly in the form of acids.<sup>8</sup> Organic arsenic, oAs, such as monomethyl-arsenic acid [MMA<sub>s</sub>(V)] and dimethylarsenic acid [DMA<sub>s</sub>(V)] are predominant in surface water and sediments.<sup>9</sup>

Both oAs [DMA<sub>s</sub>(V) and MMA<sub>s</sub>(V)] are stable in oxidative environments, and could be found in the marine water and biological samples.<sup>10</sup> Despite the fact that iAs species are predominant in natural waters, the presence of oAs has also been reported.<sup>11</sup> The toxicity of oAs species is lower than iAs species.<sup>12,13</sup> Although the main analytical interest is to determine total arsenic in water and prevailing iAs species, it is also important to develop procedures for the separation and determination of oAs species. The distribution of oAs species as a function of pH value of water is presented in Fig. 1.

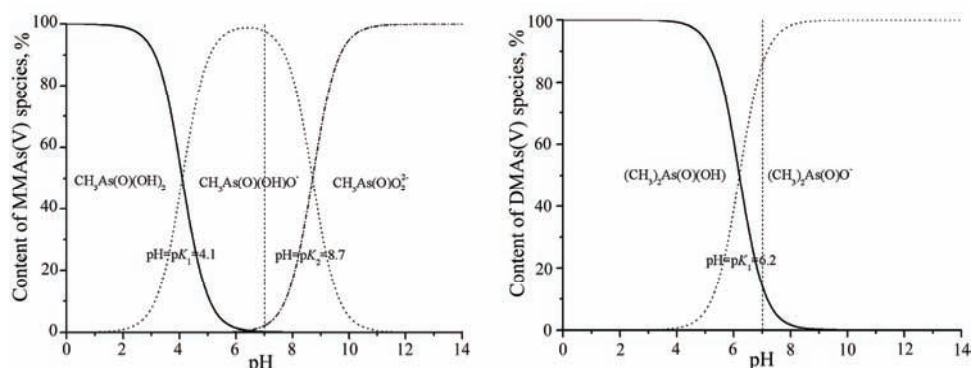


Fig. 1. Speciation of oAs compounds as a function of pH.

The investigation of the content of arsenic species and their behavior in natural waters and environment is important for chemistry and environmental protection. Several methods have been developed for the separation and measurement of arsenic species.

The most common method used to provide detection at low arsenic concentration is the hydride generation technique<sup>15–18</sup> connected with sensitive detection devices such as atomic absorption, fluorescence and atomic emission.<sup>19</sup> Inductively coupled plasma mass spectrometry (ICP–MS) and ICP optical emission spectroscopy (ICP–OES) techniques provides very low detection limits, with a greater accuracy of mass spectra detector than optical methods. The intensity of the arsenic emission is obtained by the sample entering into an ionized plasma thus producing As<sup>75</sup>. Ion chromatography<sup>20,21</sup> (IC) or ion exchange chromatographic<sup>22,23</sup> methods were coupled with ICP to provide separation and determination of arsenic species.

High-pressure liquid chromatography (HPLC) is the preferred technique used for the separation of arsenic compounds. An HPLC–ICP–MS system was used for the separation and measurement of iAs, oAs, arsenobetaine (AsB) and arsenocholine (AsC) in beer samples by the employment of an anion-exchange column using phosphate buffer as the mobile phase and perchloric acid as the extraction reagent.<sup>24</sup> Similar methods were developed using phosphate buffer with the addition of 2.0 % acetonitrile,<sup>25</sup> and using ICP atomic emission spectroscopy (ICP–AES).<sup>26</sup> An HPLC–ICP–MS system was also used for the quantification of iAs and oAs in rice and soil, whereas AsB and DMA<sub>n</sub>(V) and an unknown arsenic species were quantified in a chicken tissue.<sup>27</sup> In addition to these, pre-column reduction and complexation of As(V), MMA<sub>n</sub>(V) and DMA<sub>n</sub>(V) with L-cysteine at elevated temperature, followed by HPLC separation of the complexes on a strongly acidic cation-exchange column, and arsenic species determination by flow injection hydride generation atomic absorption spectrometry (FI–HGAAS) was achieved.<sup>28</sup> Lopez *et al.*<sup>29</sup> applied post-column derivatization by mixing an HPLC effluent with a persulfate stream before entering into thermo-reactor consisting of a loop of PTFE tubing dipped in a powdered-graphite oven heated at 140 °C. After cooling in an ice-bath, hydrochloric acid and sodium borohydride were added on-line to generate the arsine. Rahman *et al.*<sup>30</sup> achieved good separation results using SPE sorbents (polymeric organic materials comprising an ion-selective sequestering property based on molecular recognition and macrocyclic chemistry) which were coupled with graphite furnace atomic absorption spectrometry (GF–AAS). Additionally, gas chromatography (GC) was used for the determination of arsenic species in seawater. The DMA<sub>n</sub>(V) and MMA<sub>n</sub>(V) were derivatized in the sample solutions with methyl thioglycolate and the products were extracted into cyclohexane and used for the analysis.<sup>31</sup>

Moreover, a method based on the transformation of arsenic species to a colored compound using ammonium diethyldithiocarbamate (ADDC), and silver diethyl-dithiocarbamate (SDDC) is widely used.<sup>12,32</sup> Electrical differential pulse cathodic or anodic stripping voltammetry are methods that have very low detection limits.<sup>33–35</sup>

Ben Issa *et al.*<sup>22,23</sup> studied the separation and determination of iAs and oAs species in drinking water. For the separation of iAs and oAs, two types of resins, a strong basic anion exchange resin (SBAE) and hybrid resins (HY–Fe and HY–AgCl) were used. The HY–Fe and SBAE resins retained all arsenic species except DMA<sub>n</sub>(V) and As(III), respectively, which enabled the direct measurements of these species in the effluents. An HY–AgCl resin retained all iAs, which was convenient for the direct determination the concentration of oAs species in the effluent.<sup>23</sup>

As a continuation of previous work,<sup>22</sup> a method for the separation and determination of DMA<sub>n</sub>(V) using an HY resin was developed and is presented in this

paper. The hybrid system, which integrates anion exchange with adsorption, is based on the activity of hydrated iron oxides (HFO) adopted for the separation of iAs.<sup>36</sup> The hybrid resin could also be used for the selective removal of MMAs(V), thus providing separation of DMAAs(V). Although DMAAs(V) is less toxic than iAs, nevertheless, the determination of the DMAAs(V) concentration could be of appropriate significance for a better control of environmental pollution.

## EXPERIMENTAL

### Apparatus

Arsenic was analyzed by ICP–MS following the EPA method 200.8<sup>37</sup> using an Agilent 7500ce ICP–MS system (Waldbronn, Germany) equipped with an octopole collision/reaction cell, Agilent 7500 ICP–MS ChemStation software, a MicroMist nebulizer and a Peltier cooled (2.0 °C) quartz Scott-type double pass spray chamber. Calibration at levels 1.0–80.0 µg L<sup>-1</sup> was performed with an external standard solution (Fluka, Product No. 01969) by appropriate dilution. The slope of the calibration curve was 0.9999. The calibration blank and standards were prepared in 2.0 % nitric acid for all measurements. The instrument was optimized daily in terms of sensitivity, level of oxide and doubly charged ions using a tuning solution containing 1.0 µg L<sup>-1</sup> of Li, Y, Tl, Ce, Co and Mg in 2.0 % HNO<sub>3</sub> (v/v). Standard optimization procedures and criteria specified in the manufacturer's manual were followed. The sample solutions were filtered through a Millipore 0.45 µm membrane filter (Bedford, MA, USA) before injection.

The analytical accuracy and precision of the measurements were determined by analysis of certified reference materials NRC SLRS4 (Ottawa, ON, Canada) and NIST 1643e (Gaithersburg, MD, USA). The method detection limit (*MDL*) was 0.03 µg L<sup>-1</sup>.

A laboratory pH meter, Metrohm 827 (Zofingen, Switzerland) was used for the pH measurements. The accuracy of the pH meter was ±0.01 pH units.

### Reagents

The following chemical were used: HAsO<sub>2</sub>(CH<sub>3</sub>)<sub>2</sub> *p.a.*, Sigma–Aldrich (St. Louis, MO, USA); Na<sub>2</sub>AsO<sub>3</sub>CH<sub>3</sub>·6H<sub>2</sub>O *p.a.*, Sigma–Aldrich; Na<sub>2</sub>HAsO<sub>4</sub>·7H<sub>2</sub>O *p.a.*, Aldrich (Munich, Germany); NaAsO<sub>2</sub> *p.a.*, Riedel-de Haën (Buchs, Switzerland); HNO<sub>3</sub> *p.a.*, Fluka and NaOH *p.a.*, Merck. Ultra-pure water (resistivity less than 18 MΩ cm<sup>-1</sup>) produced by a Millipore Milli-Q system was used throughout the experimental work.

### Standard solutions of arsenic compounds

A monomethylarsonate, MMAs(V), working stock solution was made by dissolving 389.3 mg of Na<sub>2</sub>AsO<sub>3</sub>CH<sub>3</sub>·6H<sub>2</sub>O to 1.0 L in deionized water (100.0 mg L<sup>-1</sup> stock solution). A dimethylarsenate, DMAAs(V), working stock solution was made by dissolving 184.0 mg of HAsO<sub>2</sub>(CH<sub>3</sub>)<sub>2</sub> to 1.0 L in deionized water (100.0 mg L<sup>-1</sup> stock solution).

An As(III) stock solution (3750.0 mg L<sup>-1</sup>) was prepared by dissolving 4.9460 g sodium arsenite (NaAsO<sub>2</sub>) and 1.30 g NaOH to 1.0 L in deionized water, stored in an amber bottle at 4 °C. Under these conditions, this working stock solution was found to be stable for at least one year. An As(V) working stock solution was made by dissolving 4.1600 g Na<sub>2</sub>HAsO<sub>4</sub>·7H<sub>2</sub>O to 1.0 L in deionized water (1000.0 mg L<sup>-1</sup> stock solution), which was preserved with 0.50 % HNO<sub>3</sub>.

### *Ion exchange and hybrid resins*

The study of the separation and determination of arsenic species was performed by the use of two types of resins: SBAE and HY. SBAE resin is a strong base anionic exchange resin, Lewatit MonoPlus M500, Lanxess (Leverkusen, Germany), which is a gel-type resin based on a styrene–divinylbenzene copolymer with uniform, spherical (monodisperse), light yellow particles of 0.61 mm mean bead size. The HY resin is a hybrid macroporous monodisperse polystyrene-based resin, FO36, Lanxess with spherical, brown particles, mean bead size of 0.35 mm.<sup>35</sup> HY is a new hybrid resin developed for the removal of arsenic species based on two processes: ion exchange and adsorption.

### *Sorption procedures*

Measurements of the resin capacities were performed by two methods, *i.e.*, the standard batch and fixed bed flow techniques. In a preliminary study, evaluation of separation process efficiencies with respect to several parameters, such as pH, contact time, mass of resin and arsenic concentration, was studied. The arsenic model solution was prepared in deionized water at a concentration ranging from 0.50 to 100.0 mg L<sup>-1</sup> in the batch system and 0.50 to 5000.0 µg L<sup>-1</sup> in the fixed bed flow system.

Sorption experiments was conducted in a batch system operating under the following condition: 100 ml of an arsenic model solution with 1.0 g of resin were placed in an Erlenmeyer flask and the mixture was shaken ( $\omega = 150$  rpm) using an orbital laboratory shaker (Rotamax 120, Heidolph Instruments, Kelheim, Germany) for different times up to 12 h at room temperature. The pH was varied from 3.00 to 12.00 by adjustment with 0.1 M HCl or 0.1 M NaOH.

In the fixed bed flow system, a column of diameter 2.00 cm and length 30 cm was employed. The flow rate,  $Q$ , mass of resins,  $m$ , and empty bed volume,  $EBV$ , were adjusted to obtain the optimal time of contact,  $\tau$ , for the ion exchange/sorption. The conditions in the flow system were the following:  $Q = 1.66\text{--}2.00$  mL min<sup>-1</sup>,  $m_{\text{resin}} = 6.0\text{--}10$  g,  $EBV = 11.0\text{--}12.5$  mL,  $\tau = 6.6\text{--}7.50$  min.

### *Water samples*

Water samples were collected from the domestic tap water and wastewater from drainage channels (Vojvodina region in Serbia). Modified water was prepared by addition of ions of interest, usually present in natural water, to study the influence of their appropriate concentrations on the separation and determination of arsenic species by the proposed method. All water samples were filtered through a 0.25 µm membrane filter and collected in polyethylene bottles; if it was necessary to store for a prolonged time, the samples were acidified with HNO<sub>3</sub> and stored at 4.0 °C.

## RESULTS AND DISCUSSION

### *Preliminary investigations*

The influence of pH on the separation of arsenic species was studied in the pH range from 3.00 to 12.00, and the results are given in Fig. 2. Separation of the iAs and oAs species both at a concentration of 100 mg L<sup>-1</sup> was conducted using HY and SBAE resins in the batch system operating under the following condition: contact time  $\tau = 60$  min and shaker speed  $\omega = 150$  rpm at room temperature.

The resin capacity was calculated according to Eq. (1):

$$q = \frac{c_i - c_f}{m} V \quad (1)$$

where  $q$  is a sorption capacity in  $\mu\text{g g}^{-1}$ ,  $c_i$  is initial arsenic concentration in  $\text{mg L}^{-1}$ ,  $c_f$  is equilibrium arsenic concentration in  $\mu\text{g L}^{-1}$ ,  $V$  is the volume of the model solution in L and  $m$  is the mass of resin in g. All capacities measurements were realized in triplicate.

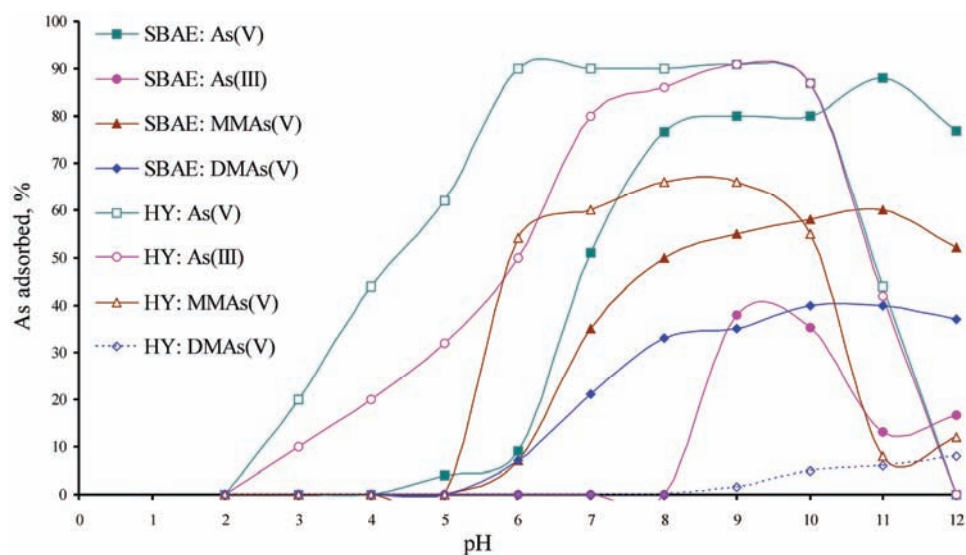


Fig. 2. Efficiency of arsenic adsorption on HY and SBAE resins *vs.* pH. Conditions:  
 $c_{\text{As(III)}} = c_{\text{As(V)}} = c_{\text{MMAAs(V)}} = c_{\text{DMAAs(V)}} = 100.0 \text{ mg L}^{-1}$ ,  $m_{\text{resin}} = 1.00 \text{ g}$ ,  $t = 20^\circ\text{C}$ ,  
 $V = 100 \text{ mL}$ ,  $\tau = 60 \text{ min}$ ,  $\omega = 150 \text{ rpm}$ .

The results presented in Fig. 2 show that the arsenic separation by the use of HY and SBAE resins was highly affected by the pH value. The adsorption of DMAAs(V) on SBAE started at pH 5.00 and on HY resin at pH 8.00. DMAAs(V) exists as neutral species at pH < 6.00 (Fig. 1), or even as cations in strongly acidic media, and thus deionized DMAAs(V) showed low affinity with respect to both resins. Bonding capacities of SBAE with respect to MMAAs(V), DMAAs(V) and As(V) species increased starting from pH 5.00 and reached a maxima at pH 11.00. The mono- and divalent anions of MMAAs(V) showed better adsorption capabilities on the SBAE resin in the pH range 7.00–12.00; a somewhat higher affinity of the divalent anion could be observed. As(III) did not bond on the SBAE resin at pH < 8.00 as it existed as neutral molecules, which is beneficial for As(III) determination in the SBAE resin effluent.<sup>22</sup>

Bonding capacities of the hydrated iron-oxide particles integrated into the HY resin with respect to iAs was beneficial at pH > 2.00. Adsorption of arsenic

species, except DMA<sub>n</sub>(V), increased from pH 2.00, small capacities changes could be observed in the pH range from 6.00 to 10.00, and subsequently, a rapid drop of the adsorption efficiency was observed. From this point of view, the HY resin could be used in the pH range from 6.00 to 8.00 for the separation and determination of DMA<sub>n</sub>(V), as well for the determination of the total iAs.<sup>22</sup>

The pH of the solution plays an important role in the control of arsenic species, which is beneficial for the arsenic separation; thus, by adjusting the pH to 7.00, SBAE resin could not retain the molecular form of As(III) while As(V) was bonded at the resin surface. Hence, the concentration of As(III) could be measured directly in the effluent from the SBAE resin. With this feature, the SBAE resin is a convenient material for the separation of iAs species.<sup>22</sup> However, the result of iAs and MMA<sub>n</sub>(V) separation from water using the HY resin suggest that HY is efficient for the mutual removal of molecular and ionic forms of iAs, as well MMA<sub>n</sub>(V) species. Thus, DMA<sub>n</sub>(V) could be measured directly in the effluent from the HY resin.

#### *Determination of resins capacities in a fixed bed flow system*

In order to develop a method for the separation and determination of DMA<sub>n</sub>(V), it was necessary to determine the capacity and the efficiency of SBAE and HY resins in a fixed bed flow system. Model solutions were prepared from deionized and from modified tap water at an arsenic concentration of 5000 µg L<sup>-1</sup>, pH 7.00. These solutions were passed through a fixed bed column:  $m_{\text{resin}} = 6.0 \text{ g}$ ,  $Q = 1.66\text{--}2.0 \text{ mL min}^{-1}$  and  $EBV = 12.5 \text{ mL}$ . The breakthrough point was considered to be the point when the arsenic concentration in the effluent was equal to or higher than 10 µg L<sup>-1</sup>, which is a good criterion for the determination of the resin capacity, as well for resin comparison. The results of the capacities determination for the HY resin are shown in Fig. 3.

The capacity of the HY resin in a fixed bed flow system for the samples prepared in deionized water was 4150 µg g<sup>-1</sup> for As(III),<sup>22</sup> 3500 µg g<sup>-1</sup> for As(V)<sup>22</sup> and 1500 µg g<sup>-1</sup> for MMA<sub>n</sub>(V),<sup>23</sup> at pH 7.00. Analogous experiments conducted with modified tap water (Fig. 3b) gave slightly lower resin capacities: 3750 µg g<sup>-1</sup> for As(III), 3330 µg g<sup>-1</sup> for As(V) and 1466 µg g<sup>-1</sup> for MMA<sub>n</sub>(V).

The high capacities provide a good area for research, especially for the separation and preconcentration of arsenic species in different water samples. The presented results indicate that at pH 7.00, DMA<sub>n</sub>(V) is not bonded by HY, while MMA<sub>n</sub>(V) show a significant affinity for the HY resin surface. Significant sorption capacities of MMA<sub>n</sub>(V) were observed in the pH range from 6.00 to 10.00, but at lower pH values, molecular forms become dominant which are less attracted by the positive resin surface. The low sorption capacity for DMA<sub>n</sub>(V) at pH > 8.00 could be due to steric interference of the two methyl groups and the resin surface groups, and such repulsive forces prevent entrance into the meso-



and micropores.<sup>38</sup> Arsenate adsorption by iron-oxide involves a ligand exchange reaction with surface hydroxyl groups, which results in different surface complexes, *e.g.*, monodentate *vs.* bidentate, mononuclear *vs.* binuclear. Arsenite adsorbs *via* a ligand exchange reaction as well forming mono- and binuclear complexes. At higher surface coverage, bidentate binuclear complex formation is a preferential type of binding, which could be a reason of the low affinity of DMA<sub>s</sub>(V) toward the HY resin surface.<sup>39,40</sup> The use of HY resin provides the possibility for quantitative separation of DMA<sub>s</sub>(V) without any interference of other arsenic species present in the sample subjected to analysis.

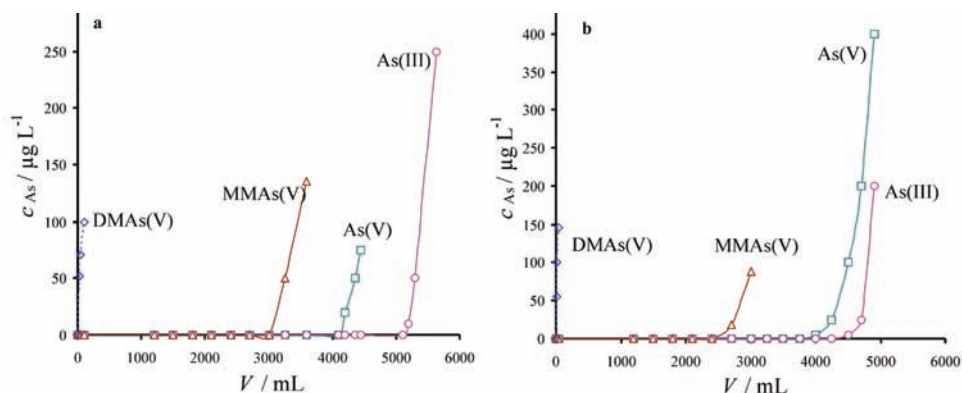


Fig. 3. Breakthrough curves for iAs and oAs species on the HY resin: a) deionized water and b) modified tap water. Conditions:  $c_{\text{As(III)}} = c_{\text{As(V)}} = c_{\text{MMAAs(V)}} = c_{\text{DMAAs(V)}} = 5000 \mu\text{g L}^{-1}$ , pH 7.00,  $m_{\text{resin}} = 6.0 \text{ g}$ ,  $Q = 1.66 \text{ mL min}^{-1}$ ,  $EBV = 12.5 \text{ mL}$ .

#### Established procedures

A simple and efficient method for the separation and determination of DMA<sub>s</sub>(V) was developed in preliminary tests and applied to the standard As solution and drinking water samples. The laboratory column was filled with 6.0 g of HY resin and rinsed with 100 ml of deionized water. The water sampling was performed according to a literature procedure<sup>41</sup> without adding any substances as stabilizers. Before the sorption experiments, the pH of the water sample (100 ml) was pH-adjusted and passed through the separation column at a flow rate of 1.66  $\text{mL min}^{-1}$ . Five portions (20.0 mL) of effluent were taken, and each fraction was adjusted to the appropriate pH with 5 % HNO<sub>3</sub> before injection into the ICP-MS instrument.

#### Application of the proposed method to the standard As solution

For the validation of the proposed method for water analyses, six samples of deionized water were spiked with different iAs and oAs concentrations to check the efficacy of DMA<sub>s</sub>(V) separation and determination. The testing was based on

the use of standard samples with the addition of iAs and oAs in the concentration range 5–100 µg L<sup>-1</sup> to approach the concentration of arsenic in natural water. The results of samples analysis prepared in deionized water with the addition of different concentrations of DMA<sub>s</sub>(V), MMA<sub>s</sub>(V), As(V) and As(III), are given in Table I.

TABLE I. Analytical data of the separation and determination of DMA<sub>s</sub>(V) species in standard solutions containing MMA<sub>s</sub>(V), As(V) and As(III) using the HY resins ( $\sigma$ —standard deviation)

Standard solution	As content, standard addition, µg L <sup>-1</sup>				Measured, µg L <sup>-1</sup> DMA <sub>s</sub> (V) average value ± $\sigma$	Recovery, % DMA <sub>s</sub> (V)
	DMA <sub>s</sub> (V)	MMA <sub>s</sub> (V)	As(V)	As(III)		
1	5.00	5.00	5.00	5.00	4.75±0.06	95.0
2	20.00	40.00	100.0	50.00	18.80±0.22	94.0
3	20.00	50.00	50.00	50.00	21.80±1.60	109.0

Good recoveries of 95.0, 94.0 and 109.0 % were obtained and the *RSD* values were 1.1, 7.50 and 7.50 % for standard solutions 1, 2 and 3, respectively.

The results of analysis of standard samples prepared in deionized water containing different concentrations of DMA<sub>s</sub>(V) and MMA<sub>s</sub>(V) are given in Table II.

Good recoveries were found in the samples at DMA<sub>s</sub>(V) concentrations of 10, 50 and 100 µg L<sup>-1</sup>, while the *RSD* values were 2.6, 4.6 and 2.4 %, respectively.

TABLE II. Analytical data of the separation and determination of DMA<sub>s</sub>(V) species in standard solutions containing MMA<sub>s</sub>(V) using the HY resin ( $\sigma$ —standard deviation)

Standard solution	As content, standard addition, µg L <sup>-1</sup>		Measured, µg L <sup>-1</sup> DMA <sub>s</sub> (V) average value ± $\sigma$	Recovery, % DMA <sub>s</sub> (V)
	DMA <sub>s</sub> (V)	MMA <sub>s</sub> (V)		
4	10.00	10.00	9.00±0.17	90.0
5	50.00	50.00	52.70±2.50	104.5
6	100.0	100.0	104.8±2.50	104.8

#### *Application of proposed method to drinking water samples*

The proposed method has been applied to drinking water samples in order to separate and determine DMA<sub>s</sub>(V). In Table III are presented results of DMA<sub>s</sub>(V) separation and determination in drinking water samples spiked with different concentrations of arsenic species. The standard addition method is useful because some unknown variations of the matrix can be prevented and this was suggested in some studies.<sup>41,42</sup> Because no water samples with known concentrations of various arsenic species were available the accuracy of the analytical results was evaluated by recovery studies.

The recovery and reproducibility of tap water samples 1–3 and modified water were good, with *RSD* values of 2.9, 7.00, 2.8 and 5.4 %, respectively.



TABLE III. Analytical data of the separation and determination of DMAAs(V) species in tap water containing MMAAs(V), As(V) and As(III) using the HY resin ( $\sigma$  – standard deviation)

Sample tap water	As content standard addition, $\mu\text{g L}^{-1}$				Measured, $\mu\text{g L}^{-1}$ DMAAs(V) average $\text{value} \pm \sigma$	Recovery, % DMAAs(V)
	DMAAs(V)	MMAAs(V)	As(V)	As(III)		
1	5.00	5.00	5.00	5.00	4.50	91.0
2	10.00	50.00	100.0	50.00	8.80 $\pm$ 0.20	88.00
3	50.00	50.00	100.0	50.00	48.10 $\pm$ 1.00	96.2
Modified	50.00	50.00	100.0	50.00	53.30 $\pm$ 2.80	106.6

*Analytical figure of merit and application*

The analytical validity of the proposed method and of the ICP–MS measurements were determined and tested by analyzing fresh water and river water certified reference materials for trace metals NIST 1643e and NRC SLRS4, of certified As concentrations of  $60.45 \pm 0.72$  and  $0.68 \pm 0.06 \mu\text{g L}^{-1}$ , respectively. The obtained results were  $61.7 \pm 0.94$  and  $0.66 \pm 0.05 \mu\text{g L}^{-1}$  total As. The standard reference materials were spiked with 10 and 25  $\mu\text{g L}^{-1}$  of DMAAs(V) in order to check the validity of the proposed method with a known standard concentration of iAs. The results of the DMAAs(V) determinations are presented in Table IV.

TABLE IV. Analytical data of the proposed separation procedure using HY resin for the determination of DMAAs(V) species in the standard reference material NIST 1643e

Standard solution	As content standard addition		Measured iAs average $\text{value} \pm \sigma$	Measured DMAAs(V) average $\text{value} \pm \sigma$	Recovery DMAAs(V)
	$\mu\text{g L}^{-1}$	DMAAs(V)			
1	10.00	61.70	61.50 $\pm$ 0.82	9.60 $\pm$ 0.20	96.0
2	25.00	61.70	60.80 $\pm$ 0.76	24.40 $\pm$ 1.50	97.6

The accuracy of the proposed method was additionally proved by analyzing five samples of wastewater from drainage channels taken from the region of Vojvodina. Only in one sample, collected in the region of the city Zrenjanin, was DMAAs(V) detected, at a level of  $1.2 \mu\text{g L}^{-1}$ , and total iAs of  $22 \mu\text{g L}^{-1}$ . Separation and determination of As(V) and As(III) species was achieved on SBAE and ICP–MS measurements gave  $21.6 \pm 0.98 \mu\text{g L}^{-1}$  of As(V) without detection of As(III). The wastewater sample was spiked with  $10 \mu\text{g L}^{-1}$  of DMAAs(V) and subjected to separation and determination of DMAAs(V). The obtained result,  $10.9 \pm 0.84 \mu\text{g L}^{-1}$ , gave unambiguous proof of the validity of proposed method for the separation and determination of DMAAs(V).

The analytic characteristics of the proposed method are given in Table V, and the experimental limit of detection was equal to the method detection limit ( $MDL$ ),  $0.03 \mu\text{g L}^{-1}$  for iAs and oAs. The achieved sensitivity is adequate for arsenic determination in non-polluted water samples.



TABLE V. Analytical characteristics of the proposed method; linear analytical range, 0.03–20 µg L<sup>-1</sup>; method detection limit (*MDL*), 0.03 µg L<sup>-1</sup>; *A*: absorbance; [As] expressed as µg L<sup>-1</sup>; *R* – correlation coefficient

Characteristic	iAs (total iAs)	oAs (total oAs)
Calibration	$A = 1.016 \times 10^4[\text{iAs}] + 4.671 \times 10^2$ $R = 0.9999$	$A = 1.022 \times 10^4[\text{oAs}] + 4.785 \times 10^2$ $R = 0.9996$

#### *Interference of inorganic ions*

The ions commonly present in tap water: chloride, sulfate, fluoride and nitrate, could potentially interfere in the proposed analytical method. The separation and determination of DMA<sub>n</sub>(V) in the presence of ions naturally present in drinking water was investigated using drinking water samples spiked by the gradual addition of the appropriate anion (Cl<sup>-</sup>, SO<sub>4</sub><sup>2-</sup>, F<sup>-</sup> and NO<sub>3</sub><sup>-</sup>) in a concentration ranging from 10 to 100 mg L<sup>-1</sup>. The interference of the ions was studied using a 10 µg L<sup>-1</sup> solution of DMA<sub>n</sub>(V) at pH 7.00, in order to determine the level of noticeable signal depression (Table VI). The presence of interference ions showed negligible effects on the reproducibility of the DMA<sub>n</sub>(V) determination providing the total dissolved salts (*TDS*) were less than 450 mg L<sup>-1</sup>. All samples were tested by ICP-MS measurements.

TABLE VI. Concentration of interfering ions (mg L<sup>-1</sup>) in tap water samples that cause noticeable signal depression when using ICP-MS

Sample	<i>TDS</i>	Cl <sup>-</sup>	SO <sub>4</sub> <sup>2-</sup>	F <sup>-</sup>	NO <sub>3</sub> <sup>-</sup>	DMA <sub>n</sub> (V), µg L <sup>-1</sup>
Modified tap water	450	52.2	53.0	0.2	3.2	9.5

The interferences of chloride and sulfate ions could be tolerated up to a concentration of 50 mg L<sup>-1</sup>. A severe problem associated with the determination of As by ICP-MS arises from the interference of chloride, which creates polyatomic species observed at *m/z* = 75. The chloride present in the sample reacts with the working gas, resulting in the formation of <sup>40</sup>Ar<sup>35</sup>Cl<sup>+</sup> (*m/z* = 75), the signal of which could interfere with those of the As species, leading to inaccurate results. The determination of arsenic in the presence of chloride was accomplished according to a procedure suggested in the literature.<sup>43</sup> Significant depression of the signal were observed for fluoride and nitrate anions at levels of 0.2 and 3.2 mg L<sup>-1</sup>, respectively. These results could not have a large influence on the method as fluoride and nitrate in drinking water are present at lower concentrations than the detection limit.

Hitherto, the developed methods for the determination of the total concentration of arsenic in natural waters (level of 1 µg L<sup>-1</sup> or less) can be achieved only by sophisticated analytical techniques for separation and measurement, such as ICP-MS and graphite furnace atomic absorption spectrometry (GF-AAS). For the measurements of iAs species, the HG-AAS<sup>15–18</sup> and hydride generation ato-

mic fluorescence spectrometry (HG–AFS)<sup>44</sup> techniques were successfully employed. However, coupled analytical techniques are the most convenient for the selective and sensitive determination of arsenic species with essentially uniform qualitative and quantitative responses. In many works, nowadays, arsenic species are determined by ICP–MS coupled with various chromatographic methods: IC,<sup>20</sup> HPLC,<sup>24–27,29</sup> or more complex system: performing pre-column<sup>28</sup> or post-column<sup>29</sup> arsenic species derivatization. In contrast to such highly sophisticated and expensive methods, the proposed procedure is cheap, simple, precise and time efficient. The separation procedure of arsenic species was highly efficient and with low interference of the ions, commonly found in water. The method could be applied routinely for monitoring the arsenic level in the various types of water samples (drinking water, ground water and wastewater).

The significance of the presented method lies in the fact that arsenic toxicity, its bioavailability and transport mechanisms highly depend on the chemical form in which it appears. The methylated arsenic species are significantly less toxic than arsenite and arsenate and thus, the determination of arsenic speciation in specific samples is of utmost significance for the consideration of the overall toxicity, which cannot be based only on total arsenic determination. Thus, the developed method represents a great improvement compared with direct ICP–MS measurements, which usually gives data of the total arsenic concentration. This method can be recommended for speciation analysis when appropriate equipment for highly sophisticated coupled techniques is not available. The proposed procedure can be adapted for on-site collection or separation of As(III), As(V) and DMA<sub>n</sub>(V) where oAs could possibly be found, such as in nature where biomethylation is caused by the activity of microorganisms,<sup>45</sup> or as the result of the use of arsenic-based pesticides.<sup>46</sup>

#### CONCLUSIONS

Studies and research on the separation and determination of arsenic species are of crucial importance for a complete understanding of the properties of elements and for the monitoring and management of natural water pollution, as well for the design of appropriate purification technologies. Two types of resins, SBAE and HY were tested. The adsorption of iAs and MMA<sub>n</sub>(V) species onto a HY resin was accomplished by adjusting the pH value of the water sample to 7.00, thus providing DMA<sub>n</sub>(V) separation and determination. The separation and pre-concentration procedures functioned well with the ICP–MS technique for the sensitive determination of DMA<sub>n</sub>(V) and iAs at low concentrations. Measurements with certified reference materials of known iAs value and spiked with different DMA<sub>n</sub>(V) concentrations proved the validity and accuracy of the applied method. Detection limit was 0.03 µg L<sup>-1</sup> and relative standard deviation (*RSD*) of all the investigated arsenic species was between 1.1–7.50 %.

The separation test showed that the resin HY could be used for separation and determination of the concentration of DMA<sub>s</sub>(V) in arsenic standard solution prepared in the laboratory and in drinking water samples spiked with different concentrations of oAs and iAs. Therefore, the obtained results related to the separation and determination of DMA<sub>s</sub>(V) indicates that the proposed method is accurate, sensitive and time saving.

*Acknowledgments.* This work was supported by the Ministry of Education and Science of the Republic of Serbia (ON142039).

#### ИЗВОД

#### РАЗДВАЈАЊЕ И ОДРЕЂИВАЊЕ ДИМЕТИЛАРСЕНАТА У ПРИРОДНИМ ВОДАМА

NURREDIN BEN ISSA, АЛЕКСАНДАР Д. МАРИНКОВИЋ и ЉУБИНКА В. РАЈАКОВИЋ

Технолошко-мешталауришки факултет, Универзитет у Београду, Карађорђева 4, 11120 Београд

У раду је приказан једноставан и ефикасан метод за раздвајање и одређивање диметиларсената, DMA<sub>s</sub>(V). За издавања DMA<sub>s</sub>(V) коришћена је хибридна смола модификована гвожђе-оксидом (HY). За одређивање концентрација арсена применењена је метода масене спектрометрије са индуковано спрегнутом плазмом (ICP-MS). Квантитативно одвајање DMA<sub>s</sub>(V) од свих врста арсена присутних у природним водама остварено је применом HY смоле уз контролу pH вредности. При pH вредности воде од 7,00 све врсте арсена у води се квантитативно везују за HY смолу изузев DMA<sub>s</sub>(V). Капацитет HY смоле је израчунат на основу одређивања тачке пробоја у проточном систему, HY смола веже више од 4150 µg g<sup>-1</sup> As(III), 3500 µg g<sup>-1</sup> As(V) и 1500 µg g<sup>-1</sup> MMA<sub>s</sub>(V). Капацитет смоле је висок и постојан и у присуству јона који су природни састојци воде. У ефлуту је одређена концентрација DMA<sub>s</sub>(V) применом ICP-MS. Предложени метод је успостављен и потврђен применом стандардних аналитичких поступака, анализом сертификованог референтног материјала и анализом узорака уз примену спољашњег стандарда и стандардног додатка. Граница одређивања била је 0,03 µg L<sup>-1</sup>, а релативна стандардна девијација (RSD) у опсегу између 1,1–7,50 %.

(Примљено 10. маја 2011, ревидирано 1 фебруара 2012)

#### REFERENCES

1. K. A. Hudson-Edwards, S. L. Houghton, A. Osborn, *Trends Anal. Chem.* **22** (2004) 745
2. R. Feeney, S. P. Kounaves, *Anal. Chem.* **72** (2000) 2222
3. V. L. Vukašinović-Pešić, M. Đikanović, N. Z. Blagojević, Lj. V. Rajaković, *Chem. Ind. Chem. Eng. Q.* **11** (2005) 44
4. D. Mohan, C. U. Pittman Jr., *J. Hazard. Mater.* **142** (2007) 1
5. A. Maiti, S. DasGupta, J. K. Basu, S. De, *Ind. Eng. Chem. Res.* **47** (2008) 1620
6. C. A. Impellitteri, *Water Res.* **38** (2004) 1207
7. C. Lomonte, M. Currell, R. J. S. Morrison, I. D. McKelvie, S. Kolev, *Anal. Chim. Acta* **583** (2007) 72
8. L. V. Rajaković, *Sep. Sci. Technol.* **27** (1992) 1423
9. P. L. Smedley, D. G. Kinniburgh, *Appl. Geochem.* **17** (2002) 517
10. B. J. Lafferty, H. Loepert, *Environ. Sci. Technol.* **39** (2005) 2120
11. O. S. Thirunavukkarasu, T. Viraraghavan, K. S. Subramanian, S. Tanjore, *Urban Water* **4** (2002) 415

12. Lj. V. Rajaković, M. Mitrović, S. Stevanović, S. Dimitrijević, *J. Serb. Chem. Soc.* **58** (1993) 131
13. N. Zhang, P. Blowers, J. Farrell, *Environ. Sci. Technol.* **39** (2005) 4816
14. I. M. M. Rahman, Z. A Begum, M. Nakano, Y. Furusho, T. Maki, H. Hasegawa, *Chemosphere* **82** (2011) 549
15. US EPA Office of Water, *Chemical Speciation of Arsenic in Water and Tissue by Hydride Generation Quartz Furnace Atomic Absorption Spectrometry*, Method 1632, August, 1998
16. Z. Zhua, J. Liub, S. Zhang, X. Na, X. Zhang, *Anal. Chim. Acta* **607** (2008) 136
17. F. T. Henry, T. M. Thorpe, *Anal. Chem.* **52** (1980) 80
18. S. Nielsen, E. H. Hansen, *Anal. Chim. Acta* **343** (1997) 5
19. P. Pohl, B. Prusisz, *Trends Anal. Chem.* **23** (2004) 63
20. E. Vassileva, A. Becker, J. A. C. Broekaert, *Anal. Chim. Acta* **441** (2001) 135
21. S. N. Ronkart, V. Laurent, P. Carbonnelle, N. Mabon, A. Copin, J. P. Barthélemy *Chemosphere* **66** (2007) 738
22. N. B. Issa, V. N. Rajaković-Ognjanović, B. M. Jovanović, Lj. V. Rajaković, *Anal. Chim. Acta* **673** (2010) 185
23. N. B. Issa, V. N. Rajaković-Ognjanović, B. M. Jovanović, Lj. V. Rajaković, *Anal. Chim. Acta* **706** (2011) 191
24. N. M. M. Coelho, C. Parrill, M. L. Cervera, A. Pastor, M. de la Guardia, *Anal. Chim. Acta* **482** (2003) 73
25. C. Demesmay, M. Olle, M. Porthault, *Fresenius J. Anal. Chem.* **348** (1994) 205
26. M. Morita, T. Uehiro, K. Fuwa, *Anal. Chem.* **53** (1981) 1806
27. I. Pizarro, M. Gómez, C. Cámaras, M. A. Palacios, *Anal. Chim. Acta* **495** (2003) 85
28. D. L. Tsalev, M. Sperling, B. Welz, *Talanta* **51** (2000) 1059
29. M. A. Lopez, M. M. Gomez, M. A. Palacios, C. Camara, *J. Anal. Chem.* **346** (1993) 643
30. I. M. M. Rahman, Z. A Begum, M. Nakano, Y. Furusho, T. Maki, H. Hasegawa, *Chemosphere* **82** (2011) 549
31. N. Campillo, R. Peñalver, P. Viñas, I. López-García, M. Hernández-Córdoba, *Talanta* **77** (2008) 793
32. J. Szkoda, J. Źmudzki, A. Grzebalska, *Bull. Vet. Inst. Pulawy* **50** (2006) 269
33. P. Salaun, B. Planer-Friedrich, C. M. G. van den Berg, *Anal. Chim. Acta* **585** (2007) 312
34. M. A. Ferreira, A. A. Barros, *Anal. Chim. Acta* **459** (2002) 151
35. K. Gibbon-Walsh, P. Salaün, C. M. G. Van den Berg, *Anal. Chim. Acta* **662** (2010) 1
36. Lanxess, Engineering Information, *Preliminary Version Arsenic Separation from Ground Water using Lewatit FO 36 Ion Exchange/Iron Oxide Hybrid System*, Leverkusen, 2007
37. USEPA, *Determination of Trace Elements in Waters and Wastes by Inductively Coupled Plasma-Mass Spectrometry. 5.4 EPA Method 200.8*, Washington, 1994
38. J. Biyan, S. Fei, G. Hu, S. Zheng, Q. Zhang, Z. Xu. *J. Hazard. Mater.* **161** (2009) 81
39. M. Grafe, M. J. Eick, P. R. Grossl, A. M. Saunders, *J. Environ. Qual.* **31** (2002) 1115
40. S. Fendorf, M. J. Eick, P. Grossl, D. L. Sparks, *Environ. Sci. Technol.* **31** (1997) 315
41. M. Segura, J. Munoz, Y. Madrid, C. Camara, *Anal. Bioanal. Chem.* **374** (2002) 513
42. J. A. Day, M. Montes-Bayon, A. P. Vonderheide, J. A. Caruso, *Anal. Bioanal. Chem.* **373** (2002) 664
43. M. Yamanaka, *Agilent Technologies Application Note 1–4* (2000)
44. L. O. Leal, R. Forteza, V. Cerdà, *Talanta* **69** (2006) 500
45. A. Zouboulis, I. Katsoyiannis, *Sep. Sci. Technol.* **37** (2002) 2859
46. R. Y. Ning, *Desalination* **143** (2002) 237.





## Colloidal chemistry-based synthesis of quantized CuInS<sub>2</sub>/Se<sub>2</sub> nanoparticles

NADICA D. ABAZOVIĆ<sup>1</sup>, DRAGANA J. JOVANOVIĆ<sup>1</sup>, MILOVAN M. STOILJKOVIĆ<sup>1#</sup>,  
MIODRAG N. MITRIĆ<sup>1</sup>, SCOTT P. AHRENKIEL<sup>2</sup>,  
JOVAN M. NEDELJKOVIĆ<sup>1</sup> and MIRJANA I. ČOMOR<sup>1\*</sup>

<sup>1</sup>Vinča Institute of Nuclear Sciences, University of Belgrade, P.O. Box 522,  
11001 Belgrade, Serbia and <sup>2</sup>South Dakota School of Mines and Technology,  
Rapid City, South Dakota 57701, USA

(Received 20 April, revised 13 December 2011)

**Abstract:** Ternary chalcogenide nanoparticles, CuInS<sub>2</sub> and CuInSe<sub>2</sub>, were synthesized in a high-temperature boiling non-polar organic solvent. X-Ray diffraction analysis revealed that both materials had a tetragonal (chalcopyrite) crystal structure. The morphology of the obtained materials was revealed by transmission electron microscopy. Agglomerated spherical CuInS<sub>2</sub> nanoparticles with broad size distribution in the range from 2 to 20 nm were obtained. In the case of CuInSe<sub>2</sub>, isolated particles with a spherical or prismatic shape in the size range from 10 to 25 nm were obtained, as well as agglomerates consisting of much smaller particles with a diameter of about 2–5 nm. The particles with the smallest diameters of both materials exhibited quantum size effects.

**Keywords:** I–III–VI<sub>2</sub> semiconductors; quantization; X-ray diffraction; optical properties.

### INTRODUCTION

I–III–VI<sub>2</sub> compounds such as CuInS<sub>2</sub> and CuInSe<sub>2</sub> (CIS), as well as Cu(In,Ga)(S,Se) (CIGS), are effective light-absorbing materials which can be used in thin-film solar cells, and printable and flexible photovoltaic devices.<sup>1</sup> These materials possess advantageous properties for solar applications since their band gap energy is at the red edge of the visible solar spectrum (bulk CuInS<sub>2</sub> and CuInSe<sub>2</sub> have band gap energies of 1.53 and 1.04 eV, respectively). CuInS<sub>2</sub> and CuInSe<sub>2</sub> are direct band-gap semiconductors with correspondingly high optical absorption coefficients,<sup>2,3</sup> and, contrary to other candidate materials for thin-film

\* Corresponding author. E-mail: mirjanac@vinca.rs

# Serbian Chemical Society member.

doi: 10.2298/JSC110420220A

solar cells such as CdTe and amorphous silicon (a-Si:H), they are stable under long-term excitation.<sup>4</sup> The highest theoretical efficiency was predicted for CuInSe<sub>2</sub> and CuInS<sub>2</sub> (25 and 28.5 %, respectively),<sup>5</sup> but the experimental record (21.5 %) has been achieved with CIGS-based solar cells.<sup>6</sup> This is significantly higher than for either CdTe or a-Si:H based devices.<sup>7</sup>

One of the hurdles currently impeding widespread commercialization of CIS-based solar cells is the difficulty of achieving controlled stoichiometry over large device areas, leading to high manufacturing costs.<sup>8</sup> CIS layers in state-of-the-art devices are deposited by a multistage co-evaporation process in which alternate copper and indium layers are exposed either to a chalcogenide source or hydrogen chalcogenide gas in the reaction chamber.<sup>9,10</sup> This process is time-consuming, the CIS stoichiometry is difficult to control, intermetallic phases can be formed and the content of S or Se can vary significantly in the films.<sup>8,11</sup> Large material losses on the deposition chamber walls also increase the cost. For these reasons, alternative CIS layer deposition strategies are desired.

One approach with the potential to produce CIS layers with controlled stoichiometry without the need for high temperature annealing is to synthesize chemically colloidal CIS nanocrystals dispersed in solvents, creating a paint or ink. Such an approach, of printable CIS inks, makes accessible a range of solution-based processing techniques and may lead to inexpensive fabrication routes for light-absorbing layers.<sup>1</sup> There are reports in the literature concerning the synthesis of I–III–VI<sub>2</sub> semiconductor nanocrystals such as CuInS<sub>2</sub>, CuInSe<sub>2</sub> and AgInS<sub>2</sub> based on either solvothermal methods or the usage of single organic precursors.<sup>12–17</sup> These approaches generally suffer from relatively low yields, poor crystallinity and poor uniformity in composition and phase of the obtained nanostructures.<sup>3,18</sup> This is not surprising considering that many of these systems have very complicated phase diagrams.<sup>19</sup> However, there are a few recent reports concerning the synthesis of colloidal CuInS<sub>2</sub> and CuInSe<sub>2</sub> nanocrystals in organic solvents avoiding the usage of single organic precursors.<sup>1,18,20–23</sup>

In this paper, a novel colloidal route for the synthesis of CuInS<sub>2</sub> and CuInSe<sub>2</sub> nanocrystals in a non-polar solvent is reported. The obtained nanocrystals could be dispersed in various non-polar solvents, becoming thereby suitable for the deposition of uniform, crack-free films onto different substrates. The in detail structural characterization of the synthesized CuInS<sub>2</sub> and CuInSe<sub>2</sub> nanocrystals was realized using transmission electron microscopy (TEM) and X-ray diffraction (XRD) analysis, while optical characterization was performed using UV–Vis spectroscopy.

## EXPERIMENTAL

### Materials

Copper(I) acetate (CuAc), indium(III) acetate (In(Ac)<sub>3</sub>), Se-pellets and trioctylphosphine (TOP) 90 % were purchased from Sigma Aldrich, while 1-octadecene (ODE) and bis(tri-

methylsilyl)sulfide (TMS) were purchased from Fluka. Myristic acid (98 %) was purchased from Alfa-Aeser. Methanol (HPLC grade) and benzene were purchased from Baker. All chemicals were of the highest purity available and were used without further purification. A standard Schlenk line was used for all the syntheses in order to avoid the presence of any oxygen.

#### Synthesis of CuInS<sub>2</sub> and CuInSe<sub>2</sub>

CuAc (01. mmol), In(Ac)<sub>3</sub> (0.1 mmol) and myristic acid (0.4 mmol), together with 6.2 cm<sup>3</sup> of ODE were introduced into a two-neck reaction flask. The flask was immersed in an oil bath at 170 °C and maintained at this temperature for 30 min under an Ar flow. Then, the flask was heated to 300 °C and 10 min after attaining the temperature, either 2 ml of ODE containing TMS (0.30 mmol) or 2 ml of TOP containing Se (0.30 mmol) were injected in order to obtain CuInS<sub>2</sub> or CuInSe<sub>2</sub>, respectively. The reaction mixtures were kept at 300 °C for 30 min and then allowed to cool spontaneously to room temperature. The obtained precipitates were washed three times with methanol and then dispersed in benzene.

#### Characterization

X-Ray diffraction (XRD) patterns of the samples were recorded using a Bruker D8 Advance diffractometer equipped with a focusing Ge-crystal primary monochromator (Johansson type) that generates CuK $\alpha$  radiation (step time: 6 or 8 s; step: 0.02 or 0.05°). The powder samples were prepared by drying washed precipitates under an Ar flow.

Micro-structural characterization of samples was performed on Hitachi H-7000 FA TEM with a W-filament. Samples were dispersed in benzene, ultrasonicated for one hour and deposited on C-coated Cu grids.

The quantitative chemical analysis of the obtained precipitates was realized by inductively coupled plasma optical emission spectroscopy (ICP–OES) (Spectroflame ICP, 2.5 kW, 27 MHz). Prior to the measurements, the samples were dissolved in hydrochloric acid. The measurements were performed by measuring the intensity of the radiation emitted by each element at specific wavelengths ( $\lambda_{\text{em}} = 324.754$  nm for Cu and 325.609 nm for In). The concentration (in ppm) of both elements were calculated using a series of standard solutions, the results were transformed into the number of atoms of each element. These numbers were used for the determination of the Cu/In ratio in the synthesized samples: 0.55 in CuInS<sub>2</sub> and 0.63 in CuInSe<sub>2</sub>.

Diluted benzene dispersions of synthesized CuInS<sub>2</sub> and CuInSe<sub>2</sub> were used for optical measurements. For UV/Vis absorption spectrometry, an Evolution 600 UV/Vis spectrophotometer (Thermo Scientific) was used. Emission measurements were performed on a Perkin Elmer LS 45 luminescence spectrometer.

## RESULTS AND DISCUSSION

The X-ray diffraction patterns of the synthesized CuInS<sub>2</sub> and CuInSe<sub>2</sub> are shown in Fig. 1. The XRD pattern shown in Fig. 1a matches well with the literature data for tetragonal (chalcopyrite)<sup>21</sup> CuInS<sub>2</sub>. The obtained peaks can be assigned to the (112), (200), (204)/(220) and (312)/(116) crystalline planes. The crystalline structure of the synthesized CuInSe<sub>2</sub> is presented in Fig. 1b. The main reflections that correspond well with tetragonal (chalcopyrite) CuInSe<sub>2</sub> structure can be noticed. First, there is reflection from the (112) plane, then (204)/(220), (312)/(116), (004)/(200) and very weak from the (103) plane. All peaks are slightly

shifted to larger  $2\theta$  values compared to literature data,<sup>15</sup> indicating that crystalline lattice parameters are orderly changed, most likely due to the non-stoichiometric ratio between Cu and In and/or the small size of the particles. The sharp peaks at  $2\theta < 26^\circ$  can be assigned to TOP/TOPO adsorbed on the surface of the CuInSe<sub>2</sub> nanoparticles. In addition, there is a peak denoted with star at about  $43^\circ$  in Figs. 1a and 1b, which can be assigned to either metallic copper<sup>24</sup> or to an indium rich phase (CuIn<sub>11</sub>S<sub>17</sub>).<sup>25</sup>

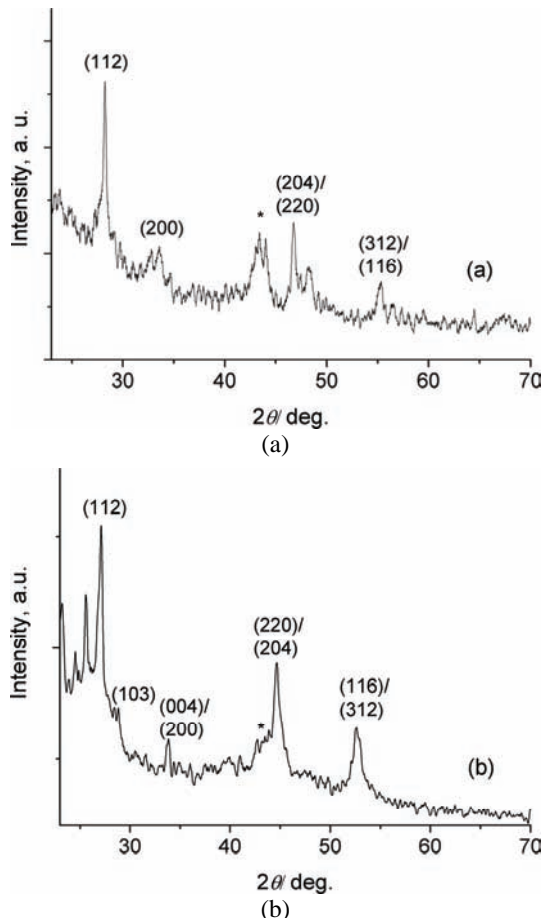


Fig. 1. The XRD patterns of a) CuInS<sub>2</sub> and b) CuInSe<sub>2</sub>.

As can be seen from the XRD patterns of both materials, the peaks have an irregular shape – the effect is the most obvious for the (112) peaks, which indicates that crystals of, at least, two sizes were present in the materials. The wide base of the peaks originates from smaller, while the sharp maximum of the peaks corresponds to larger crystallites. The average crystalline domain size of both materials was estimated using XFIT and FOURYA.<sup>26</sup> The grain size was found to be 20 and 15 nm for CuInS<sub>2</sub> and CuInSe<sub>2</sub>, respectively.

The morphology of the CuInS<sub>2</sub> and CuInSe<sub>2</sub> samples was studied using TEM. Typical TEM images are presented in Fig. 2. Agglomerated spherical CuInS<sub>2</sub> nanoparticles with a broad size distribution in the range from 2 to 20 nm can be seen in Fig. 2a. This observation is in agreement with literature data concerning the morphology of CuInS<sub>2</sub> synthesized in different ways.<sup>13,15</sup> Practically, it was impossible to find isolated particles due to the usage of a non-coordinating solvent (ODE), which cannot act as a surfactant and prevent aggregation of the particles. The best observation is presented in the inset of Fig. 2a; a small fraction of nearly mono dispersed particles of about 8 nm in diameter is presented. Unfortunately, TEM images of CuInS<sub>2</sub> could not be used for size distribution statistics because of the agglomeration. The CuInSe<sub>2</sub> nanoparticles were much better dispersed on the grid (Fig. 2b). The size distribution was broad (2–25 nm), and isolated particles with spherical or prismatic shape can be seen. The size distribution statistics was performed and the results are presented in Figs. 2c and 2d. The larger fraction of spherical and prismatic particles has sizes of about 13 nm, smaller particles organized as agglomerates have diameters  $\leq 5$  nm. The observed morphologies are the consequence of the growth mechanism. As pointed out in the literature,<sup>21</sup> after formation of the primary particles, the growth proceeds through Ostwald ripening and aggregation. For Ostwald ripening, a complexion agent is necessary (in the present case, it is myristic acid) and if it is not present the growth can proceed only through aggregation. It should be mentioned that there is reasonably good agreement in the size estimation from TEM and XRD measurements.

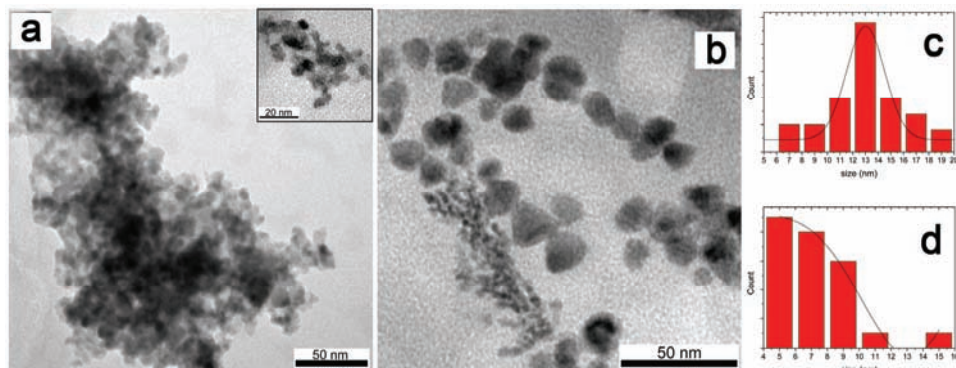


Fig. 2. Typical TEM images of a) CuInS<sub>2</sub> and b) CuInSe<sub>2</sub>, and the size distribution histograms (c and d) of the CuInSe<sub>2</sub> nanoparticles.

The absorption onset of each product was determined by a least-squares fit of the linear region of a  $(Ah\nu)^2$  vs.  $h\nu$  plot ( $A$  = absorbance,  $h$  = Planck's constant, and  $\nu$  = frequency), as presented in Fig. 3. Due to the position of their absorption threshold, band gaps of 2.02 eV for CuInS<sub>2</sub> and 2.13 eV for CuInSe<sub>2</sub>

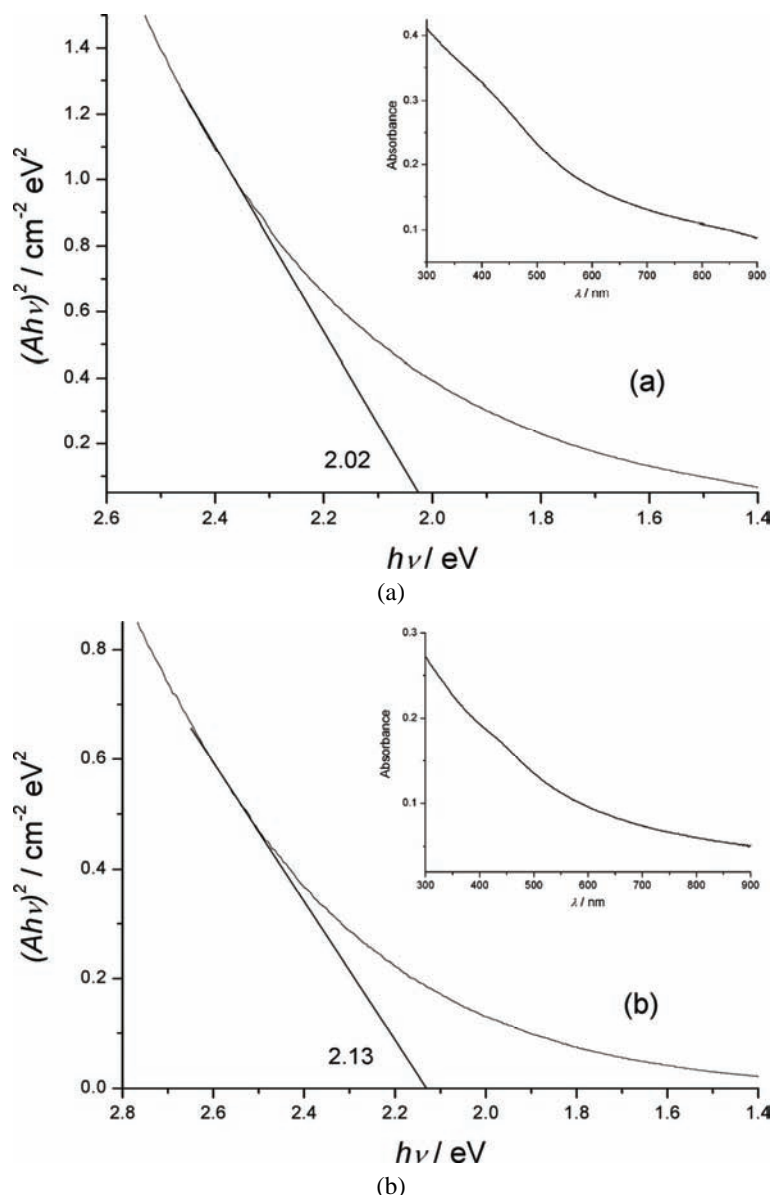


Fig. 3. Plots of  $(Ah\nu)^2$  vs. energy for a) CuInS<sub>2</sub> and b) CuInSe<sub>2</sub> nanoparticles. The insets show the absorption spectrum of the corresponding colloidal dispersions.

are obtained. In order to correlate the optical properties of the synthesized nanoparticles of both materials with size, the effective mass approximation model (Eq. (1)) was used to calculate the size of the particles from the increase of the effective band gap energies:<sup>27</sup>

$$\Delta E = \frac{\hbar^2 \pi^2}{2R^2} \left( \frac{1}{m_e} + \frac{1}{m_h} \right) - \frac{1.8e^2}{\epsilon R} \quad (1)$$

where  $\Delta E$  is the increase of the band gap energy,  $m_e$  and  $m_h$  are the effective masses of electrons and holes, respectively,  $\epsilon$  is the dielectric constant and  $R$  is the radius. Values for CuInS<sub>2</sub> ( $m_e = 0.16$ ,  $m_h = 1.3$  and  $\epsilon = 11$ ) and CuInSe<sub>2</sub> ( $m_e = 0.082$ ,  $m_h = 0.71$  and  $\epsilon = 15$ ) were taken from literature.<sup>15</sup> The increase of the band gap energy ( $\Delta E$ ) was estimated to be 0.5 and 1 eV for CuInS<sub>2</sub> and CuInSe<sub>2</sub>, respectively. Using these values, the calculated diameters of the nanoparticles were found to be about 2 and 3 nm for CuInS<sub>2</sub> and CuInSe<sub>2</sub>, respectively. Although these values are smaller compared to values estimated from the TEM measurements, it should be emphasized that they are similar to the size of the primary particles of which the larger agglomerates are composed. The absorption spectra were obtained using benzene dispersions of the obtained samples where agglomeration is negligible.

Theoretical calculations have shown that the Wannier–Mott bulk exciton radiiuses are 4.1 and 10.6 nm for CuInS<sub>2</sub> and CuInSe<sub>2</sub>, respectively.<sup>15</sup> According to particle sizing performed by TEM and XRD, the smallest particles of both materials should be in the weak confinement regime and quantum effects due to reduced dimensionality could be expected. The optical characterization also revealed quantum confinement. The absorption spectra of dispersed CuInS<sub>2</sub> and CuInSe<sub>2</sub> are shown in the insets in Figure 3. In both cases, rather featureless absorption spectra were obtained with tail towards the infrared region and a shoulder in the spectral range 400 to 500 nm. The presence of the absorption tail can be explained by light scattering due to the presence of agglomerated particles. On the other hand, the presence of shoulder instead of a well-resolved exciton band is the consequence of the rather broad size distributions of the CuInS<sub>2</sub> and CuInSe<sub>2</sub> nanoparticles.

In order to reveal the ratio between copper and indium in the synthesized materials, assuming that peaks marked with a star in Figs. 1a and 1b can be assigned to non-stoichiometric In rich compounds, ICP–OES measurements were performed. One of the most attractive properties of CuIn(S,Se) compounds is that they appear to tolerate a large range of anion-to-cation off stoichiometry, which is manifested by the existence of a series of ordered defect compounds (ODC) with large variations in their Cu/In/(S,Se) atomic ratios.<sup>28</sup> These ODCs generally possess wider band gap and type of conductivity can be changed with changes of Cu/In ratio from p to n. The measurements indicated Cu/In ratios of about 0.55 and 0.63 for CuInS<sub>2</sub> and CuInSe<sub>2</sub>, respectively. Both materials are indium-rich and consequently n-type conductivity can be expected.<sup>29</sup>

The materials obtained in this study showed no detectable emission, contrary to literature data.<sup>21</sup> The nature of the surface ligands plays an important role in

the PL efficiency of CuIn(S,Se)<sub>2</sub> nanocrystals, as was shown by Castro *et al.*<sup>13</sup> Obviously the choice of non-coordinating solvent/surfactants (ODE/TOP) proved themselves excellent for quenching emission and making the photogenerated charges more available for use in photovoltaic devices. This will be the subject of future experiments.

#### CONCLUSIONS

A simple synthetic procedure for the preparation of CuInS<sub>2</sub> and CuInSe<sub>2</sub> nanoparticles has been presented. The obtained materials had a tetragonal (chalcopyrite) crystalline structure. XRD results indicated broad particle size distributions, all in nano dimensions. TEM measurements also revealed the presence of nanoparticles of different dimensions and a tendency of the CuInS<sub>2</sub> nanoparticles to form agglomerates. The particles of smallest dimensions of both materials exhibit size quantization effects due to reduced dimensionality. The effective mass approximation model was used to correlate the optical properties of the obtained colloidal nanoparticles with their diameters.

*Acknowledgments.* Financial support for this study was granted by the Ministry of Education and Science of the Republic of Serbia (Project ON172056).

#### ИЗВОД

#### СИНТЕЗА КВАНТИЗИРАНИХ НАНОЧЕСТИЦА CuInS<sub>2</sub>/Se<sub>2</sub> КОЛОИДНО-ХЕМИЈСКОМ МЕТОДОМ

НАДИЦА Д. АБАЗОВИЋ<sup>1</sup>, ДРАГАНА Ј. ЈОВАНОВИЋ<sup>1</sup>, МИЛОВАН М. СТОИЉКОВИЋ<sup>1</sup>, МИОДРАГ Н. МИТРИЋ<sup>1</sup>,  
SCOTT P. AHRENKIEL<sup>2</sup>, ЈОВАН М. НЕДЕЉКОВИЋ<sup>1</sup> и МИРЈАНА И. ЧОМОР<sup>1</sup>

<sup>1</sup>Институут за нуклеарне науке "Винча", Универзитет у Београду, бб. бр. 522, 11001 Београд и <sup>2</sup>South Dakota  
School of Mines and Technology, Rapid City, South Dakota 57701, USA

Наночестице тернarnих халкогенида, CuInS<sub>2</sub> и CuInSe<sub>2</sub>, синтетисане су у неполарним, органским растворачима високе тачке кључаша. Дифракција X-зрака показала је да оба материјала имају тетрагоналну (халкопиритну) кристалну структуру. Употребом трансмисионе електронске микроскопије откривено је да су честице сферног облика нано-димензија. Наночестице CuInS<sub>2</sub> формирају агрегате и имају широку расподелу величина честица од 2–20 nm. У случају CuInSe<sub>2</sub>, добијене су изоловане честице сферног и призматичног облика, димензија од 10–25 nm као и агломерати који се састоје од честица знатно мањих димензија, од 2–5 nm. Оба материјала показују квантизациони ефекат услед нанодимензија.

(Примљено 10. априла, ревидирано 13. децембра 2011)

#### REFERENCES

1. M. G. Panthani, V. Akhavan, B. Goodfellow, J. P. Schmidtke, L. Dunn, A. Dobadalapur, P. F. Barbara, B. A. Korgel, *J. Am. Chem. Soc.* **130** (2008) 16770
2. W. E. Devaney, W. S. Chen, J. M. Stewart, R. A. Mickelsen, *IEEE Trans. Electron Devices* **37** (1990) 428
3. R. Scheer, T. Walter, H. W. Schock, M. L. Fearheiley, H. J. Lewerenz, *Appl. Phys. Lett.* **63** (1993) 3294

4. J.-F. Guillemoles, L. Kronik, D. Cahen, U. Rau, A. Jasenek, H.-W. Schock, *J. Phys. Chem., B* **104** (2000) 4849
5. S. Siebentritt, *Thin Solid Films* **403–404** (2002) 1
6. J. S. Ward, K. Ramanathan, F. S. Hasoon, T. J. Coutts, J. Keane, M. A. Contreras, T. Moriarty, R. Noufi, *Prog. Photovoltaics Res. Appl.* **10** (2002) 41
7. M. A. Green, K. Emery, D. L. King, Y. Hishikawa, W. Warta, *Prog. Photovoltaics Res. Appl.* **15** (2007) 35
8. M. Powalla, B. Dimmler, *Thin Solid Films* **361–362** (2000) 540
9. I. Repins, M. A. Contreras, B. Egaas, C. De Hart, J. Scharf, C. L. Perkins, B. To, R. Noufi, *Prog. Photovoltaics Res. Appl.* **16** (2008) 235
10. A. Contreras, B. Egaas, K. Ramanathan, J. Hiltner, A. Swartzlander, F. Hasoon, R. Noufi, *Prog. Photovoltaics Res. Appl.* **7** (1999) 311
11. H.-W. Schock, R. Noufi, *Prog. Photovoltaics Res. Appl.* **8** (2000) 151
12. H. I. Elim, W. Ji, M.-T. Ng, J. J. Vittal, *Appl. Phys. Lett.* **90** (2007) 033106
13. S. L. Castro, S. G. Bailey, R. P. Raffaelle, K. K. Banger, A. F. Hepp, *J. Phys. Chem., B* **108** (2004) 12429
14. K. K. Banger, M. H.-C. Jin, J. D. Harris, P. E. Fanwick, A. F. Hepp, *Inorg. Chem.* **42** (2003) 7713
15. S. L. Castro, S. G. Bailey, R. P. Raffaelle, K. K. Banger, A. F. Hepp, *Chem. Mater.* **15** (2003) 3142
16. B. Li, Y. Xie, J. Huang, Y. Qian, *Adv. Mater.* **11** (1999) 1456
17. C. Czekelius, M. Hilgendorff, L. Spanhel, I. Bedja, M. Lerch, G. Müller, U. Bloeck, D.-S. Su, M. Giersig, *Adv. Mater.* **11** (1999) 643
18. S.-H. Choi, E.-G. Kim, T. Hyeon, *J. Am. Chem. Soc.* **128** (2006) 2520
19. A. Ghezelbash, B. A. Korgel, *Langmuir* **21** (2005) 9451
20. M. A. Malik, P. O'Brien, N. Revaprasadu, *Adv. Mater.* **11** (1999) 1441
21. H. Zhong, Y. Zhou, M. Ye, Y. He, J. Ye, C. He, C. Yang, Y. Li, *Chem. Mater.* **20** (2008) 6434
22. M. Kruszynska, H. Borchert, J. Parisi, J. Kolny-Olesiak, *J. Am. Chem. Soc.* **132** (2010) 15976
23. K. Nose, T. Omata, S. Otsuka-Yao-Matsuo, *J. Phys. Chem., C* **113** (2009) 3455
24. M. Salavati-Niasari, F. Davar, *Mat. Lett.* **63** (2009) 441
25. R. P. Wijesundera, W. Siripala, *Sol. Energy Mater. Sol. Cells* **81** (2004) 147
26. R. W. Cheary, A. A. Coelho, *Programs XFIT and FOURYA*, deposited in CCP14 Powder Diffraction Library, Engineering and Physical Sciences Research Council, Daresbury Laboratory, Warrington, England, <http://www.ccp14.ac.uk/tutorial/xfit-95/xfit.htm> (1996)
27. L. Brus, *J. Phys. Chem.* **90** (1986) 2555
28. R. R. Philip, B. Pradeep, *Thin Solid Films* **472** (2005) 136
29. K. Yoshino, K. Nomoto, A. Kinoshita, T. Ikari, Y. Akaki, T. Yoshitake, *J. Mater. Sci. Mater. Electron.* **19** (2008) 301.







## Comparative analyses of the diffusion coefficients from thyme for different extraction processes

SLOBODAN S. PETROVIĆ<sup>1</sup>, JASNA IVANOVIĆ<sup>2\*</sup>, STOJA MILOVANOVIĆ<sup>2</sup>  
and IRENA ŽIŽOVIĆ<sup>2</sup>

<sup>1</sup>BIOSS – PS i ostali, Bulevar oslobođenja 401i, 11000 Belgrade, Serbia and <sup>2</sup>University of Belgrade, Faculty of Technology and Metallurgy, Kariđeljova 4, 11120 Belgrade, Serbia

(Received 11 June, revised 31 October 2011)

**Abstract:** This work was aimed at analyzing the kinetics and mass transfer phenomena for different extraction processes from thyme (*Thymus vulgaris* L.) leaves. Different extraction processes with ethanol were studied, *i.e.*, Soxhlet extraction and ultrasound-assisted batch extraction on the laboratory scale, as well as pilot plant batch extraction with mixing. The extraction processes with ethanol were compared to the process of supercritical carbon dioxide extraction performed at 10 MPa and 40 °C. The experimental data were analyzed by a mathematical model derived from the Fick's second law to determine and compare the diffusion coefficients in the periods of constant and decreasing extraction rates. In the fast extraction period, the values of the diffusion coefficients were one to three orders of magnitude higher compared to those determined for the period of slow extraction. The highest diffusion coefficient was recorded for the fast extraction period of supercritical fluid extraction. In the cases of the extraction processes with ethanol, ultrasound, stirring and increasing extraction temperature enhanced the mass transfer rate in the washing phase. On the other hand, ultrasound contributed the most to the increase of mass transfer rate in the period of slow extraction.

**Key words:** *Thymus vulgaris*; ethanol extraction; supercritical extraction; extraction kinetics; modelling; diffusion coefficients.

### INTRODUCTION

Common thyme (*Thymus vulgaris* L.) is a perennial shrub native to southern Europe, widely cultivated for its strong flavour, resulting from its content of thymol. Due to their antimicrobial, antioxidant and antifungal activity, flavour properties and aroma-active constituents (thymol, carvacrol, *p*-cymene, limonene and  $\gamma$ -terpinene), thyme essential oils and extracts have been widely applied as additives in the food and cosmetic industries thereby increasing the economic

\*Corresponding author. E-mail: jasnai@tmf.bg.ac.rs  
doi: 10.2298/JSC110616009P

value of this crop worldwide.<sup>1,2</sup> In recent investigations, thyme was identified as a valuable raw material for the production of antibacterial agents, whereby thyme isolates showed stronger antibacterial activity than those of sage and rosemary.<sup>3</sup>

Nowadays, different extraction techniques have been widely investigated and applied to obtain valuable natural compounds from plant material for commercial application in the food, pharmaceutical and cosmetic industries.<sup>4</sup> Steam distillation is an appropriate technique for the isolation of volatile components from plant materials, such as essential oils, some amines and organic acids, as well as other, relatively volatile compounds, insoluble in water. Since it is performed at elevated temperature, it requires substantial energy consumption and may cause thermal decomposition of the components of the essential oil, resulting in flavour changes.<sup>5</sup> Extraction with organic solvents or water is used for the isolation of thermolabile substances from plant materials. The organic solvents are removed from the extracts by evaporation under vacuum to obtain concretes which are further subjected to degreasing with ethanol to obtain essential oils for application in the cosmetic and perfumery industries. Processes of extraction with organic solvents are limited by the compound solubility in the specific solvent used, and hence the quality and quantity of the extracted mixture are determined by the type of extractant applied.<sup>4</sup> Solvent extraction in a Soxhlet apparatus enables the isolation and enrichment of compounds of medium and low volatility and thermal stability. It allows a high recovery, but has a number of shortcomings, such as long extraction times, large consumption of solvents, cooling water and electric energy and often unsatisfactory reproducibility.<sup>6</sup> These shortcomings have led to the consideration of the use of new so-called “green” separation techniques with shortened extraction time, reduced organic solvent consumption, and increased pollution prevention, such as microwave extraction, supercritical fluid extraction, ultrasound extraction, ultrafiltration, flash distillation, the controlled pressure drop process and sub-critical water extraction. Nowadays, extraction processes for the isolation of phytochemicals under extreme or non-classical conditions are constantly being developed in applied research and industry.<sup>7,8</sup>

Ultrasound-assisted extraction (USE) is considered as an emerging potential technology that could improve heat and mass transfer of the solutes and increase the efficiency of the isolation of bioactive principles from plant materials. Ultrasound waves produce a cavitation effect that facilitates the erosion of the solute from the interfacial surfaces of a plant material and the release of the extractable compounds by disrupting the plant cell walls.<sup>6,7,9,10</sup> The USE process thus enables high reproducibility along with a reduction of the solvent consumption and extraction time. Several classes of food components, such as aromas, pigments, antioxidants, and other organic and mineral compounds, have been efficiently isolated by a USE process from a variety of matrices (mainly animal tissues, food and plant materials).<sup>7</sup> Scanning electron micrographs have provided evidence of

the mechanical effects of ultrasound, mainly shown by the destruction of cell walls and release of cell contents, leading to more effective mass transfer in solid phase as well.<sup>11</sup> The average time of ultrasonic extraction typically ranges from a few to 30 min, although it can be as long as 70 min, whereby the recoveries obtained during this time are comparable to those obtained after a dozen or so hours of Soxhlet extraction, performed at the same temperature.<sup>6,10</sup> The extraction conditions could be optimized with respect to time, polarity and amount of solvent, as well as the mass and kind of sample, whereby solvent polarity and extraction time have the greatest effect on the recovery.<sup>12</sup> The extraction could be realised at room temperature, which makes it suitable for the extraction of thermally labile compounds. The need for the separation of the organic solvent from the extract is a disadvantage of this technique.

The process of supercritical fluid extraction (SFE) has gained a lot of attention for the extraction of bioactive principles from herbs and spices, especially in the field of high value added compounds, such as pharmaceuticals and nutraceuticals. In order to isolate essential oil rich extracts from aromatic herbs and spices, the SFE process is optimally performed under mild pressure (9–10 MPa) and temperature (40–50 °C) conditions.<sup>13</sup> The SFE process is superior to the conventional extraction processes in a variety of ways: speed of extraction, completeness of extraction, elimination of organic solvents, suitability for thermally sensitive compounds, simplified procedure, selectivity, reduced environmental hazard/non-toxicity and cost savings. Due to their low viscosity and higher diffusivity compared to liquids, supercritical fluids have better transport properties than liquids, and can diffuse through solids more easily.

Knowledge of the mechanism and kinetics of extraction processes is generally needed for optimizing the operating conditions and extraction process design. Independent of the type of plant material or solvent polarity, two extraction periods could be observed: a) a rapid increase in the concentration of the extractable substances in the solvent in the initial stage of the process, known as the washing or the fast extraction period and b) a slow increase in the concentration of the extractable substances in the solvent with increasing progress of the extraction, known as the slow extraction period. Mathematical modelling of extraction processes from different herbaceous materials has been of great importance for design purposes because it allows generalization of the experimental results and successful prediction of the extraction kinetics. A mathematical model based on the second Fick's Law, which was introduced by Crank,<sup>14</sup> has been widely used to describe the process of unsteady diffusion in the solid phase for different extraction processes and particle geometries.<sup>14–20</sup>

In this study, a model based on the Fick's Second Law<sup>14</sup> was used to estimate and compare the diffusion coefficients for different extraction processes from thyme leaves. The method proposed by Osburn and Katz,<sup>18</sup> which considers

two parallel diffusion processes in the solid, was used to determine and compare the diffusion coefficients in the periods of so-called fast and slow extraction. Comparative analysis of diffusion coefficients was provided in order to investigate and quantify the influence of the extraction temperature, ultrasound and stirring on the mass transfer rate during ethanol extraction as well as to compare different extraction processes with ethanol and supercritical carbon dioxide with respect to the diffusion coefficients.

## EXPERIMENTAL

### *Materials*

Dried leaves of *Thymus vulgaris* L. (crop 2009) were supplied by the Institute for Medicinal Plant Research "Dr. Josif Pančić" (Belgrade, Serbia). The moisture content of the air-dried plant material, determined by Karl Fischer volumetric titration, was 10.9 mass %. The ground plant material (average particle diameter of 0.4 mm) was used for the extractions. Ethanol (96 %, Alba, Novi Sad, Serbia) and demi water (NIS Petrol Rafinerija naftne, Novi Sad, Serbia) were used to prepare the solvent mixture of ethanol and water (70:30 v/v) for the solvent extractions. Commercial carbon dioxide (99 % purity) supplied by Messer-Tehnogas (Serbia) was used for the supercritical extraction.

### *Soxhlet extraction*

Ground dried thyme leaves (50 g) were placed in a thimble-holder and continuously filled with condensed fresh solvent from a distillation flask filled with 600 ml of ethanol aqueous solution (70 % v/v) for approximately 16 h (the solvent to feed ratio was 12:1). Each time when the liquid reached the overflow level, the solution in the thimble-holder was siphoned back into the distillation flask, carrying the extracted solutes into the bulk liquid. After each extraction cycle, 5 ml of the solution was taken from the flask, filtered and evaporated to the dryness using a rotary vacuum evaporator (Devarot, Elektromedicina, Ljubljana, Slovenia).

The mass of the extract was determined and the extraction yield ( $Y$ ) was calculated from the formula:

$$Y (\%, \text{w} / \text{w}) = 100 \frac{m_e}{m_{pm}} \quad (1)$$

where  $m_e$  is the mass of the extract and  $m_{pm}$  is the mass of the raw material.

### *Ultrasonic-assisted extraction*

The batch ultrasonic-assisted extraction was performed in an open rectangular ultrasonic cleaner bath (Bodelon Sonorex, RK 52, 60 W, internal dimensions: 150 mm×140 mm×100 mm, Bodelon Electronic, Munich, Germany) using the indirect sonication mode at 35 kHz. Ground plant material (20 g) was added into round bottom flask filled with 240 ml of ethanol aqueous solution (70 % v/v) and subjected to ultrasound-assisted extraction (solvent to feed ratio 12:1). The flask with the sample was partially immersed into the ultrasonic bath, filled with water and sonicated for 90 min at 40 °C ( $\pm 1.0$  °C). In specific time intervals (5, 10, 15, 25, 35, 45, 60, 75 and 90 min), 4 ml of the solution were taken from the flask, filtered and evaporated to the dryness using a rotary vacuum evaporator. The mass of the extract was determined and the yield of extraction was calculated by Eq. (1).

#### Pilot-scale extraction

The pilot-scale extraction (PSE) from thyme was performed in a self-made batch apparatus presented in Fig. 1. The batch extractor was filled with 600 g of the ground plant material and 7.2 dm<sup>3</sup> of ethanol aqueous solution (70 % v/v) (solvent to feed ratio 12:1). The extractions were performed at 40 °C and at the boiling temperature of the ethanol aqueous solution (80.5 °C) for 2 h. The temperature of the water bath was regulated and maintained at a constant level ( $\pm 0.5$  °C). In specific time intervals (10, 30, 60, 120, 180 and 240 min), 30 ml of the solution were taken from the flask and filtered. The solvent was removed from the filtered samples using a rotary vacuum evaporator and the differential mass of the extract was determined. The extraction yield was calculated by Eq. (1).

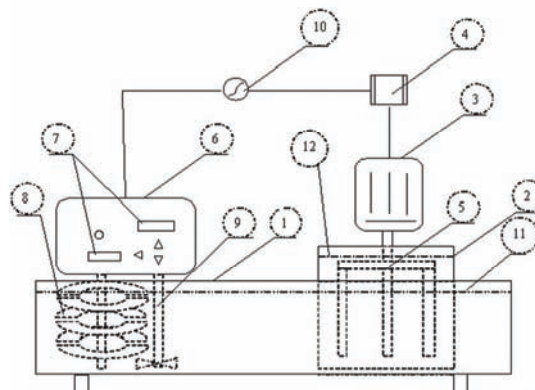


Fig. 1. Scheme of the pilot-scale extraction apparatus: 1 – water bath; 2 – extraction vessel; 3 – electromotor; 4 – frequency regulator; 5 – mixer; 6 – thermoregulation unit; 7 – temperature indicator controller; 8 – heaters; 9 – water bath mixer; 10 – electric power source; 11 – water level in the bath; 12 – level of the solvent and plant material in the vessel.

#### Supercritical CO<sub>2</sub> extraction

Extraction with supercritical carbon dioxide was performed in an Autoclave Engineers SCE Screening System with a 150 cm<sup>3</sup> extractor, which was previously described in detail.<sup>21</sup> The extractions were performed at 10 MPa and 40 °C in order to isolate the essential oil rich extracts and to minimize the yield of higher molecular weight compounds.<sup>13</sup> The initial mass of the plant material used for the extraction was 32 g. At the beginning of the SFE, the plant material was exposed to the influence of the supercritical fluid for one hour under the extraction conditions (without flow of the supercritical carbon dioxide) as a pre-treatment. The chosen pre-treatment of the herbaceous matrix enhances the rate of the SFE due to the glandular trichomes cracking during the exposure to supercritical fluid.<sup>22</sup> After one hour of pre-treatment, continuous flow of supercritical fluid was established. Extraction was realized until total exhaustion of the plant material and maximal extraction yield was determined after consumption of 94.3 kgCO<sub>2</sub> kg<sup>-1</sup> plant material (*i.e.*, after 5 h of extraction). The mass flow rate of the CO<sub>2</sub> was 0.66 kg h<sup>-1</sup>. The experiment was performed in triplicate.

### Mathematical model

Chosen extraction processes were analyzed with the diffusion model proposed by Crank,<sup>14</sup> which is derived from the Fick's Second Law.<sup>14</sup>

The model used in this study was based on the following assumptions:<sup>15-18</sup> a) the solid particles are considered as spheres with a diameter of  $2R$ ; b) the solute is initially homogeneously contained in the solid; c) the solute content in the solid varies with time and distance; d) the extraction of solute occurs in a two-step process, *i.e.*, a constant rate and a decreasing rate stage; e) thermodynamic equilibrium is established at the interface and f) the porous solid is considered as a pseudo-homogeneous medium.

According to the study of Osburn and Katz,<sup>18</sup> who investigated the kinetics of extraction from lamina soybean flakes, it was necessary to consider the presence of two parallel diffusion processes inside the solid; one faster and one slower. This method can also be applied to describe of the extraction from different particle geometries (spheres or flat plates).<sup>15-18</sup> The mass transfer from the spherical particles is described by the following equation:<sup>15,16,18</sup>

$$\frac{c_{\infty} - c}{c_{\infty}} = F_1 \exp\left\{-\frac{\pi^2 D_1 t}{R^2}\right\} + F_2 \exp\left\{-\frac{\pi^2 D_2 t}{R^2}\right\} \quad (2)$$

where:  $F_1 = 6f_1/\pi^2$  and  $F_2 = 6f_2/\pi^2$  are the fractions of the solute that are extracted with diffusion coefficients  $D_1$  and  $D_2$ , respectively,  $f_1$  and  $f_2$  are constants,  $t$  is the extraction time and  $R$  is the radius of the spherical particles. In the later stages of the extraction, only the second term on the right hand side of Eq. (2) remains significant. Therefore, the parameter  $D_2$  could be obtained from the slope and the parameter  $f_2$  from the intercept of the curve when  $\ln(c_{\infty}/(c_{\infty} - c))$  is plotted as function of  $t$ . In the earlier stages of the extraction, the second exponential term is close to unity and  $D_1$  and  $f_1$  could be determined from the same plot.<sup>15</sup>

## RESULTS AND DISCUSSION

### Extraction kinetics study

The determined extraction yields obtained by the employed methods are presented in Table I. The extraction yields for the extraction processes with ethanol are plotted as function of the extraction time in Figs. 2 and 3. The extraction curve for the supercritical extraction process is presented as a plot of extraction yields vs. specific amount of supercritical carbon dioxide consumed ( $m_{\text{CO}_2}$ ) in Fig. 4.

TABLE I. The yields obtained by laboratory and pilot-scale extraction from thyme leaves

Extraction type	Notation	$T / ^\circ\text{C}$	$t / \text{h}$	$t_{90}^{\text{a}} / \text{h}$	$V_s^{\text{b}} / \text{l}$	Ultrasound	Stirring	$Y^{\text{c}} / \%$
<b>Laboratory scale</b>								
Soxhlet	SE	80.5	15	10.0	0.60	No	No	$29.80 \pm 2.16$
Ultrasonic	USE	40.0	1.5	1.25	0.24	Yes	No	$18.5 \pm 0.75$
Supercritical	SFE	40.0	5.0	1.60	4.8	No	No	$1.15 \pm 0.15$
<b>Pilot plant scale</b>								
Batch solvent	PSE1	40.0	2.0	1.40	7.2	No	Yes	$21.23 \pm 0.52$
	PSE2	80.5	2.0	0.66	7.2	No	Yes	$27.60 \pm 0.37$

<sup>a</sup>Time required for the achievement of 90 % recovery of extractable substances in the given process; <sup>b</sup>volume of solvent (70 % v/v aqueous solution of ethanol or supercritical carbon dioxide); <sup>c</sup>averaged values of extraction yields determined in triplicate with the absolute deviation



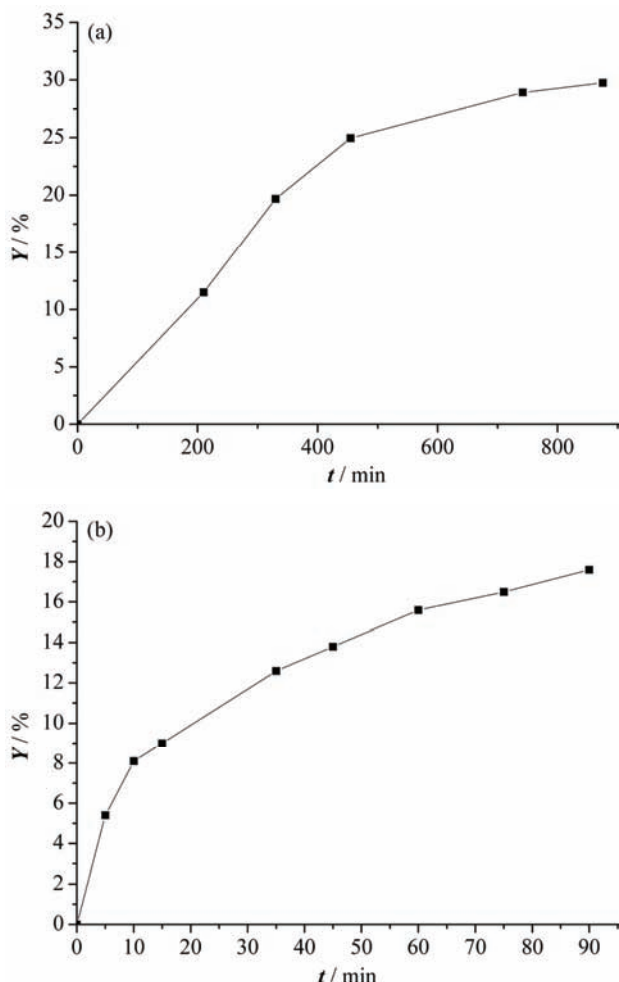


Fig. 2. Kinetics of thyme extraction a) in the Soxhlet apparatus and b) by ultrasonic-assisted extraction.

As expected, much higher extraction yields were obtained by the solvent extractions due to the lower selectivity of the aqueous ethanolic solution compared to that of supercritical carbon dioxide. According to the presented results, 1.5 h of ultrasonic extraction at 40 °C enabled 85 % recovery of thyme extract achieved by the Soxhlet extraction at a higher temperature (80.5 °C) and for a much longer extraction time ( $\approx$ 15 h) with the same solvent. This can be explained by the beneficial effects of ultrasound waves to the extraction efficiency that have been assigned to mass transfer intensification, cell disruption, improved penetration and capillary effects.<sup>9–11</sup>

Considering the kinetic plots (Figs. 2–4), the presence of two extraction stages were noticed: a constant rate stage followed by a stage of decreasing rate. Namely, transfer of the extractible substances from thyme included: a solid to

liquid (or supercritical carbon dioxide) phase transfer, corresponding to the extraction of the easy available solute, from exogenous glands disrupted by milling, by simple washing, and b) a molecular diffusion of the inaccessible fraction of solute (intact glandular trichomes) throughout the porous herbaceous matrix.

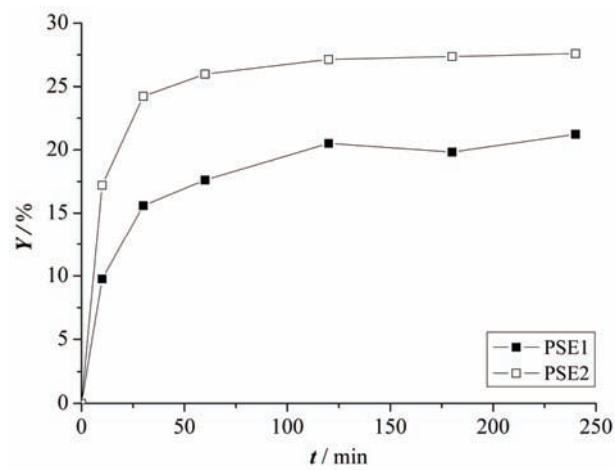


Fig. 3. Influence of temperature on the kinetics of thyme extraction by the ethanol–water mixture on the pilot-scale.

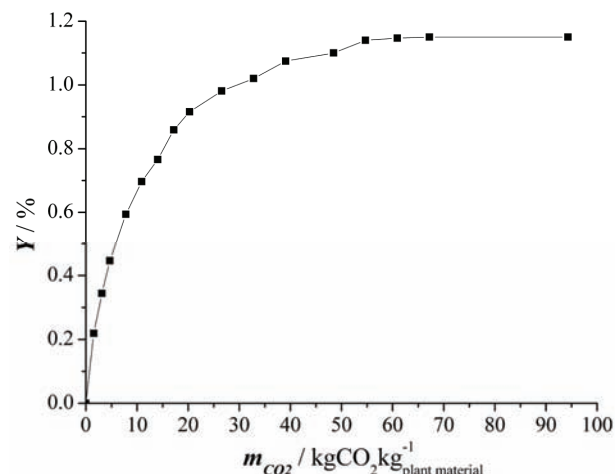


Fig. 4. Extraction yield as a function of the specific amount of supercritical carbon dioxide for the SFE at 10 MPa and 40 °C.

The shape of extraction curves in the Figs. 2b and 3 and the results presented in the Table I indicated that the rate of solvent extractions within the initial washing stage was enhanced by increasing temperature, stirring and ultrasound. Moreover, the rate of solvent extraction during the slow extraction period was particularly enhanced by ultrasound. As for the SFE process, the applied pre-treatment of the plant material (exposure to supercritical carbon dioxide) led to the cracking of additional glandular trichomes, which contributed to an increase of the extraction rate within the early stage of the SFE process.

According to the presented kinetic data, the time required for achievement of satisfactory recovery of extractable substances (90 % recovery), denoted as  $t_{90}$ , can be determined (Table I). The rate of achievement of a satisfactory yield of extract was noticeably affected by the nature of the employed solvent. The highest recovery rate was achieved in the supercritical extraction process (1.60 h). An increase of the extraction temperature in the case of the pilot plant extraction also increased the rate of achievement of a satisfactory extraction yield (0.66 instead of 2 h).

#### *Evaluation of the diffusion coefficients*

Equilibrium concentrations (or saturation concentrations) of thyme extracts in ethanol aqueous solution or supercritical carbon dioxide at infinite time ( $c_\infty$ ) represent concentrations of solute in solvent when all resistances are overcome. Since the ethanol extractions are batch processes and SFE is characterized by a continuous flow of the supercritical fluid, different procedures were used to determine  $c_\infty$ . Equilibrium concentrations of extractable substances for extraction with ethanol at a given temperature were determined by exhaustion of the plant material. In the case of the SFE process,  $c_\infty$  was determined by the following procedure: milled plant material was placed in the extractor vessel and pressurized to the extraction conditions. Sudden fast depressurization followed in order to disrupt the untouched glandular trichomes and plant cells and to minimize cell wall resistance in the extraction process. The extraction vessel was pressurized again and the solubility of saturation was determined from the slope of the extraction curve in the early stages of extraction. The obtained  $c_\infty$  values are presented in Table II.

TABLE II. Corresponding values of  $c_\infty$  of extractable substances from thyme for laboratory and pilot-scale extraction processes

Extraction type	Notation	$c_\infty / \text{kg m}^{-3}$
Laboratory scale		
Soxhlet	SE	27.1
Ultrasonic	USE	16.9
Supercritical	SFE	0.90
Pilot plant scale		
Batch solvent	PSE1	24.0
	PSE2	27.0

The corresponding plots of the function  $\ln(c_\infty/(c_\infty - c))$  against the extraction time are presented in Figs. 5–7 for the fast stage as well as for the slower stage of the chosen extraction processes.

During the SFE process, the concentration of extractable substances in the supercritical carbon dioxide, which flows continuously, decreased with time due

to exhaustion of the plant material, and therefore the function  $\ln(c_\infty/(c_\infty - c))$  against  $t$  had a downward trend (Fig. 7). However, this function had an upward trend for USE, SE and PSE as batch processes due to the enrichment of ethanol with solute over time (Figs. 5 and 6).

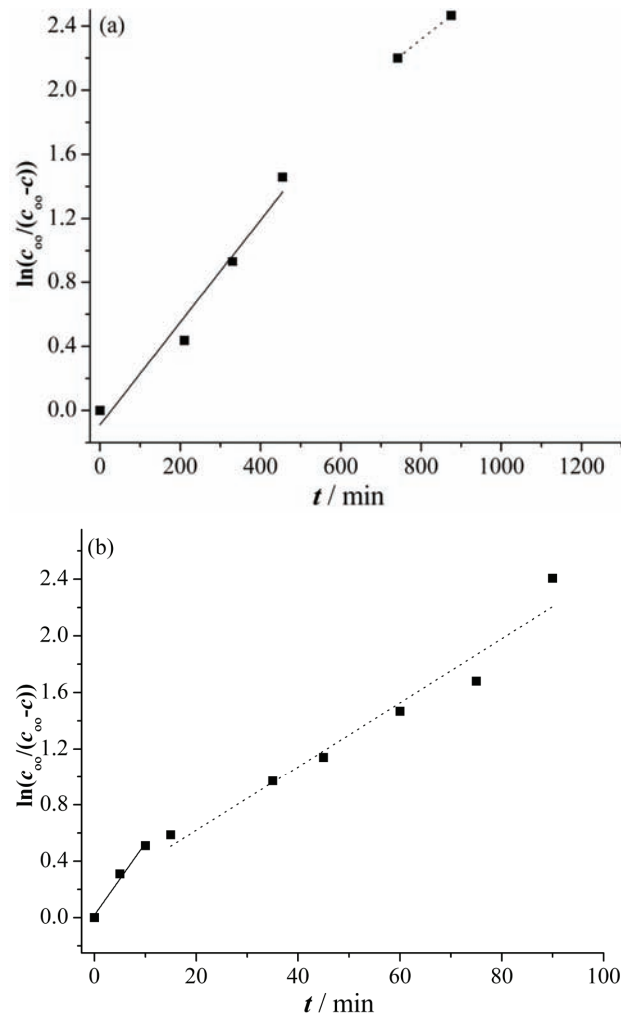


Fig. 5. Plot of the function  $\ln(c_\infty/(c_\infty - c))$  against time for the fast first and the later slower second stage of the laboratory-scale a) Soxhlet extraction at 80.5 °C, and b) ultrasonic-assisted extraction (USE) of thyme at 40 °C (— fast extraction; --- slow extraction).

The corresponding diffusion coefficients for the periods of constant and decreasing extraction rate,  $D_1$  and  $D_2$ , respectively, are presented in Table III. Diffusion coefficients in the initial washing period were one to three (in the case of the SFE process) orders of magnitude higher compared to those for the period of slow extraction. Moreover, the calculated value of the diffusion coefficient for the SFE process in the washing period was two or three orders of magnitude

higher compared to those reported for the extraction processes with ethanol. This was expected since supercritical fluids penetrate into samples of plant material almost as well as gases, due to their low viscosity. At the same time, their dissolving power is similar to those of liquids.<sup>6</sup> In addition, there was a higher content of lower molecular weight compounds in the thyme supercritical extract (mainly essential oil with thymol as the most abundant compound<sup>3,23,24</sup>) than in the thyme ethanol extracts, which also contributes to faster diffusion rate of the solute in the case of the thyme SFE. Recently, phenylindolizine was identified as main component of the thyme ethanol extract.<sup>25</sup>

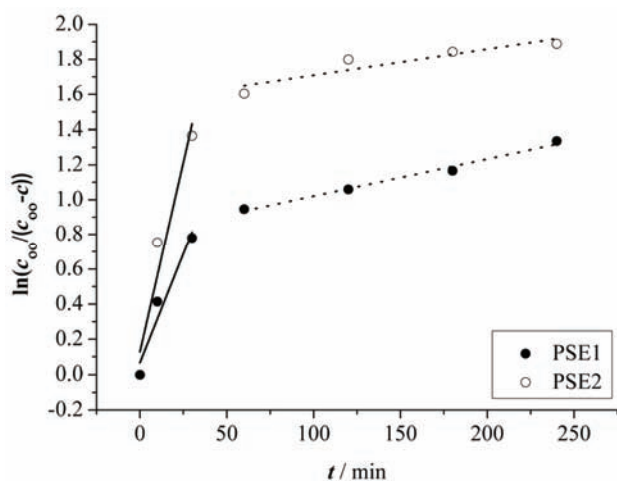


Fig. 6. Plot of the function  $\ln(c_\infty/(c_\infty - c))$  against time for the fast first and the later slower second stage of the pilot-scale extraction of thyme at different temperatures (PSE1 and PSE2); — fast extraction; ---- slow extraction).

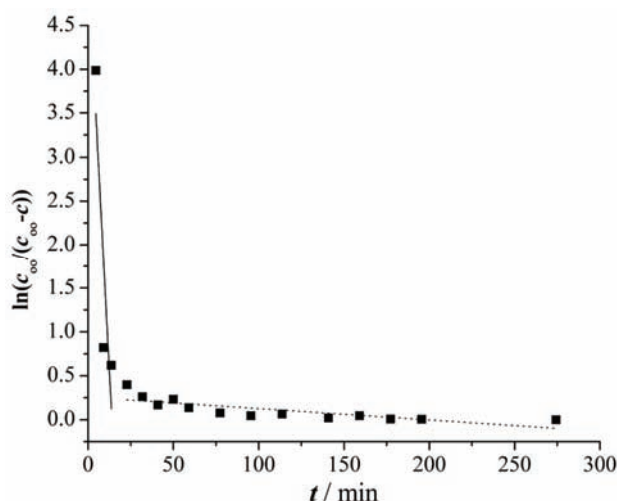


Fig. 7. Plot of the function  $\ln(c_\infty/(c_\infty - c))$  against time for the fast first and the later slower second stage of SFE (— fast extraction; ---- slow extraction).

Considering the solvent extractions, the mass transfer rate described by  $D_1$  could be increased by ultrasound, temperature increase or by stirring within the initial washing phase, while ultrasound particularly affected the mass transfer rate during the slow period of extraction (described by  $D_2$ ) (Table III).

TABLE III. Diffusion coefficients of solute obtained for different extraction processes of thyme

Extraction method	$f_1$	$f_2$	$F_1$	$F_2$	$D_1 \times 10^{10} / \text{m}^2 \text{s}^{-1}$	$D_2 \times 10^{11} / \text{m}^2 \text{s}^{-1}$
Laboratory scale						
SE	0.842	0.802	0.512	0.488	0.13	0.81
USE	0.253	1.392	0.153	0.846	2.07	9.18
SFE	0.370	1.274	0.225	0.775	15.0	0.523
Pilot plant scale						
PSE1	0.910	0.732	0.554	0.446	4.04	3.41
PSE2	1.298	0.346	0.790	0.210	7.04	2.43

During the batch extraction of thyme with ethanol on the pilot plant scale, a temperature increase from 40 to 80.5 °C enhanced the extraction efficiency due to its positive effect on the solubility of the solutes. The temperature increase also enhanced the mass transfer rate in the washing phase due to the reduced viscosity at elevated temperatures. Agitation enabled enhancement of the mass transfer of solute particularly in the period of fast extraction (washing period), which was confirmed by the one order of magnitude higher diffusion coefficients for the PSE compared to the SE process at the same temperature (80.5 °C) (Table III).

To the best of our knowledge, there are no data available in the open literature on the values of the diffusion coefficients in extraction processes from thyme, except in one previously published study<sup>23</sup> in which the diffusion coefficient for the mass transfer through the glandular trichomes membrane in the SFE process was determined using mathematical modelling on the micro-scale.<sup>22</sup> Obtained value of the diffusion coefficient through the peltate gland membrane was  $3.5 \times 10^{-12} \text{ m}^2 \text{s}^{-1}$ .<sup>23</sup> This diffusion coefficient corresponds to the diffusion coefficient in the process of the slow extraction (after the easily accessible oil is exhausted), which was determined in this study to be  $5.32 \times 10^{-12} \text{ m}^2 \text{s}^{-1}$  (Table III) using the mathematical model based on the Fick's Second Law. The similar values of the diffusion coefficients can be explained by the same extraction conditions (10 MPa and 40 °C), as well as by the similar chemical composition of the extracts, mainly composed of essential oil.

Herodež *et al.*<sup>17</sup> investigated the kinetics of extraction from balm (*Melissa officinalis* L.) belonging to the same plant family as thyme (Lamiaceae) with an ethanol:methanol:2-propanol ratio 90:5:5 v/v in an ultrasonic bath for 1 h at room temperature. The authors used the same mathematical model as applied in this study except they considered the solid particles as flat plates with a thickness of  $2L$  and reported one order of magnitude lower diffusion coefficients of carnosic,

ursolic and oleanolic acids for the period of the fast extraction (order of magnitude  $10^{-11} \text{ m}^2 \text{ s}^{-1}$ ) as well as for the period of slow extraction ( $10^{-13}$ – $10^{-12} \text{ m}^2 \text{ s}^{-1}$ ) compared to the values obtained in this investigation. The reason for this lies in the fact that the higher molecular weight compounds present in the balm leaves (carnosic, ursolic and oleanolic acid with molecular weight of 332.43–456.71 kg kmol $^{-1}$ ) need more time to diffuse from the solid particle than the compounds present in the thyme ethanol extract. Reportedly,<sup>24,25</sup> the thymol (molecular weight 150.22 kg kmol $^{-1}$ ) content in a thyme ethanol extract was still very high (8 %) and phenylindolizine (molecular weight 193.25 kg kmol $^{-1}$ ) was identified as the most abundant component. The lower values of diffusion coefficients reported by Herodež *et al.*<sup>17</sup> could be also result from performing the ethanol extraction at a lower temperature (room temperature) than the temperatures applied in this study (40 and 80.5 °C).

#### CONCLUSIONS

An analysis of the mass transfer phenomena in the extraction of phytochemicals on the laboratory and pilot plant scale is necessary for process design. This work provides new data on the values of the diffusion coefficients in different extraction processes from thyme. In the fast extraction period, the diffusion coefficients were one to three orders of magnitude higher compared to those in the period of slow extraction. The highest diffusion coefficient was reported for the early stage of the SFE process, which was due to the physical properties of supercritical carbon dioxide. Concerning the solvent extractions, the mass transfer rate in the period of fast extraction and the corresponding diffusion coefficient can be enhanced by a temperature increase, ultrasound and stirring. The mass transfer rate and corresponding diffusion coefficients in the period of slow extraction was most affected by ultrasound.

#### NOMENCLATURE

$c$	Concentration of solute in the solution at time $t$ , kg m $^{-3}$
$c_\infty$	Concentration of the solute in the solution at infinite time ( $t \rightarrow \infty$ ), kg m $^{-3}$
$D_1$	Diffusion coefficient in the constant extraction rate period, m $^2 \text{ s}^{-1}$
$D_2$	Diffusion coefficient in the decreasing extraction rate period, m $^2 \text{ s}^{-1}$
$F_1, F_2$	Fractions of the solute, which are extracted with diffusion coefficients $D_1$ and $D_2$ , respectively
$f_1, f_2$	Parameters obtained from the intercept of the curve when $\ln(c_\infty/(c_\infty - c))$ is plotted as a function of the extraction time $t$
$m_e$	Mass of the extract, g
$m_{\text{CO}_2}$	Specific amount of supercritical carbon dioxide consumed, kg CO $_2$ kg $^{-1}$ plant material
$m_{\text{pm}}$	Mass of the plant material
$R$	Radius of the spherical particles, mm
$T$	Temperature, °C
$t$	Extraction time, min

- $t_{90}$  Extraction time required for the achievement of 90 % recovery of the extractible substances under the given extraction conditions and extractant  
 $V_s$  Volume of solvent (70 % v/v aqueous solution of ethanol or supercritical carbon dioxide)  
 $Y$  Extraction yield, mass %.

*Acknowledgments.* Financial support of this work by the Serbian Ministry of Education and Science, Project III 45017, is gratefully acknowledged.

#### ИЗВОД

#### УПОРЕДНА АНАЛИЗА КОЕФИЦИЈЕНТА ДИФУЗИЈЕ ЗА РАЗЛИЧИТЕ ПРОЦЕСЕ ЕКСТРАКЦИЈЕ ИЗ ТАМЈАНА

СЛОБОДАН С. ПЕТРОВИЋ<sup>1</sup>, ЈАСНА ИВАНОВИЋ<sup>2</sup>, СТОЈА МИЛОВАНОВИЋ<sup>2</sup> И ИРЕНА ЖИЖОВИЋ<sup>2</sup>

<sup>1</sup>БИОСС – ПС и осћали, Булевар ослобођења 401и, 11000 Београд и <sup>2</sup>Универзитет у Београду, Технолошко-међалуршки факултет, Карнеџијева 4, ћ. др. 3503, 11120 Београд

Циљ овог рада била је анализа кинетике и феномена преноса масе за различите процесе екстракције из листа тимијана (*Thymus vulgaris* L.). Испитани су различити поступци екстракције са воденим раствором етанола: екстракција у апаратури по Сокслету, шаржна ултразвучна екстракција на лабораторијском нивоу као и шаржна екстракција са мешањем на полуиндустријском нивоу. Процеси екстракције са етанолом су поређени са процесом екстракције са наткритичним угљеник(IV)-оксидом на 10 МРа и 40 °C. Експериментални подаци су анализирани помоћу математичког модела заснованог на другом Фиковом закону у циљу одређивања и поређења коефицијената дифузије у периоду константне и опадајуће брзине екстракције. У периоду брзе екстракције, вредности коефицијената дифузије су биле један до три реда величине веће у односу на вредности коефицијената дифузије за период споре екстракције. Највећа вредност коефицијента дифузије била је одређена за период брзе екстракције код процеса наткритичне екстракције. Код процеса екстракција са етанолом, примена ултразвука, мешање и повећање температуре су позитивно утицали на брзину преноса масе у периоду испирања. С друге стране, највећи утицај на повећање брзине преноса масе у периоду споре екстракције имала је примена ултразвука.

(Примљено 11. јуна, ревидирано 31. октобра 2011)

#### REFERENCES

1. A. L. Dawidowicz, E. Rado, D. Wianowska, M. Mardarowicz, J. Gawdzik, *Talanta* **76** (2008) 878
2. E. Al-Dein Mohammed Al-Ramamneh, *Ind. Crop. Prod.* **30** (2009) 389
3. J. Ivanovic, D. Misic, I. Zizovic, M. Ristic, *Food Control* **25** (2012) 110
4. L. Wang, C. L. Weller, *Trends Food Sci. Tech.* **17** (2006) 300
5. A. Ammann, D. C. Hinz, R. S. Addleman, C. M. Wai, B. W. Wenclawiak, *Fresenius J. Anal. Chem.* **364** (1999) 650
6. G. Romanik, E. Gilgenast, A. Przyjazny, M. Kamiński, *J. Biochem. Biophys. Met.* **70** (2007) 253
7. F. Chemat, Z. Huma, M. K. Khan, *Ultrason. Sonochem.* **18** (2011) 813
8. E. Y. Kenig, *Chem. Eng. Res. Des.* **86** (2008) 1059
9. M. Toma, M. Vinotoru, L. Paniwnyk, T. J. Mason, *Ultrason. Sonochem.* **8** (2001) 137
10. M. Vinotoru, *Ultrason. Sonochem.* **8** (2001) 303

11. S. Chemat, A. Lagha, H. AitAmar, P. V. Bartels, F. Chemat, *Flav. Fragr. J.* **19** (2004) 188
12. M. I. S. Melecchi, V. F. Peres, C. Dariva, C. A. Zini, F. C. Abad, M. M. Martinez, E. B. Caramão, *Ultrason. Sonochem.* **13** (2006) 242
13. E. Reverchon, I. De Marco, *J. Supercrit. Fluids* **38** (2006) 146
14. J. Crank, *The mathematics of diffusion*, Oxford University Press, Oxford, 1975
15. M. Škerget, M. Bezjak, K. Makovšek, Ž. Knez, *Acta Chim. Slov.* **57** (2010) 60
16. M. Hojnik, M. Škerget, Ž. Knez, *LWT Food Sci. Technol.* **41** (2008) 2008
17. Š. S. Herodež, M. Hadolin, M. Škerget, Ž. Knez, *Food Chem.* **80** (2003) 275
18. J. O. Osburn, D. L. Katz, *Trans. Am. Inst. Chem. Eng.* **40** (1944) 511
19. D.A. Şaşmas, *J. Am. Oil Chem. Soc.* **73** (1996) 669
20. D. T. Veličković, D. M. Milenović, D. S. Ristić, V. B. Veljković, *Biochem. Eng. J.* **42** (2008) 97
21. I. Zizovic, M. Stamenic, A. Orlovic, D. Skala, *J. Supercrit. Fluids* **39** (2007) 338
22. I. Zizovic, M. Stamenic, A. Orlovic, D. Skala, *Chem. Eng. Sci.* **60** (2005) 6747
23. J. Ivanovic, I. Zizovic, M. Ristic, M. Stamenic, D. Skala, *J. Supercrit. Fluids* **55** (2011) 983
24. Z. P. Zeković, Ž. D. Lepojević, S. L. Markov, S. G. Milošević, *Acta Periodica Technol.* **33** (2002) 1
25. K. Bayoub, T. Baibai, D. Mountassif, A. Retmane, A. Soukri, *Afr. J. Biotechnol.* **9** (2010) 4251.





## Transesterification of linoleic and oleic sunflower oils to biodiesel using CaO as a solid base catalyst

ZLATICA PREDOJEVIĆ<sup>\*\*</sup>, BILJANA ŠKRBIĆ<sup>#</sup> and NATAŠA ĐURIŠIĆ-MLADENOVIĆ

Faculty of Technology, University of Novi Sad, Bulevar cara Lazara 1,  
21000 Novi Sad, Serbia

(Received 24 August, revised 24 November 2011)

**Abstract:** The purpose of this work was to characterize biodiesel (*i.e.*, methyl esters, MEs) produced from linoleic and oleic sunflower oils (LSO and OSO, respectively) by alkali transesterification with methanol using CaO as a heterogeneous catalyst under different reaction conditions. The parameters investigated were the methanol/oil mole ratio (4.5:1, 6:1, 7.5:1, 9:1 and 12:1) and the mass ratio of CaO to oil (2 and 3 %). The physical and chemical properties of the feedstocks and the MEs, such as density at 15 °C, kinematic viscosity at 40 °C, acid value, iodine value, saponification value, cetane index and fatty acid (methyl ester) composition, were determined in order to investigate the effects of the properties of the LSO and OSO and reaction parameters on the product characteristics, yields and purity. The properties of the feedstocks had a decisive effect on the physical and chemical properties of the MEs. The studied reaction conditions did not significantly affect the properties of the MEs. The produced MEs generally met the criteria required for commercial biodiesel; in fact, the only exception was the iodine value of the ME produced from LSO. The product yields only slightly changed with the applied conditions; the highest yield (99.22 %) was obtained for the ME-LSO produced at 6 mol % methanol to oil ratio, while the lowest one (93.20 %) was for ME-OSO produced under the lowest methanol/oil mole ratio (4.5:1). The applied amounts of catalyst had a similar influence on the oil conversion to biodiesel. The yields of the ME-LSOs were, in general, somewhat higher than those obtained for the ME-OSOs under the same conditions, which was attributed to the influence of the respective acid value and viscosity of the feedstock.

**Keywords:** biodiesel; calcium oxide; heterogeneous catalysis; transesterification; linoleic and oleic sunflower oils.

\* Corresponding author. E-mail: pzlatica@uns.ac.rs

<sup>#</sup> Serbian Chemical Society member.

doi: 10.2298/JSC110824206P

## INTRODUCTION

Biodiesel is a non-petroleum-based fuel defined as fatty acid methyl or ethyl esters produced by transesterification of triglycerides, the main constituents of vegetable oils or animal fats, with a short chain alcohol (methanol or ethanol) in the presence of a suitable catalyst. This fuel may be regarded as a mineral diesel substitute with the advantage of reducing greenhouse emissions because it is a renewable resource. However, the high cost of biodiesel is the major obstacle for its commercialization. An important contribution to the final cost arises from the catalytic transesterification. The primary commercial process used today for biodiesel production is alkali catalyzed transesterification, performed in batch or continuous stirred tank reactors at temperatures ranging from 60 to 200 °C using homogeneous catalysts, most frequently NaOH or KOH dissolved in methanol.<sup>1</sup> However, the use of homogeneous base catalysts requires neutralization and a difficult separation from the final reaction mixture, which lead to a series of environmental problems related to the use of high amounts of solvents and energy. Furthermore, the operational problems in the conventional production process are associated with the catalyst (*e.g.*, NaOH and KOH) because they are hazardous, caustic and corrosive.<sup>1</sup> Replacement of the homogeneous catalysts by heterogeneous solid catalysts has various advantages, such as, lower consumption of the catalysts, easier separation from the reaction mixture and the possibility of recycling the catalyst, lower production costs and less environmental endangerment since there is no need for purification of waste effluents. Therefore, the possibility of replacing the homogeneous with heterogeneous solid catalysts in biodiesel production is of increasing interest. In recent years, a considerable research effort is being devoted to the heterogeneous catalyzed methanolysis of vegetable oils. As a result, a great variety of catalysts, such as alkali earth metals oxides and hydroxides,<sup>2–4</sup> alkali metals hydroxides or salts supported on  $\gamma$ -alumina,<sup>5–7</sup> zeolites,<sup>8</sup> hydrotalcites,<sup>9</sup> etc., have hitherto been used under different reaction conditions and with variable degrees of success.

Among the alkali earth oxides, CaO is one of the solids that has displayed higher transesterification activities.<sup>10,11</sup> The application of CaO as a solid base catalyst for soybean oil transesterification was investigated by Liu *et al.*<sup>3</sup> and a reaction mechanism was proposed. The catalyst lifetime was longer than that of calcined  $K_2CO_3/\gamma Al_2O_3$  and  $KF/\gamma Al_2O_3$  catalysts. CaO maintained its activity even after being repeatedly used for 20 cycles and the biodiesel yield at 1.5 h was not substantially affected in the repeated experiments. Granados *et al.*<sup>2</sup> studied the activity of activated CaO as a heterogeneous catalyst in the conversion of sunflower oil to biodiesel. They demonstrated that CaO could be reutilized for eight runs without significant deactivation, stressing the possibility of its use as compared with the conventional homogeneous catalyst, KOH dissolved in methanol. Even though the transesterification activity of CaO is not as large as that

of KOH or NaOH homogeneous catalysts, this could be compensated for by employing a larger concentration of CaO, as long as the CaO can be reutilized for a greater number of runs.<sup>2</sup> Veljković *et al.*<sup>4</sup> examined the methanolysis of sunflower oil in the presence of CaO in order to determine the optimal temperature for CaO calcination.

The purpose of this work was to study the transesterification of two types of sunflower oils, differing in their unsaturated fatty acids profiles (*i.e.*, primarily in their contents of linoleic and oleic acids), to biodiesel using methanol and CaO, as a solid base catalyst. The aim was to investigate the effects of the properties of the feedstocks and the transesterification reaction conditions, such as the methanol/oil molar ratio and the catalyst/oil mass ratio, on the properties, yields and purity of the obtained methyl esters. This is the first study that explores simultaneously the heterogeneous conversion of these two types of sunflower oils to biodiesel.

## EXPERIMENTAL

### Materials and methods

To prepare biodiesel by alkali catalyzed transesterification, linoleic and oleic sunflower oils (LSO and OSO, respectively) were used. Since there is insufficient information on the working parameters for the heterogeneous CaO transesterification of such oils, especially of OSO, it was decided to work with refined oils, despite the fact that they cost much more than the biodiesel to be produced from them; similarly, many researchers have used refined edible oils in the first stages of their studies in order to investigate the influence of the basic properties of the oily feedstocks and of the working conditions on the properties and yields of the obtained biodiesel, thereby avoiding the introduction of impurities into the process.<sup>3,12-15</sup> Methanol chromatographic grade (99.9 %), and CaO (ReagentPlus 99.9 % trace metals basis) in a form of powder were supplied by Aldrich, while the reference standard for the gas chromatographic determination of the fatty acid methyl esters was obtained from Supelco (Bellefonte, USA). Concerning the CaO powder, the supplier notes that *ca.* 10 % of the mass is lost by calcinations at 1000 °C, indicating that CaO was partially carbonated and hydrated. Such CaO was stored under vacuum in a desiccator with silica gel and KOH pellets to remove H<sub>2</sub>O and CO<sub>2</sub> from the residual desiccator atmosphere, as previously described by Granados *et al.*<sup>2</sup>

### Transesterification procedure

Methyl esters were synthesized in a batch type reactor using CaO powder as the catalyst. All experiments were performed in a three-neck round-bottom flask equipped with a thermometer, reflux condenser and magnetic stirrer, which was immersed in a water bath. In all batches, 150 g of oil was used in the reaction. The transesterification reaction was performed using different methanol/oil mole ratios (4.5:1, 6:1, 7.5:1, 9:1 and 12:1) and various amounts of catalyst relative to the mass of oil (2 and 3 %). The mixture was vigorously stirred at 400 rpm and at 65 °C (*i.e.*, around the boiling point of the mixture) under methanol reflux for the required reaction time of 1.5 h, in accordance to a previous study of Liu *et al.*<sup>3</sup> According to the results of Liu *et al.*,<sup>3</sup> the chosen temperature of 65 °C is an optimum reaction temperature for the transesterification of oil to biodiesel using solid CaO; it was found that at lower temperatures, reaction rate was slow and the biodiesel yield was low, while a more rapid reaction

rate could be obtained at higher temperatures, but at temperatures higher than 65 °C, the methanol vaporized and formed a large number of bubbles that could inhibit the reaction on the interfaces in the three-phase system methanol–oil–catalyst.<sup>3</sup> After completion of the reaction, the mixture was poured into a separation funnel and left for separate for 12 h. The upper layer of esters was then filtered through filter paper and the residual methanol from the filtrate was removed *via* rotary evaporation (at 60 °C and 20 kPa) prior to analysis. A similar transesterification procedure was used previously but with different solid base catalysts, *i.e.*, CaO,<sup>3</sup> NaX zeolite with a KOH coating<sup>8</sup> and KNO<sub>3</sub> loaded alumina.<sup>5,6</sup>

#### *Characterization of feedstocks and methyl esters*

Most of the physical and chemical properties of the used feedstocks (LSO and OSO) and the obtained methyl esters (designated as ME-LSO and ME-OSO, respectively) were determined by the methods listed in the SRPS EN 14214:2005 standard,<sup>16</sup> which defines the requirements and test methods for fatty acid methyl esters (FAME) for use in diesel engines.

Measurements of the density at 15 °C by hydrometer method and of the kinematic viscosity at 40 °C were realized according to SRPS EN ISO 3675:2005<sup>17</sup> and SRPS ISO 3104:2003,<sup>18</sup> respectively. The acid value (AV) was determined by titration in accordance to EN 14104:2003;<sup>19</sup> the iodine value (IV) was obtained by the Hannus method (EN 14111:2003).<sup>20</sup> Even though it is not required by SRPS EN 14214:2005,<sup>16</sup> the saponification value (SV) was also determined using the titration method described in EN ISO 3657:2003.<sup>21</sup> This property was previously used for biodiesel characterization.<sup>22–25</sup> The method for the estimation of the cetane index (CI) based on the saponification (SV) and iodine (IV) values was previously described<sup>26</sup> as simpler and more convenient than the experimental procedure for the determination of the cetane number utilizing a cetane engine (SRPS ISO 4264:2002).<sup>27</sup> For CI calculation, the Krisnangkura Equation as follows was used:<sup>26</sup>

$$CI = 46.3 + 5458/SV - 0.225IV \quad (1)$$

This equation is not recommended for feedstock characterization as it was previously documented that the cetane indices of oils are generally much lower than those of methyl ester derivates despite the fact that they have similar SVs and IVs.<sup>26</sup> Thus, a discussion on the CI of the feedstocks will not be made.

The methyl ester composition of biodiesel was obtained using a gas chromatograph (GC) equipped with DB-WAX 52 column (Supelco) and a flame ionization detector (FID).

All the properties were analyzed in two replicates and the final results are given as average values.

#### *Principal component analysis (PCA)*

PCA is a multivariate analytical tool used to reduce a set of original variables and to extract a small number of latent factors (principal components, PCs) for analyzing relationships among the observed variables (*i.e.*, physical and chemical properties of biodiesels in this study) and for classification of samples (*i.e.*, biodiesels produced under different working conditions). The newly extracted variables, *i.e.*, PCs, are linear combinations of the original ones and are sorted in descending order according to the amount of variance that they account for in the original set of variables. The loadings express how well the principal components correlate with the old variables. PCA shows which kinds of variables are similar to each other, *i.e.*, carry comparable information, and which ones are unique. Relationships among the samples could be seen on the score plots, whereas the loading plots show the extent to which each variable contributes to the sample separation (grouping). Alternatively, variable loadings and sample scores can be combined into a unique graphical presentation called a biplot. Since

the magnitude of the loadings and scores are not the same, it is advisable to divide each loading and score value with respective to the maximum value obtained for a particular PC; in this way, the biplot presents the relative positions of the element loadings and the sample scores within the range from -1 to +1. Thus, the interpretation of the correlations among variables and their impact on the classification of the samples could be more evident. It is also possible to search for the possible presence of outliers using PC biplots. Outliers are in fact measurements that are far removed from the others in the plot because they have exceptionally high and/or low concentrations of the variables.<sup>28-30</sup>

In this study, the input data set consisting of columns with physical and chemical properties determined in this investigation and of rows with biodiesels produced under different conditions were firstly mean-centered (column means subtracted from each matrix element). Then each matrix element was divided by the standard deviation of the respective column and the established matrix was submitted to PCA. The number of PCs extracted from the variables was determined by the Kaiser Rule.<sup>31</sup> This criterion retains only PCs with eigenvalues that exceed one. The algorithm of PCA can be found in standard textbooks.<sup>32</sup>

## RESULTS AND DISCUSSION

### *Effects of the properties of the feedstocks on the biodiesel properties*

The physical and chemical properties of the LSO and OSO used as the feedstocks for transesterifications are given in Table I.

TABLE I. Physical and chemical properties of linoleic (LSO) and oleic (OSO) refined sunflower oils used as feedstocks for methyl esters preparation by heterogeneous transesterification

Property		LSO	OSO
Density at 15 °C, g cm <sup>-3</sup>		0.927	0.920
Kinematic viscosity at 40 °C, mm <sup>2</sup> s <sup>-1</sup>		25.75	30.32
Acid value, mg KOH g <sup>-1</sup> oil		0.05	0.41
Iodine value, g I <sub>2</sub> per 100 g		134.16	107.03
Saponification value, mg KOH g <sup>-1</sup> oil		194	191
Fatty acid composition, mass %			
C16:0	Palmitic	6.18	5.20
C18:0	Stearic	3.98	3.36
C18:1	Oleic	21.13	58.91
C18:2	Linoleic	66.79	32.24
C18:3	Linolenic	<0.20	0.20
C20:0	Arachidic	0.20	<0.20
C22:0	Behenic	0.67	<0.20
C24:0	Tetracosanoic	0.24	<0.20
Total unsaturated		87.92	91.35
Total saturated		11.27	8.56

It could be seen that the main differences between the used feedstocks were in acid and iodine values, and the contents of oleic and linoleic acids. The OSO had an almost 3 times higher content of oleic acid, while its acid values was 8 times higher than that of LSO. However, this higher acid value was still far

below the recommendation given for the acid value of feedstocks of less than 2 mg KOH g<sup>-1</sup> (*i.e.*, 1 %)<sup>24</sup> for the case of alkaline transesterification. The LSO had a 2 times higher content of linoleic acid and 1.25 times higher iodine value than the OSO. The remaining characteristics analyzed in oils did not differ by more than 1.2 times, and some of the observed differences coincided with the observation of Purdy,<sup>33</sup> who found that high oleic sunflower oils had higher viscosities and lower densities, and lower iodine and saponification values than the “normal” (linoleic) oils, as direct consequences of the higher oleic acid content.

The physical and chemical properties of methyl esters obtained from LSO and OSO (ME-LSO and ME-OSO, respectively) on application of different conditions during the transesterification are given in Tables II and III, respectively.

TABLE II. Characterization of the methyl esters obtained from linoleic sunflower oils (ME-LSO) by transesterification under different experimental conditions (Av. – average values of the parameters)

Parameter	Methanol:oil mole ratio										RSD %	
	4.5:1					6:1						
	Catalyst:oil, mass %		7.5:1		9:1		12:1		Av.			
	2	3	2	3	2	3	2	3	2	3		
Density at 15 °C, kg m <sup>-3</sup>	889	889	886	887	886	886	887	886	887	886	887 0.13	
Kinematic viscosity at 40 °C, m <sup>2</sup> s <sup>-1</sup>	4.29	4.25	4.15	3.96	3.98	4.07	3.93	3.76	4.43	4.01	4.08 4.86	
Acid value, mg KOH g <sup>-1</sup> oil	0.05	0.09	0.05	<0.04	0.06	<0.04	0.06	0.06	0.05	0.04	0.06 25.88	
Iodine value, g I <sub>2</sub> per 100 g	130	129	131	133	131	131	131	131	130	131	0.79	
Saponification value, mg KOH g <sup>-1</sup> oil	178	182	187	188	186	185	184	189	178	188	184 2.17	
Cetane index (CI)	47.8	47.2	46.1	45.6	46.3	46.7	46.4	45.8	47.5	46.2	46.6 1.57	
Fatty acid methyl ester composition, mass %												
Palmitic C16:0	6.78	6.47	6.42	6.30	6.69	6.68	7.06	6.73	6.43	6.39	6.59 3.53	
Stearic C18:0	3.75	3.43	3.55	3.35	3.28	3.48	3.70	3.39	3.71	3.34	3.50 4.89	
Oleic C18:1	22.1	22.8	21.8	23.4	23.8	22.6	22.2	22.5	21.7	22.5	22.6 3.00	
Linoleic C18:2	67.3	67.1	68.1	65.7	65.9	67.2	67.1	67.3	67.2	66.6	66.9 1.04	

To gain a better insight into the latent structure (hidden regularities) of the obtained data and to investigate similarities and dissimilarities of the produced biodiesel samples, PCA was applied on the determined physical and chemical properties and the biplot is shown in Fig. 1. Two PCs were retained explaining 86.3 % of the total variance in the data. A clear separation of MEs synthesized from LSO and OSO was obtained on the PC1 vs. PC2 biplot (Fig. 1), with all the ME-LSOs located on the right side of the plot and all the ME-OSOs on the left. The variables governing the sample separation were those with the highest load-



ings on PC1, *i.e.*, iodine value, density and the contents of C16:0-, C18:0-, and C18:2-methyl esters, which had positive loadings, and the cetane index and the content of methyl ester of the C18:1 acid that had negative PC1 loadings. Due to higher contents of the C16:0-, C18:0-, and C18:2- methyl esters, and also of higher iodine values, the ME-LSOs were clearly separated from the ME-OSOs, characterized by a higher cetane index and content of C18:1-methyl ester than the former. The outliers were the biodiesels obtained from both types of feedstocks using the lowest methanol/oil mole ratio (4.5:1) and the ME-LSO obtained with a 12:1 mole ratio of methanol to oil and 2 mass % of catalyst to oil, and ME-OSO synthesized with a 6:1 mole ratio of methanol to oil and 2 mass % of catalyst to oil.

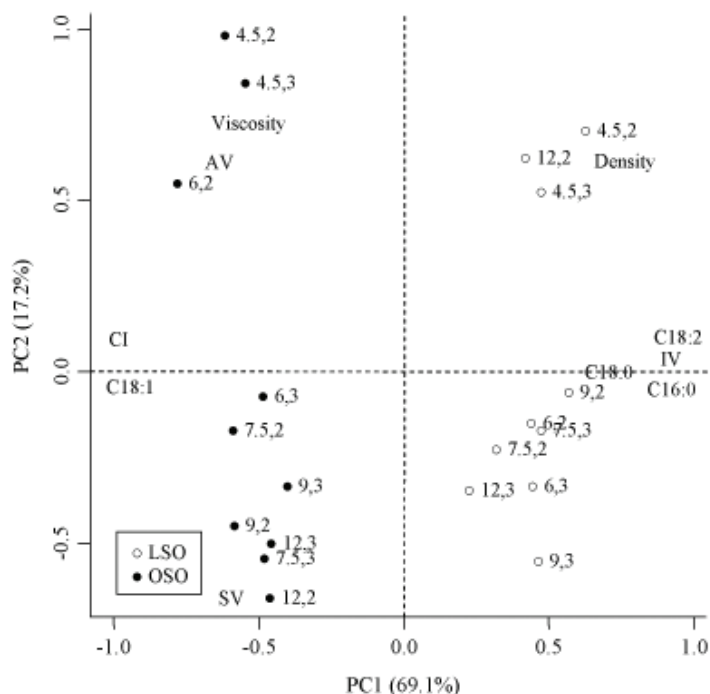


Fig. 1. The PCA biplot PC1 vs. PC2 obtained for the input data set consisting of the physical and chemical properties of the biodiesel produced under the investigated experimental conditions (the first digit indicates the molar ratio of methanol to oil, while the second is mass percentage of catalyst to oil). Percentages given in parentheses are the shares of the total variance explained by each PC.

#### Density at 15 °C

Fuel density is a property important mainly in airless combustion systems because it influences the efficiency of the fuel atomization.<sup>34</sup> The small difference seen between density values of the feedstocks (LSO and OSO, Table I) was also observed between the respective methyl esters (ME-LSO and ME-OSO,

Tables II and III); namely, regardless of the applied working parameters, the ME-LSOs produced from LSO, which was slightly denser than OSO, always had slightly higher densities than the ME-OSOs. This was expected since it is a well-known fact that biodiesel density is influenced primarily by the choice of vegetable oil and, to some extent, by the applied purification steps, since it depends primarily on the content of methyl esters and slightly on the quantity of residual methanol (up to 0.2 % m/m according to SRPS EN 14214<sup>16,24</sup>). The mean values of density for ME-LSOs and ME-OSOs were 0.887 and 0.884 g cm<sup>-3</sup> (Tables II and III) with deviations lower than 0.20 %, calculated as the relative standard deviation, *RSD* (ratio of the standard deviation and the average value of all values obtained for a particular property of the MEs from one feedstock, regardless of the working conditions, multiplied by 100). This implied that working parameters applied in this study had no influence on the densities of the MEs, coinciding with the fact that this biodiesel characteristic depends primarily on the origin of the feedstock.<sup>35</sup> The percentages of the decrease in density between the feedstocks and the corresponding methyl esters (calculated as the ratios of the density differences between a particular SO and ME and the initial density values for the SO multiplied by 100) were about 4 %. This reduction rate was very similar to the one obtained in a previous study of Predojević,<sup>24</sup> who obtained a 5 % reduction of the densities of the feedstocks when a homogenous two-step alkali transesterification procedure was applied on waste frying sunflower oils. Obviously, regardless of the feedstock and the system applied (homogenous or heterogeneous), the density of feedstocks could be reduced by ≈4–5 % on alkali transesterification. All MEs met the density value specified by SRPS EN 14214,<sup>16</sup> *i.e.*, were within the range 0.860–0.900 g cm<sup>-3</sup> at 15 °C.

TABLE III. Characterization of methyl esters obtained from oleic sunflower oil (ME-OSO) by transesterification under different experimental conditions (Av. – average values of the parameters)

Parameter	Methanol:oil mole ratio										Av. %	
	4.5:1					6:1						
	7.5:1					9:1						
	2	3	2	3	2	3	2	3	2	3		
Density at 15 °C, kg m <sup>-3</sup>	887	887	884	884	883	883	883	884	883	882	884 0.19	
Kinematic viscosity at 40 °C, m <sup>2</sup> s <sup>-1</sup>	4.78	4.86	4.75	4.30	4.14	4.40	4.35	4.23	4.03	4.18	4.40 6.66	
Acid value, mg KOH g <sup>-1</sup> oil	0.38	0.23	0.36	0.11	0.20	<0.04	0.08	0.05	0.10	0.05	0.16 80.8	
Iodine value, g I <sub>2</sub> per 100 g	104	102	105	102	101	102	103	103	105	103	103 1.29	
Saponification value, mg KOH g <sup>-1</sup> oil	187	186	188	186	187	192	191	188	191	187	188 1.18	
Cetane index (CI)	52.0	52.8	51.7	52.7	52.9	51.7	51.7	52.2	51.1	52.1	52.1 1.11	

TABLE III. Continued

Parameter	Methanol:oil mole ratio										Av.	RSD %			
	4.5:1					6:1		7.5:1		9:1					
	Catalyst:oil, mass %														
	2	3	2	3	2	3	2	3	2	3	2	3			
Fatty acid methyl ester composition, mass %															
Palmitic	C16:0	5.08	4.92	4.84	5.73	4.90	4.85	5.16	5.40	4.90	5.06	5.08			
Stearic	C18:0	3.06	3.25	2.79	2.96	3.04	3.49	2.96	3.29	3.30	3.27	3.14			
Oleic	C18:1	59.6	58.9	58.5	59.6	58.1	57.4	60.1	58.9	59.6	57.9	58.8			
Linoleic	C18:2	32.2	32.6	32.6	31.7	33.6	33.2	31.8	32.7	32.1	33.6	32.6			

*Kinematic viscosity at 40 °C*

Even more than density, the kinematic viscosity at 40 °C is an important property regarding fuel atomization and distribution. The viscosities of the ME-LSOs were slightly lower than those of the ME-OSOs (Tables II and III, respectively), as was the case for the viscosities of their respective feedstocks (Table I). The average viscosity of the ME-LSOs was 4.08 mm<sup>2</sup> s<sup>-1</sup>, while that of the ME-OSOs was 4.40 mm<sup>2</sup> s<sup>-1</sup>. The respective *RSD* values were 4.86 and 6.66 %, respectively, which coincide with the *RSD* values calculated for the contents of fatty acid (primarily stearic) methyl esters in the produced MEs. Thus, the observed dispersion of the viscosities among the MEs could be ascribed to the changes of viscosities influenced by slight changes in the FAME composition of the MEs. The produced methyl esters met the required values that must be between 3.5–5.0 mm<sup>2</sup> s<sup>-1</sup>.<sup>16</sup>

The viscosities of the MEs were about 6–7 times lower than those of their respective oils. The average decrease in the viscosities going from the feedstocks to the corresponding MEs due to the applied transesterification method was about 85 % (calculated by dividing the difference between the viscosities of the SO and the respective ME with the viscosity of the SO, and finally multiplying by 100 to obtain the percentage value). A similar reduction rate for the viscosity ( $\approx$ 89 %) was obtained in a previous study of Predojević,<sup>24</sup> in which a homogenous two-step alkali transesterification procedure for biodiesel production from the waste frying sunflower oils was applied.

*Acid value*

The acid value measures the content of free fatty acids in sample, which have influence on fuel aging. It is measured in terms of the quantity of KOH required to neutralize sample. As it has been previously mentioned, base catalyzed transesterification is very sensitive to the content of free fatty acids in the feedstocks, which should not exceed 2 mg KOH g<sup>-1</sup> recommended as a limit to avoid deactivation of the catalyst, and the formation of soaps and emulsions.<sup>24</sup> In this



study, the acid values of the feedstocks were well below this limit, since refined oils were used (due to reasons explained previously), which did not have a decisive influence on the efficiency of the applied process. The acid values of the MEs were less than  $0.5 \text{ mg KOH g}^{-1}$ , specified as the maximum allowed value according to SRPS EN 14214.<sup>16</sup> The average acid value of the ME-LSOs was  $0.06 \text{ mg KOH g}$  with an *RSD* of  $\approx 26\%$  (Table II), while of ME-OSOs it was  $0.16 \text{ mg KOH g}^{-1}$  with an *RSD* of  $\approx 81\%$  (Table III). The *RSD* value for the ME-LSOs could not be ascribed to the influence of the different working parameters on the acid values, since all the values were rather small ( $<0.04\text{--}0.09 \text{ mg KOH g}^{-1}$ ), *i.e.*, near the method detection limit and also similar to the value determined for the LSO ( $0.05 \text{ mg KOH g}^{-1}$ ); thus, the calculated *RSD* ( $\approx 26\%$ ) more probably reflects the experimental error in the acid values determination at levels near the detection limit. However, the acid values of the ME-OSOs covered a wider range ( $<0.04\text{--}0.38 \text{ mg KOH g}^{-1}$ ) than was the case with the values for the ME-LSOs, indicating, most probably, an influence of the different working conditions on this property. In Table III, it could be seen that higher acid values were obtained for the ME-OSOs produced using the lower methanol/oil mole ratios (4.5:1 and 6:1) and the lower catalyst/oil mass ratio (2%). Apparently, no (or only a very slight) neutralization of the free fatty acid in the SO by CaO occurred in these cases. With a methanol/oil ratio of 7.5:1, a 50% reduction of the initial acid value of the feedstock was achieved with 2% catalyst/oil mass ratio, while acid value was reduced below the method detection limit when the catalyst/oil mass ratio was 3%. With the two highest levels of the methanol/oil molar ratios applied in this study (9:1 and 12:1), the acid values of the produced methyl esters were very low and comparable with the ones obtained under the same conditions from LSO.

#### Iodine value

The iodine value (*IV*) is a measure of the average amount of unsaturation of fats and oils and is expressed in terms of the number of centigrams of iodine absorbed per gram of sample (or g I<sub>2</sub> per 100 g oil, *i.e.* % of iodine absorbed by the oil).<sup>36</sup> The MEs obtained in this study had *IVs* in a very narrow range, *i.e.*, 129–133 g I<sub>2</sub> per 100 g for ME-LSO and 101–105 g I<sub>2</sub> per 100 g for ME-OSO. The higher iodine values of the ME-LSOs could be related to their higher content of linoleic acid with two double bonds (C18:2), since *IV* is proportional to the number of double bonds and the amount of a fatty compound.<sup>36</sup> Comparing the iodine values of the SOs and the respective MEs, it could be seen that this property was not influenced by the transesterification procedure, since the MEs had almost the same iodine values as their feedstocks. Obviously, this property depends strongly on the feedstock origin and this finding could be supported by the low

RSD values calculated for the IVs of the MEs, irrespective of the applied working parameters (Tables II and III).

The IV is currently the most usual parameter for assessing the oxidative stability of biodiesel, since it is well known that the auto-oxidation of unsaturated fatty compounds proceeds at rates depending on the number and position of the double bonds.<sup>37</sup> The rationale is that the higher the unsaturation of biodiesel, the higher the tendency of the unsaturated compounds to polymerize and form engine deposits. Many automotive biodiesel standards specify an upper IV limit for fuel; for example, Europe's EN 14214<sup>16</sup> standard allows a maximum of 120 g I<sub>2</sub> per 100 g of biodiesel for use as diesel fuel, Germany's DIN 51606<sup>38</sup> set maximum IV at 115 g I<sub>2</sub> per 100 g, while according to the South African Standard SANS 1935<sup>39</sup> for biodiesel, IV of biodiesel should be less than 140 g I<sub>2</sub> per 100 g. The USA ASTM D6751<sup>40</sup> does not specify the IV as a requirement for biodiesel. It should be emphasized that the European and German specifications result in a *de facto* ban on soy-based biodiesel, which often have IV higher than 120 g I<sub>2</sub> per 100 g (*e.g.*, 120–143 g I<sub>2</sub> per 100 g).<sup>36</sup> Furthermore, virgin sunflower oils are also known for typically higher iodine values (*e.g.*, 110–143 g I<sub>2</sub> per 100 g) because of their higher levels of unsaturated fatty acids, primarily linoleic acid (two double bonds) than other vegetable oils (*e.g.* the IVs of corn, palm and rapeseed oils are in ranges 103–128 g I<sub>2</sub> per 100 g, 50–55 g I<sub>2</sub> per 100 g, and 94–120 g I<sub>2</sub> per 100 g, respectively).<sup>36</sup> Accordingly, the ME-LSOs with IVs higher than the limit of 120 g I<sub>2</sub> per 100 g (Table II) were not in compliance with the biodiesel standard SRPS EN 14214,<sup>16</sup> while the ME-OSOs met this requirement. However, there are some studies implying that higher IVs of ME-LSOs (ranged from 129–133 g I<sub>2</sub> per 100 g, Table II) do not necessarily indicate an unsuitable oxidative stability of the biodiesel. Namely, Knothe<sup>36</sup> explained that the difference between the IV of rapeseed methyl esters (115) and soy methyl ester (131) was low, not causing engine deposition. Moreover, Prankl *et al.*<sup>41</sup> found no significant differences in engine use of rapeseed methyl ester, sunflower methyl ester and camelina methyl ester, which had IVs of 107, 132, and 150, respectively. There is some evidence that, for example, storage conditions may have a greater influence on oxidation than the IV.<sup>42</sup>

#### Saponification value

The saponification value (SV) represents the milligrams of KOH required to saponify one gram of fat or oil. The SV of fatty acid methyl esters increases with decreasing molecular mass; for instance, the SV of methyl palmitate is 207.45, while those of methyl oleate, linoleate and linolenate are 189.23, 190.53 and 191.84 mg KOH g<sup>-1</sup>.<sup>36</sup> For biodiesel, the overall SV depends on the amount of each ester and its molecular mass (*i.e.*, individual SV).

The results in Tables II and III indicate that the produced esters had saponification values similar to those of the corresponding oils; namely, the mean value for the ME-LSOs was 184 mg KOH g<sup>-1</sup> oil (5 % lower than the initial SV of the feedstock LSO, Table I), while for the ME-OSO, the average value was 188 mg KOH g<sup>-1</sup> oil (1.6 % lower than the initial SV of the feedstock OSO, Table I). This was not surprising knowing that a triglyceride has 3 fatty acid chains; hence, each triglyceride will give 3 methyl esters during transesterification; thus, stoichiometrically, it may be expected that the same number of fatty acid carbon chains in the neat feedstock oil and the biodiesel will react with the same amount of KOH giving soaps, *i.e.*, their SVs will be the same. It should be noted that in this study, the SV was determined only for the purpose of calculating the cetane index according to Krisnangkura.<sup>26</sup> The SV is not a restricted property of biodiesel according to the EU and the Serbian standards, for this reason, it was not regularly determined in the relevant literature studies. For the MEs produced in the study of Šiler-Marinković and Tomašević<sup>23</sup> from sunflower seeds by *in situ* transesterification and for those produced from waste frying sunflower oils in the study of Predojević,<sup>25</sup> the respective SVs were 179–186 mg KOH g<sup>-1</sup> oil and 204–212 mg KOH g<sup>-1</sup> oil. Thus, the MEs obtained in the present study had saponification values in the range of those found in the literature.

The low levels of the *RSDs* obtained for the SVs of the MEs (Tables II and III) indicated that the working conditions of the transesterification reaction did not influence this property. Thus, the results clearly indicated that the SV of the biodiesel originated from the feedstock quality.

#### Cetane index

As an alternative to the cetane number, the cetane index is also an indicator of ignition quality of a fuel and it is related to the time that passes between injection of the fuel into the cylinder and onset of ignition.<sup>43</sup> Krisnagkura<sup>26</sup> proposed Eq. (1) for the estimation of cetane index (*CI*) based on the SV and *IV*, recommending it not be used for oils, only for methyl esters. Namely, it was previously documented that despite the fact that triglycerides (*i.e.*, feedstock oils) and the respective MEs have similar SVs and *IVs*, as was also obtained in this study, the cetane indices of oils are generally much lower than those of the corresponding methyl ester derivates.<sup>44</sup> Thus, the *CI* values of the SOs were not calculated. In this work, the ME-LSOs had lower *CI* values (the mean was 46.6) than the ME-OSOs (the mean was 52.1). Šiler-Marinković and Tomašević<sup>23</sup> also used the *CI* for the characterization of methyl esters produced from crude (linoleic) sunflower oils, and the estimated values ranged from 49.7 to 50.9. The differences between the *CI* values of the respective MEs expressed as the *RSD* values were rather low (below 1.6 %, see Tables II and III) regardless of the applied working parame-

ters, implying that *CI* was also a property influenced primarily by the feedstock origin.

#### Fatty acid composition

The compositions of fatty acid methyl esters of the produced biodiesels are presented in Tables II and III; only the major components are given, not those present in amounts equal to or less than 1 mass %. It could be seen that the biodiesels had almost the same composition as the feedstocks (Table I). The ME-LSO consisted mainly of linoleic (C 18:2) > oleic (C 18:1) > palmitic (C 16:0) > stearic (C 18:0) acids, while oleic acid (C 18:1) was dominant in the ME-OSOs over linoleic (C 18:2) > palmitic (C 16:0) > stearic (C 18:0) acids. Regardless of the applied working parameters, similar fatty acid profiles were observed in the biodiesels with *RSDs* of up to about 7 %. Thus, it could be concluded that applied transesterification conditions did not change the methyl ester composition of the feedstocks.

#### Effects of the properties of the feedstocks and the working parameters on biodiesel yield and purity

The changes in the biodiesel yield as a function of the methanol/oil molar ratios and the catalysis/oil mass ratios are graphically illustrated in Fig. 2. The product yield is defined as mass percentage of final product relative to the initial mass of oil introduced into the transesterification.<sup>45</sup> The results presented in Fig. 2

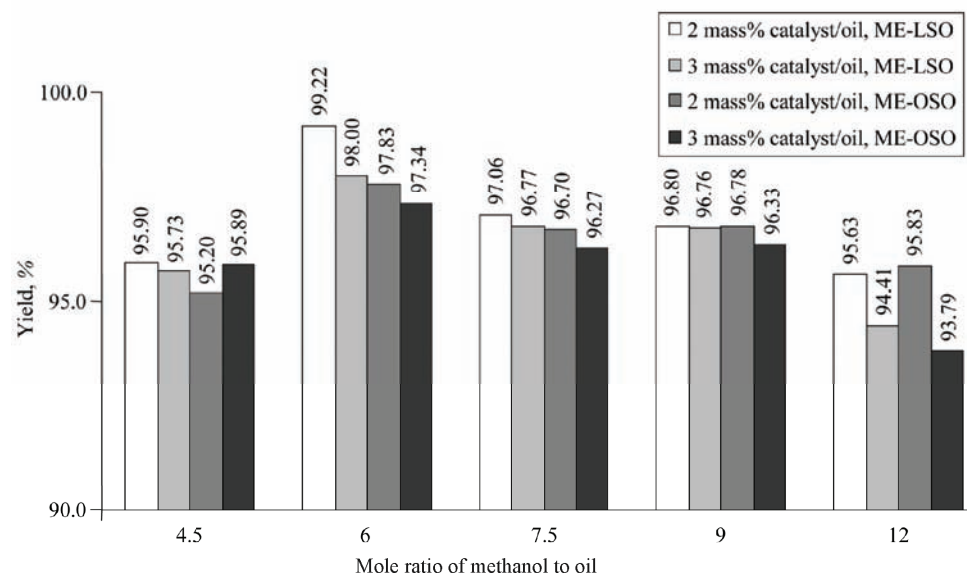


Fig. 2. Effects of the methanol to oil mole ratio and of the catalyst to oil mass ratio on the biodiesel yield.

show that the yields were rather similar with slightly higher values obtained at a methanol/oil ratio of 6 mol % and when the lower amount of catalyst relative to oil was used. To be more specific, the highest yield of ≈99 % (Fig. 2) was obtained by transesterification of LSO at a CaO/oil mass ratio of 2 % and a methanol/oil ratio of 6:1.

The molar ratio of methanol to oil is one of the important parameters that affect the conversion to methyl esters. Stoichiometrically, 3 moles of methanol are required for each mole of triglyceride; but, in practice, the presence of a sufficient amount of methanol during the transesterification reaction is essential to break the glycerin–fatty acid linkages and to improve the biodiesel yields by shifting the equilibrium to the right-hand side of the reaction.<sup>46,47</sup> The employment of excess methanol is also one of the better options for improving the rate of the heterogeneous transesterification reaction, which is diffusion-controlled dependent on mass transfer in a three phase (oil–methanol–catalyst) system.<sup>46</sup> When the mass transfer is limited in the system, it could be much slower than the reaction rate. On the other hand, excess methanol should be avoided, since it also decreases the catalyst content,<sup>3</sup> leading to lower yields, as can be seen for the methanol/oil ratio of 12:1 used in this study (Fig. 2). The product yield was not increased with increasing the methanol/oil mole ratio beyond 6:1; however, it should be taken into account that at a slightly higher methanol amount, as was previously discussed, a more intensive acid value reduction was seen for the ME-OSOs.

The effect of the different amounts of CaO on the biodiesel yield was negligible; a kinetic study at shorter reaction time (<1.5 h) would probably have shown more obviously that the 3 % catalyst results in a faster reaction. The most obvious differences in the yields were observed at the methanol/oil ratio of 12:1, when ≈1.5 % lower yields were obtained for a mass ratio of CaO to oil (either LSO or OSO) of 3 % (Figure 2). Nevertheless, this could also be ascribed to dilution of the catalyst due to the excess of methanol, as mentioned previously. However, the differences between the yields obtained for different mass ratios could be regarded as negligible and this might also be the consequence of a similar and limited dissolution of CaO in methanol (0.035 mass %) previously studied by Granados *et al.*<sup>2</sup> Namely, they reasoned that if the reaction is caused by active homogeneous species related to the dissolution of CaO in methanol, similar yields should be obtained on using different loadings of catalyst, since the presence of homogenous species is in principle controlled by the solubility product of the solid in the reaction media and therefore a constant value of dissolved CaO should be obtained irrespective of the CaO amount used in catalytic reaction.

The yields of the ME-LSOs were in general somewhat higher than those obtained for the ME-OSOs under the same conditions. Since the main differences between the feedstocks, LSO and OSO, were in their acid values and viscosity (Table I), it might be presumed that these parameters also influenced the bio-

diesel yields. This is in agreement with previous observations of Felizardo *et al.*<sup>34</sup> and Predojević,<sup>25</sup> who found that the lowest biodiesel yields after alkali transesterification were obtained with more acidic feedstocks, because of the more pronounced deactivation of the catalyst and the soap formation by the free fatty acids from the feedstock. Moreover, Leung and Guo<sup>45</sup> concluded that a higher viscosity of the oil could also have a negative impact on the product yield, slowing down dissolution of the oils in the methanol and reducing the contact between oil and methanol molecules, consequently leading to a lower conversion of triglycerides. Thus, slightly higher yields of the ME-LSOs over the ME-OSOs could be ascribed to the lower acid value and the viscosity of the LSO compared to the OSO.

The purity of biodiesel product denoted by its ester content is defined as the mass percentage of methyl esters in the final product. In fact, it closely represents the percentage of triglycerides converted to methyl esters.<sup>45</sup> The purity of the ME-LSO produced with the highest yield under a methanol/oil mole ratio of 6:1 and a catalyst/oil mass ratio of 2 % is shown in Fig. 3. According to SRPS EN 14214,<sup>16</sup> the minimum acceptable purity for biodiesel is 96.5 % in methyl esters. With respect to the obtained results (Fig. 3), the produced biodiesel satisfied this requirement.

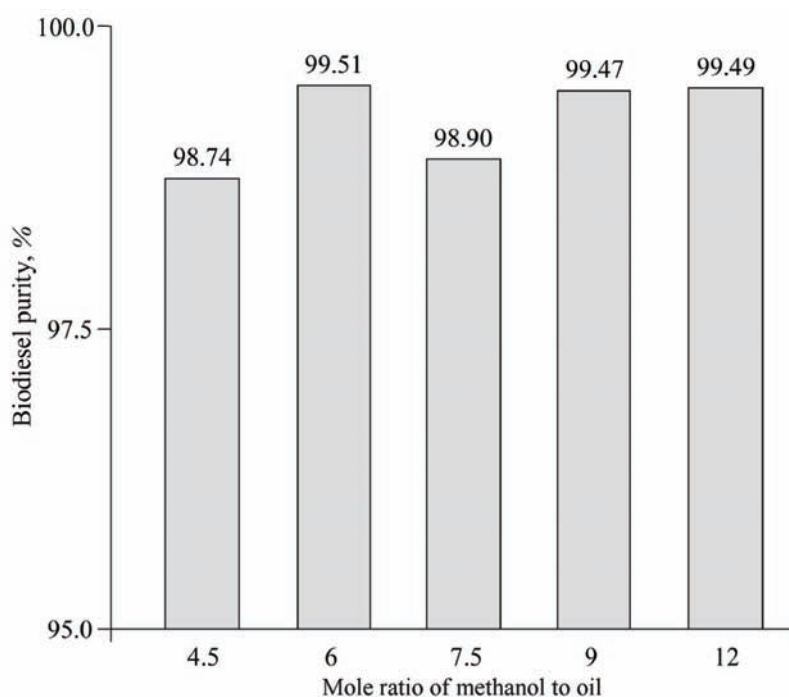


Fig. 3. Purity of methyl esters obtained by heterogeneous alkali transesterification of linoleic sunflower oil with a catalyst/oil ratio of 2 mass % and different methanol/oil ratios.

### CONCLUSIONS

The feedstock origin has a detrimental impact on the physical and chemical properties of the produced biodiesel. Of all the biodiesel properties analyzed, the acid value seems to be the only one influenced by the reaction conditions varied in this study. The heterogeneous transesterification of sunflower oils with different amounts of unsaturated fatty acids could be efficiently accomplished using a 6:1 mole ratio of methanol to oil, with either a 2 or a 3 % CaO/oil mass ratio, and holding the reaction mixture at 65 °C for 1.5 h. The results also indicated that a higher methanol/oil ratio could be favorable in the case of a feedstock with a higher acid value, since under such conditions, reduction of the acid value in the biodiesel would be more pronounced. The biodiesel produced generally met the criteria required of a diesel substitute; in fact, the only exception was in the case of the iodine value of the biodiesel produced from the feedstock with iodine value higher than the value required by the SRPS EN 14214 standard,<sup>16</sup> which defines the requirements for fatty acid methyl esters to be used in a diesel engine, since this property remained almost unchanged during the transesterification reaction. However, there is evidence that a biodiesel with an iodine value of ≈130 g I<sub>2</sub> per 100 g oil would be oxidatively stable. The yields of the biodiesels were above 93 %, while their purities were above the minimum acceptable purity value of 96.5 %, according to SRPS EN 14214<sup>16</sup>

*Acknowledgement.* The results obtained in this article are part of the Project No. 172050 funded by the Ministry of Education and Science of the Republic of Serbia.

### ИЗВОД

#### ТРАНСЕСТЕРИФИКАЦИЈА СУНЦОКРЕТОВОГ УЉА ЛИНОЛНОГ И ОЛЕИНСКОГ ТИПА У БИОДИЗЕЛ КОРИШЋЕЊЕМ CaO КАО БАЗНОГ КАТАЛИЗATORА

ЗЛАТИЦА Ј. ПРЕДОЈЕВИЋ, БИЉАНА Д. ШКРБИЋ И НАТАША ЂУРИШИЋ-МЛАДЕНОВИЋ

*Технолошки факултет, Универзитет у Новом Саду, Булевар цара Лазара 1, 21000 Нови Сад*

Сврха овог рада је карактеризација биодизела (тј. метил естера, ME) произведеног из сунцокретовог уља линолног и олеинског типа (ЛСУ и ОСУ, респективно) алкалном трансестерификацијом са метанолом и CaO хетерогеним базним катализатором, под различитим реакцијоним условима. У току реакције варирани су следећи параметри: молски однос метанол/уље (4,5:1; 6:1; 7,5:1; 9:1 и 12:1) и масени однос CaO према уљу (2 и 3 %). Испитивана су следећа физичко-хемијска својства сировине и ME, као што су: густина на 15 °C, кинематска вискозност на 40 °C, киселински број, јодни број, сапонификацијони број, цетански индекс, састав масних киселина (метил-естера), у циљу испитивања утицаја ЛСУ и ОСУ и параметара реакције на принос, чистоћу и карактеристике произведеног биодизела. Својства сировина имала су изразити утицај на физичка и хемијска својства ME, међутим, вредности већине карактеристика ME, нису се значајно разликовале варирањем услова реакције. Генерално, карактеристике добијеног ME задовољавају стандардом прописане критеријуме комерцијалног биодизела, а једини изузетак је вредност јодног броја ME произведеног од сунцокретовог уља ЛСУ типа. При испитиваним реакцијоним условима постиже се незнатна промена приноса; највећи принос (99,22 %) добијен је за ME–ЛСУ произведеног при мол-

ском односу метанол/уље 6:1, а најнижи (93,20 %) је за МЕ–ОСУ при најнижој вредности молског односа метанол/уље (4,5:1). Масени односи катализатор/уље су имали сличан утицај на конверзију уља у биодизел. Приноси МЕ–ЛСУ су нешто већи у односу на приносе МЕ–ОСУ под истим реакционим условима, што се може објаснити утицајем киселинског броја и вискозности одговарајуће сировине.

(Примљено 24. августа, ревидирано 24. новембра 2011)

#### REFERENCES

- K. G. Georgogianni, A. K. Katsoulidis, P. J. Pomonis, G. Manos, M. G. Kontominas, *Fuel Process. Technol.* **90** (2009) 1016
- M. L. Granados, M. D. Zafra Poves, D. Martin Alonso, R. Mariscal, F. Cabello Galisteo, R. Moreno-Tost, J. Santmaria, J. L. G. Fierro, *Appl. Catal. B* **73** (2007) 317
- X. Liu, H. He, Y. Wang, Sh. Zhu, X. Piao, *Fuel* **87** (2008) 216
- V. B. Veljković, O. S. Stamenković, Z. B. Todorović, M. L. Lazić, D. U. Skala, *Fuel* **88** (2009) 1554
- W. Xie, H. Peng, L. Chen, *Appl. Catal., A* **300** (2006) 67
- W. Xie, H. Li, *J. Mol. Catal., A* **255** (2006) 1
- C. S. MacLeod, A. P. Harvey, A. F. Lee, K. Wilson, *Chem. Eng. J.* **135** (2008) 63
- W. Xie, X. Huang, H. Li, *Bioresour. Technol.* **98** (2007) 936
- W. Xie, H. Peng, L. Chena, *J. Mol. Catal., A* **246** (2006) 24
- S. Gryglewich, *Bioresour. Technol.* **70** (1999) 249
- S. Gryglewich, *Appl. Catal., A* **192** (2000) 23
- H. K. Kim, B. S. Kang, M. J. Kim, M. Young, Y. M. Park, D. K. Kimb, J. S. Lee, K. Y. Kwan-Young Lee, *Catal. Today* **93–95** (2004) 315
- G. Arazmend, E. Arguiñena, I. Campo, L. M. Gandía, *Chem. Eng. J.* **122** (2008) 31
- G. Arazmendi, I. Campo, E. Arguiñena, M. Sánchez, M. Montes, L. M. Gandía, *Chem. Eng. J.* **134** (2007) 123
- Z. Yang, W. Xie, *Fuel Process. Technol.* **88** (2007) 631
- SRPS EN 14214:2005, *Automotive fuels. Fatty acid methyl esters (FAME) for diesel engines-Requirements and test methods*. Standardization Institute, Belgrade, Serbia, 2005
- SRPS EN ISO 3675:2005, *Crude petroleum and liquid petroleum products - Laboratory determination of density - Hydrometer method*, Standardization Institute, Belgrade, Serbia, 2005
- SRPS ISO 3104:2003, *Petroleum products – Transparent and opaque liquids – Determination of kinematic viscosity and calculation of dynamic viscosity*, Belgrade, Serbia, 2003
- EN 14104:2003, *Fatty and oil derivatives – Fatty Acid Methyl Esters (FAME) – Determination of acid value*, CEN Brussels, Belgium, 2003
- EN 14111:2003, *Fat and oil derivatives. Fatty acid methyl esters (FAME). Determination of iodine value*, CEN Brussels, Belgium, 2003
- EN ISO 3657:2003, *Animal and vegetable fats and oils. Determination of saponification value*, CEN Brussels, Belgium, 2003
- F. Karaosmanoğlu, K. B. Ciğizoglu, M. Tüter, S. Ertekin, *Energ. Fuels* **10** (1996) 890
- S. S. Šiler-Marinković, V. A. Tomašević, *Fuel* **77** (1998) 1389
- Z. Predojević, *Fuel* **87** (2008) 3522
- Z. Predojević, B. Škrbić, *J. Serb. Chem. Soc.* **74** (2009) 993
- K. Krisnangkura, *J. Am. Oil Chem. Soc.* **3** (1986) 552



27. SRPS ISO 4264:2002, *Petroleum products – Calculation of cetane index of middle – distillate fuels by the four-variable equation*, Belgrade, Serbia, 2002
28. B. Škrbić, N. Đurišić-Mladenović, *Chemosphere* **68** (2007) 2144
29. B. Škrbić, N. Đurišić-Mladenović, *Chemosphere* **80** (2010) 1360
30. T. Stafilov, B. Škrbić, J. Klanova, P. Čupr, I. Holoubek, M. Kočov, N. Đurišić-Mladenović, *J. Chemomet.* **25** (2011) 262
31. H. F. Kaiser, J. Rice, *Educ. Psychol. Meas.* **34** (1974) 111
32. K. Varmuza, P. Filzmoser, *Introduction to multivariate statistical analysis in chemometrics*, Taylor & Francis – CRC-Press, Boca Raton, FL, USA, 2009
33. R. Purdy, *J. Am. Oil Chem. Soc.* **63** (1986) 1062
34. P. Felizardo, M. J. Neiva Correia, I. Raposo, J. F. Mendes, R. Berkemeier, J. M. Bordado, *Waste Manage.* **26** (2006) 487
35. M. Mittelbach, *Bioresour. Technol.* **56** (1996) 7
36. G. Knothe, *J. Am. Oil Chem. Soc.* **79** (2002) 847
37. E. N. Frankel, *Lipid oxidation*, The Oily Press, Dundee, UK, 1998, p. 19
38. DIN 51606, *Liquid fuels; diesel fuel of vegetable oil methylester (PME); requirements*, Deutsches Institut für Normung, Beurh Verlag GmbH, Berlin, Germany, 1994
39. South African Standard SANS 1935: 2011, *Automotive biodiesel. Fatty acid methyl esters (FAME) for diesel engines-Requirements and test methods*. SABS Standards Division, Pretoria, South Africa, 2011
40. ASTM D6751, *Standard Specification for Biodiesel Fuel Blend Stock (B100) for Middle Distillate Fuels*, American Society for Testing and Materials, Philadelphia, PA, USA, 2011
41. H. Prankl, M. Wörgötter, J. Rathbauer, *Technical performance of vegetable oil methyl esters with a high iodine number*, in *Proceedings of the 4<sup>th</sup> Biomass Conference of the Americas*, R. P. Overend, E. Chornet, Eds., Elsevier Science, Oxford, UK, 1999, p. 805
42. P. Bondioli, L. Folegatti, *Riv. Ital. Sostanze Grasse* **73** (1996) 349
43. G. Knothe, *Fuel Process. Technol.* **86** (2005) 1059
44. G. H. Pischinger, R. W. Siekmann, A. M. Falcon, F. R. Fernandes, *Methylesters of Plant Oils as Diesel Fuels, Either Straight or in Blends*, in *Proceedings of the International Conference on Plant and Vegetable Oils as Fuels*, American Society of Agricultural Engineers, Fargo, ND, USA, 1982, p. 198
45. D. Y. C. Leung., Y. Guo, *Fuel Process. Technol.* **87** (2006) 883
46. Z. Yang, W. Xie, *Fuel Process. Technol.* **88** (2007) 631
47. Y. C. Sharma, B. Singh, S. N. Upadhyay, *Fuel* **87** (2008) 2355.



## Soil acidity and mobile aluminum status in pseudogley soils in the Čačak–Kraljevo Basin

IVICA G. ĐALOVIĆ<sup>1\*</sup>, ĐORĐE S. JOCKOVIĆ<sup>1</sup>, GORAN J. DUGALIĆ<sup>2</sup>, GORAN F. BEKAVAC<sup>1</sup>, BOŽANA PURAR<sup>1</sup>, SRĐAN I. ŠEREMEŠIĆ<sup>3</sup> and MILAN Đ. JOCKOVIĆ<sup>1</sup>

<sup>1</sup>Institute of Field and Vegetable Crops, Maksima Gorkog 30, 21000 Novi Sad, Serbia,

<sup>2</sup>University of Kragujevac, Faculty of Agronomy, Cara Dušana 34, 32000 Čačak,

Serbia and <sup>3</sup>University of Novi Sad, Faculty of Agriculture,  
Dositeja Obradovića 8, 21000 Novi Sad, Serbia

(Received 29 June, revised 2 November 2011)

**Abstract:** Soil acidity and aluminum toxicity are considered the most damaging soil conditions affecting the growth of most crops. This paper reviews the results of tests of pH, exchangeable acidity and the mobile aluminum (Al) concentration in profiles of pseudogley soils from the Čačak–Kraljevo Basin. For these purposes, 102 soil pits were dug in 2009 in several sites around the Čačak–Kraljevo Basin. The tests encompassed 54 field, 28 meadow, and 20 forest soil samples. Samples of soil in a disturbed state were taken from the Ah and Eg horizons (102 samples), from the B<sub>1</sub>tg horizon in 39 field, 24 meadow and 15 forest pits (a total of 78 samples) and from the B<sub>2</sub>tg horizon in 14 field, 11 meadow, and 4 forest pits (a total of 29 samples). The mean pH values (1 M KCl) of the tested soil profiles were 4.28, 3.90 and 3.80 for the Ah, Eg and B<sub>1</sub>tg horizons, respectively. The soil pH of the forest samples was lower than those in the meadow and arable land samples (mean values of 4.06, 3.97 and 3.85 for arable land, meadow and forest samples, respectively). The soil acidification was especially intensive in the deep horizons; thus, 27 (Ah), 77 (Eg) and 87 % (B<sub>1</sub>tg) of the soil samples had a pH value below 4.0. The mean values of the total exchangeable acidity (TEA) were 1.55, 2.33 and 3.40 meq (100 g)<sup>-1</sup> for the Ah, Eg and B<sub>1</sub>tg horizons, respectively. The TEA values in the forest soils were considerably higher (3.39 meq (100 g)<sup>-1</sup>) than those in the arable and meadow soils (1.96 and 1.93 meq (100 g)<sup>-1</sup>, respectively). The mean mobile Al contents of the tested soil samples were 11.02, 19.58 and 28.33 mg Al (100 g)<sup>-1</sup> for the Ah, Eg and B<sub>1</sub>tg horizons, respectively. According to the pH and TEA values, mobile Al was considerably higher in the forest soils (a mean value of 26.08 mg Al (100 g)<sup>-1</sup>) than in the arable and meadow soils (mean values of 16.85 and 16.00 mg Al (100 g)<sup>-1</sup>, respectively). The Eg and B<sub>1</sub>tg horizons of the forest soil had

\* Corresponding author. E-mail: maizescience@yahoo.com; ivica.djalovic@ifvns.ns.ac.rs

# Serbian Chemical Society member.

doi: 10.2298/JSC110629201D

especially high mobile Al contents (mean values of 28.50 and 32.95 mg Al (100 g)<sup>-1</sup>, respectively). High levels of mobile Al were especially frequent in the forest soils, with 35 (Ah), 85.0 (Eg) and 93.3 % (B<sub>1tg</sub>) of the tested samples ranging above 10 mg Al (100 g)<sup>-1</sup>.

**Keywords:** soil; acidity; aluminum; pseudogley.

## INTRODUCTION

Soil acidity limits crop production on 30–40 % of the world's arable land and up to 60 % of the world's potentially arable land. There are several estimates of the extent of acid soils in the world. Van Wambeke<sup>1</sup> reported acid soils covering 1,455 million ha, or about 11 % of the total global land surface, while Von Uexküll and Mutert<sup>2</sup> estimated that acid soils (defined as soils with pH < 5.5 in the top layer) covered 3,950 million ha, or around 30 % of global arable land, with a growing trend. These results are in agreement with those of Eswaran *et al.*<sup>3</sup>, who estimated that globally around 26 % of the total ice-free land is constrained for crop production by soil acidity. Acid soils occur mainly in two global belts: the northern belt, with a cold, humid temperate climate, and the southern tropical belt, with warm and humid conditions.<sup>2</sup>

In Serbia, acid soils are widespread, accounting for over 60 % of the total arable land. These are mostly lowland or hillside types of pseudogley or their leached variants, acid vertisols, podzolic eutric cambisols, diluvial, brown or leached brown soils of mountainous regions, which are rather poor in bases, medium to heavily acid, with very poor texture and low organic content. These soils are more or less ill suited for the cultivation of most cereal crops.<sup>4,5</sup> Most acid soils are located in Central Serbia and in Kosovo and Metohija. With the exception of soils in major river valleys (formed on alluvial deposits) and soils formed on calcareous, marine and lake sediments and limestones, nearly all regions of Central Serbia have soils that are acid to some degree.<sup>6</sup>

The acidity of these soils, their high contents of H<sup>+</sup> and low contents of essential plant nutrients, primarily P and Ca, are limiting factors for high and stable yields of cultivated cereal crops. Apart from acidity, these soils are also often characterized by high contents of toxic forms of Al, Fe and Mn, and by deficits caused by leaching or decreased availability of P, Ca, Mg and some other micro-nutrients, especially Mo, Zn and B.<sup>6–8</sup>

Aluminum (Al) toxicity is the primary factor that limits crop production on strongly acidic soils. At soil pH values at or below 5, toxic forms of Al dissolve into the soil solution, inhibiting root growth and function and thus reducing crop yield. Mineral soils contain large amounts of Al, most of which is locked in aluminosilicates or Al oxides of the clay fraction and does not pose a toxicity hazard. Upon soil acidification, a fraction of this Al becomes soluble and potentially toxic to plants. Thus, acidic mineral soils are practically synonymous with

Al toxicity. Intensification of the process of solubilization of Al compounds is connected with the degree of soil acidification caused by the washing out of alkaline metals ions ( $\text{Na}^+$ ,  $\text{K}^+$ ,  $\text{Ca}^{2+}$  and  $\text{Mg}^{2+}$ ) from the soil and a decrease in the pH of the soil solutions. The determination of the content of available Al (exchangeable and in the soil solution) is essential for an evaluation of the risk of plant production on acid soils, in which it can occur in concentrations toxic for plants and microorganisms.<sup>9</sup>

The objective of this study was to test the pH value, exchangeable acidity and mobile aluminum (Al) status in the profiles of pseudogley soils of the Čačak–Kraljevo Basin.

## EXPERIMENTAL

### *General characteristics of the Čačak–Kraljevo Basin*

Čačak–Kraljevo Basin is located in western Serbia. It is a narrow belt approximately 70 km long in the NW–SE direction and 5 to 18 km wide. The Kablar, Ovčar, Troglav, Stolovi, Goč, Suvobor, Vujno and Kotlenik Mountains border the basin in the SW and NE directions. The pseudogley soils of this area (approximately 32,000 hectares situated mainly between 180 and 200 m above sea level) were formed on the diluvial–Holocene terrace of the Western Morava River and its tributaries. The low productivity of these soils is, to a smaller or a greater extent, the result of unfavorable physical and chemical properties over all the observed parameters of these properties, starting from physiological depth, over texture, structure, porosity to the air and water regime, *i.e.*, from the amount of easily mobile Al ions and exchangeable adsorbed base cations to the degree of base and H-ions saturation. It is characterized with a basic profile structure of the A–Eg–Btg type, and with conditions that create a transition horizon Eg/Btg, buried beneath the Btg (fossil) humus horizon of meadow soil.<sup>10</sup> Based on the development of the physical and chemical properties in the pseudogley, eluvial (Ah, Ahp and Eg) and alluvial (Btg) horizons could be distinguished. In addition, there are significant differences between the varieties of forest, meadow and field pseudogley, especially in the humus horizon.

### *Sampling and chemical analysis*

A total of 102 soil pits were dug in 2009 at several locations around the Čačak–Kraljevo Basin. The tests encompassed 54 field, 28 meadow, and 20 forest soil profiles. Samples of soil in the disturbed state were taken from the humus and Eg horizons (102 samples), from the B<sub>1</sub>tg horizon in 39 field, 24 meadow and 15 forest soil profiles (a total of 78 samples) and from the B<sub>2</sub>tg horizon in 14 field, 11 meadow, and 4 forest soil profiles (a total of 29 samples). In the laboratory, the exchangeable acidity was determined in a 1 M KCl soil solution (pH 6.0) using a potentiometer with a glass electrode, as well as by the Sokolov Method, in which the content of Al ions in the extract is determined in addition to the total exchangeable acidity ( $\text{H}^+ + \text{Al}^{3+}$ ). Exchangeable Al ( $\text{Al}_{\text{KCl}}$ ) and exchangeable acidity ( $\text{meq (100 g)}^{-1}$ ) were determined by extraction with 1 M KCl (1:2.5), shaken for 1 h and titration (the Sokolov Method).<sup>11</sup> For the evaluation of the  $\text{Al}^{3+}$  in the extracts of 1 mol L<sup>-1</sup> KCl solution, 1:10 (v/v) soil/solution ratio, the following procedures were used: titrimetric method (standard method). Primarily, the exchangeable acidity ( $\text{Al}^{3+} + \text{H}^{+}_{\text{tit}}$ ) was determined by titrations of 25 mL KCl extract with 0.025 mol L<sup>-1</sup> NaOH, using 1.0 g L<sup>-1</sup> phenolphthalein as an indicator (titration from colorless to pink). Then, the concentration of mobile  $\text{Al}^{3+}$  was obtained by back-titration

of the same KCl extract, previously used, after the acidification with a drop of HCl and addition of 40 g L<sup>-1</sup> NaF, with 0.025 mol L<sup>-1</sup> HCl (titration from pink to colorless).<sup>11</sup>

#### RESULTS AND DISCUSSION

Aluminum (Al) toxicity is considered as the main growth- and yield-limiting factor on soils with pH below 5.0.<sup>12</sup> Soil acidity is a serious agricultural problem in many parts of the world, affecting as much as 40 % of the world's arable land.<sup>13</sup>

Al toxicity is affected by many factors, such as pH, concentration of Al, temperature, and concentrations of cations and anions in the culture solution. The critical soil pH at which sufficient Al becomes soluble to be toxic is difficult to predict because it depends on many other factors, including clay mineralogy, organic matter, other cations and anions and total salts.<sup>14,15</sup> In general, Al starts to dissolve when the pH<sub>Ca</sub> is lower than 5.5, while below 4.5, there is a marked increase in the extractable Al. The content of soluble Al ions in soils ranges from 1–33 ppm, but seldom exceeds 4 ppm. Increased concentrations of aluminum (for many plant species as low as 1–2 ppm) inhibit root cell division and elongation, resulting in poor root development, reduction of water and nutrient uptake, drought susceptibility, and subsequently in a significant decrease in yield.<sup>16,17</sup> Al interferes with the uptake, transport and utilization of essential nutrients, including Ca, Mg, K, P, Cu, Fe, Mn and Zn.<sup>18,19</sup>

The results of this study showed that the content of exchangeable Al in pseudogleys is highly variable, depending on the locality and profile depth. Its dynamics depends mostly on the soil pH (active, exchangeable or hydrolytic acidity). The mean pH (1 mol L<sup>-1</sup> KCl) of the tested soil profiles were 4.28, 3.90 and 3.80, for Ah, Eg and B<sub>1tg</sub> horizons, respectively. In addition, the pH of the forest soil profiles was lower in comparison with the meadow and arable land profiles (mean values of 4.06, 3.97 and 3.85, for arable land, meadow soil and forest soil, respectively). Soil acidification was especially intensive in deep soil horizons since 27 (Ah), 77 (Eg) and 87 % (B<sub>1tg</sub>) of the soil profiles had a pH below 4.0 (Table I; Fig. 1).

Soil reaction is one of the best parameters for an estimation of the exchangeable Al content. Al solubility increases at active soil acidities below 5.5. In addition to soil reaction, Al dynamics is also affected by other factors, especially the soil organic matter content and composition. Acid cations in complexes or chelates with organic matter are not readily exchangeable by normal exchange reactions.<sup>20,21</sup>

The mean values of the total exchangeable acidity (TEA) in the tested soil profiles were 1.55, 2.33 and 3.40 meq (100 g)<sup>-1</sup>, for the Ah, Eg and B<sub>1tg</sub> horizons, respectively. However, it was considerably higher in the forest soils (mean 3.39 meq (100 g)<sup>-1</sup>) than in the arable and meadow soils (means 1.96 and 1.93, respectively). The deep horizons (Eg and B<sub>1tg</sub>) of the meadow and forest soil pro-

files had especially high *TEA* values. Especially high frequencies of high *TEA* values (over 3.0 meq (100 g)<sup>-1</sup>) were found in the forest soil profiles (Table I; Fig. 2).

TABLE I. Distribution of pH (1 M KCl, in % of total), total exchangeable acidity (*TEA* as sum of H<sup>+</sup> and Al<sup>3+</sup>, in % of total) and mobile aluminum in soil profiles (in % of total); a = arable land; m = meadow; f = forest

Horizon	<i>n</i>	pH (1 M KCl)				<i>TEA</i>				Mobile Al			
		pH Range				>5 <1.0 1–2 2–3 >3.0 <3.0				3–6 6–10 >10			
		< 4.0	4.1–4.5	4.6–5.1	>5	<1.0	1–2	2–3	>3.0	<3.0	3–6	6–10	>10
Ah (a)	54	18.5	57.5	22.2	1.8	86.8	13.2	0.0	0.0	63.0	18.5	11.1	7.4
Ah (m)	28	20.8	75.0	4.2	0.0	85.2	14.8	0.0	0.0	64.4	17.8	7.1	10.7
Ah (f)	20	55.0	30.0	5.0	10.0	55.0	20.0	5.0	20.0	40.0	10.0	15.0	35.0
Ah (total)	102	26.5	56.1	14.3	3.1	80.0	15.0	1.0	4.0	58.8	16.3	10.8	14.1
Eg (a)	54	64.8	27.8	7.4	0.0	35.8	37.8	22.6	3.8	20.4	13.0	12.9	53.7
Eg (m)	28	91.7	8.3	0.0	0.0	18.5	63.0	11.1	7.4	10.7	7.1	21.4	60.8
Eg (f)	20	90.0	10.0	0.0	0.0	10.0	20.0	30.0	40.0	0.0	15.0	0.0	85.0
Eg (total)	102	76.5	19.4	4.1	0.0	26.0	41.0	21.0	12.0	13.7	11.8	12.8	61.7
B <sub>1</sub> tg (a)	39	76.9	20.5	2.6	0.0	24.3	18.9	24.3	32.5	12.8	12.8	7.7	66.7
B <sub>1</sub> tg (m)	24	95.0	5.0	0.0	0.0	8.7	21.7	39.2	30.4	0.0	8.3	12.5	79.2
B <sub>1</sub> tg (f)	15	100	0.0	0.0	0.0	0.0	21.4	28.6	50.0	0.0	0.0	6.7	93.3
B <sub>1</sub> tg (total)	78	86.9	11.8	1.3	0.0	14.8	20.3	29.6	35.3	6.4	9.0	8.9	75.7
B <sub>2</sub> tg (total)	29	90.2	6.6	3.2	0.0	14.8	27.6	36.5	21.1	0.0	14.2	13.5	72.3

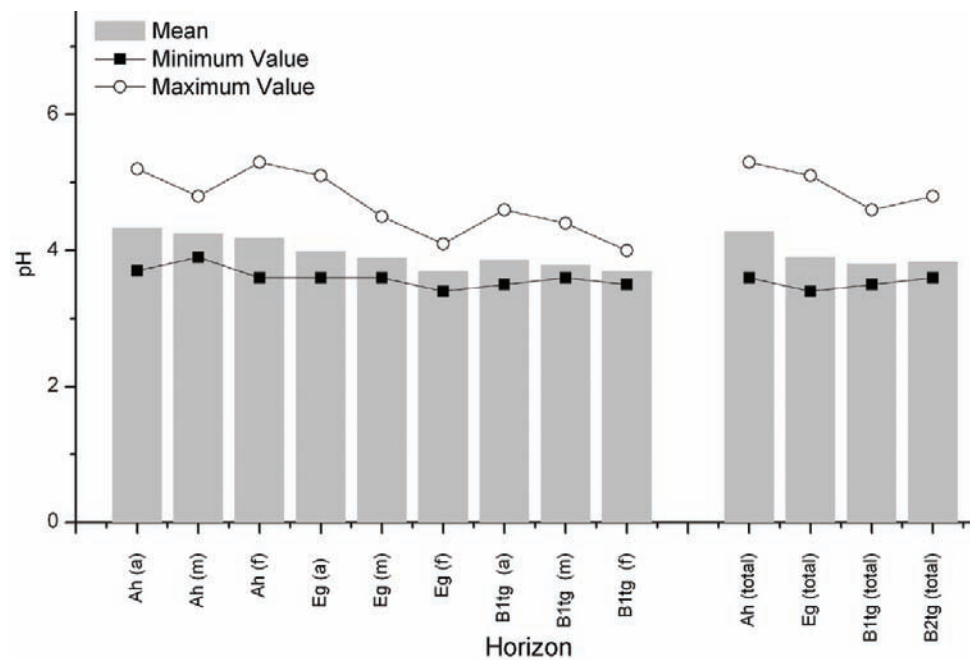


Fig. 1. Distribution of pH (1 M KCl) in the soil profiles.

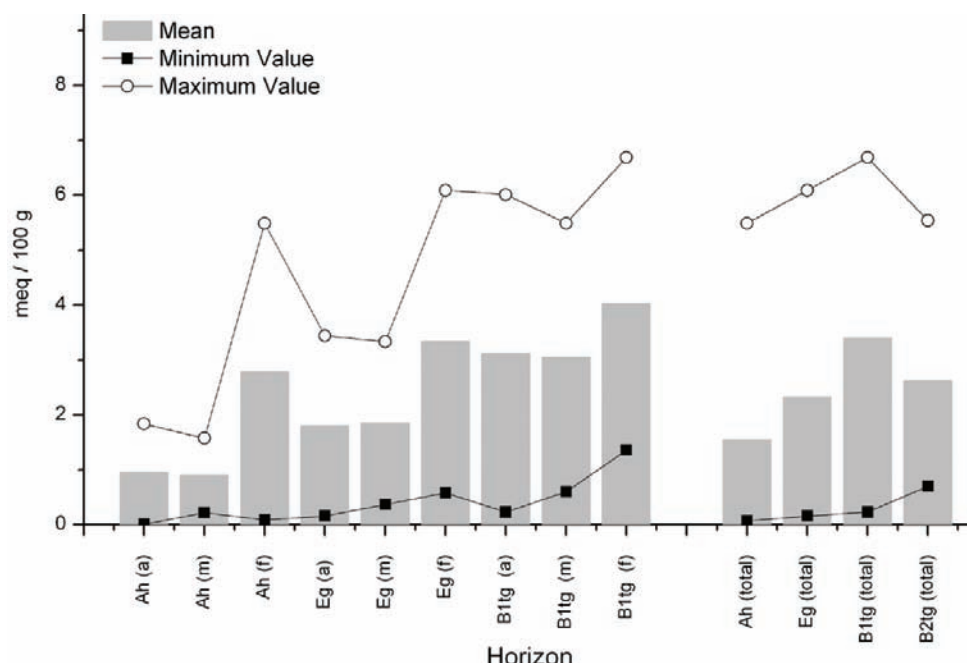


Fig. 2. Distribution of total exchangeable acidity (*TEA*) (sum of  $H^+$  and  $Al^{3+}$ ) in the soil profiles (meq (100 g) $^{-1}$  soil).

The mean mobile Al contents in the tested soil profiles were 11.02, 19.58 and 28.33 mg Al (100 g) $^{-1}$  for the Ah, Eg and B<sub>1</sub>tg horizons, respectively. In accordance with soil pH and *TEA*, the mobile Al in the forest soils was considerably higher (mean 26.08 mg Al (100 g) $^{-1}$ ) than in arable and meadows soils (means 16.85 and 16.00 mg Al (100 g) $^{-1}$ , respectively). The Eg and B<sub>1</sub>tg horizons of the forest soil profiles had especially high mobile Al contents (means 28.50 and 32.95 mg Al (100 g) $^{-1}$ , respectively). The frequency of high levels of mobile Al was especially high in the forest soils since 35 (Ah), 85.0 (Eg) and 93.3 % (B<sub>1</sub>tg) of the tested profiles were in the range above 10 mg Al (100 g) $^{-1}$  (Table I, Fig. 3).

High contents of mobile aluminum in pseudogley soil were also observed by Osaki *et al.*,<sup>22</sup> Abreu *et al.*<sup>23</sup> and Mládková *et al.*<sup>24</sup>

Increased *TEA* values are characteristic for soils in which acidification processes are rather far advanced, the reaction of their soil solutions being fairly acidic, with pH values lower than 5.0. This is typical of the pseudogley in the Čačak-Kraljevo Basin, the most widely distributed soil type in the location. As, for the same *TEA* value, an increased concentration of Al ions is much more dangerous for plants than  $H^+$  at the same concentration, plants increasingly suffer if a high share of Al ions is present in the soil. Already at 6–10 mg (100 g) $^{-1}$  of read-

ily mobile Al in the soil, plant growth is retarded to a greater or lesser extent depending on the crop in question.<sup>25</sup> High TEA values created predominantly by Al ions is one of the most important causes for the low productivity of the pseudogley in the studied basin, where average yields of cultivated plants, despite the application of fertilizers and different agrotechnical measures, are low and vary greatly in dependence on the weather conditions of the year.

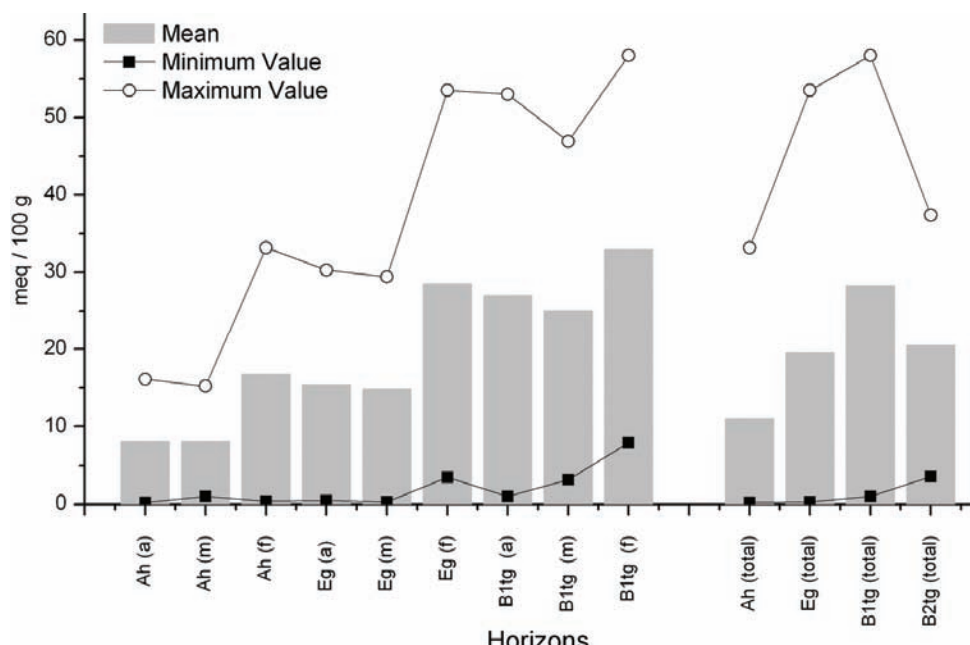


Fig. 3. Distribution of mobile aluminum in the soil profiles (meq (100 g)<sup>-1</sup> soil).

The sources of the available Al (in the soil solution and exchangeable Al) are the aluminum contained in aluminosilicates, amorphous and crystalline Al oxides, organically bound Al, Al in interlayers of three-layered minerals, etc. The content of these forms in stagnosols depends on the parent rock composition, the intensity of the processes of clay leaching and other colloids, the weathering process, organic matter content and other soil characteristics.<sup>26</sup>

In studies of different soil types, many researchers concluded that the content of Al oxides is not proportional to the content of exchangeable Al.<sup>27,28</sup> The form of the Al plays a decisive role in its potential bioavailability and toxicity. The toxicity of aluminum to plants qualitatively decreases in the order: Al<sub>13</sub> (not in the form of phosphates or silicates), Al<sup>3+</sup>, Al(OH)<sup>2+</sup> and Al(OH)<sub>2</sub><sup>+</sup>. Aluminum bound in fluoride or organic complexes and Al(OH)<sub>3</sub> are supposed to be non-toxic.<sup>29</sup> The complexation of Al by natural organic substances is of considerable significance in regulating the concentrations of the highly toxic Al<sup>3+</sup> in acid soils

and natural waters.<sup>30</sup> The distribution of toxic Al<sup>3+</sup> is particularly affected by the contents of humic and fulvic acids in the surface soil horizons. Aluminum complexes with both types of acids decrease the toxic impact of Al<sup>3+</sup> by decreasing its bioavailability and activity in the soil solution.<sup>31,32</sup>

The investigations of stagnosols from Serbia showed that the content of exchangeable Al increased significantly with increasing contents of less available Al forms, Al<sub>Cu</sub>, Al<sub>EDTA</sub> and Al<sub>dit</sub>, but the correlation with amorphous Al was low.<sup>26</sup> These findings were explained with possibility of EDTA and CuCl<sub>2</sub> to extract the organic Al, Al in interlayers of three-layered minerals and other Al forms comprised in the amorphous Al. The results of the present study indicate that further research on the mobility of Al reserves in different types of acid soils is required.

Lime is widely known as the most effective means for correcting soil acidity. The direct effect of soil amendment through lime is a change in the soil pH. Its application usually results in significant reduction of exchangeable Al, allowing for a more efficient uptake of N and P.<sup>33</sup> Osei<sup>34</sup> studied the effects of different lime application rates and time of application on some chemical properties of an acid soil. Significant increase in pH (> 28 %) was obtained at all soil sampling depths. Available P also increased significantly (> 90 %). Exchangeable Al was completely eliminated when most of the soil samples had pH > 5.0. The results clearly indicated that liming as a management practice, could be used to alleviate or prevent acidification of pseudogley soil.

Strategies to overcome the negative effects of Al on plant growth in these soils include the application of lime to raise the soil pH and lower the soil exchangeable Al, and the use of crop species that are resistant to Al-toxic soils. The incorporation of lime fertilizers alleviates soil acidity, provides calcium to plants, increases the amount of plant available phosphorus, provides mineralization of organic and harvest residues, and decreases the amount of toxic substances and heavy metals in the soil. Chemical amendment (melioration) of acid soils (soil adaptation to the plant) and the breeding and selection of tolerant genotypes (plant adaptation to the soil) are two complementary possibilities to alleviate the problems related to increasing the productivity of acid soils.<sup>35</sup>

#### CONCLUSIONS

Aluminum (Al) toxicity is considered as the main growth- and yield-limiting factor on soils with pH below 5.0. The obtained results showed variability of the soil properties among the examined sites, and the deeper soil horizons have higher contents of mobile Al. The mean mobile Al contents of the tested soil samples were 11.02, 19.58 and 28.33 mg Al 100 g<sup>-1</sup> for the Ah, Eg and B<sub>1tg</sub> horizons, respectively. It was found that increasing TEA and lower pH significantly contributed to an increase in Al toxicity. The mobile Al was significantly higher in the pseudogley of forest soils (26.08 mg Al (100 g)<sup>-1</sup>) than in the arable and

meadow soils (16.85 and 16.00 mg Al (100 g)<sup>-1</sup>, respectively). To explain fully the role and toxicity of Al in soil productivity, the TEA, pH, Ca and soil organic matter must be controlled. Finally, to prevent manifestation of Al toxicity on plants growing in pseudogley and similar acid soils, it is necessary to conduct preliminary soil analyses, particularly of the deeper soil horizons. Chemical amendment (melioration) of acid soils (soil adaptation to the plant) and the breeding and selection of tolerant genotypes (plant adaptation to the soil) are two complementary possibilities for solving the problems related to increasing the productivity of acid soils.

*Acknowledgment.* This research was supported by a grant from the Ministry of Education and Science of the Republic of Serbia (Project No. TR 31073).

#### И З В О Д

#### КИСЕЛОСТ И САДРЖАЈ ПОКРЕТЉИВОГ АЛУМИНИЈУМА У ПСЕУДОГЛЕЈНИМ ЗЕМЉИШТИМА ЧАЧАНСКО-КРАЉЕВАЧКЕ КОТЛИНЕ

ИВИЦА Г. ЂАЛОВИЋ<sup>1</sup>, ЂОРЂЕ С. ЈОЦКОВИЋ<sup>1</sup>, ГОРАН Ј. ДУГАЛИЋ<sup>2</sup>, ГОРАН Ф. БЕКАВАЦ<sup>1</sup>, БОЖАНА ПУРАР<sup>1</sup>,  
СРЂАН И. ШЕРЕМЕШИЋ<sup>3</sup> и МИЛАН Ђ. ЈОЦКОВИЋ<sup>1</sup>

<sup>1</sup>Институција за раштарство и поштарство, Максима Горкоћ 30, 21000, Нови Сад, <sup>2</sup>Агрономски факултет,  
Универзитет у Краљеву, Цара Душана 34, 32000, Чачак и <sup>3</sup>Полојтврдни факултет,  
Универзитет у Новом Саду, Доситеја Обрадовића 8, 21000, Нови Сад

Киселост земљишта и токсичност алуминијума се сматрају најважнијим факторима који ограничавају раст биљака на киселим земљиштима. У овом раду су испитивани pH вредност земљишта и садржај покретљивог алуминијума (Al) у профилма земљишта псеудоглеја Чачанско-краљевачке котлине. Укупно 102 земљишна профила су отворена током 2009. године на појединим локалитетима Чачанско-краљевачке котлине. Истраживањима је обухваћено 54 узорка са ораница, 28 са ливада и 20 узорака из профила који су отворени под шумском вегетацијом. Из отворених профила, узети су узорци земљишта у поремећеном стању из Ah и Eg хоризонта (102 профила), а затим из B<sub>1tg</sub> хоризонта са 39 ораница, 24 ливаде и 15 шумских профила (укупно 78) и из B<sub>2tg</sub> хоризонта 14 ораница, 11 ливада и 4 шумска профила (укупно 29). Просечна pH вредност (1 M KCl) испитиваних земљишних профила је 4,28, 3,90 и 3,80, за Ah, Eg и B<sub>1tg</sub> хоризонте. Такође, pH вредност земљишта шумских профила је низка у поређењу са ливадама и обрадивим земљиштем (4,06, 3,97 и 3,85, за обрадиво земљиште, ливаде и шуме). Земљишна киселост је посебно изражена у дубљим хоризонтима, јер 27 (Ah), 77 (Eg) и 87 % (B<sub>1tg</sub>) земљишних профила имају pH вредност нижу од 4,0. Средња укупна разменјива киселост (TEA) испитиваних земљишних профила је 1,55, 2,33 и 3,40 meq (100 g)<sup>-1</sup>, у Ah, Eg и B<sub>1tg</sub> хоризонтима. Међутим, код шумским земљиштима TEA је знатно виша (просечно 3,39 meq (100 g)<sup>-1</sup>) него код обрадивог земљишта и ливада (1,96 и 1,93). Просечан садржај покретљивог Al у испитиваним земљиштима је 11,02, 19,58 и 28,33 mg Al (100 g)<sup>-1</sup>, у Ah, Eg и B<sub>1tg</sub> хоризонтима. Услед разлика у pH и TEA вредностима његов садржај у шумским земљиштима је знатно виши (просечно 26,08 mg Al (100 g)<sup>-1</sup>) него код обрадивог земљишта и ливада (16,85 и 16,00 Al (100 g)<sup>-1</sup>). Eg и B<sub>1tg</sub> хоризонти шумског земљишта имају посебно висок садржај покретљивог Al (28,50 и 32,95 mg Al (100 g)<sup>-1</sup>). Учесталост високог нивоа покретљивог Al у шумским земљиштима постоји због тога што 35 (Ah), 85,0 (Eg) и 93,3 % (B<sub>1tg</sub>) испитиваних профила поседују више од 10 mg Al (100 g)<sup>-1</sup>.

(Примљено 29. јуна, ревидирано 2. новембра 2011)

## REFERENCES

1. A. V. Wambeke, *Formation, distribution and consequences of acid soils in agricultural development*, In *Proceedings of Workshop on Plant Adaptation to Mineral Stress in Problem Soils*, J. M. Wright, A. S. Ferrari, Eds., *Spec. Publ. Cornell Univ. Agric. Exp. Stn.*, Ithaca, NY, 1976, p. 15
2. H. R. von Uexkull, E. Mutert, *Plant Soil* **171** (1995) 1
3. H. Eswaran, P. Reich, F. Beinroth, *Global distribution of soils with acidity*, in *Plant–Soil Interactions at Low pH*, A. C. Moniz, Ed., *Brazilian Soil Sci. Soc.*, Sao Paulo, Brazil, 1997, p. 159.
4. M. Jakovljević, M. Kresović, S. Blagojević, S. Antić-Mladenović, *J. Serb. Chem. Soc.* **70** (2005) 765
5. M. Kresović, M. Jakovljević, S. Blagojević, S. Maksimović, *J. Serb. Chem. Soc.* **74** (2009) 93
6. I. Dalović, I. Maksimović, R. Kastori, M. Jelić, *Proc. Nat. Sci. Matica Srpska Novi Sad* **118** (2010) 107
7. A. L. Narro, J. C. Perez, S. Pandey, J. Crossa, F. Salazar, M. P. Arias, *Implications of soil-acidity tolerant maize cultivars to increase production in developing countries*, In *Plant nutrient acquisition: New perspectives*, N. Ae, J. Arihara, K. Okada, A. Srinivasan, Eds., Springer Verlag, Tokyo, Japan, 2001, p. 447
8. Z. Jovanovic, I. Djalovic, M. Tolimir, M. Cvijovic, *Cereal Res. Commun.* **35** (2007) 1325
9. V. Mrvić, M. Jakovljević, D. Stevanović, D. Čakmak, M. Zdravković, *J. Serb. Chem. Soc.* **73** (2008) 673
10. G. Dugalić, B. Gajić, *Soil Plant* **51** (2002) 141
11. M. Jakovljevic, M. Pantovic, S. Blagojevic, *Laboratory Manual of Soil and Water Chemistry*, Faculty of Agriculture, Belgrade, 1995, p. 57 (in Serbian)
12. C. D. Foy, *Adv. Soil Sci.* **9** (1992) 97
13. A. Haug, *Crit. Rev. Plant Sci.* **1** (1984) 345
14. P. A. V. Hees, U. S. Lundstrom, M. Starr, R. Giesler, *Geoderma* **94** (2000) 289
15. D. A. Samac, M. Tesfaye, *Plant Cell Tiss. Org.* **75** (2003) 189
16. C. D. Foy, *Commun Soil Sci. Plant Anal.* **19** (1988) 959
17. T. Mossor-Pietraszewska, *Acta Biochim. Pol.* **48** (2001) 673
18. R. B. Clark, *Plant Soil* **47** (1977) 653
19. G. Tyler, T. Olsson, *Plant Soil* **230** (2001) 307
20. F. Dijkstra, R. Fitzhugh, *Geoderma* **114** (2003) 33
21. M. Jelić, J. Milivojević, S. Trifunović, I. Đalović, D. Milošev, S. Šeremešić, *J. Serb. Chem. Soc.* **76** (2011) 781
22. M. Osaki, T. Watanabe, T. Tadano, *Soil Sci. Plant Nutr.* **43** (1997) 551
23. C. H. Abreu, J. T. Muraoka, A. F. Lavorante, *Sci. Agric. (Piracicaba, Braz.)* **60** (2003) 543
24. L. Mládková, L. Bordvka, O. Drábek, *Soil Sci. Plant Nutr.* **51** (2005) 741
25. Z. Rengel, *Biometals* **17** (2004) 669
26. V Mrvić, M. Jakovljević, M. Stevanović, D. Čakmak, *Plant Soil Environ.* **53** (2007) 482
27. E. Alvarez, C. Monterroso, L. M. Fernandez Marcos, *For. Ecol. Manage.* **166** (2002) 193
28. E. Garcia-Rodeja, J. Novoa, X. Pontevedra, A. Martinez-Cortizas, P. Buurman, *Catena* **56** (2004) 155
29. G. Sposito, *The Environmental Chemistry of Aluminum*, CRC Press, Boca Raton, FL, USA, 1996

30. D. Berggren, J. Mulder, *Geochim. Cosmochim. Acta* **59** (1995) 4167
31. F. Vardar, M. Ünal, *Adv. Mol. Biol.* **1** (2007) 1
32. L. M. Adams, J. O. Hawke, S. H. N. Nilsson, J. K. Powell, *Aust. J. Soil Res.* **38** (2000) 141
33. B. Raij, J. A. Quaggio, *Methods used for diagnosis and correction of soil acidity in Brazil: an overview*, in *Plant–Soil Interactions at Low pH*, A. C. Moniz, Ed., Brazilian Soil Sci. Soc., São Paulo, Brazil, 1997, p. 205
34. A. B. Osei, *Soil Use Manage.* **11** (1995) 25
35. C. Welcker, C. The, B. Andreau, C. Deleon, S. N. Parentoni, F. J. Bernal, C. Zonkeng, F. Salazar, L. Nano, A. Charcosset, W. J. Horst, *Crop Sci.* **45** (2005) 2405.





## Short-time effects of the herbicide nicosulfuron on the biochemical activity of Chernozem soil

LJILJANA RADIVOJEVIĆ<sup>1</sup>, SLAVICA GAŠIĆ<sup>1\*</sup>, LJILJANA ŠANTRIĆ<sup>1</sup>,  
JELENA GAJIĆ UMILJENDIĆ<sup>1</sup> and DRAGANA MARISAVLJEVIĆ<sup>2</sup>

<sup>1</sup>Institute of Pesticides and Environmental Protection, Banatska 31b, P. O. Box 163,  
11080 Belgrade, Serbia and <sup>2</sup>Institute for Plant Protection and Environment,  
Teodora Dražera 9, P. O. Box 33-79, 11000 Belgrade, Serbia

(Received 8 August, revised 27 December 2011)

**Abstract:** Short-time effects of the herbicide nicosulfuron on the biochemical activity of soil were investigated. Nicosulfuron rates of 0.3, 1.5 and 3.0 mg kg<sup>-1</sup> of soil were laboratory-tested on Chernozem soil. The change in the dehydrogenase activity, in microbial biomass carbon, soil respiration and the metabolic coefficient ( $q_{CO_2}$ ) were examined. Samples were collected for the analysis 1, 7, 14, 21, 30 and 60 days after nicosulfuron application. The obtained results indicated that the effect of nicosulfuron on the soil biochemical activity depended on its application rate and duration of activity, and the effect was either stimulating or inhibiting. However, the changes detected were found to be transient and, therefore, there is no real risk of the compound disrupting the balance of biochemical processes in Chernozem soil.

**Keywords:** nicosulfuron; Chernozem soil; dehydrogenase; biomass carbon; respiration.

### INTRODUCTION

The perfect pesticide should be toxic only to the target organisms, be totally biodegradable to CO<sub>2</sub> and H<sub>2</sub>O, and should not leave intermediate compounds in environment or be leached into the groundwater. Unfortunately, this is rarely the case and the widespread use of pesticides in contemporary agriculture is of increasing concern. The main problems in a real system arising from the use of pesticides in agriculture are their toxicity to non-target organisms and the environment, and their persistence in soil.<sup>1</sup>

The toxicity of pesticides has been examined individually in a variety of soils under different conditions and there is mounting evidence that the biological

\*Corresponding author. E-mail: slavica.gasic@pesting.org.rs  
doi: 10.2298/JSC110825004R

parameters of soil may be used as early and sensitive indicators of soil ecological stress.<sup>2–4</sup>

Some researchers<sup>5</sup> proposed a set of soil quality indicators that are sensitive to changes in soil management, and integrate biological, physical and chemical properties. In discussions about soil quality indicators, other researchers<sup>6</sup> included microbial biomass carbon, enzyme activity and soil respiration as biological indicators.

Sulfonylureas are class of herbicides characterized by high biochemical activity at low application rates. Modern pesticides tend to be applied at much lower doses than older compounds, but this does not mean they are less harmful to non-target organisms, as environmental risk arises from dose and activity, not just from the dose alone.<sup>7</sup> Sulfonylurea herbicides were introduced in the 1980s and have become valuable tools for weed management in agricultural production. Depending on crop type and local legislation, the application rates of these herbicides range from 2 g to 150 g a.i ha<sup>-1</sup>. Although the mode of action of this herbicide class has been reported,<sup>8–10</sup> little additional information is available on the overall effects of this herbicide class on the biochemical properties of soil.

Nicosulfuron, 1-(4,6-dimethoxypyrimidin-2-yl)-3-(3-dimethylcarbamoyl-2-pyridyl sulfonyl) urea), a member of this class, is a common agricultural herbicide used to control most annual and perennial grasses and several broad-leaved weeds in maize.

Microbial degradation critically affects the fate and behavior of pesticides in soil. The microbial population in soil constitutes a complex biochemical system capable of producing unique enzymes that degrade a large number of pesticides. Establishment of the degradation pathway of a pesticide in soil is difficult, but the use of various biochemical indicators can help the impact of a pesticide on soil to be better understood. Biochemical indicators, such as soil enzymes, biomass, respiration, *etc.*, are often used to characterize the effects of pesticides on the environment.<sup>11</sup>

The objective of the present study was to investigate, under laboratory conditions, the effects of nicosulfuron on the biochemical properties of soil by measuring different parameters, *i.e.*, microbial biomass carbon, dehydrogenase activity, soil respiration and the microbiological metabolic coefficient ( $q_{CO_2}$ ).

## EXPERIMENTAL

The pesticide (herbicide) nicosulfuron, 1-(4,6-dimethoxypyrimidin-2-yl)-3-(3-dimethylcarbamoyl-2-pyridylsulfonyl)urea, tested in the experiment was a technical grade product of BASF, Germany. The rates of application were 0.3, 1.5 and 3.0 mg kg<sup>-1</sup> soil. The lowest concentration tested was the label rate (0.3 mg kg<sup>-1</sup>), while the other two were five and ten times higher than the recommended dose. The experiment was performed in Chernozem soil with a clay loam texture (pH 7.10, organic matter, 3.32 %, sand, 21 %, silt, 49 %, and clay, 30 %) at Zemun Polje, Belgrade. The soil chosen for the study had never been previously treated

with pesticides. Various management practices would have otherwise affected the soil microbial populations. In this way, it was possible to control the effects of the chosen pesticide (nicosulfuron).

The dehydrogenase activity, microbial biomass carbon and soil respiration were examined as relevant biochemical indicators.<sup>12-15</sup>

The soil samples were collected from the upper layer (0–10 cm), carefully dried, sieved to <5 mm mesh and stored at 4 °C. Before use, the soil was air-dried at room temperature for 24 h. Each herbicide concentration was pipetted onto the surface of 1 kg of soil before homogenization on a rotary stirrer for 30 min. After homogenization, the soil was portioned into pots. Untreated soil served as the control. The experiments were conducted in four replicates. The pots were kept in a controlled-environment chamber at 20±2 °C, 50 % air humidity and a 12/12 h day/night photoperiod throughout the experiments. The soil humidity was maintained at 50 % field capacity. Samples were collected for analysis 1, 7, 14, 21, 30 and 60 days after nicosulfuron application.

The activity of the enzyme dehydrogenase was determined according to Tabatabai.<sup>16</sup> The soil samples were prepared by incubation with triphenyltetrazonium chloride (TTC) under moist conditions at 37 °C for 24 h. Determination of triphenylformazan (TPF), which is derived from triphenyltetrazonium chloride (TTC) as a product of enzyme activity, was realized spectrophotometrically. The measurements were performed at a wavelength of 485 nm (Gilford stasar III, model 2400) and the enzyme activity is given as µg TPF g<sup>-1</sup> soil.

Fumigation-extraction<sup>17</sup> was employed to determine the microbial biomass carbon. The samples were fumigated with alcohol-free chloroform (CHCl<sub>3</sub>) under moist conditions for 24 h. After incubation, the carbon was extracted with a 0.5 M solution of potassium sulfate (K<sub>2</sub>SO<sub>4</sub>) and its content determined by titration with a 0.0333 M solution of Mohr salt ((NH<sub>4</sub>)<sub>2</sub>Fe(SO<sub>4</sub>)<sub>2</sub>) in the presence of phenylanthranilic acid as the indicator. Non-fumigated samples were extracted under the same conditions. The microbial biomass carbon was calculated based on a difference between carbon in the fumigated and non-fumigated samples using the factor 0.38.<sup>18</sup> The results are presented in µg C g<sup>-1</sup> soil.

The Walter method<sup>19</sup> was employed to determine the soil respiration. The soil samples were incubated with sodium hydroxide under moist conditions at room temperature for 24 h. The carbon dioxide (CO<sub>2</sub>) released during soil respiration was absorbed by 0.1 M solution of sodium hydroxide (NaOH), and CO<sub>2</sub> content was determined by titration with 0.1 M hydrochloric acid (HCl) in the presence of an appropriate indicator (phenolphthalein, Methyl Orange). The results are presented in µg CO<sub>2</sub> g<sup>-1</sup> soil.

The microbiological metabolic coefficient ( $q_{CO_2}$ ) was computed from the ratio of the intensity soil respiration and the microbial biomass.<sup>20</sup>

Statistical data processing was realized using PC Anova software. *F*-test was applied to all variables and their interactions and, in the case of a significant result in the individual comparisons, the LSD test was applied. Probability levels of 0.05 and 0.01 were used as significance criteria.

## RESULTS AND DISCUSSION

Dehydrogenase activity is a measure of microbial metabolism and thus of the microbial oxidative activity in a soil. The soil enzyme activity is believed to be sensitive to pollution and has been proposed as an index of soil degradation. Dehydrogenase is thought to be an indicator of the overall microbial activity, because it occurs intracellularly in all living microbial cells and is linked with

microbial oxidation–reduction processes. It is a specific kind of enzyme that plays a significant role in the biological oxidation of soil organic matter by transferring protons and electrons from substrates to acceptors. The dehydrogenase activity of a is considered a valuable parameter for assessing the side effects of herbicide treatments on the soil microbial biomass.<sup>21</sup>

The effect of nicosulfuron on the enzyme activity is shown in Fig. 1, from which it can be seen that the dehydrogenase activity decreased for all applied nicosulfuron concentrations from the 1<sup>st</sup> to the 30<sup>th</sup> day. The decrease ranged from 5.1–25.8 % for the 0.3 mg concentration to 3.4–30.1 % for 1.5 mg kg<sup>-1</sup> of soil and 4.4–42.7 % for 3.0 mg kg<sup>-1</sup> of soil, and the found differences were statistically significant ( $P < 0.01$ ). The decreased dehydrogenase activity was the result of the impact of the herbicide on the soil microorganisms. Actually, any toxicant from the external environment added to a soil may inhibit the microorganisms and thus the dehydrogenase enzymes. The altered enzyme activity depended on the concentration and duration of nicosulfuron activity. There was an increase in enzyme activity from 30<sup>th</sup> to 60<sup>th</sup> day, and the values of treated and untreated soils were similar at the end of the examination period.

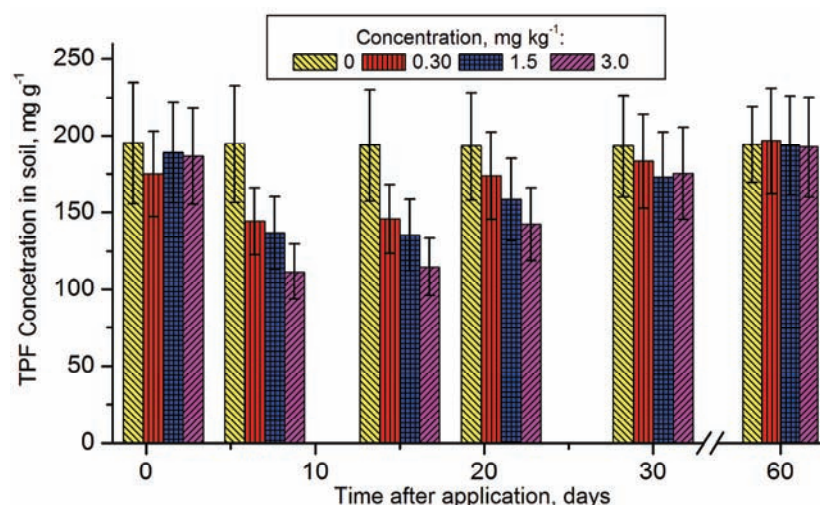


Fig. 1. Effect of nicosulfuron on the dehydrogenase activity.

These results are in accordance with the results of other authors who investigated the effects of different pesticides on dehydrogenase activity.<sup>22–27</sup> However, Ming *et al.*<sup>28</sup> reported that butachlor stimulated the soil microorganisms as well as the dehydrogenase activity. Radivojević *et al.*<sup>29</sup> investigated the effects of the herbicide metribuzin on the activity of some enzymes in soil. They found that the effect depended on the treatment rate, exposure time, enzyme group and that it initially inhibited but finally became stimulating at the end of the experiment.

Soil microbial biomass is defined as the living part of the organic matter of a soil. The composition of the soil microbial biomass varies depending on the soil characteristics. The soil microbial biomass increases or decreases in response to changes in soil management. Therefore, biomass measurement can indicate the effects of a pesticide on a soil and it is an important parameter in ecological tests. Data showing the effect of nicosulfuron on the biomass carbon are presented in Fig. 2. The highest biomass carbon ( $2033.2 \mu\text{g C g}^{-1}$  soil) was found for a nicosulfuron concentration of  $3.0 \text{ mg kg}^{-1}$  of soil (7 days after application) and the lowest ( $408.7 \mu\text{g C g}^{-1}$  soil) for a concentration of  $3.0 \text{ mg kg}^{-1}$  of soil (1 day after application).

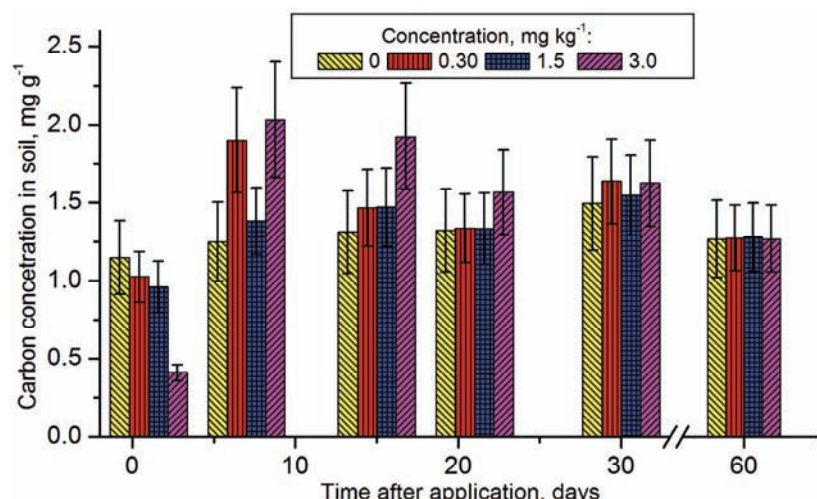


Fig. 2. Effect of nicosulfuron on the microbial biomass carbon.

These results indicate that nicosulfuron influenced the microbial biomass carbon, particularly at the beginning of the experiment, as a significant decrease in the microbial biomass carbon was observed on the first day. However, after one week and until the end of experiment (60<sup>th</sup> day), an increase in the biomass in relation to the applied concentration was recorded. This is not strange as it was assumed that the most dramatic decrease in the biomass carbon would occur immediately after pesticide application, when the concentration of the compound in the soil solution was the highest.<sup>30</sup> Many authors believe<sup>31–34</sup> that the biomass carbon later increases primarily due to restored populations of living organisms that are able to adapt to the particular pesticide present in the soil. Therefore, a new biomass that is metabolically very active and participates in various biochemical processes in the soil is formed. There have been other reports on the activity of different pesticides in relation to biomass carbon. The effects of long-term cumulative field application of the pesticides benomyl, chlorfenvinphos, aldicarb,

triadimefon and glyphosate on soil microbial biomass and mineralization of the soil organic matter were investigated. The addition of aldiocarb consistently increased the microbial biomass, due to its beneficial effect on crop growth, but this effect was not influenced by the rate of organic matter mineralization. However, in general, the continued application of these pesticides for up to 19 years, at slightly higher than the recommended rates, had very little effect on the soil microbial population.<sup>35</sup> On the contrary, Duah-Yentumi and Johnson<sup>36</sup> reported a dramatic reduction in the soil biomass following vinclosolin application, but for other pesticides, such as carbofuran, cabosulfan, simazine, paraquat, *etc.*, they concluded that there were substantially different effects on soil biomass production by single or repeated application. It can be concluded that almost every pesticide has a different impact on the microbial biomass, as there is no general rule for their behavior. Still, it is very important to know the influence as microbial biomass reflects the effects of pesticide contaminants on the overall microbial population.

The biochemical activity of a soil, therefore, can be quantified by measuring CO<sub>2</sub> evolution. Carbon dioxide evolution is often used to characterize the effects of pesticides on the soil microflora. Soil respiration is one of the oldest and still the most frequently used parameter for quantifying activity in soil.<sup>37</sup> Soil respiration, as indicated by oxygen consumption and CO<sub>2</sub> evolution is considered as an indicator of microbiological activity, although it should be interpreted with caution. The rate of soil respiration depends on the physiological condition of the organisms and the edaphic conditions, such as temperature and soil moisture. Soil respiration measurements are often useful when made in conjunction with other response parameters, as was the case in this investigation.

The effect of nicosulfuron on soil respiration primarily depended on the pesticide concentration (Fig. 3). The respiration intensity at a nicosulfuron concentration of 3.0 mg kg<sup>-1</sup> of soil ranged between 2.8 (1 day after application) and 6.9 µg CO<sub>2</sub> g<sup>-1</sup> soil (15 days after application). At all concentrations, the respiration was reduced 2.5–40.2 % one day after application. Between the 7<sup>th</sup> and 15<sup>th</sup> day, an increase in respiration (21.7–56.4 %) was observed for all applied concentrations. A statistically significant increase in respiration ( $P<0.01$ ) was detected for a concentration of 3.0 mg kg<sup>-1</sup> of soil until 21 and 30 days after application. The degree of respiration inhibition increased with increasing nicosulfuron concentration at the beginning of the experiment but there was an increase in respiration at the end of the investigation. Thus, the more drastic the effect, the greater is the potential for recolonization of the treated soil.

Respiration gives a measure of the overall microbial activity and is considered as a bioindicator of soil quality.<sup>38</sup> Soil respiration has been frequently used for assessing the side effects of pesticides, such as atrazine, pentachlorophenol, 4-chloroanile and chloroacetamide, and it was found that atrazine caused minor

effects but the other pesticides stimulated respiration.<sup>39</sup> Araujo *et al.*<sup>40</sup> studied changes in microbial activity caused by glyphosate application and the result was an increase of 10–15 % in the respiration. Other researchers<sup>41,42</sup> reported that rimsulfuronmethyl had no effect on respiration but that rimsulfuron greatly reduced the intensity of this process.

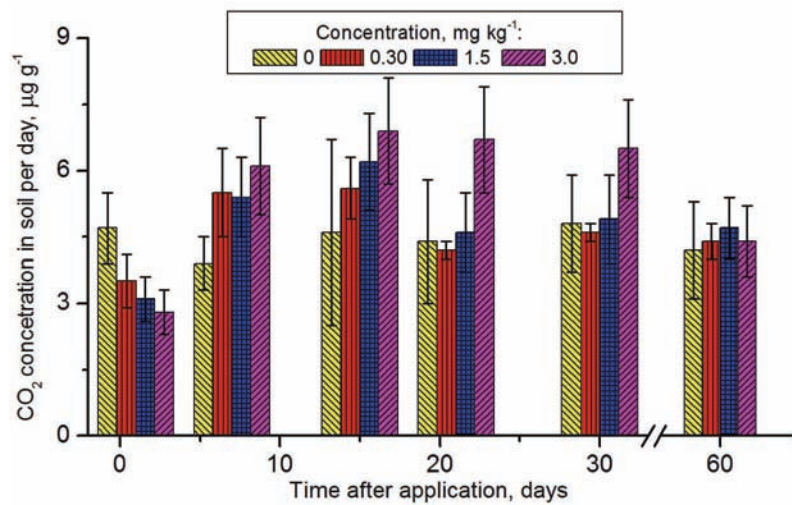


Fig. 3. Effect of nicosulfuron on soil respiration.

Based on literature data, it is not clear enough if the degree of soil respiration is influenced by the catabolic activity of the microbiological community or by changing microbial biomass. Based on the results obtained in the present study, it could be concluded that changes in biomass carbon influences changes in respiration.

The ratio between soil respiration and the soil microbial biomass of the microorganisms presents a safe way to evaluate microbial activity. This ratio, named metabolic coefficient ( $q_{CO_2}$ ), was proposed by Anderson and Domsch<sup>43</sup> and is directly related to the fact that the biomass of the soil microorganisms becomes more efficient in utilizing the ecosystem resources. This coefficient is indicative of the activity of the microorganisms in soil. The degree of disturbance of the microbial community by anthropogenic impacts can be comparable to that caused by natural stress (drying-wetting and freeze-thawing), yet the duration of anthropogenic exposure is much longer, which makes it more harmful. An increase in the soil  $q_{CO_2}$  was observed after various anthropogenic disturbances: heavy metal contamination<sup>44,45</sup> or long term exposure to pesticides.<sup>46,47</sup> Therefore, the metabolic coefficient is used as a measure of microorganism stress because of different harmful influences. Thus, soil under stress would present higher  $q_{CO_2}$ .

values than non-stressed soils.<sup>48</sup> The comparison of the metabolic coefficients in the affected and intact soil could be used to quantify different impacts.

In this investigation, increased values of the metabolic coefficient were recorded on the 1<sup>st</sup> (3.0 mg kg<sup>-1</sup> of soil), 15<sup>th</sup> (1.5 mg kg<sup>-1</sup> of soil), 21<sup>st</sup> (3.0 mg kg<sup>-1</sup> of soil) and 30<sup>th</sup> (0.3 and 3.0 mg kg<sup>-1</sup> of soil) day of the experiment (Fig. 4). Reduced coefficient values were recorded after the 1<sup>st</sup> (0.3 and 1.5 mg kg<sup>-1</sup> of soil), 7<sup>th</sup> (0.3 and 3.0 mg kg<sup>-1</sup> of soil) and 21<sup>st</sup> (0.3 mg kg<sup>-1</sup> of soil) days. All differences detected were statistically significant ( $P < 0.01$  or  $P < 0.05$ ).

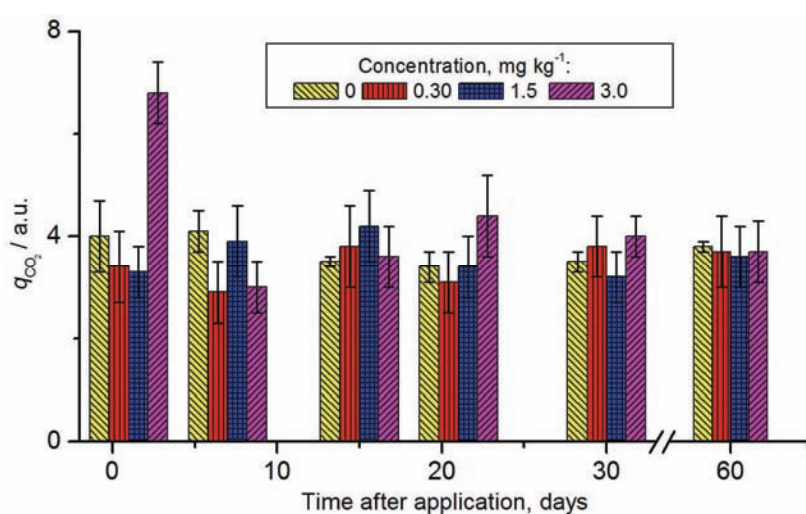


Fig. 4. Variation of the metabolic coefficient ( $q_{CO_2}$ ) in the presence of nicosulfuron.

The increased values of the metabolic coefficient were induced by the adverse effects of nicosulfuron on the biochemical activity of soil. The period in which an increase in the metabolic coefficient was recorded was in accordance with the time when significant changes in dehydrogenase activity, microbial biomass carbon and intensity of soil respiration were registered. Bearing in mind the fact that the level of the metabolic coefficient reached the control level after 30 days, it was concluded that the harmful effect of nicosulfuron decreased with time. We are of the opinion that this occurred because of the microbial degradation of the nicosulfuron and restoration of the microbial community with microorganism groups that could use nicosulfuron as a source of nutrients and energy for physiological processes.

The results obtained in the present study are in accordance with the results of other authors. Increased values of the metabolic coefficient were found 21 days after application of glyphosphate and dinoseb.<sup>47</sup> Larger values were found in the case of dinoseb compared to glyphosphate, which is not strange bearing in mind the greater toxicity of dinoseb. Radivojevic *et al.*<sup>15</sup> showed that atrazine had in-

creased the values of the coefficient  $q_{CO_2}$  30 days after application. In addition, it was found that there was an increase by 20–55 % in the metabolic coefficient after application of metalaxy1.<sup>45</sup>

Finally, it should be mentioned that the data presented herein suggest difficulties in the employment of biochemical parameters as indicators of nicosulfuron impact on soil, as different results were acquired depending on the biochemical parameter examined, the rate of application and the post-treatment time. In the literature, contrasting and opposing results of the impact of different pesticides on the biochemical parameters are reported. According to the present investigation, it seems that, of the examined parameters, the dehydrogenase activity was the most useful indicator of nicosulfuron impact on soil.

#### CONCLUSIONS

This short-term study, which lasted for 60 days, showed that soil microbial activities, such as soil respiration, dehydrogenase, soil biomass carbon and the metabolic coefficient changed on application of the herbicide nicosulfuron. Under the employed experimental conditions, the short-term use of nicosulfuron caused different effects on the biochemical activity in soil. The influence of nicosulfuron depended on the rate of application and the duration of activity, and was either stimulating or inhibitory. The impact of nicosulfuron on the dehydrogenase activity was consistently negative for each herbicide concentration and depended on the rate of application. Based on the microbial biomass carbon, soil respiration and the metabolic coefficient ( $q_{CO_2}$ ), non consistent positive or negative effects of nicosulfuron were observed and the effects persisted until the 60<sup>th</sup> day.

The present study indicated that the application of nicosulfuron, either at the recommended or multiplied doses, influences temporary changes in character and intensity, which suggests that there is no real risk of causing a disruption of the existing balance of the soil biochemical processes. The microbial activities seemed to recover after the application. However, regarding pesticide application, laboratory results may not necessarily reflect the situation under field conditions, because in the field many factors could mask or reduce the potential toxicity of pesticides. Therefore, field studies would be a more realistic approach before general conclusions on the effect of nicosulfuron on the biochemical activity in soil are made.

*Acknowledgment.* The authors are grateful to the Ministry of Education and Science of the Republic of Serbia for financial support (Project No. TR 31043 and Project No. III46008).

И З В О Д

КРАТКОРОЧНО ДЕЛОВАЊЕ НИКОСУЛФУРОНА НА  
БИОХЕМИЈСКУ АКТИВНОСТ ЧЕРНОЗЕМА

ЉИЉАНА РАДИВОЈЕВИЋ<sup>1</sup>, СЛАВИЦА ГАШИЋ<sup>1</sup>, ЉИЉАНА ШАНТРИЋ<sup>1</sup>, ЈЕЛЕНА ГАЛИЋ УМИЉЕНДИЋ<sup>1</sup>  
и ДРАГАНА МАРИСАВЉЕВИЋ<sup>2</sup>

<sup>1</sup>Институти за пресипације и заштиту животне средине, Банатска 31б, Ј. Ђр. 163, 11080 Београд

<sup>2</sup>Институти за заштиту биља и животне средине, Теодора Драјзера 9, Ј. Ђр. 33–79, 11000 Београд

У раду је испитивано краткорочно деловање хербицида никосулфурон на биохемијску активност земљишта. Оглед је постављен у лабораторијским условима на земљишту типа глиновита иловача. Никосулфурон је примењен у количинама од 0,3, 1,5 и 3,0 mg kg<sup>-1</sup> земљишта. Праћени су следећи биохемијски параметри: активност ензима дехидрогеназе, промене микробиолошке биомасе угљеника, респирација (дисање) земљишта као и метаболитички кофицијент ( $q_{CO_2}$ ). Узорци за анализе узимани су 1, 7, 14, 21, 30 и 60 дана после примене никосулфурона. Добијени резултати су показали да је утицај никосулфурона на биохемијску активност земљишта зависио од примењене количине и дужине деловања, те је у зависности од тога, било стимулативно или инхибиторно. Међутим, утврђене промене су биле пролазног карактера, тако да може да се сматра да нема реалног ризика од нарушавања равнотеже биохемијских процеса у земљишту под утицајем овог једињења.

(Примљено 8. августа, ревидирано 27. децембра 2011)

#### REFERENCES

1. M. Ros, M. Goberna, J. L. Moreno, T. Fernandez, C. Garcia, H. Insan, J. A. Pascual, *Appl. Soil Ecol.* **34** (2006) 93
2. G. Dinelli, A. Vicari, *J. Environ. Qual.* **27** (1998) 1459
3. K. Debosz, P. H. Rasmussen, A. R. Pedersen, *Appl. Soil Ecol.* **13** (1999) 209
4. C. Accinelli, C. Screpanti, G. Dinelli, A. Vicari, *Int. J. Environ. Anal. Chem.* **82** (2002) 519
5. J. W. Doran, D. G. Fraser, M. N. Culik, W. C. Liebhard, *Am. J. Altern. Agric.* **2** (1987) 99
6. D. L. Karlen, M. J. Mausbach, M. J. Doran, J. W. Cline, R. F. Harris, G. E. Schuman, *Soil Sci. Soc. Am. J.* **61** (1997) 4
7. M. P. Greaves, in *Proceedings of an International Crop Protection Conference*, Brighton, UK, 1987, p. 501
8. J. M. Green, J. F. Uldrich, *Weed Sci.* **41** (1993) 508
9. M. A. Baghestani, E. Zand, S. Soufizadeh, A. Eskandari, R. P. Azar, M. Veysi., N. Nasirzadeh, *Crop Prot.* **26** (2007) 936
10. S. R. Sikkema, N. Soltani, P. H. Sikkema, D. E. Robinson, *Crop Prot.* **27** (2008) 695
11. A. Chowdhury, S. Pradhan, M. Saha, N. Sanyal, *Indian J. Microbiol.* **48** (2008) 114
12. E. Grossbard, H. A. Davis, *Weed Res.* **16** (1996) 163
13. G. S. Burns, *Soil Biol. Biochem.* **14** (1982) 423
14. P. R. Hargreaves, P. C. Brooks, P. R. Ross, P. R. Poulton, *Soil. Biol. Biochem.* **35** (2003) 401
15. Lj. Radivojević, S. Gašić, Lj. Šantrić, R. Stanković-Kalezić, *J. Serb. Chem. Soc.* **73** (2008) 951
16. M. A. Tabatabai, *Soil Enzymes. Method of soil analysis*, Part 2, American Society of Agronomy, Soil Science Society of America, Madison, WI, USA, 1982, p. 903
17. D. S. Jenkinson, S. A. Davidson, D. S. Powlson, *Soil Biol. Biochem.* **8** (1979) 521

18. E. D. Vance, P. C. Brooks, D. S. Jenkinson, *Soil Biol. Biochem.* **19** (1987) 703
19. H. Walter, *Ber. Dtsch. Bot. Ges.* **65** (1952) 175
20. T. H. Anderson, K. H. Domsch, *Soil Biol. Biochem.* **22** (1990) 251
21. Z. Stepniewska, A. Wolinska, R. Lipinska, *Int. Agrophys.* **21** (2007) 101
22. H. A. Davies, M. P. Greaves, *Weed Res.* **21** (1981) 205
23. N. Milošević, M. Govđedarica, M. Živanović, M. Jarak, Đ. Papić, *Pesticides* **10** (1995) 129 (in Serbian)
24. M. Govđedarica, N. Milošević, M. Jarak, B. Konstantinović, S. Đurić, *Acta Herbologica* **6** (1997) 39
25. S. Junnila, H. Heinonen-Tanski, L. R. Ervio, P. Laitinen, *Weed Res.* **34** (1999) 413
26. B. K. Singh, A. Walker, D. J. Wright, in *Proceedings of Symposium Pesticide Behavior in Soil and Water*, Brighton, UK, 2001, p. 145
27. A. Monkiedje, M. O. Ilbori, M. Spitteler, *Soil Biol. Biochem.* **34** (2002) 1939
28. H. Ming, Y. Ye, Z. Chen, W. Wu, D. Yufeng, *J. Environ. Sci. Health., B* **36** (2001) 581
29. Lj. Radivojević, Lj. Šantrić, R. Stanković-Kalezić, D. Brkić, V. Janjić, *Pesticides* **18** (2003) 99 (in Serbian)
30. D. A. Wardle, D. Parkinson, *Plant Soil* **134** (1991) 2093
31. T. Harden, R. G. Joergensen, B. Mayer, V. Wolters, *Soil Biol. Biochem.* **25** (1993) 679
32. R. G. Joergensen, P. C. Brookes, D. S. Jenkinson, *Soil Biol. Biochem.* **22** (1990) 1129
33. D. A. Wardle, G. W. Yeates, K. S. Nocholson, K. I. Bonner, R. N. Watson, *Soil. Biol. Biochem.* **31** (1999) 1707
34. J. A. Entry, P. K. Donnelly, W. H. Emmingham, *Appl. Soil. Ecol.* **2** (1995) 74
35. M. R. Hart, P. C. Brookes, *Soil Biol. Biochem.* **28** (1996) 1641
36. S. Duah-Yentumi, D. B. Johnson, *Soil Biol. Biochem.* **18** (1986) 629
37. K. Alef, in *Methods in applied soil microbiology and biochemistry*, K. Alef, P. Nannipieri, Eds., London Academic, London, UK, 1995, p. 215
38. M. Dutta, D. Sarder, R. Pal, R. K. Kole, *Environ. Monit. Assess.* **160** (2010) 385
39. L. I. Zelles, I. Scheunert, F. Korte, *J. Environ. Sci. Health., B* **20** (1985) 457
40. A. S. F. Araujo, R. T. R. Monteiro, R. B. Abarkeli, *Chemosphere* **52** (2003) 799
41. S. Đorđević, M. Govđedarica, S. Ajder, L. Stefanović, *Contemp. Agricul.* **42** (1994) 125 (in Serbian)
42. Lj. Radivojević, Lj. Šantrić, J. Gajić Umiljendić, *Pesticides* **26** (2011) 135 (in Serbian)
43. T. H. Anderson, K. H. Domosch, *Biol. Fertil. Soils* **1** (1985) 81
44. G. Valsecchi, C. Gigliotti, A. Farini, *Biol. Fertil. Soils* **20** (1995) 253
45. W. J. Jones, N. D. Ananyeva, *Biol. Fertil. Soils* **33** (2001) 477
46. N. D. Anayeva, E. V. Balgodatskaya, T. S. Demkina, *Eurasian Soil Sci.* **30** (1997) 1010
47. D. A. Wardle, G. W. Yeates, K. S. Nocholson, K. I. Bonner, R. N. Watson, *Soil Biol. Biochem.* **31** (1999) 1707
48. S. A. P. Fernandes, W. Bettoli, C. C. Cerri, *Appl. Soil. Ecol.* **30** (2005) 65.





***Errata*** (printed version only)

Issue No. 5 (2012), Vol. 77, back cover – Contents:

– lines 20–22 from below should read:

<i>M. Adimi, M. Salimi, M. Nekoei, E. Pourbasheer and A. Beheshti: A quantitative structure–activity relationship study on histamine receptor antagonists using the genetic algorithm–multi-parameter linear regression method .....</i>	639
--	-----